X-ray microscopy

Chris Jacobsen

Department of Physics & Astronomy

Stony Brook University, NY, USA

Chris.Jacobsen@stonybrook.edu

Slides at `http://tinyurl.com/ye9ldvb`

Long Island, New York, USA

Stony Brook University

National Synchrotron Light Source, Brookhaven National Laboratory

X-ray microscopy group at Stony Brook

Jan Steinbrener, Lisseth Gavilan, Xiaojing Huang, Christian Holzner, Rachel Mak, Josh Turner, Johanna Nelson, Chris Jacobsen, Robert Towers. Not shown: Sue Wirick, Chris Peltzer.

Phase contrast and fluorescence
Spectromicroscopy
XDM/CXDI

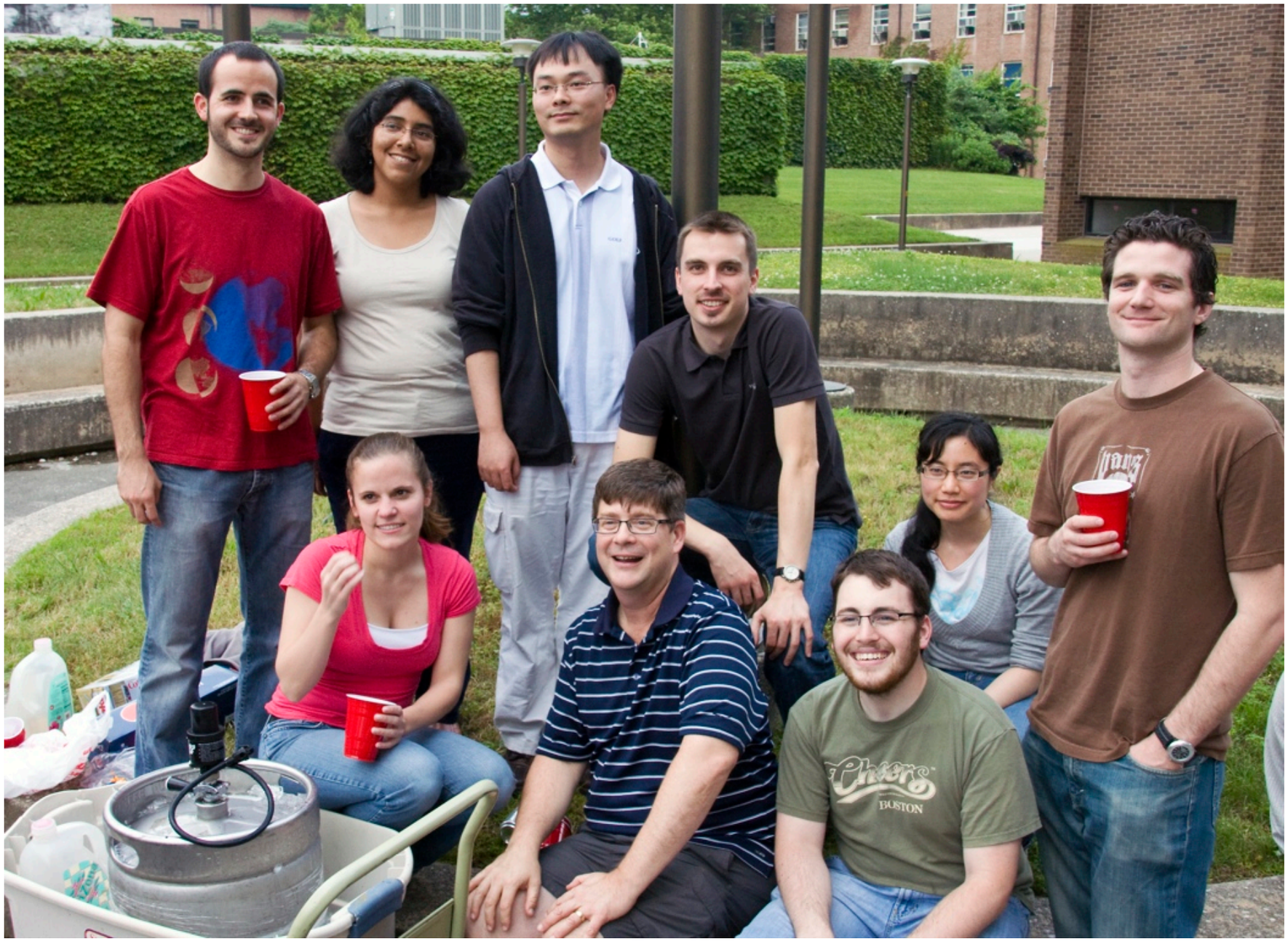

Summer at Stony Brook: groups take turns sponsoring the 4:30 pm Friday beer keg

Wilhelm Röntgen
Universität Würzburg
Dec. 1895

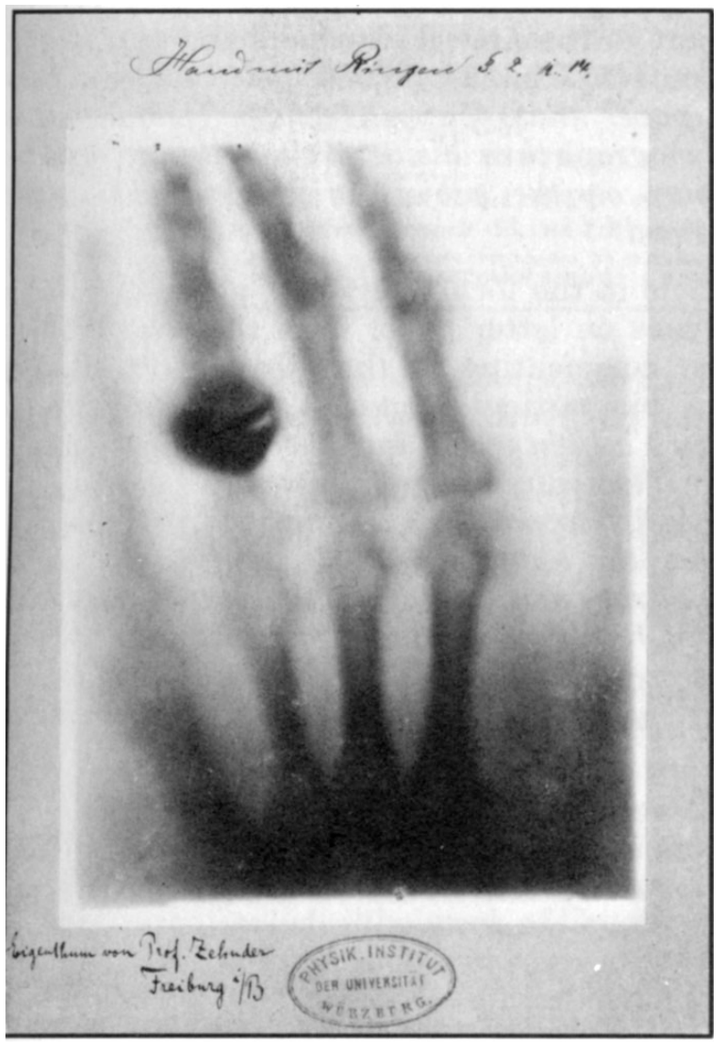

Michael Pupin
Columbia University/New York
Feb. 1896

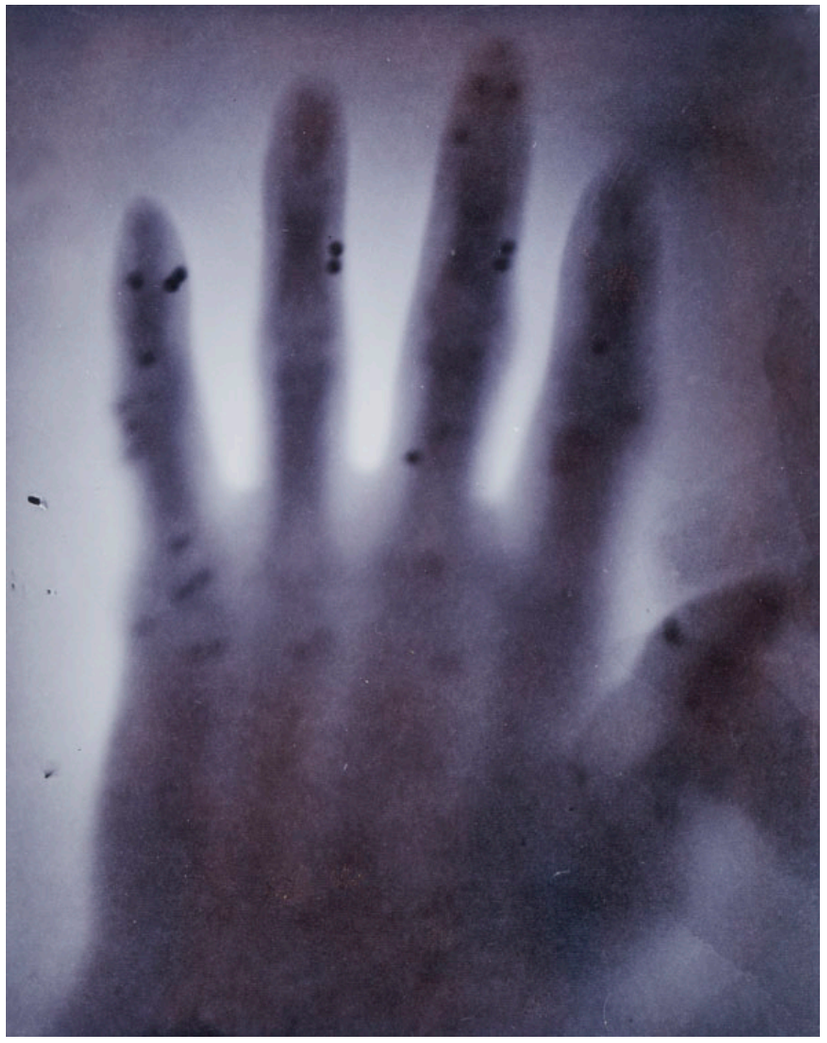

"This is of the hand of a gentleman resident in New York, who, while on a hunting trip in England a few months ago, was so unfortunate as to discharge his gun into his right hand, no less than forty shot lodging in the palm and fingers. The hand has since healed completely; but the shot remain in it, the doctors being unable to remove them, because unable to determine their exact location. The result is that the hand is almost useless, and often painful." - Cleveland Moffett, McClure's Magazine, April 1896

The X-ray Microscope

It would be a big improvement on microscopes using light or electrons, for X-rays combine short wavelengths, giving fine resolution, and penetration. The main problems standing in the way have now been solved.

SCIENTIFIC AMERICAN

Established 1845

Some further problems were solved after 1949...

Grazing incidence mirror optics: Kirkpatrick and Baez, 1949; Wolter 1952

Zone plate optics: Baez 1960; Schmahl and Rudolph 1969; Ceglio 1980

Synchrotron radiation: Horowitz and Howell 1972; Aoki *et al*., 1972; Niemann, Schmahl *et al*., 1976

Scanning: Horowitz and Howell 1972; Rarback, Kirz *et al*., 1980

Fluorescence: Horowitz and Howell 1972; Sparks 1980

Cryo: Schneider *et al*., 1995; Maser, Jacobsen *et al*., 1996

Tomography: Haddad *et al*., 1994; Schneider, Weiss *et al*. 1998

NEXAFS spectromicroscopy: Ade, Kirz *et al*., 1992

Historical comments

- Following Röntgen: use visible light microscopes to examine detail of x-ray micrographs on film.
- 1940's & 1950's: reflective optics (Kirkpatrick & Baez; Wolter)
- 1960's: point source projection (Cosslett, Nixon and others)
- "modern" era with zone plates:
  - UV holography for fabrication, full-field imaging using synchrotron: Schmahl et al., Göttingen [Optik **29**, 577--585 (1969); Applied Optics **15**, 1883--1884 (1976)]
  - Electron beam lithography for zone plate fabrication: proposed by Sayre [IBM technical report RC 3974 (#17965), 1972], and first implemented by Ceglio *et al.*, *J. Vac. Sci. Tech. B* **1**, 1285 (1983) and Kern *et al.*, *SPIE* **447**, 204 (1984).
  - Scanning microscopy with zone plates: Kirz et al., Stony Brook [Scanned Image Microscopy, E.A. Ash, Editor. 1980: London. p. 449]

X rays

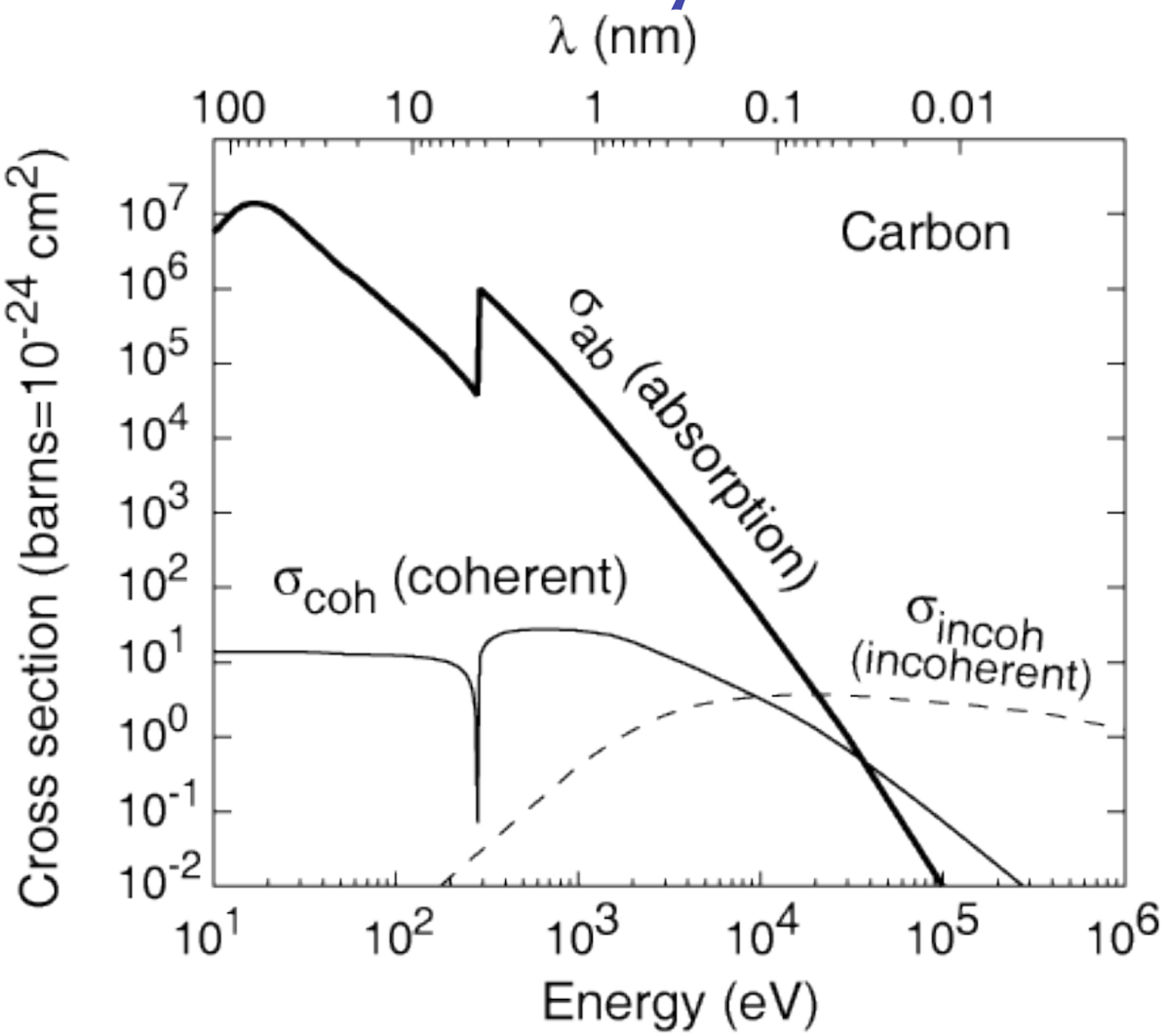

- Absorption dominates
- Inelastic scattering is weak
- No multiple scattering

Electrons

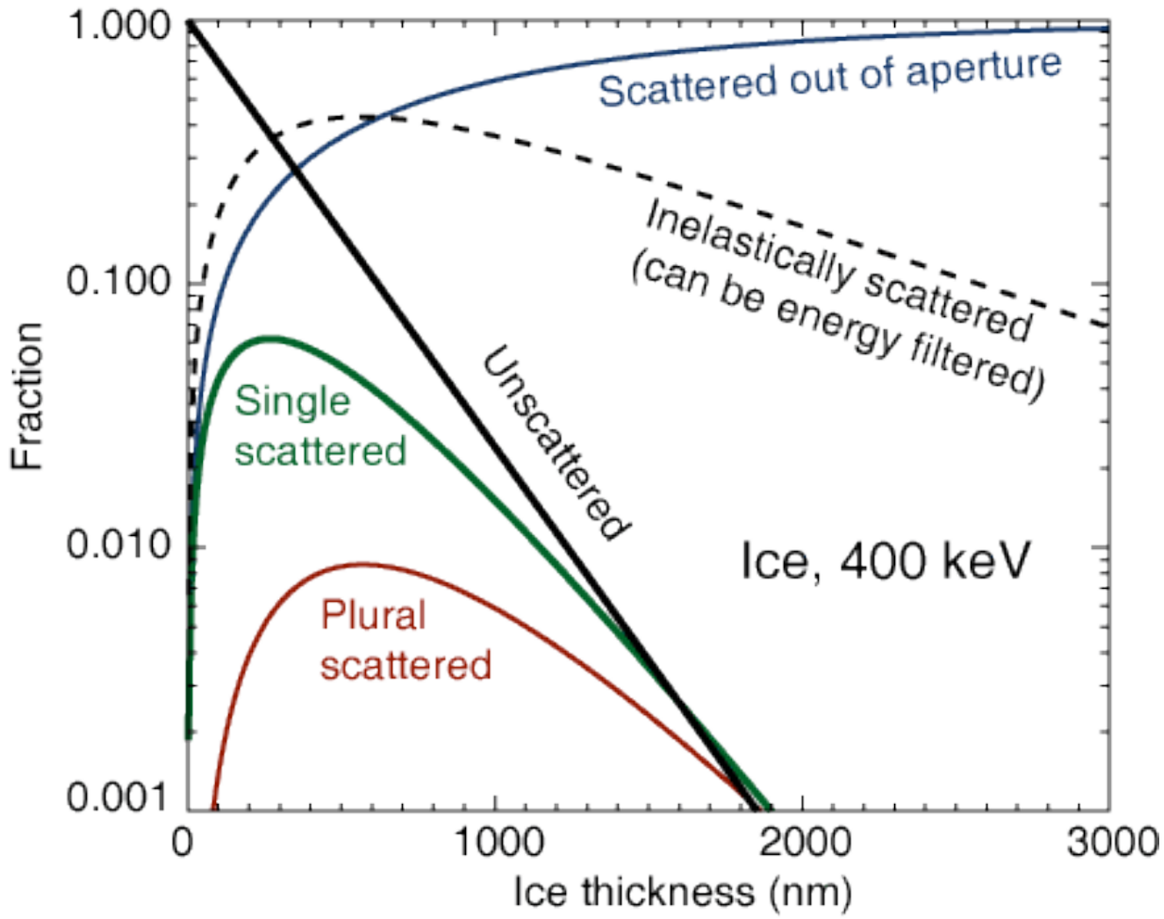

- Inelastic scattering dominates (energy filters)
- Multiple scattering often present
- High contrast from small things

The refractive index

- Damped, driven harmonic oscillator

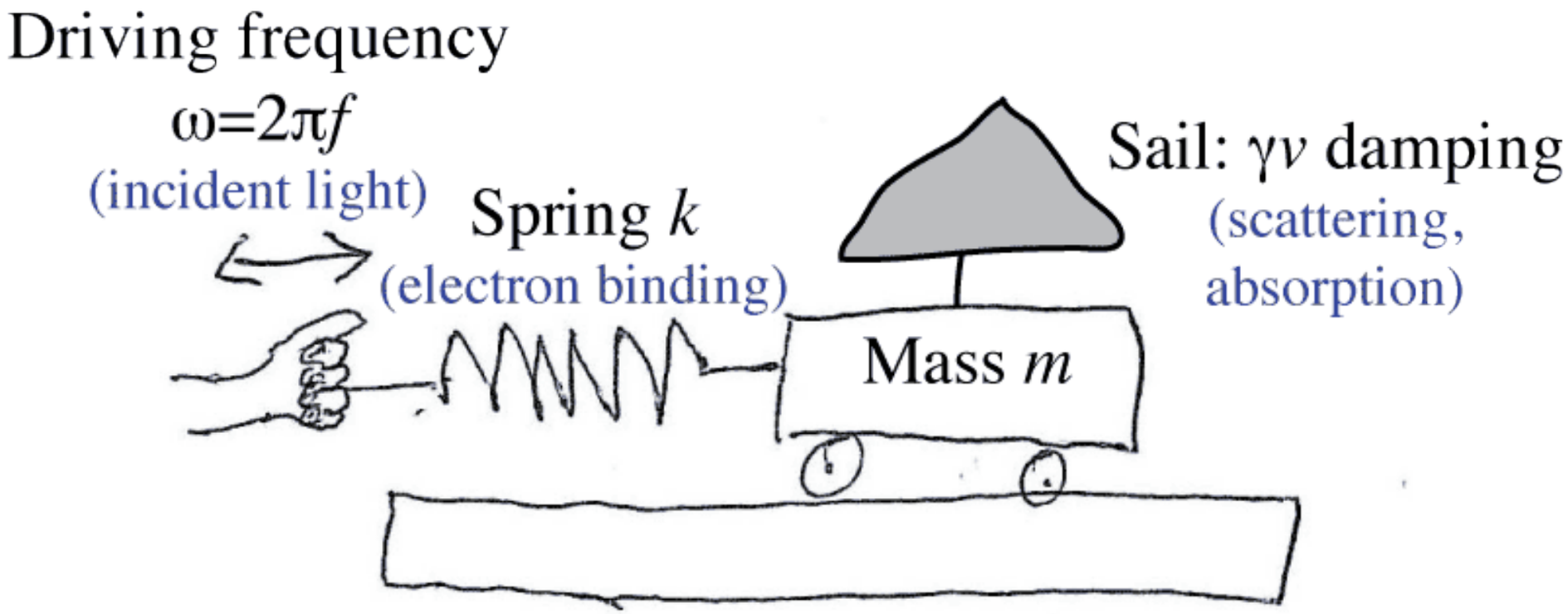

- Damping: scattering, absorption
- Driving: incident electromagnetic wave ω
- Harmonic oscillator: electron quantum state with energy $\hbar\omega_0 = \hbar\sqrt{k/m}$

Damped, driven harmonic oscillator

- Single resonance: absorption peak, phase shift across resonance

$$Q = \omega_0/\gamma$$

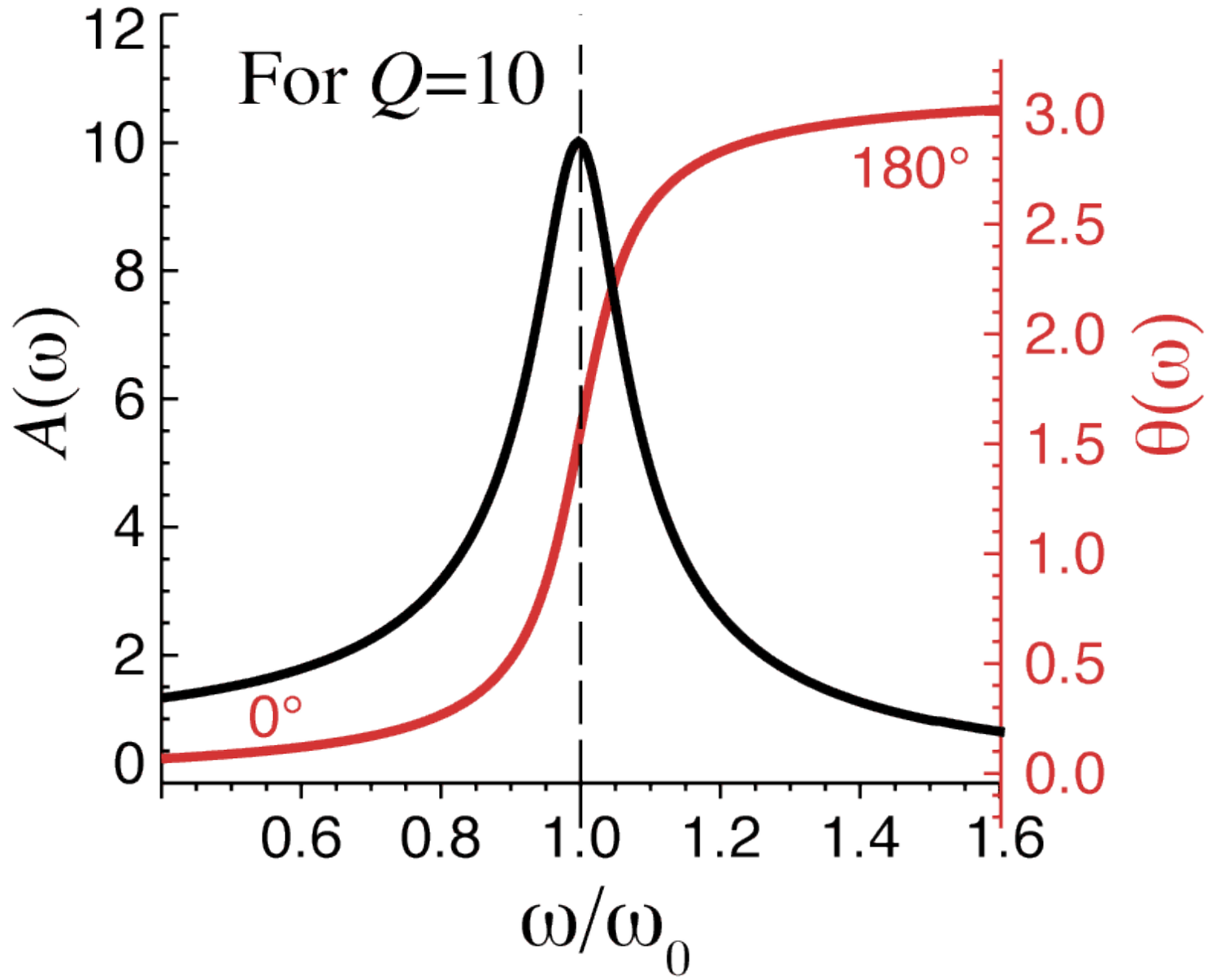

The preponderance of plasmons

Dividing line between low and high frequency limits of refractive index

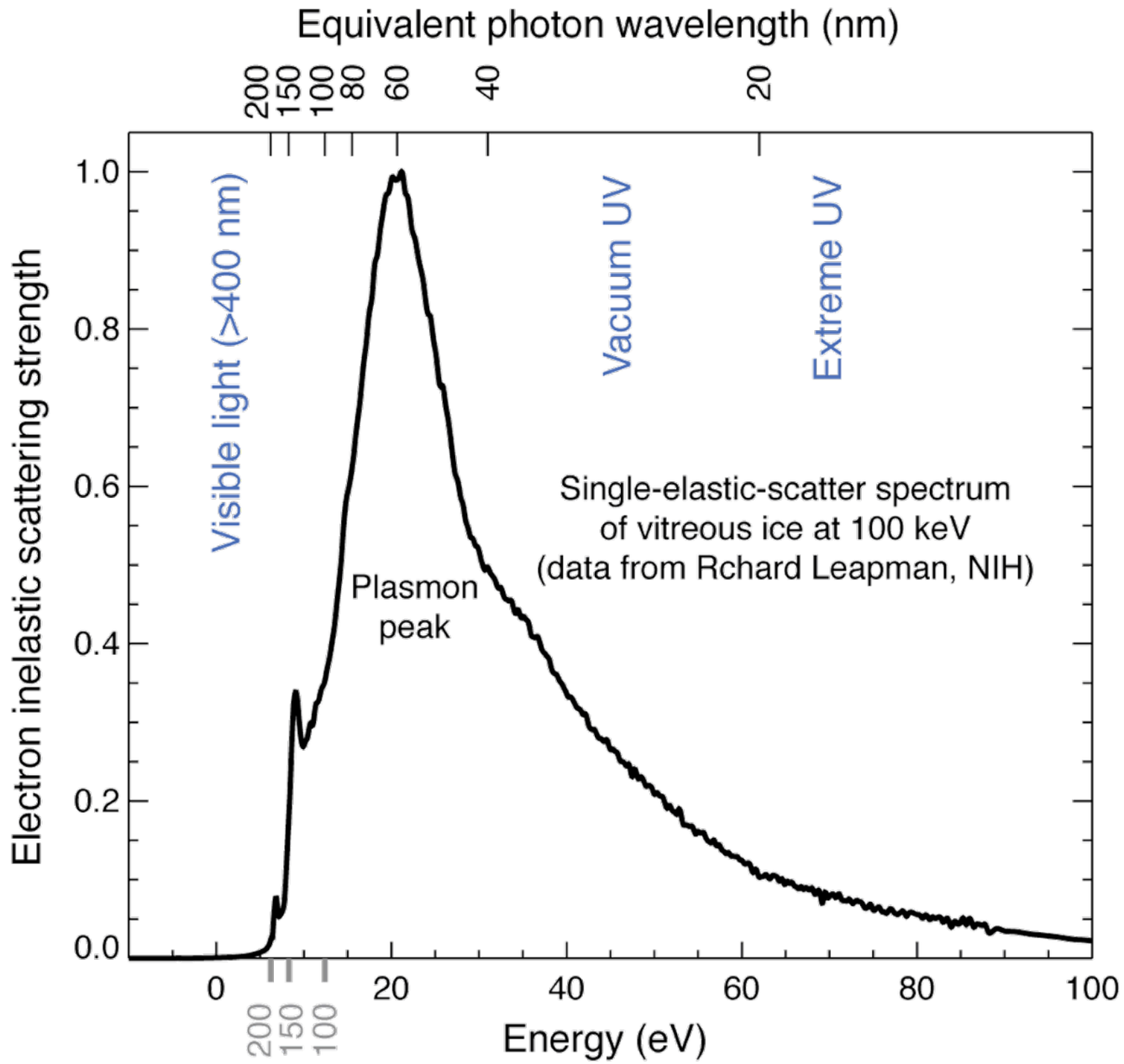

Dispersion in glasses

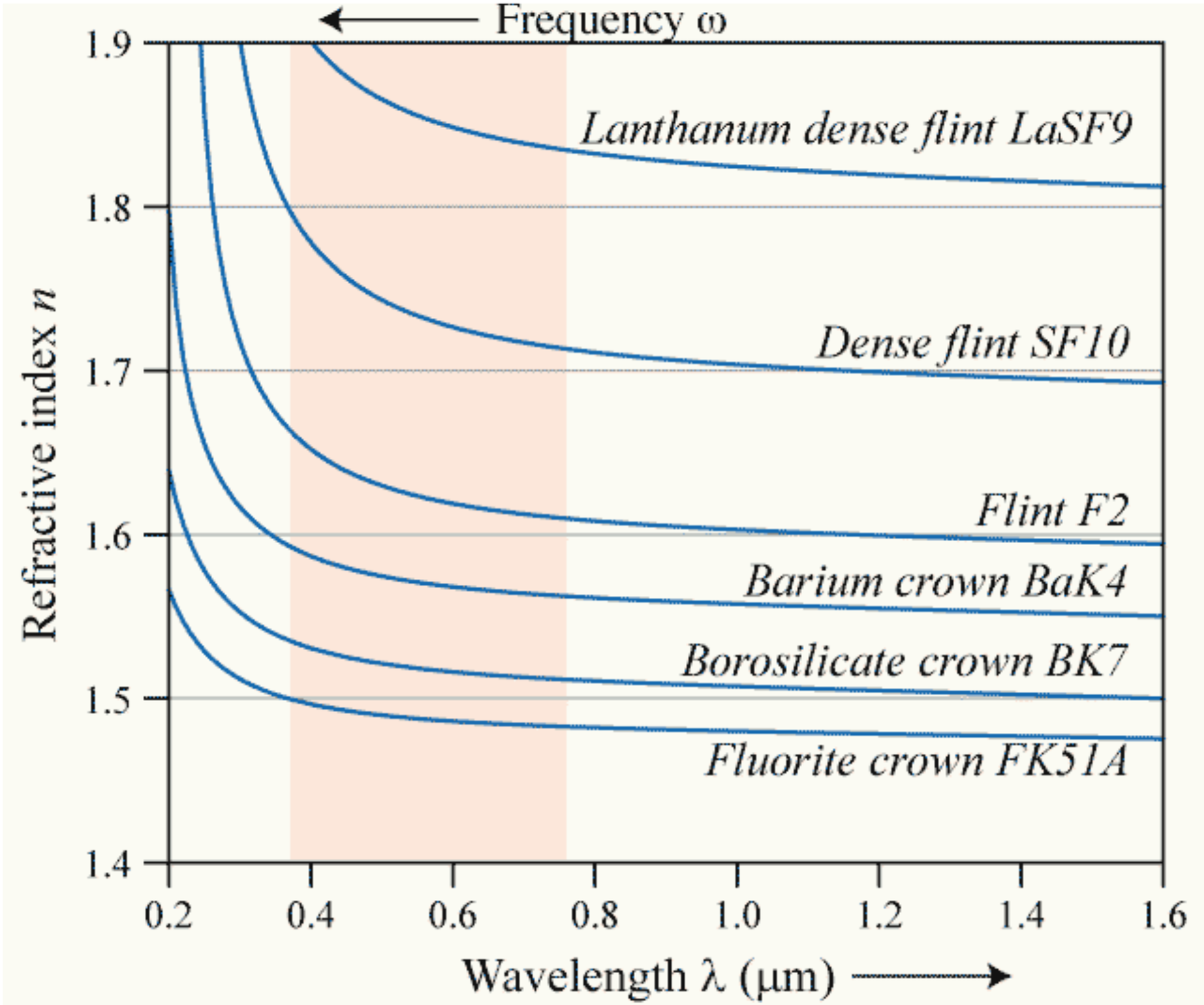

Mysteries of the refractive index

Write refractive index as

$$n = 1 - \frac{n_a r_e}{2\pi}\lambda^2\left(f_1 + if_2\right) = 1 - \alpha\lambda^2\left(f_1 + if_2\right)$$

Phase velocity is faster than light in vacuum!

$$v_p = \frac{w}{k} \approx c\left(1 + \alpha\, f_1\lambda^2\right)$$

Prisms refract x rays the opposite way from visible light!
Phase is advanced rather than retarded! Total external reflection with critical angle

$$\theta_c \approx \sqrt{2\alpha\,\lambda^2 f_1}$$

But group velocity is OK:

$$v_g = \frac{dw}{dk} \approx c\left(1 - \alpha\, f_1\lambda^2\right)$$

Lassen sich Brechungsexponenten der Körper für Röntgenstrahlen experimentell ermitteln?

Von A. Einstein.

(Eingegangen am 21. März 1918.)

Vor einigen Tagen erhielt ich von Herrn Prof. A. KÖHLER (Wiesbaden) eine kurze Arbeit [1]), in welcher eine auffallende Erscheinung bei Röntgenaufnahmen geschildert ist, die sich bisher nicht hat deuten lassen. Die reproduzierten Aufnahmen — zu meist menschliche Gliedmaßen darstellend — zeigen an der Kontur einen hellen Saum von etwa 1 mm Breite, in welchem die Platte heller bestrahlt zu sein scheint als in der (nicht beschatteten) Umgebung des Röntgenbildes.

Ich möchte die Fachgenossen auf diese Erscheinung hinweisen und beifügen, daß die Erscheinung wahrscheinlich auf Totalreflexion beruht. Nach der klassischen Dispersionstheorie müssen wir erwarten, daß der Brechungsexponent n für Röntgenstrahlen nahe an 1 liegt, aber im allgemeinen doch von 1 verschieden ist. n wird kleiner bzw. größer als 1 sein, je nachdem der Einfluß derjenigen Elektronen auf die Dispersion überwiegt, deren Eigenfrequenz kleiner oder größer ist als die Frequenz der Röntgenstrahlen. Die Schwierigkeit einer Bestimmung von n liegt darin, daß $(n-1)$ sehr klein ist (etwa 10^{-6}). Es ist aber leicht einzusehen, daß bei nahezu streifender Inzidenz der Röntgenstrahlen im Falle $n < 1$ eine nachweisbare Totalreflexion auftreten muß.

X-ray refractive index

Refractive index: based on a damped, driven harmonic oscillator model in the limit of high frequency and low damping:

$$n = 1 - \frac{n_a r_e}{2\pi}\lambda^2\left(f_1 + if_2\right)$$

where n_a gives atoms/volume, r_e=2.82×10^{-15} m is the classical radius of the electron, and (f_1+if_2) specify the atom's oscillator strength at a given photon energy

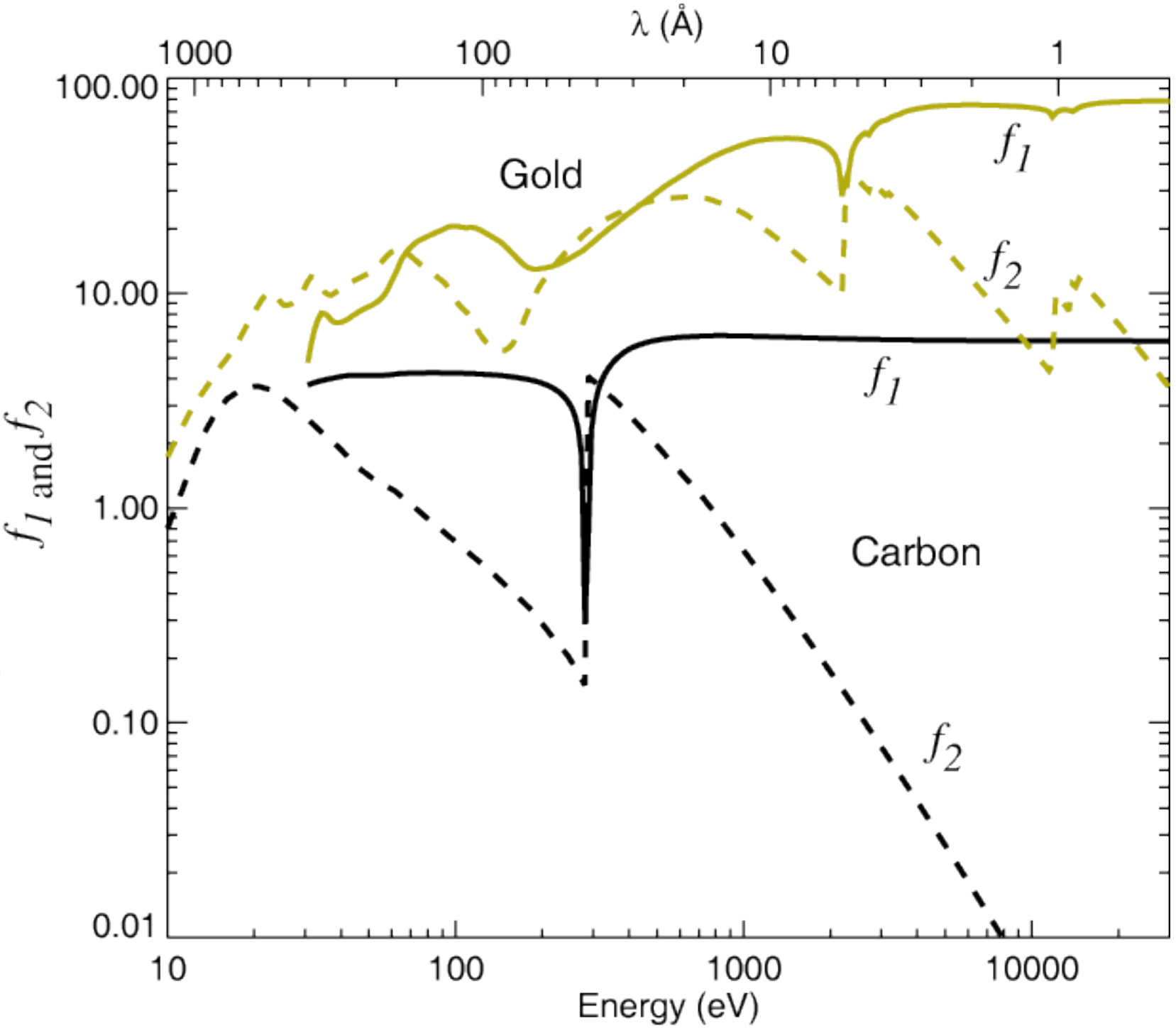

Phase velocity greater than group velocity

X rays in media

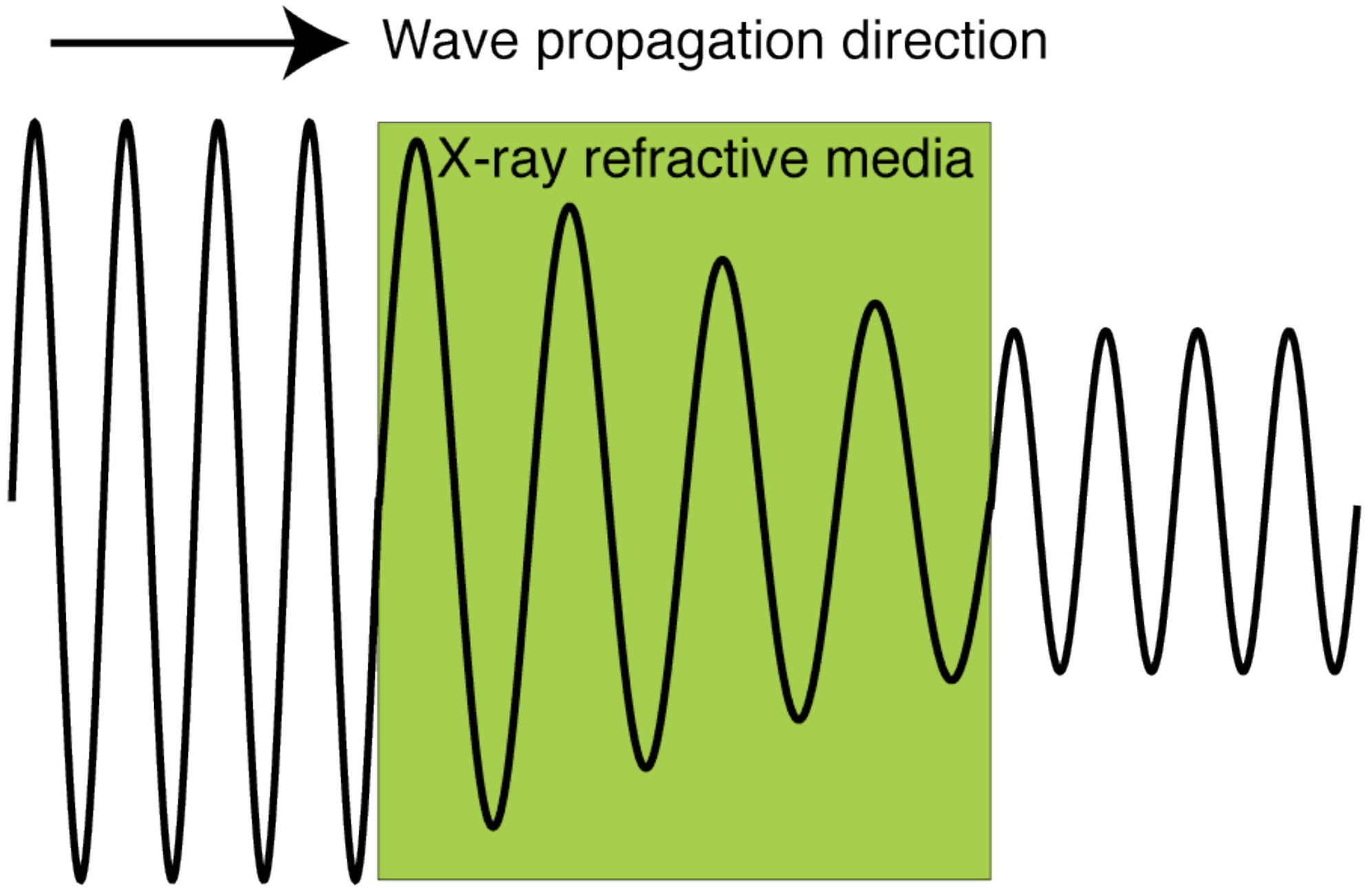

Electron interactions

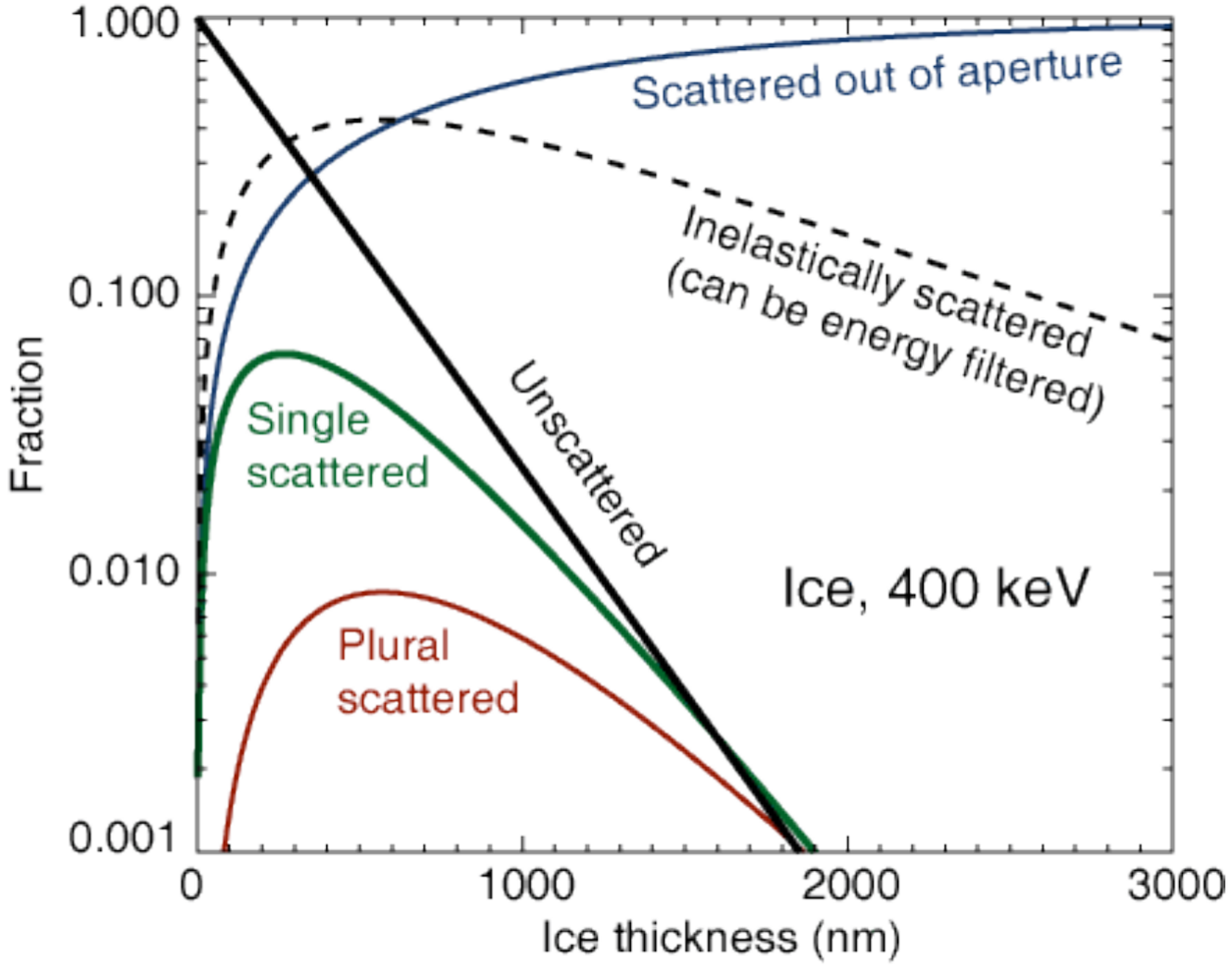

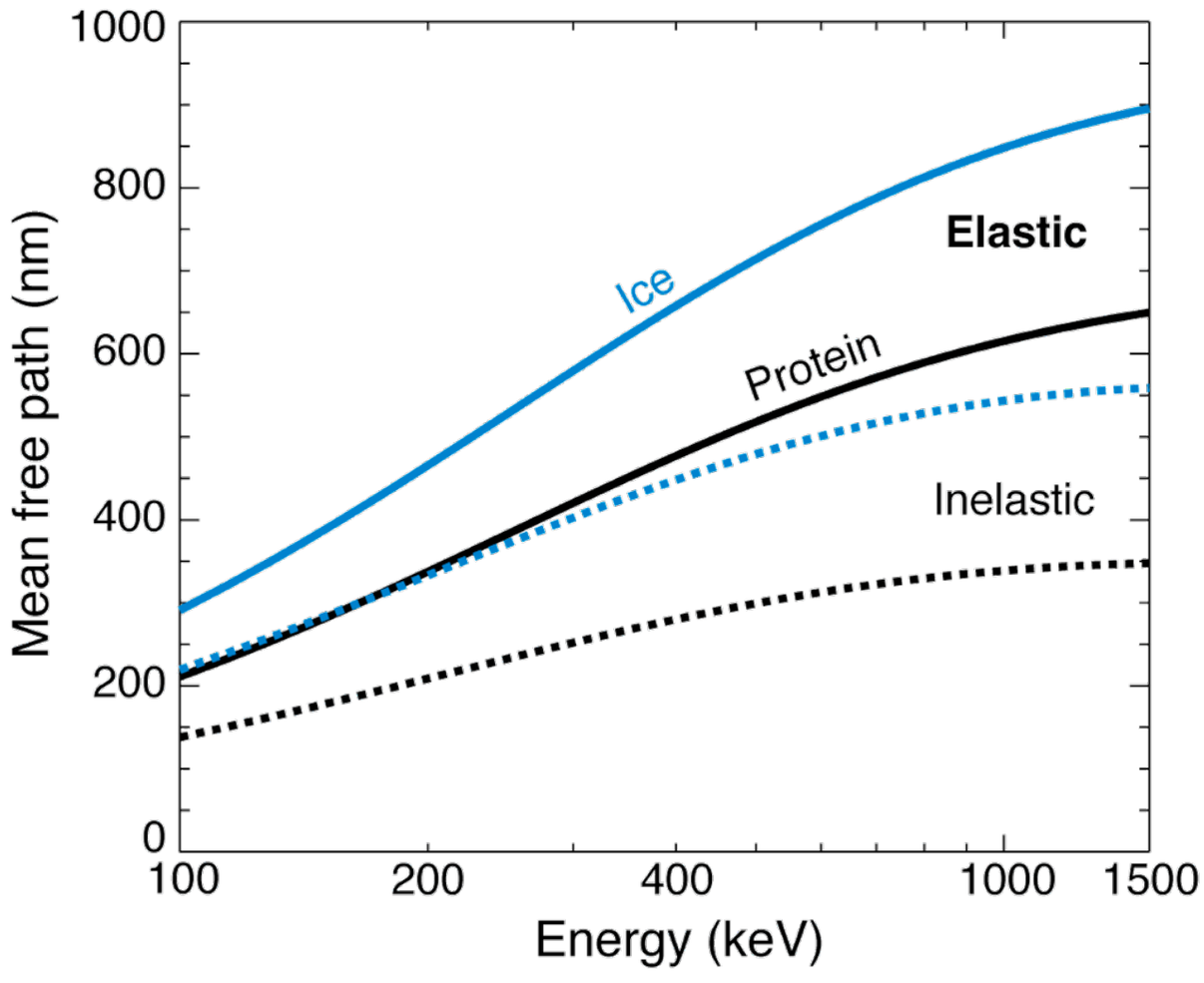

These plots: Jacobsen, Medenwaldt, and Williams, in **X-ray Microscopy & Spectromicroscopy** (Springer, 1998)

X rays and electrons

Consider penetration distance: 1/*e* absorption length for x rays, scattering mean free paths for electrons

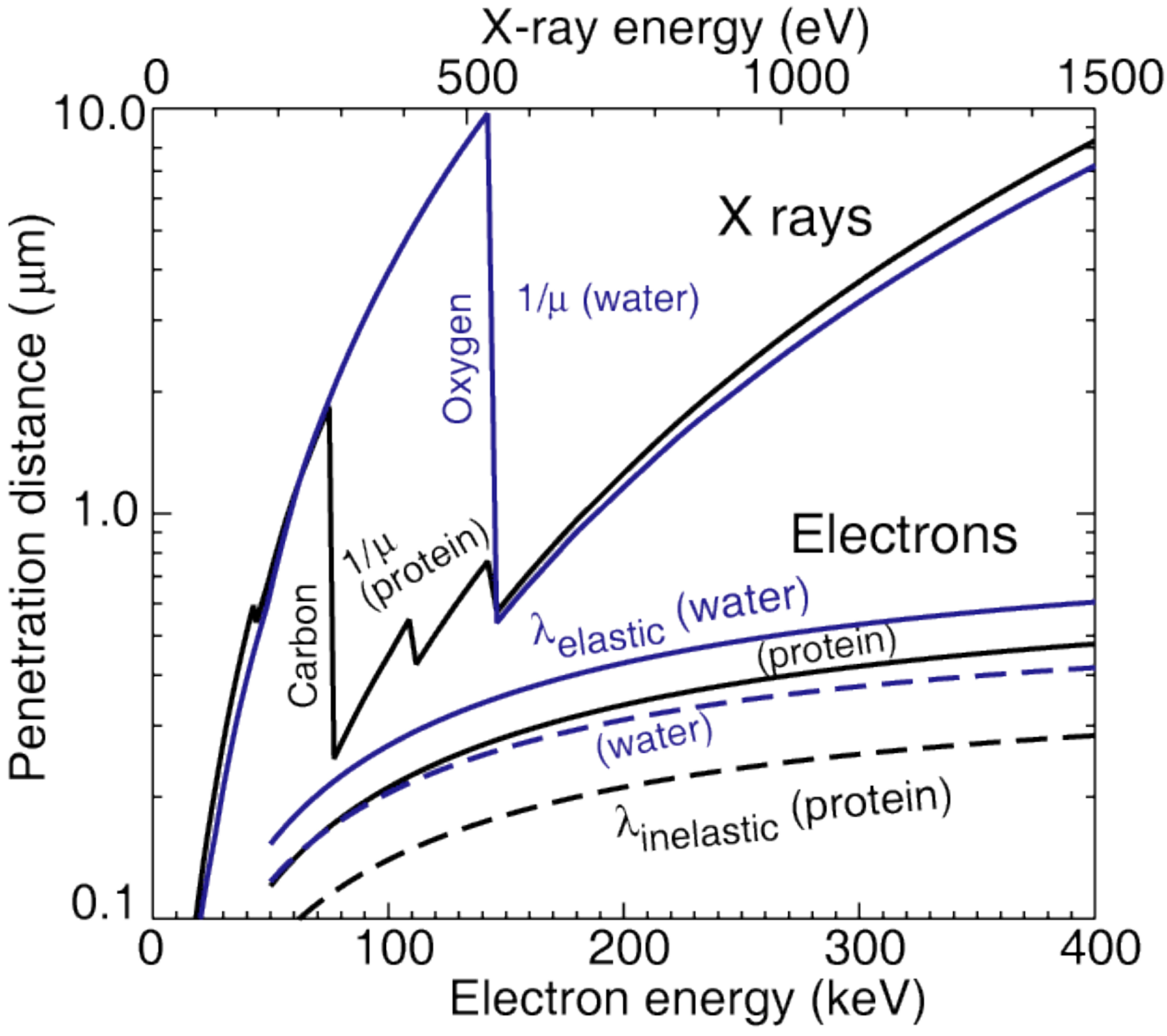

Electrons: inelastic energy deposition

Inelastic scattering: energy transfer of 35-45 eV

At 100 keV, 1 $e^-/nm^2 \Rightarrow 3.2x10^4$ Gray

(1 Gray=1 J/kg)

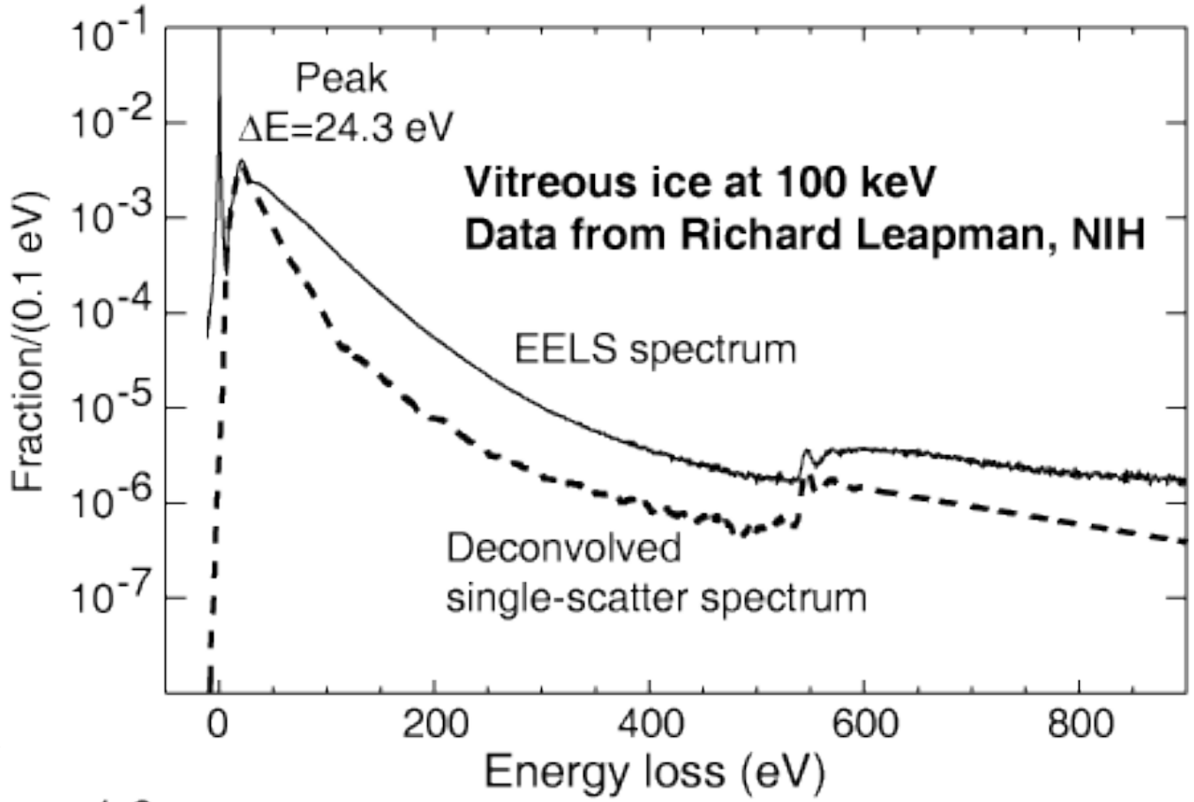

X rays are better than electrons for thick specimens

- λ=100-10 nm: minimum penetration in entire electromagnetic spectrum.
- No more than 1 high-resolution image of wet, soft samples unless frozen.
- At energies >3 keV, opportunities for thick specimens.

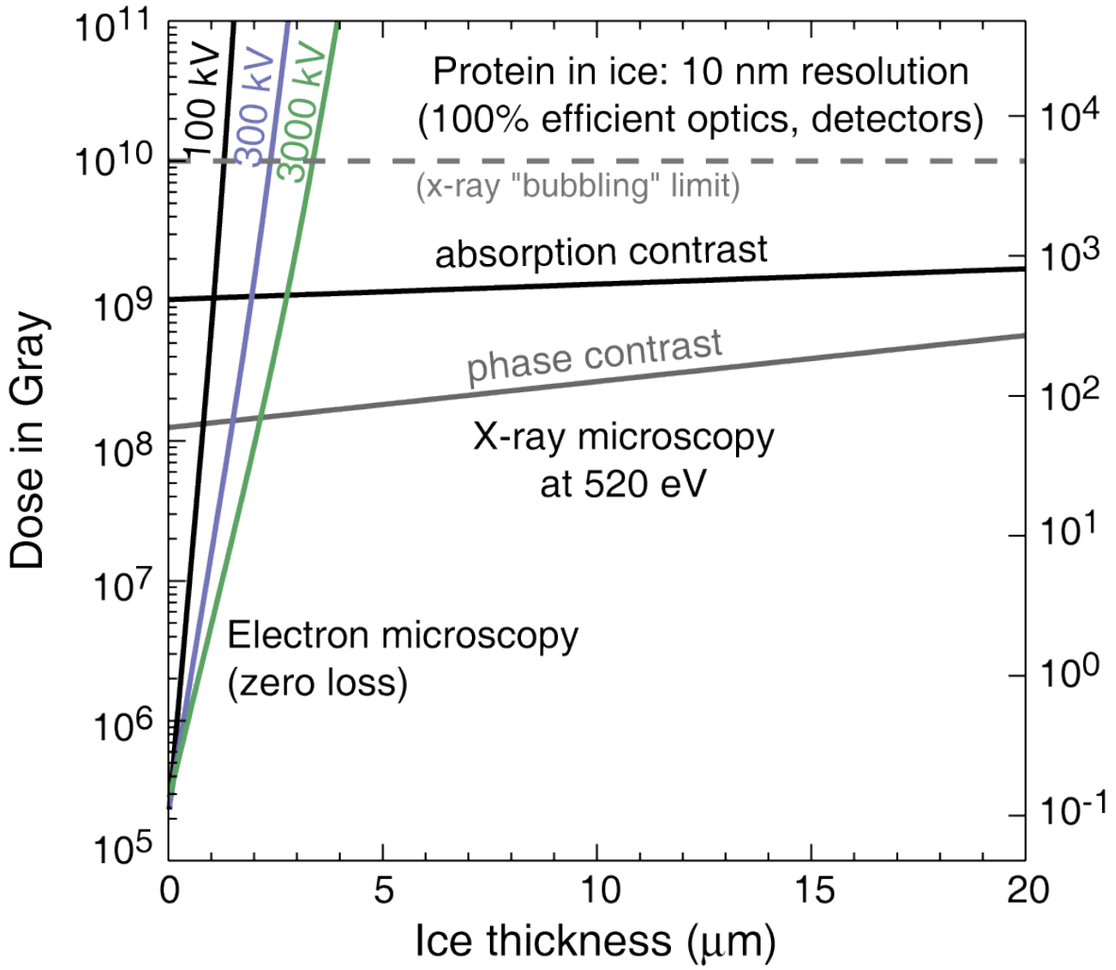

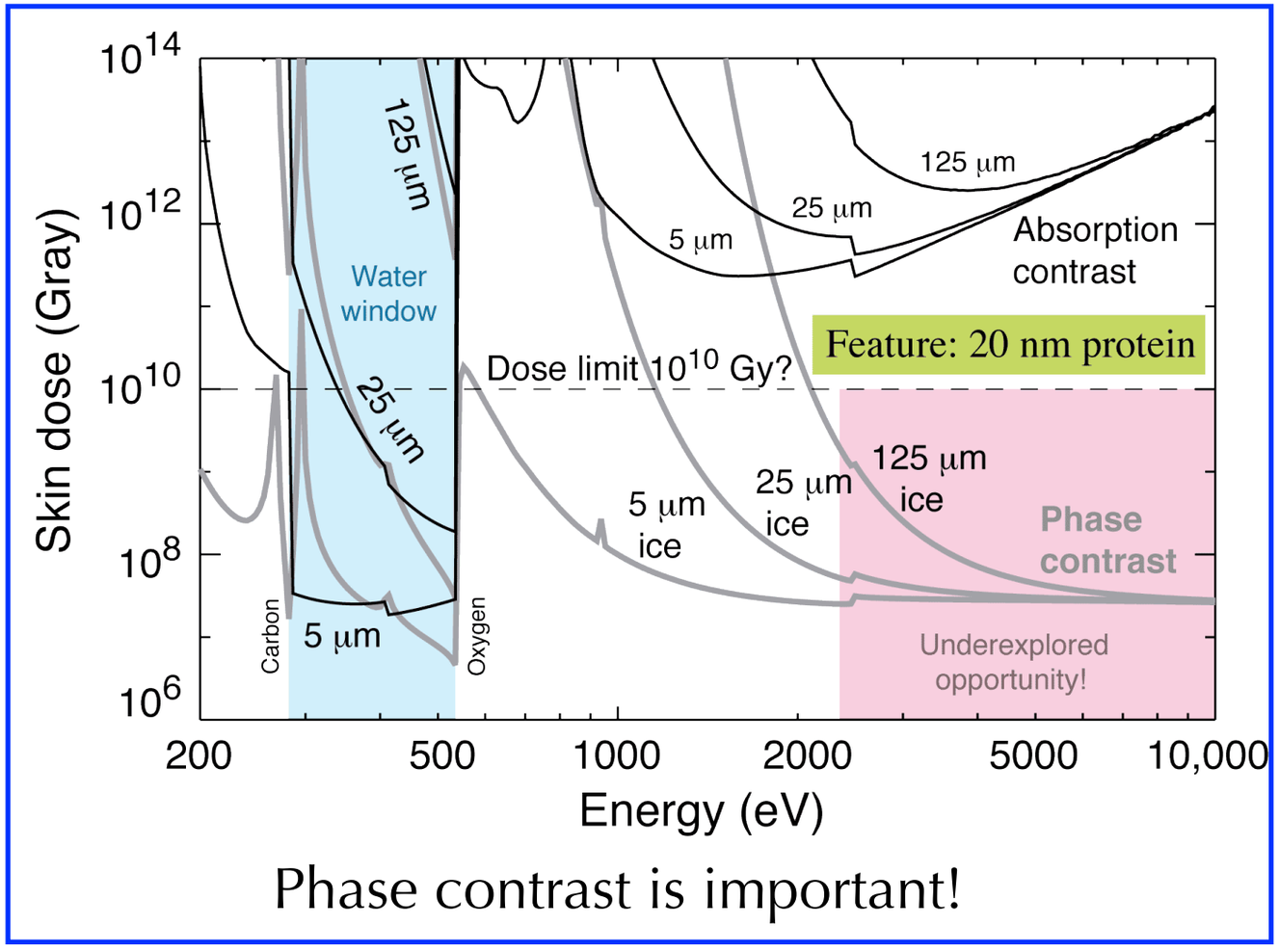

Phase contrast is important!

These plots: based on Jacobsen, Medenwaldt, and Williams, in **X-ray Microscopy & Spectromicroscopy** (Springer, 1998). See also Sayre *et al.*, *Science* **196**, 1339 (1977).

Detecting trace elements

- Differential absorption is great for soft x-ray spectromicroscopy, but at >1% concentration.
- X-ray fluorescence: **~1000x better sensitivity** than electrons for trace elemental mapping (ion concentrations etc.). Parts per billion!

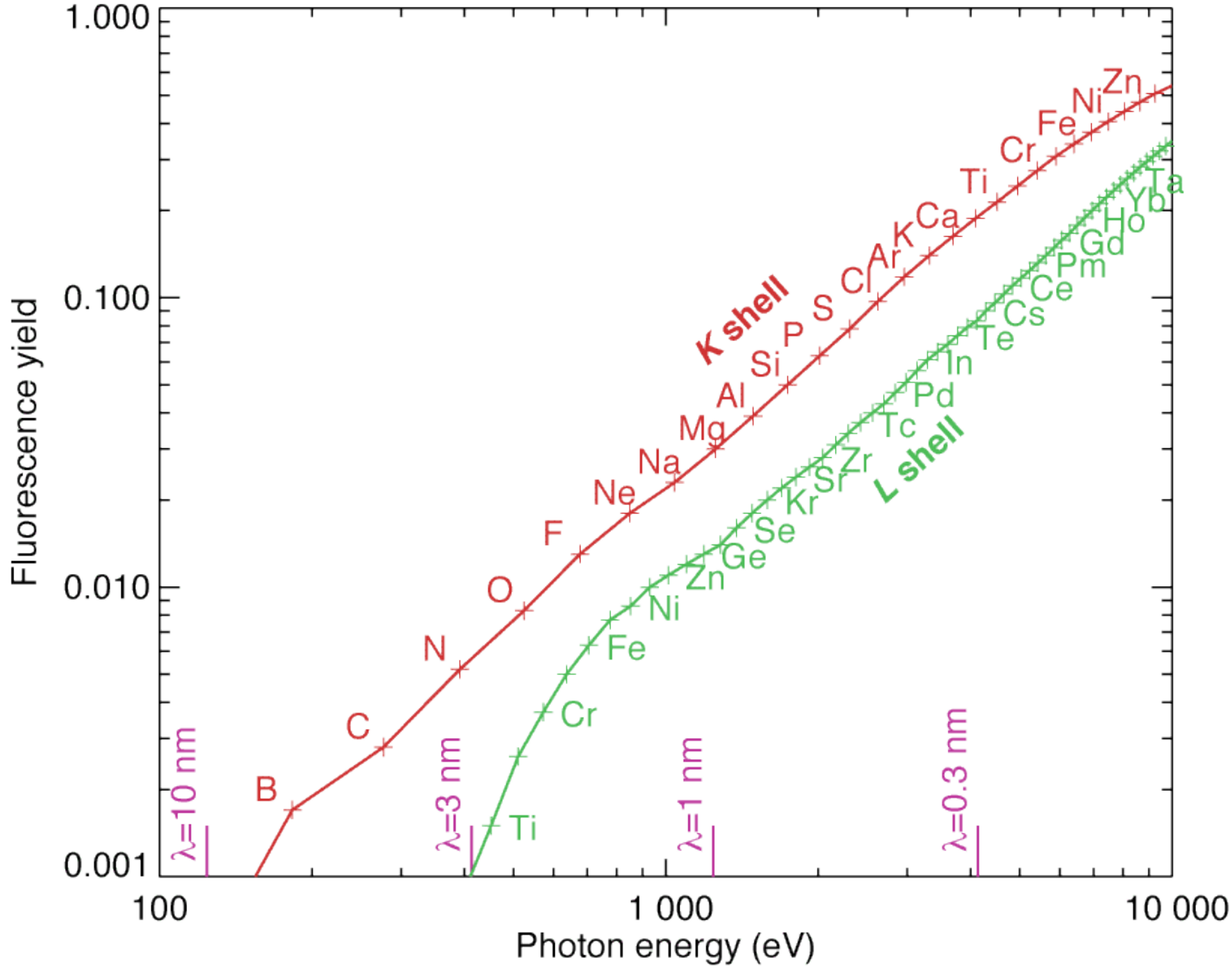

Fluorescence: trace element concentrations

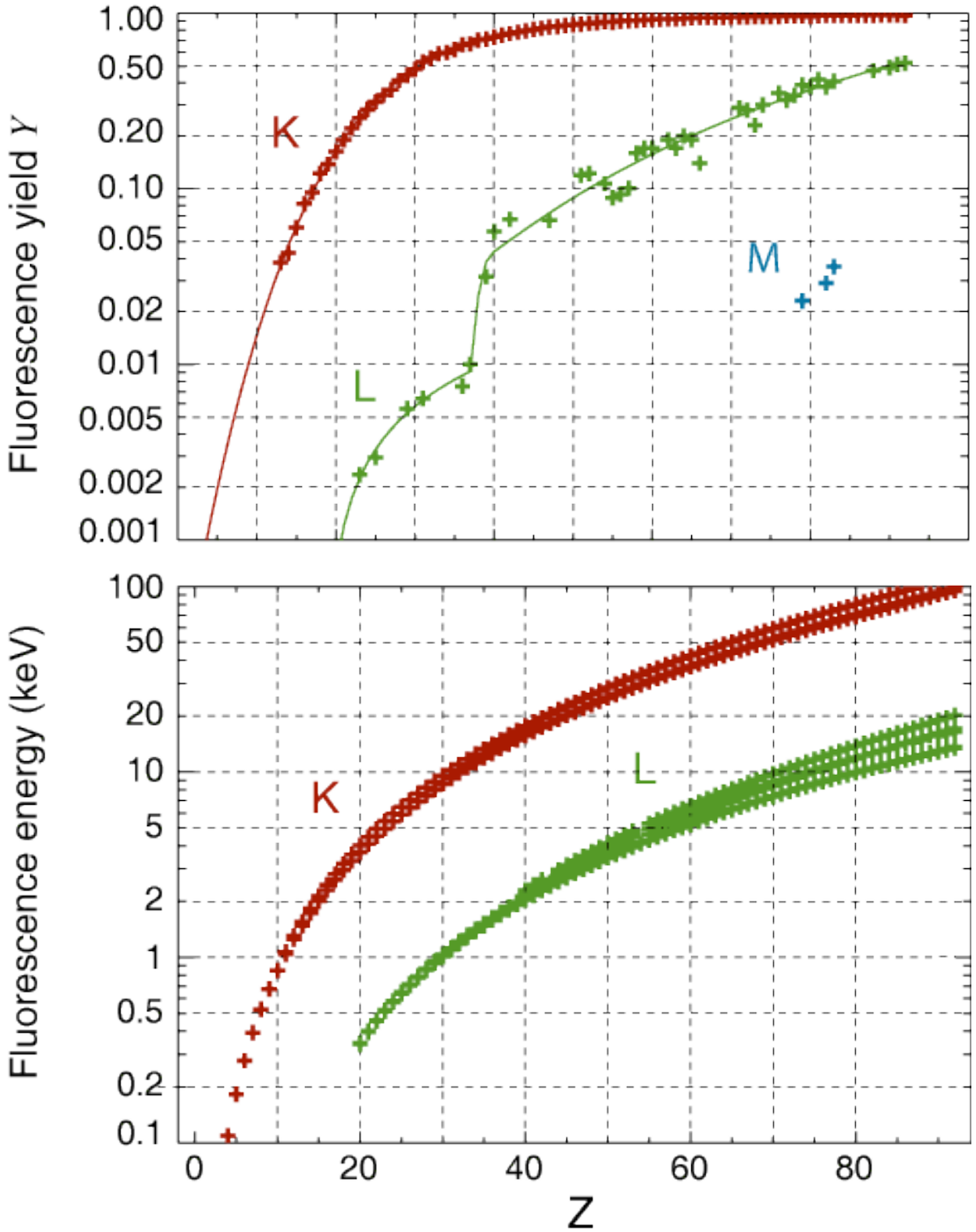

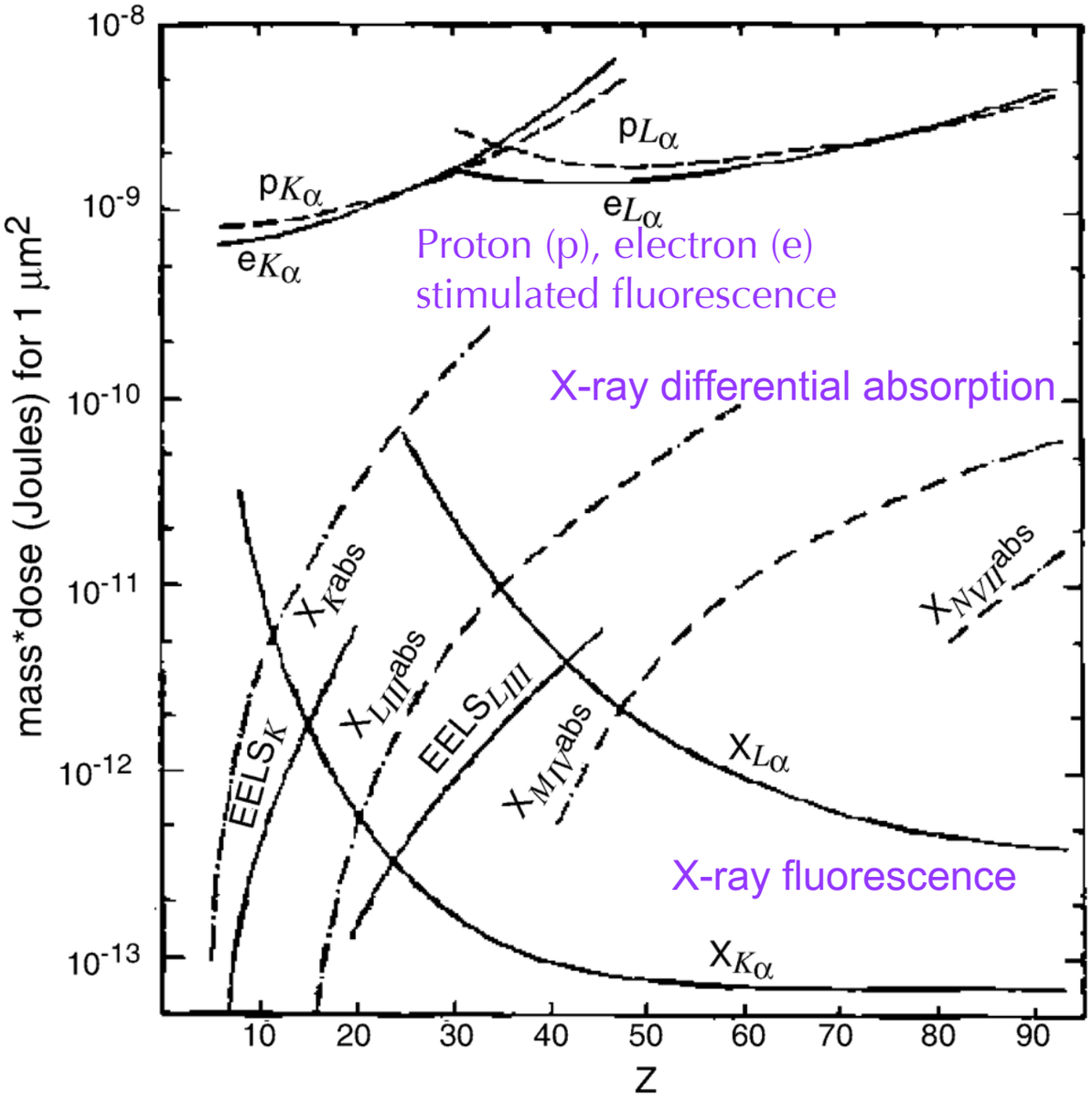

J. Kirz, in *Scanning Electron Microscopy* **2**, 1980, p. 239. EELS=electron energy loss spectroscopy. Hard-to-find reprint: http://tinyurl.com/2eu7q4

Total internal reflection

- Snell's law: $n_1 \sin\theta_1 = n_2 \sin\theta_2$
- When $\theta_1 = 90°$, we have $\sin\theta_2 = n_1/n_2$

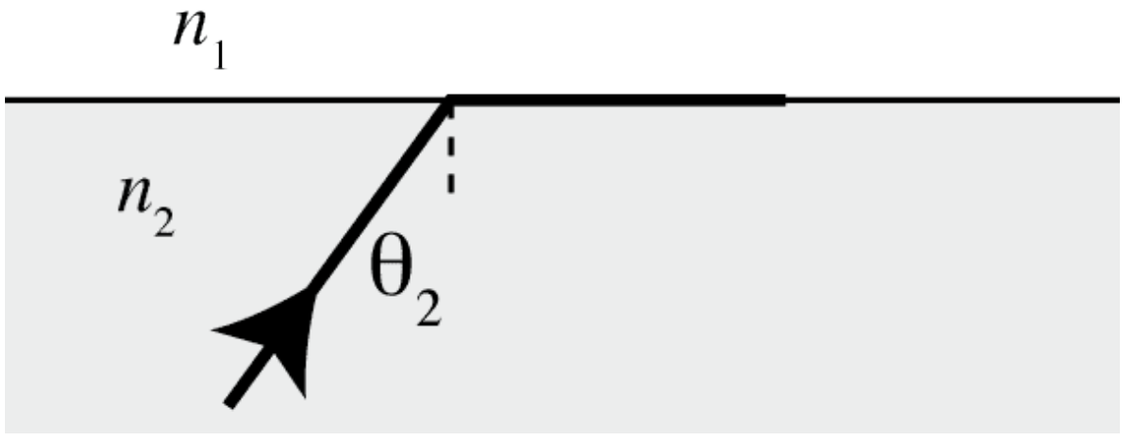

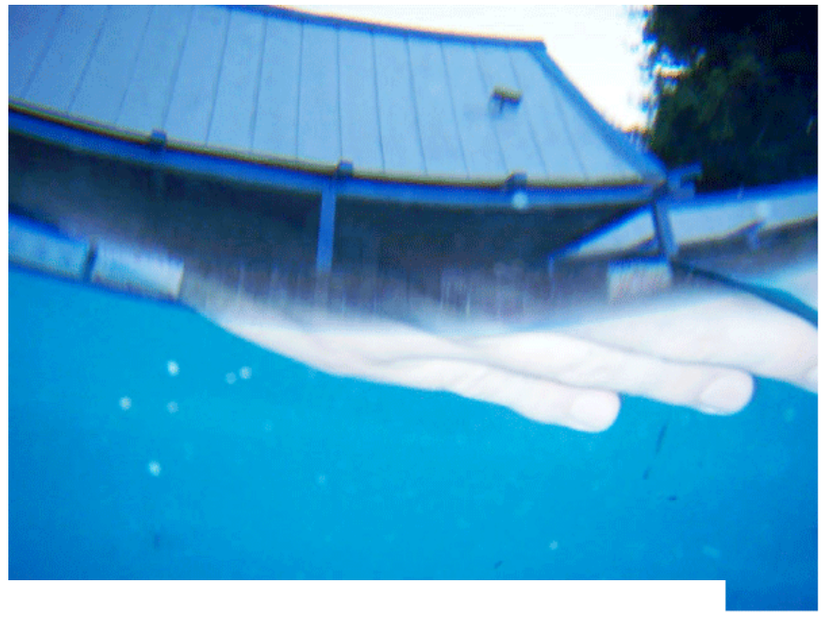

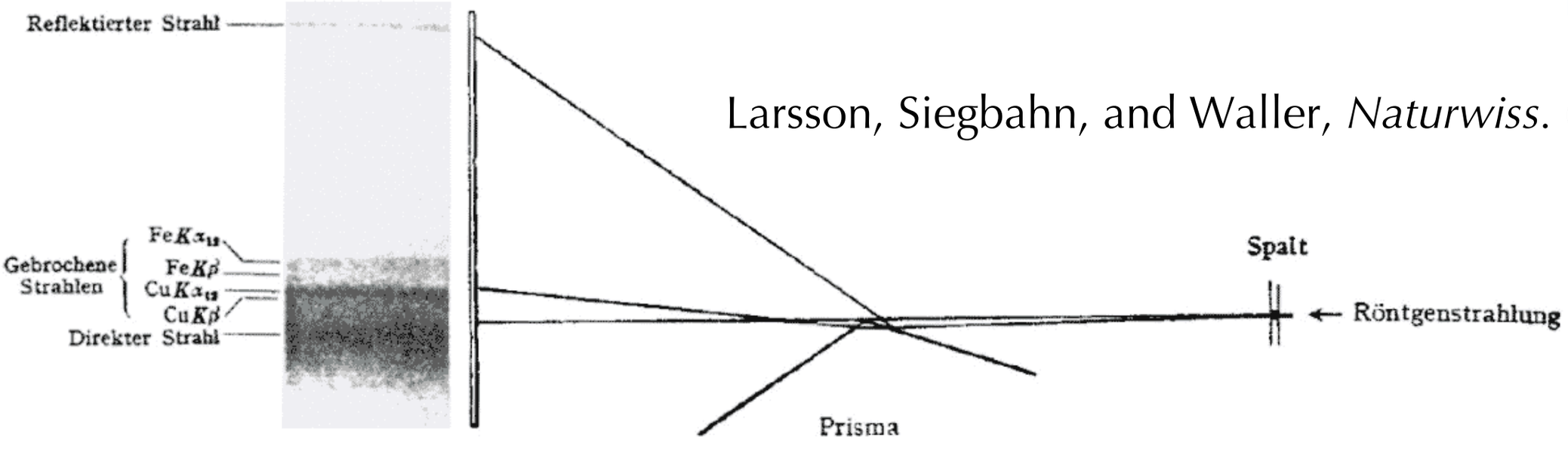

Larsson, Siegbahn, and Waller, *Naturwiss.* (1924)

Reflective x-ray optics

- Grazing incidence critical angle for mirror reflection:

$$\cos\theta_C = 1 - \alpha\lambda^2 f_1 \quad \text{or} \quad \theta_C \approx \lambda\sqrt{2\alpha f_1}$$

- Use two orthogonal cylinders for 2D focusing: Kirkpatrick and Baez, *J. Opt. Soc. Am.* **38**, 766 (1948)

Mimura, Yamauchi *et al.*, *Appl. Phys. Lett.* **90**, 051903 (2007): 25 nm using elastic emission machining.

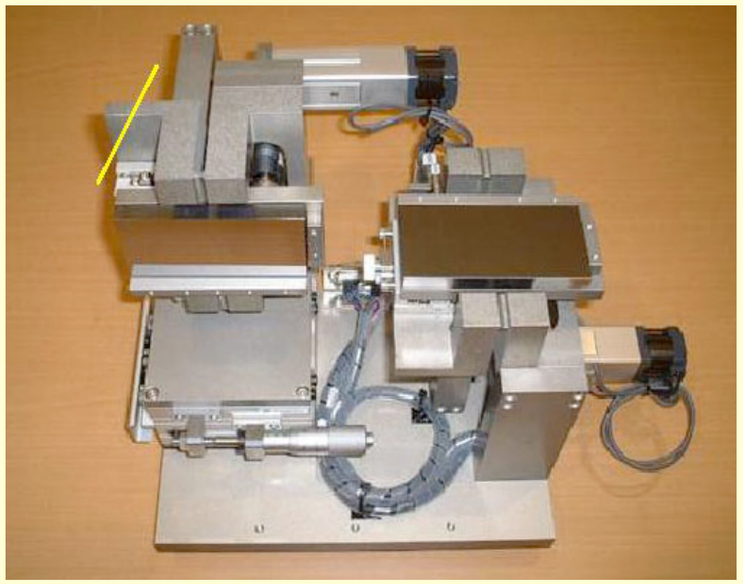

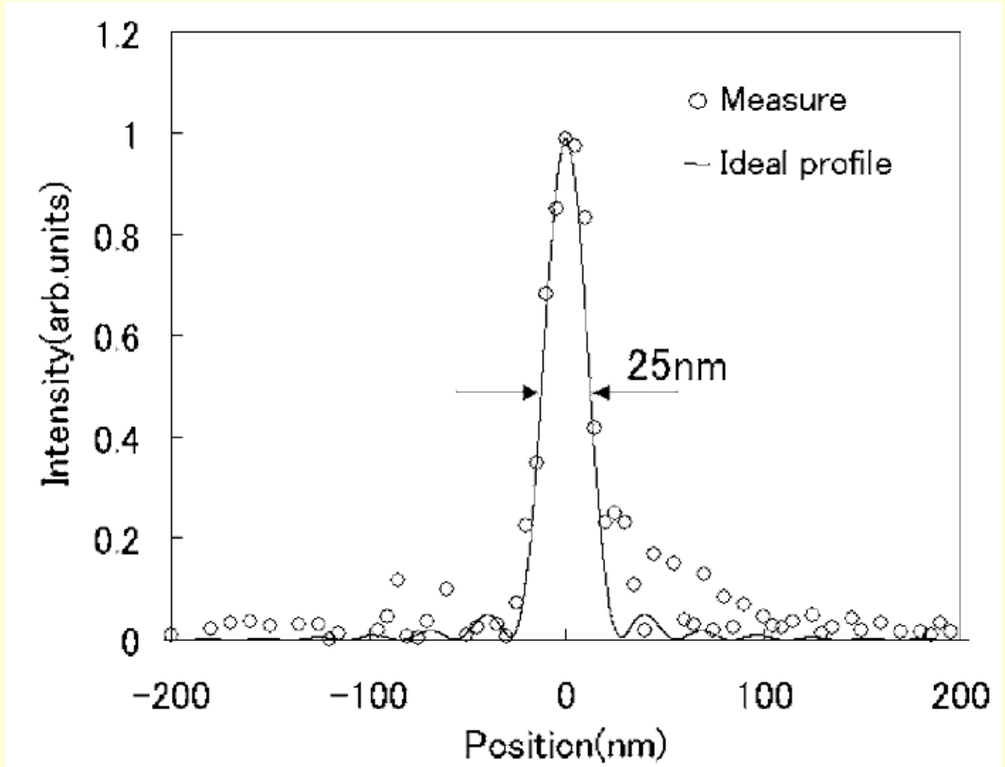

Synthetic multilayer mirrors: work well at approx. $\lambda \geq 10$ nm

Compound refractive lenses

- Röntgen tried to make lenses, but found no focusing.
- Focal length of one lens is long – so combine many lenses! Tomie; Snigirev *et al.*, *Nature* **384**, 49 (1996); Lengeler *et al.*, *J. Synch. Rad.* **9**, 119 (2002).
- Resolution approaching 100 nm at 5-10 keV with parabolic beryllium lenses

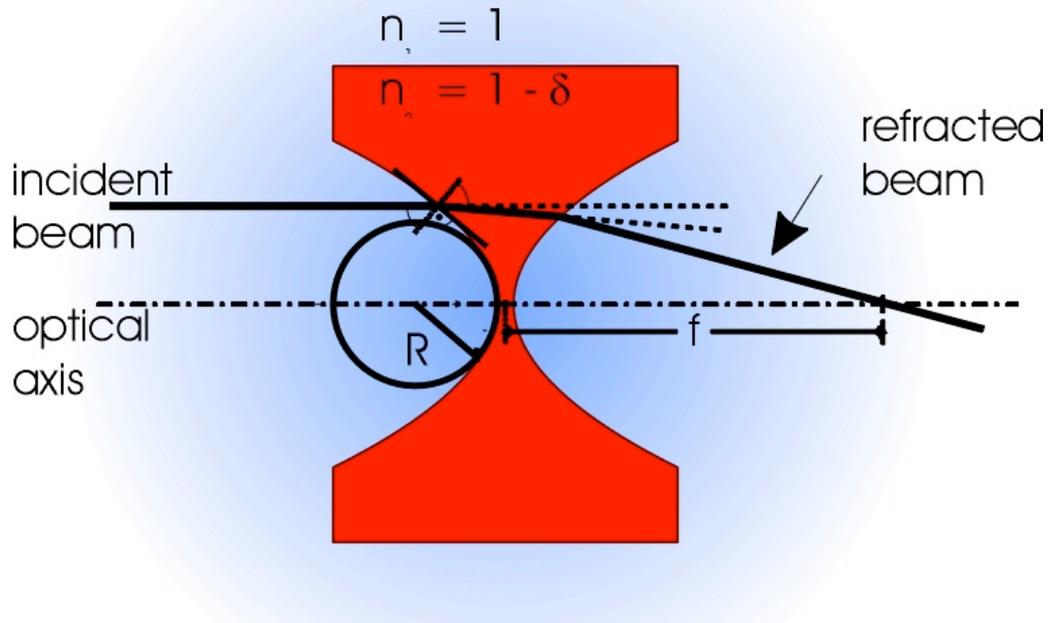

Compound refractive lenses at Universität Aachen

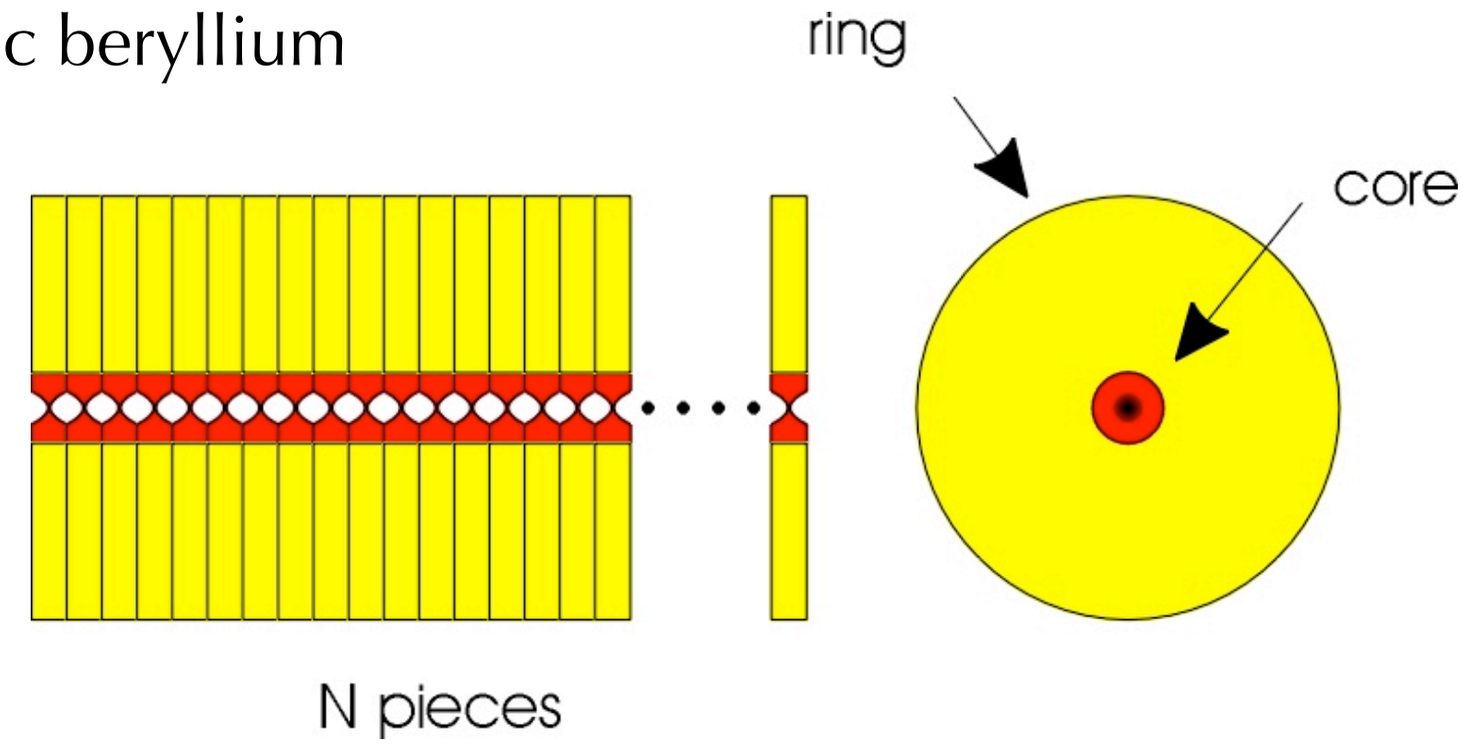

X-ray focusing: Fresnel zone plates

- Diffractive optics: radially varied grating spacing
- Largest diffraction angle is given by outermost (finest) zone width dr_N as $\theta=\lambda/(2dr_N)$
- Rayleigh resolution is $0.61\,\lambda/(\theta)=1.22dr_N$
- Zones must be positioned to ~1/3 width over diameter (10 nm in 100 μm, or $1{:}10^4$)

Diameter d, outermost zone width dr_N, focal length f, wavelength λ:

$$d\ dr_N = f\ \lambda$$

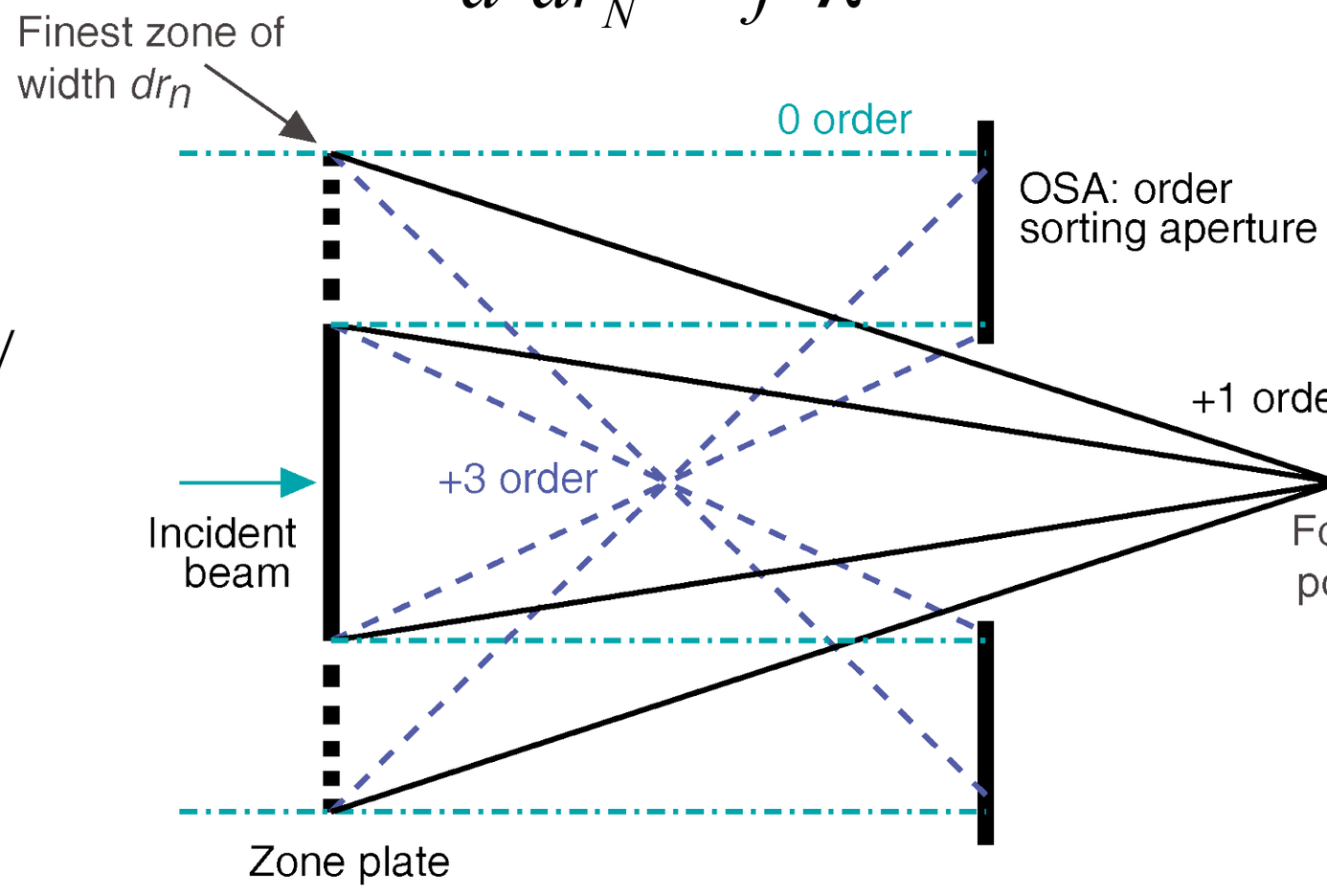

Central stop and order sorting aperture (OSA) to isolate first order focus

Fresnel zone plate images

R. W. Wood (1898): zone plate figure drawn with a pen and a compass! Photographically reduced

PLATE 2. ZONE-PLATE, FROM A DRAWING.

Zone plate efficiency and thickness

For binary zones, 1:1 mark:space ratio.

See Kirz, *J. Opt. Soc. Am.* **64**, 301 (1974)

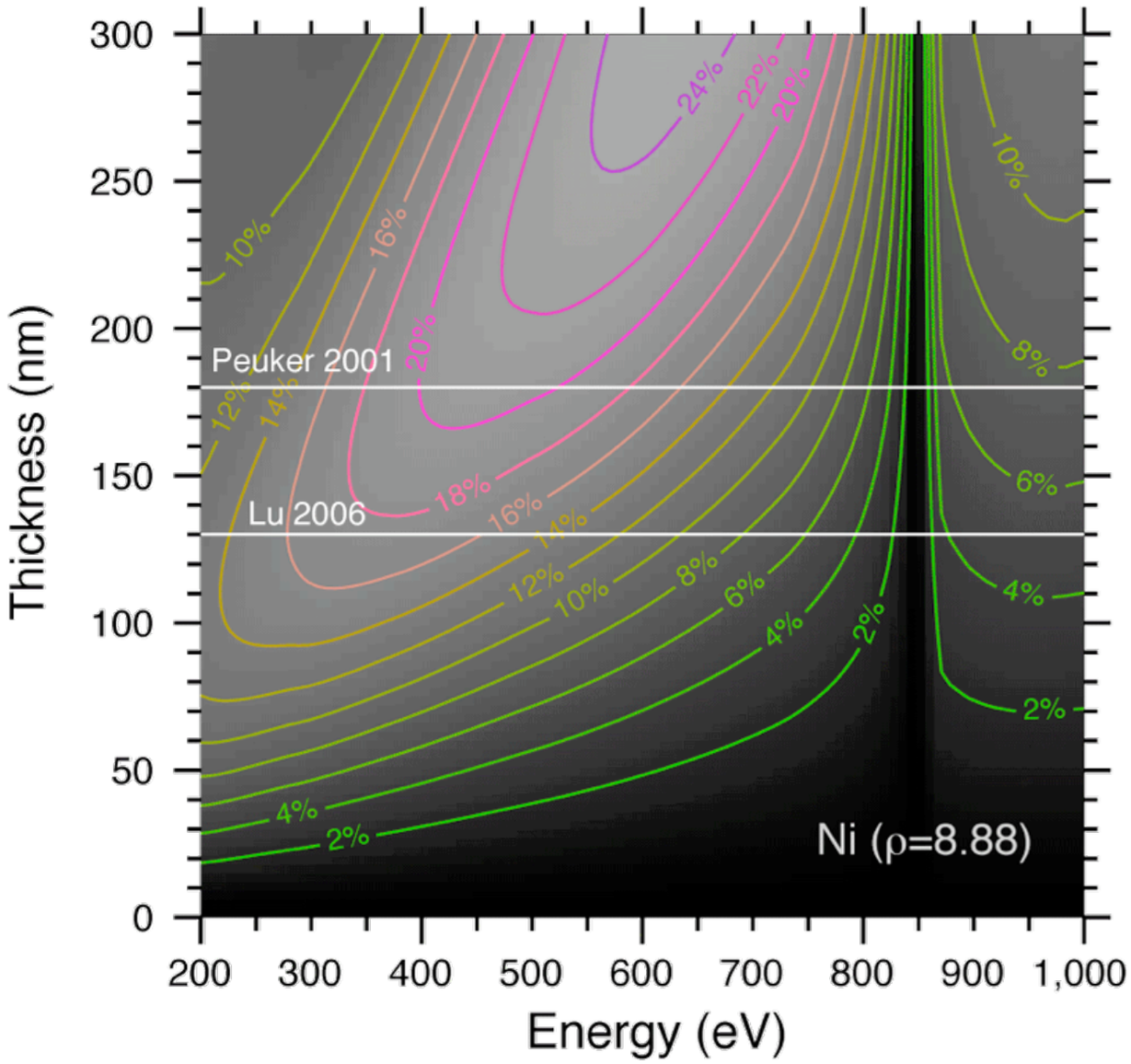

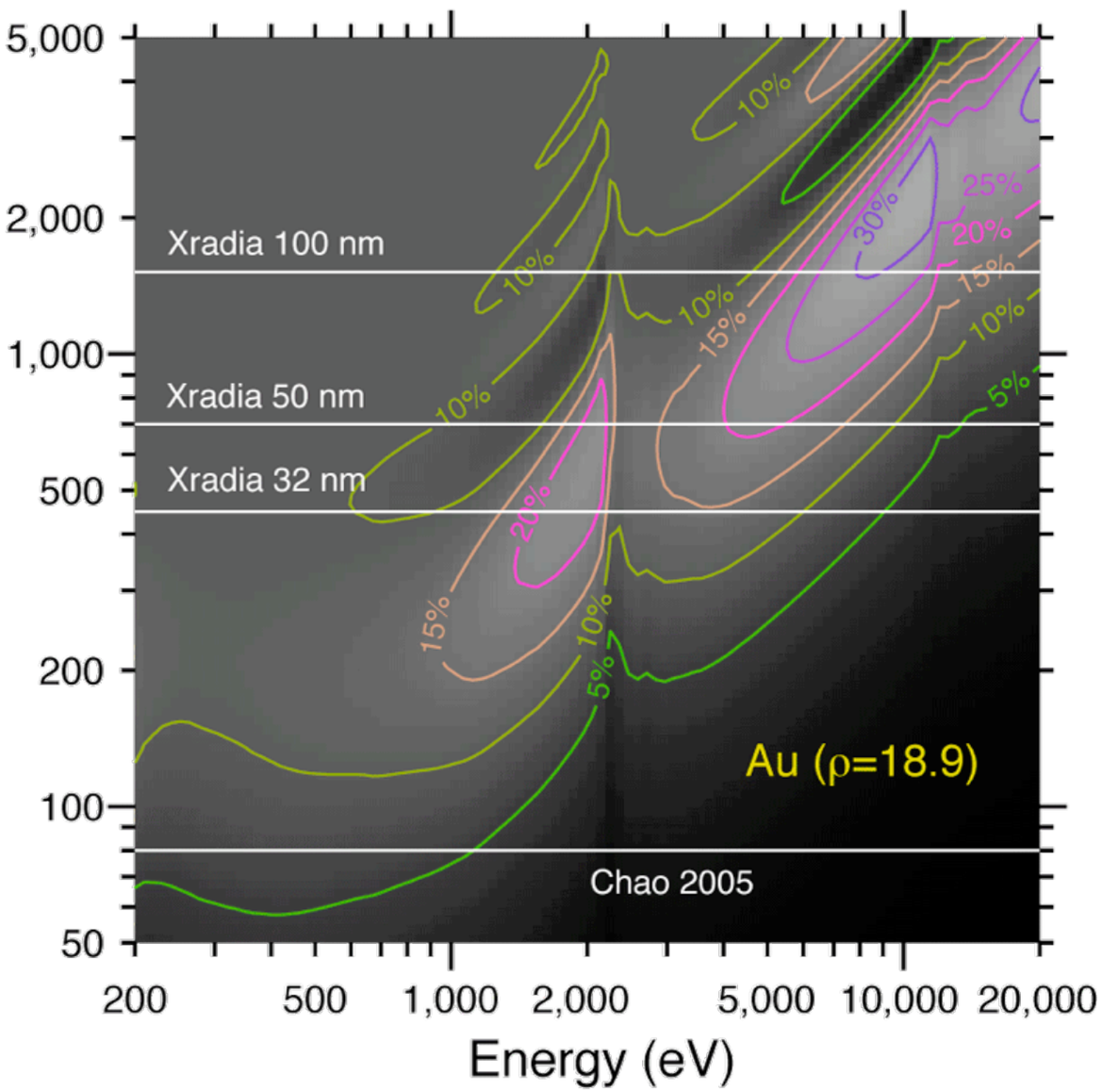

Zone plates by electron beam lithography

- Electron beam lithography: produces the finest possible structures (other than what nature can be persuaded to make by itself)
- M. Lu, A. Stein (PhD 2002; now BNL), S. Spector (PhD 1998; now Lincoln Lab), C. Jacobsen (Stony Brook)
- D. Tennant (Lucent/New Jersey Nanotech Consortium)
- JEOL JBX-9300FS: 1 nA into 4 nm spot, 1.2 nm over 500 μm, 100 keV

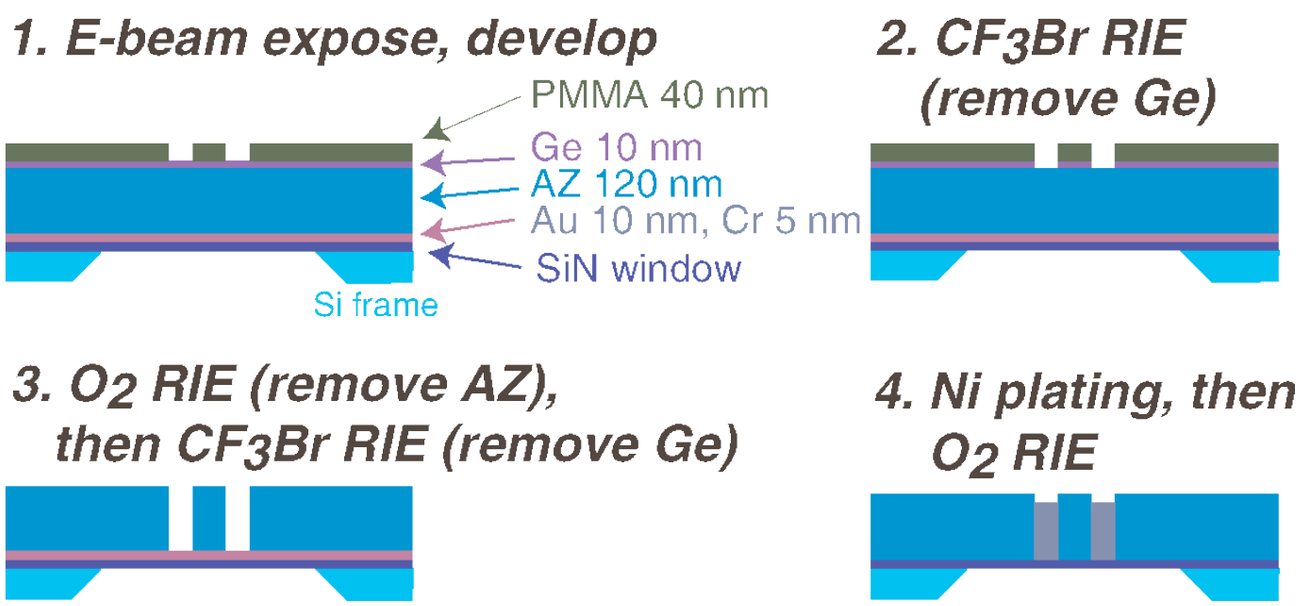

A. Stein and JBX-9300FS

Fresnel Zone Plates in nickel

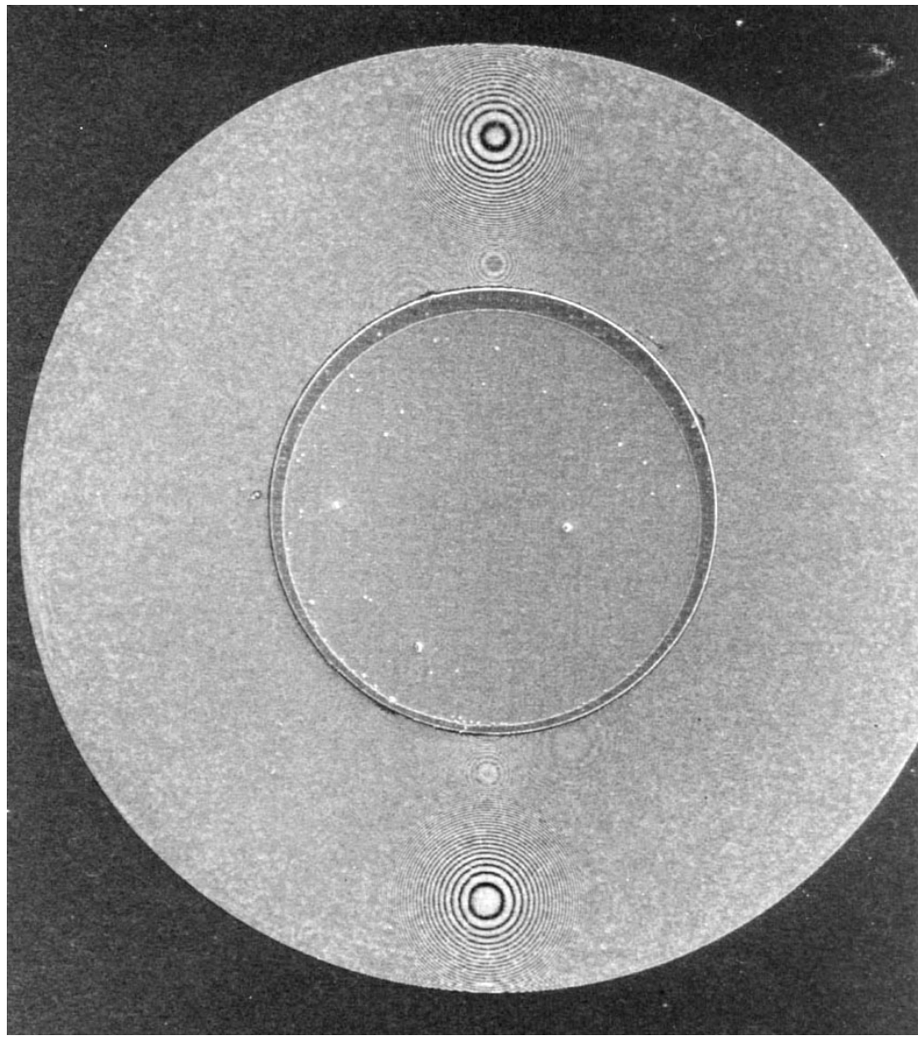

Diameter: 160 μm or about 3x diameter of one hair (A. Stein)

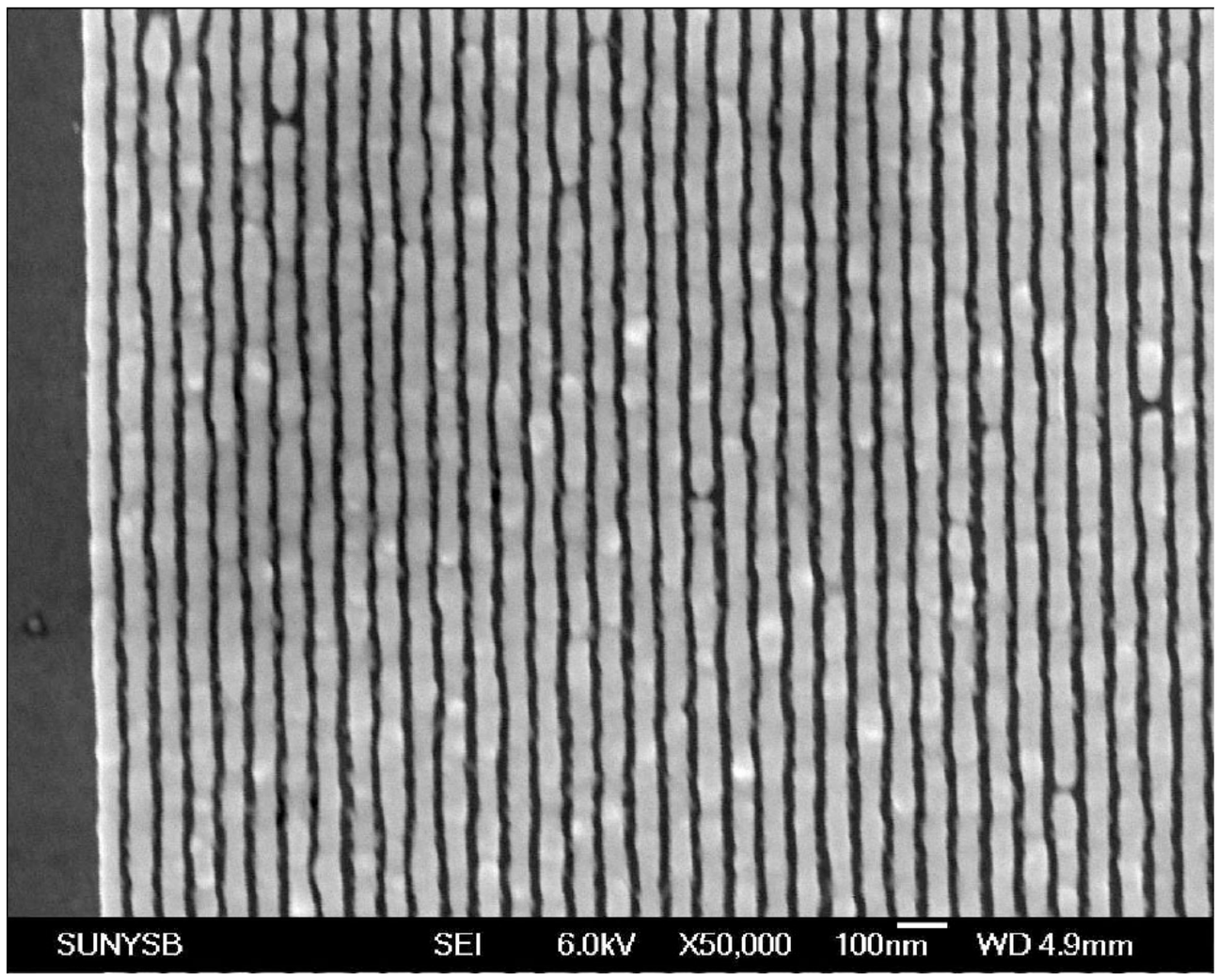

Finest linewidth: 0.030 μm or 30 nm, or about 150 atoms across (M. Lu)

Fabrication of zone plates

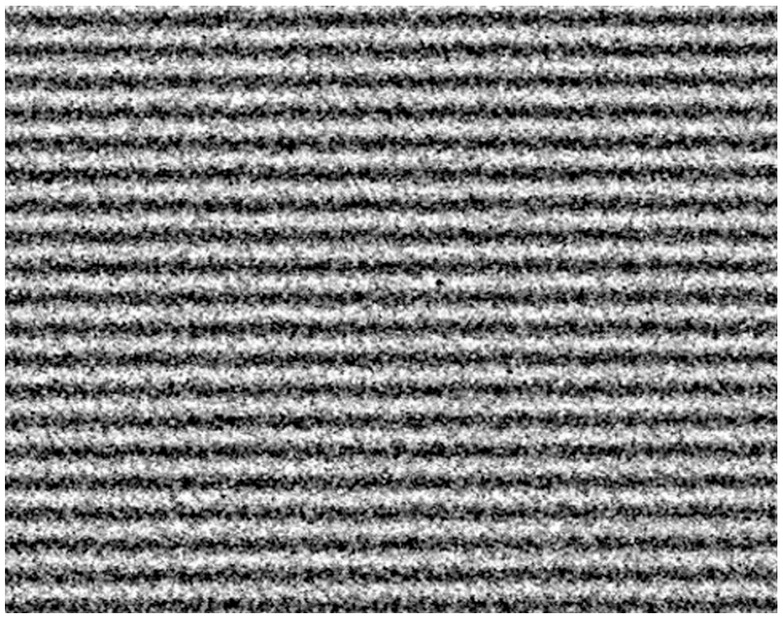

15.1 nm half-pitch multilayer slice imaged with a 15 nm outermost zone width zone plate. Chao et al., Nature **435**, 1210 (2005). But efficiency only ~3%. Other results: 9.2% at 20 nm: Peuker, Appl. Phys. Lett. **78**, 2208 (2001)

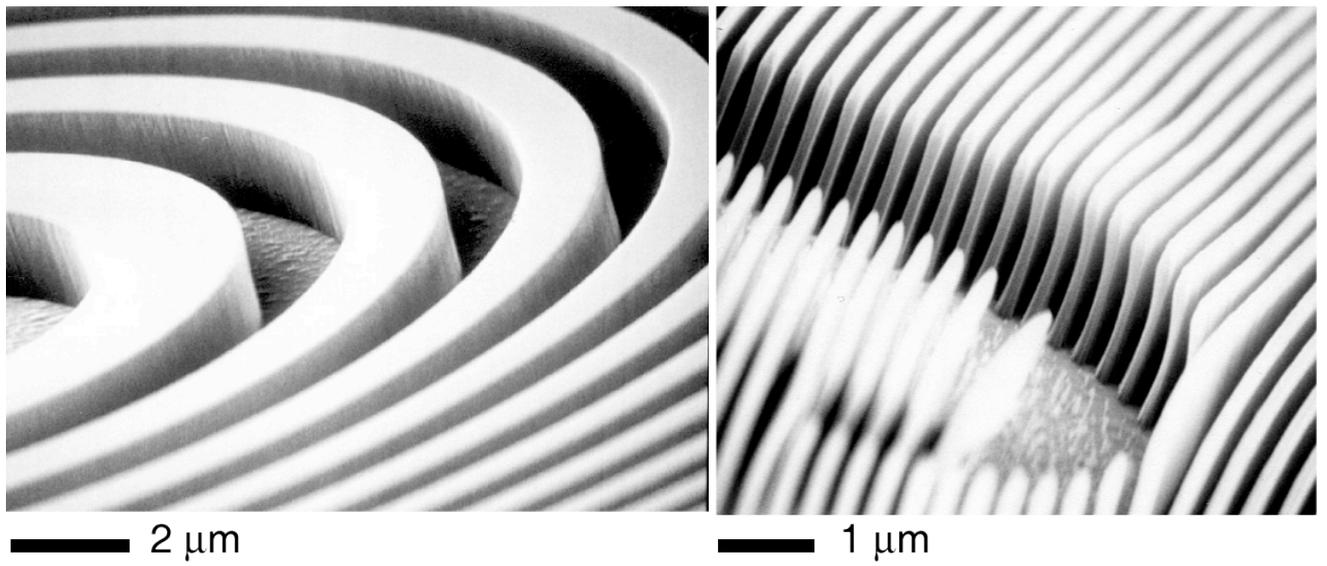

Gold zone plates, Xradia, Inc.: 70 nm outermost zones, 1 μm thick

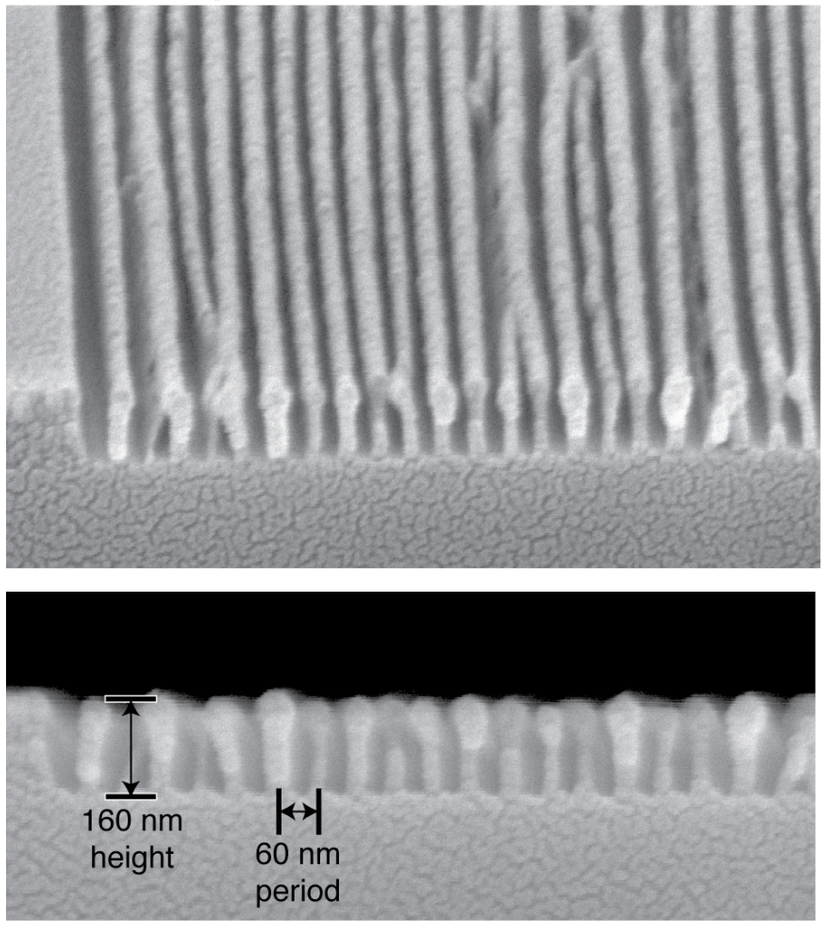

Test structures showing fabrication challenges (M. Lu)

Zone plate fabrication examples

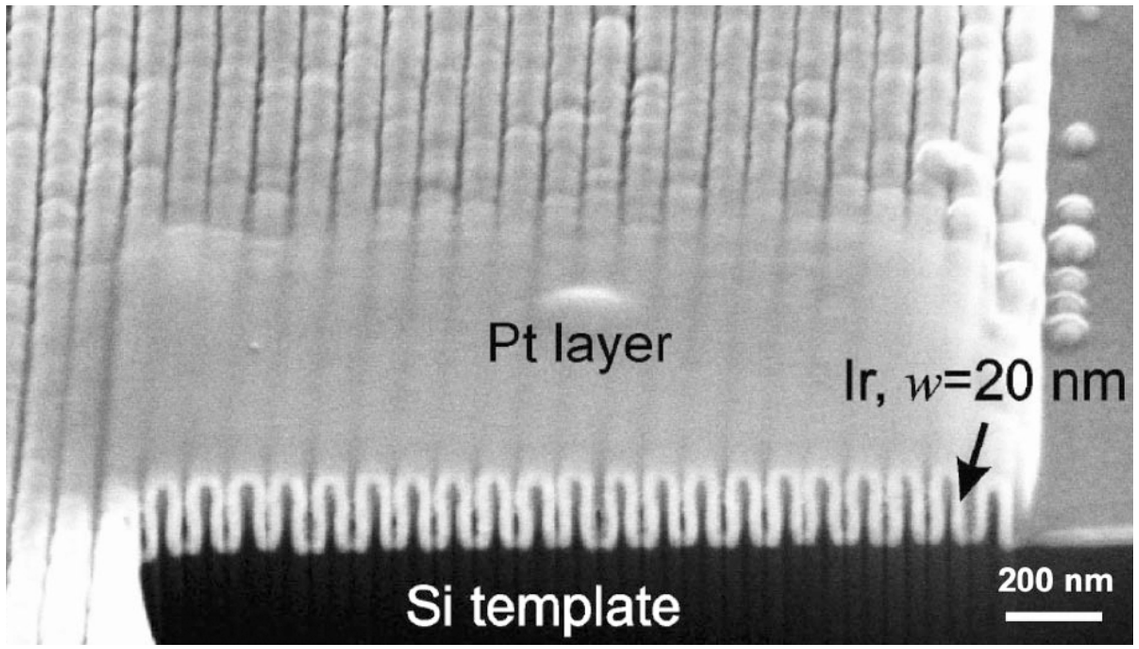

PSI, 20 nm wide, 170 nm tall Ir, 100 μm diameter:
Jefimovs *et al.*, *Phys. Rev. Lett.* **99**, 264801 (2007).

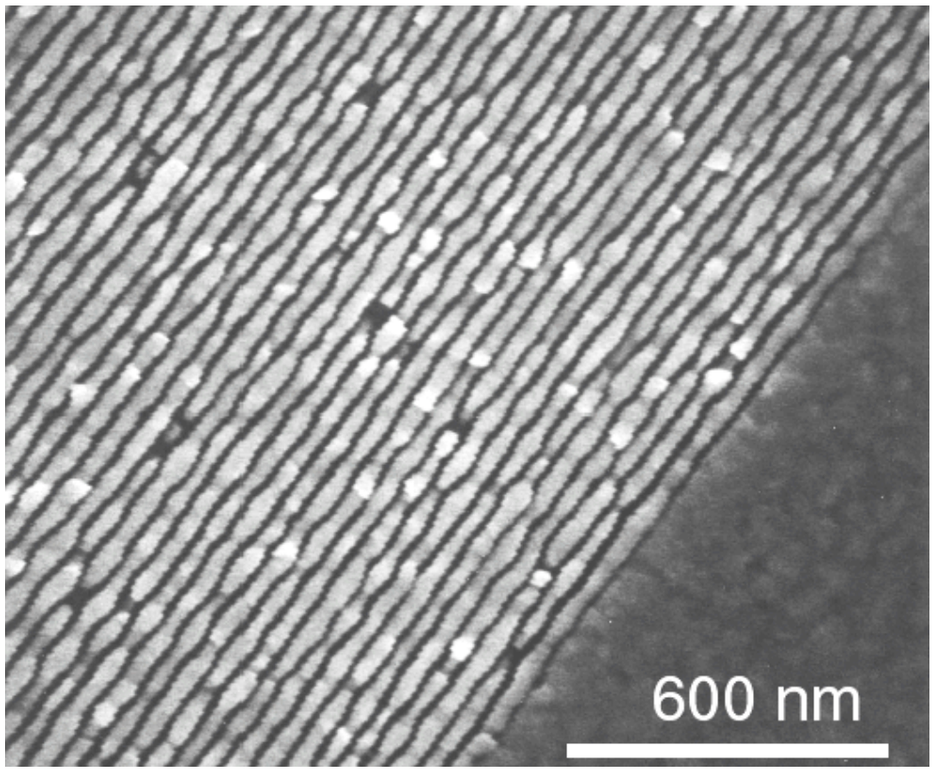

Stony Brook, 18 nm wide, 60 nm tall Ni, 80 μm diameter:
Spector *et al.*, *J. Vac. Sci. Tech. B* **15**, 2872 (1997).

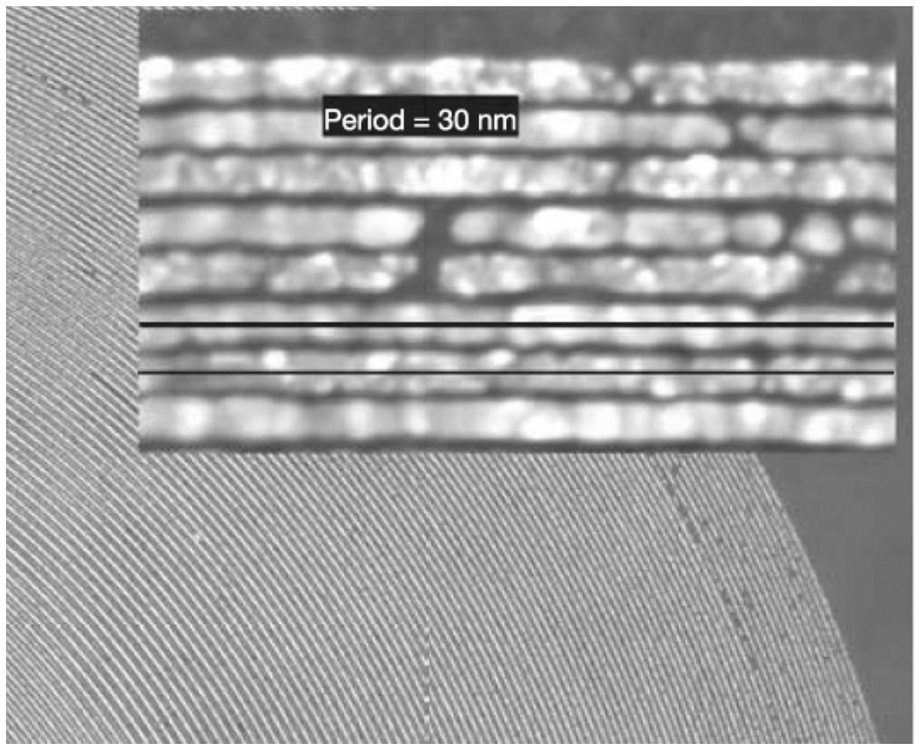

CXRO/LBL, 15 nm wide, 80 nm tall Au, 30 μm diameter:
Chao *et al.*, *Nature* **435**, 1210 (2005).

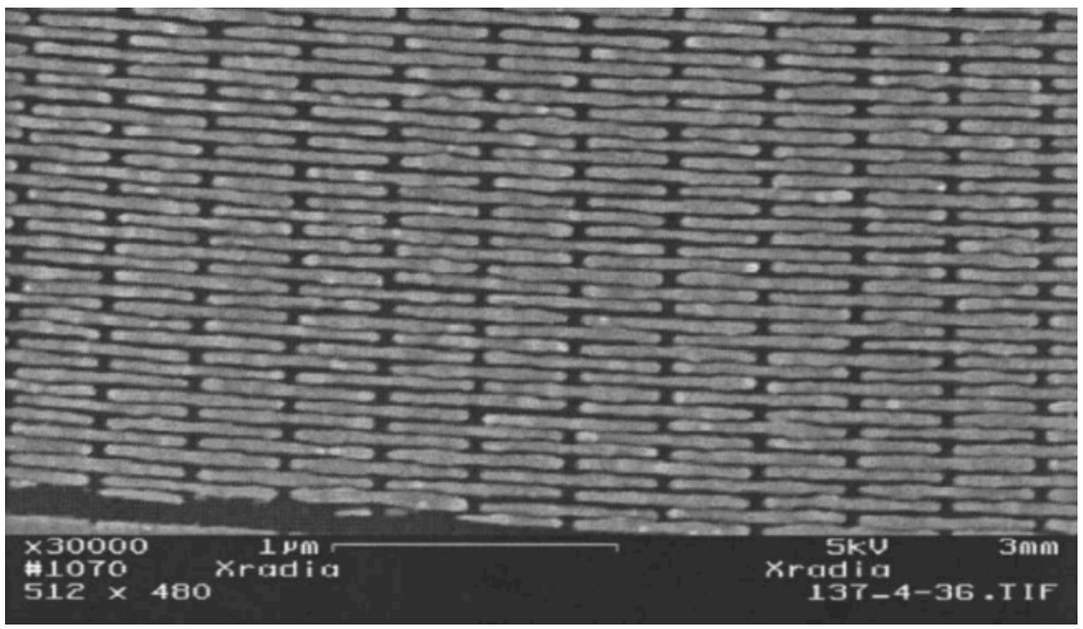

Xradia, 24 nm wide, 300 nm tall Au, 133 μm diameter:
Feng *et al.*, *J. Vac. Sci. Tech. B* **25**, 2004 (2007).

Multilayer Laue lenses

- Forget top-down circles, and go sideways! Start by depositing thinnest zones first on a flat substrate, and work your way up to thicker zones. Cross two 1D lenses for 2D focusing. Maser et al., *SPIE* **5539**, 185 (2004)
- For thick optics, you want to tilt to be on the Bragg condition anyway [Maser, PhD thesis; Maser and Schmahl, *Opt. Comm.* **89**, 355 (1992)]

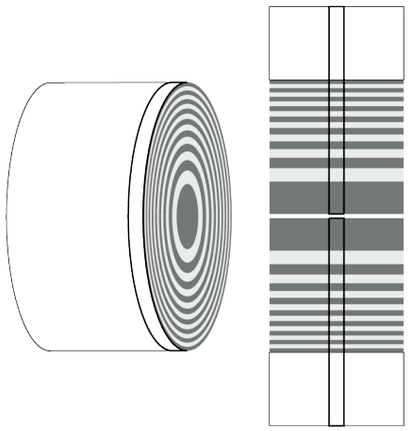

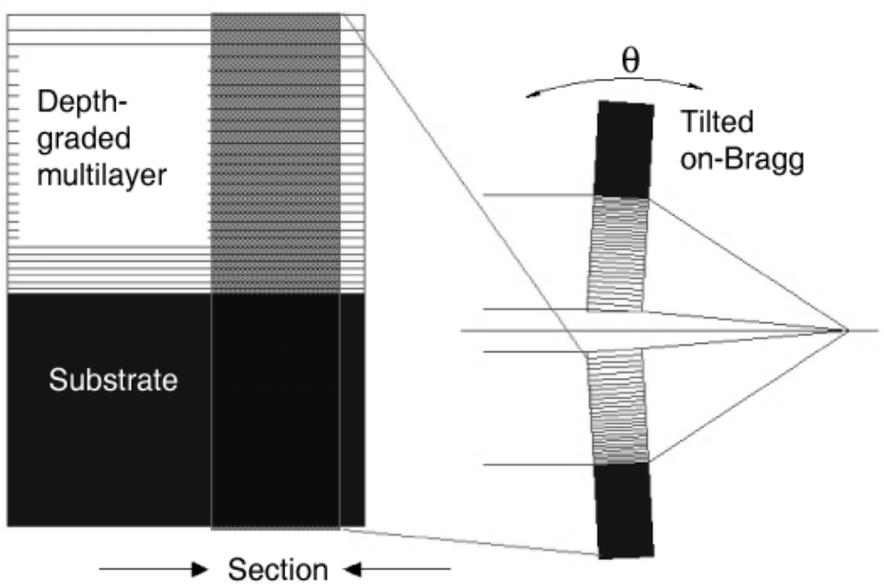

Maser et al., *SPIE* **5539**, 185 (2004)

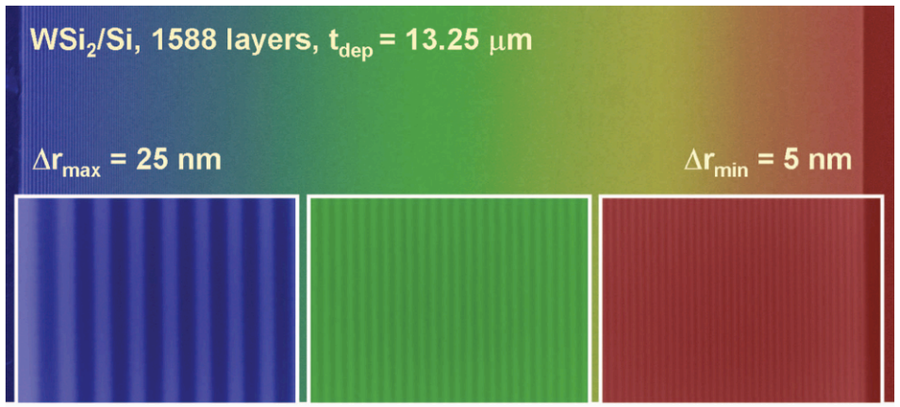

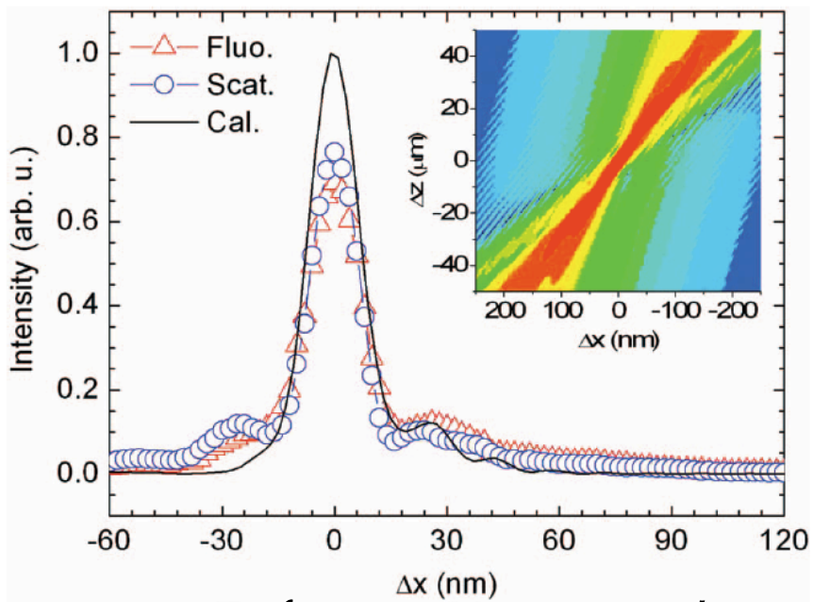

16 nm 1D focus: Kang *et al.*, *Appl. Phys. Lett.* **92**, 21114 (2008)

X-ray optics: best published resolution

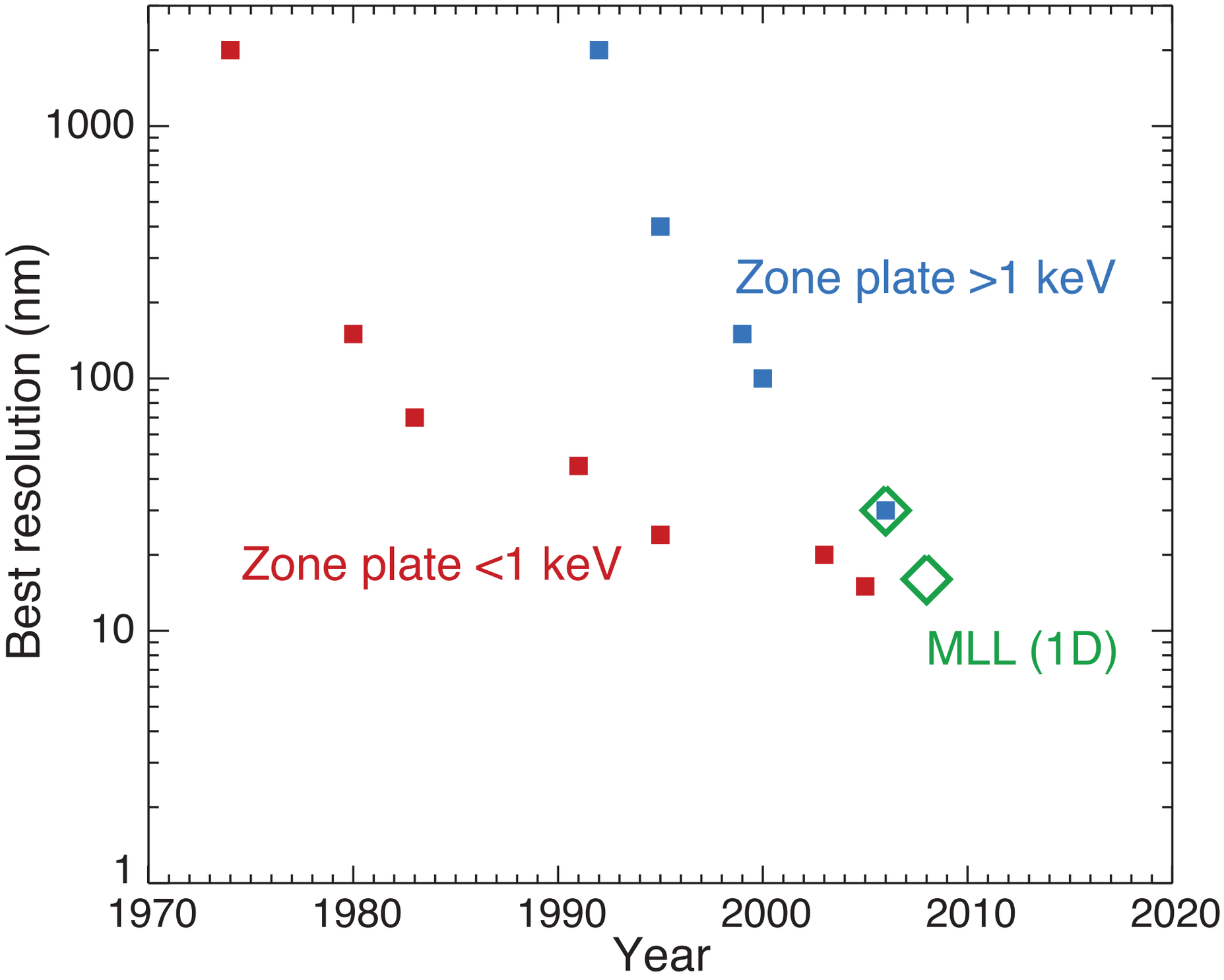

Zone plate microscopes

TXM

- Incoherent illumination; works well with a bending magnet, with fast imaging
- More pixels (e.g., 2048^2)
- Moderate spectral resolution in most cases - but new instrument at BESSY, Berlin!

STXM

- Coherent illumination; works best with an undulator
- Less dose to sample (~10% efficient ZP)
- Better suited to conventional grating monochromator [high E/(ΔE)]
- Microprobes: fluorescence etc.

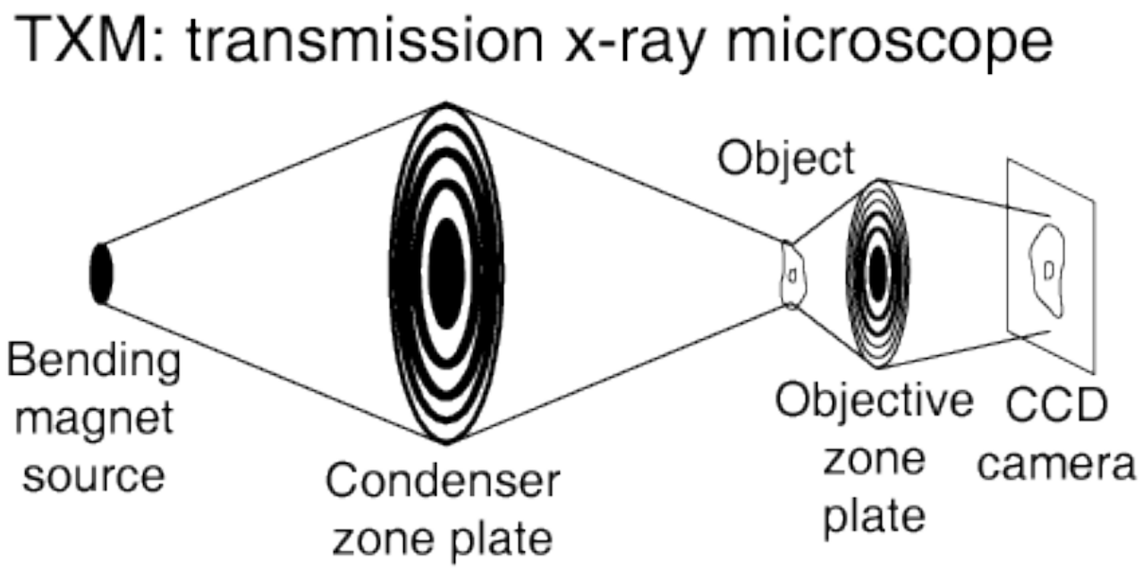

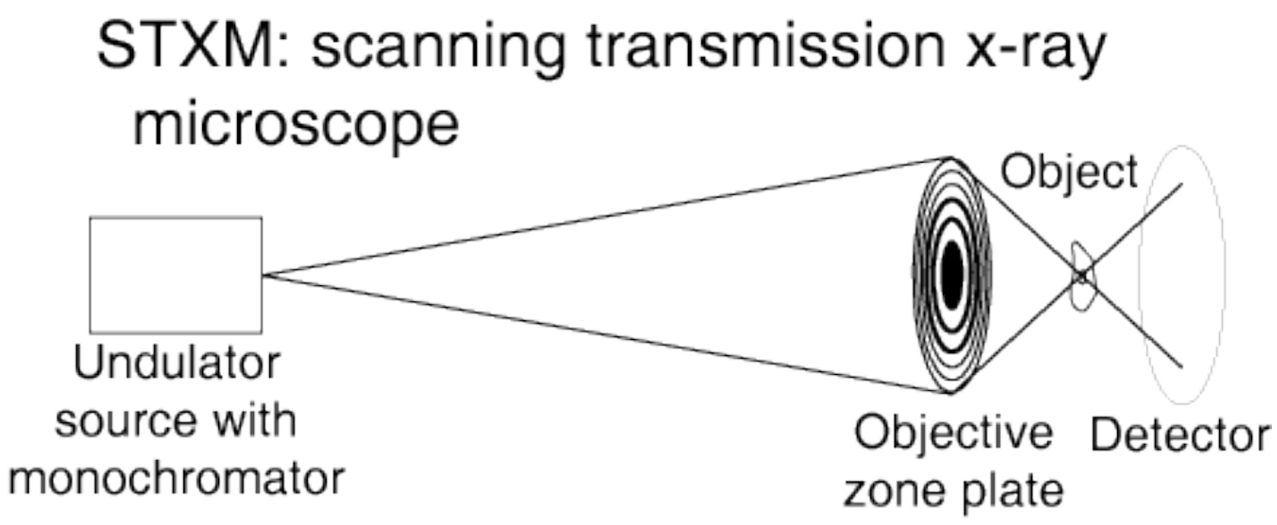

Scanning and full-field

- General property of lenses: preserve size•angle product (Liouville's Theorem), so

$$h\theta = h'\theta'$$

- Microprobe/STXM: want $h' < \delta$ so that diffraction limit of optic rather than geometrical image of source dominates spot size
- Rayleigh resolution of $\delta = 0.61\frac{\lambda}{\theta}$ thus gives phase space of

$$(2\delta)(2\theta) = 2.44\lambda$$

- Full-field: each pixel in object is diffraction limit of optic, but can have many pixels simultaneously!

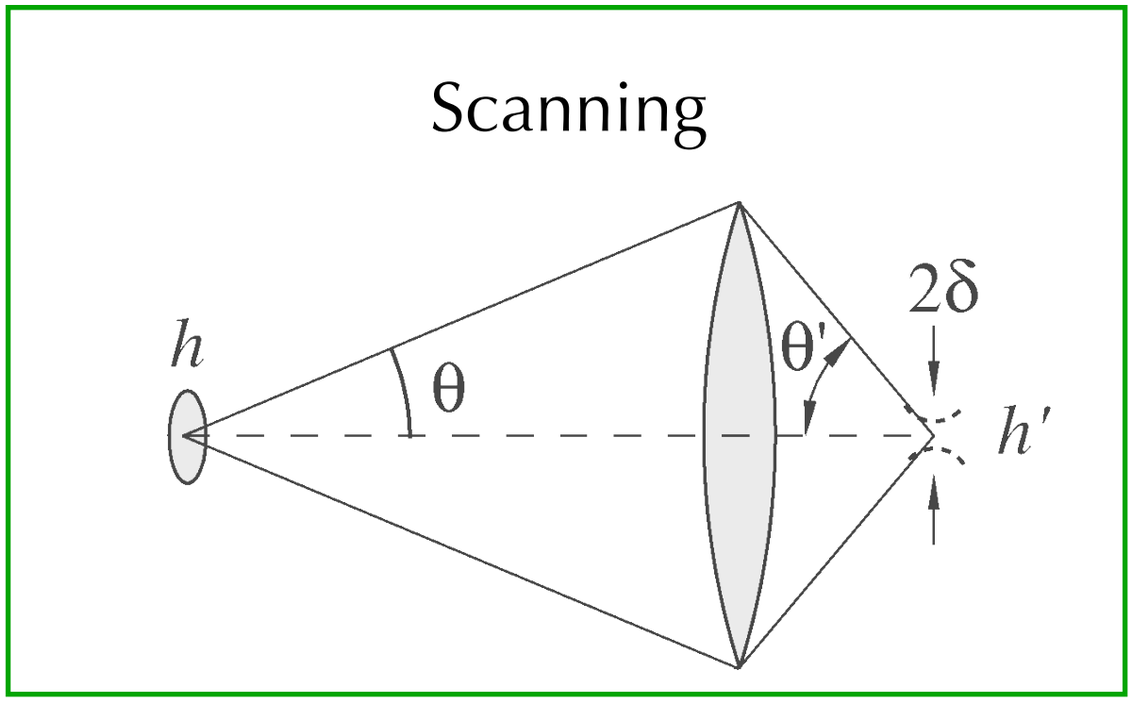

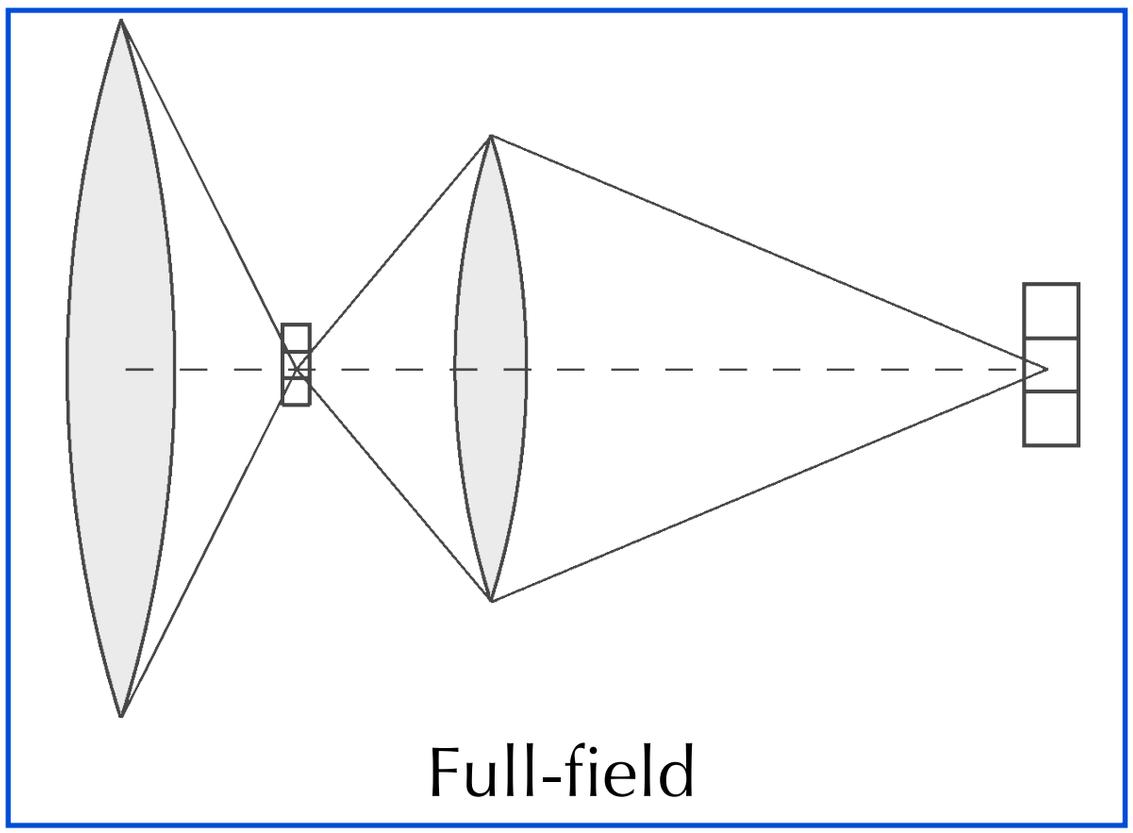

Controlling spatial coherence

- Coherent flux: phase space area of λ in each dimension. Coherent flux is $B \bullet \lambda^2$. Green, BNL-50522 (1976); Kondratenko and Skrinsky, Opt. Spectr. **42**, 189 (1977).
- Spatial filter: pinhole at the focus of a lens. Passes only the spatially coherent fraction of an incident beam.

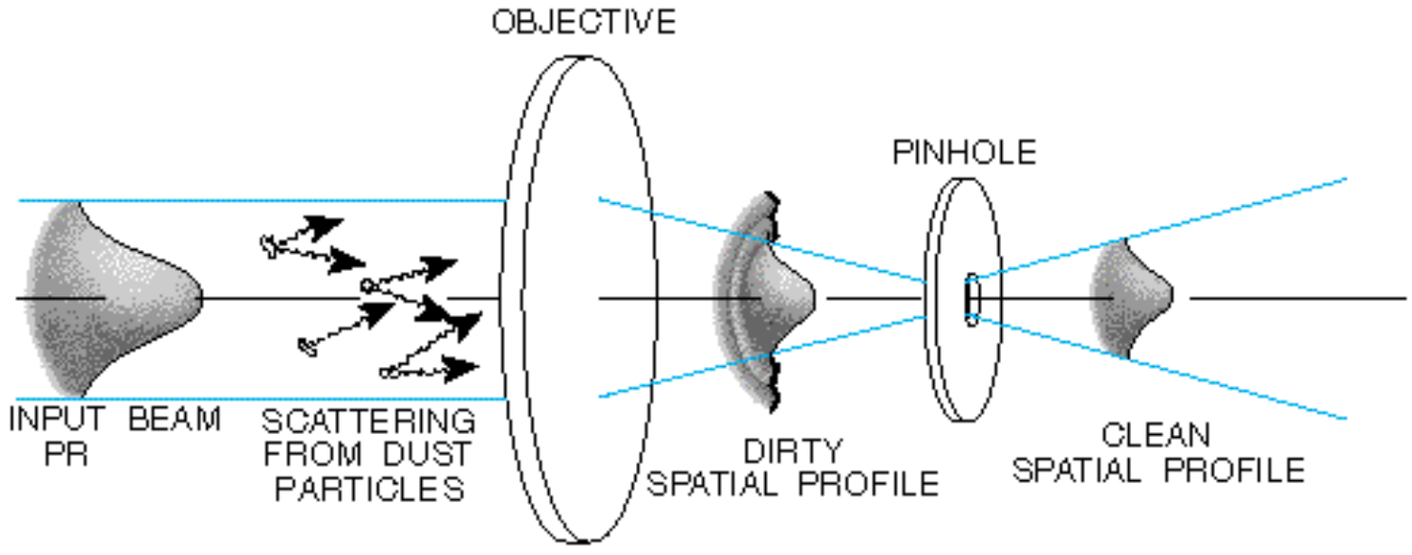

Diagram, photo from Newport catalog

Effects of spatial incoherence on STXM

How close must $p=h\theta$ be to λ?

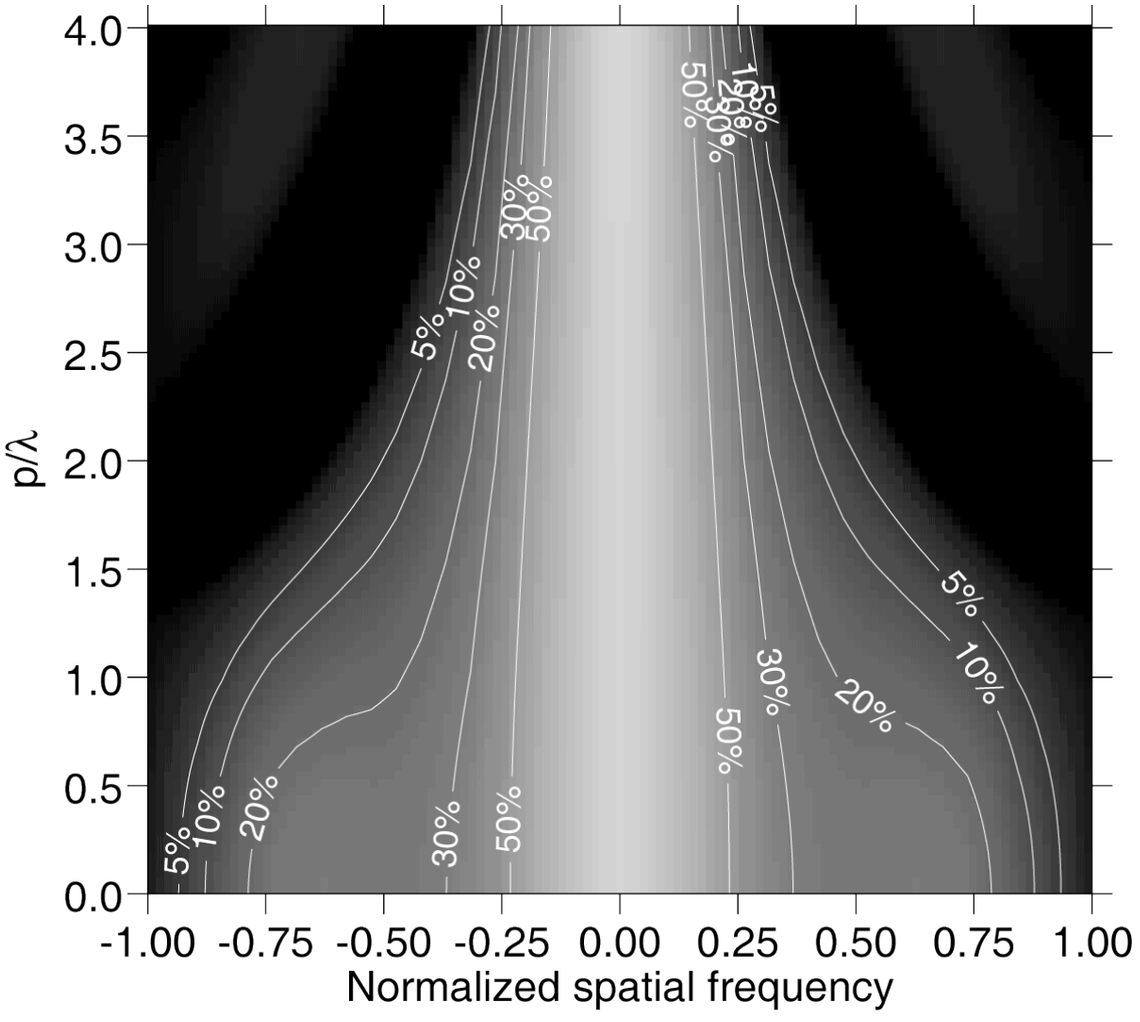

Effect on modulation transfer function MTF
(50% central stop)

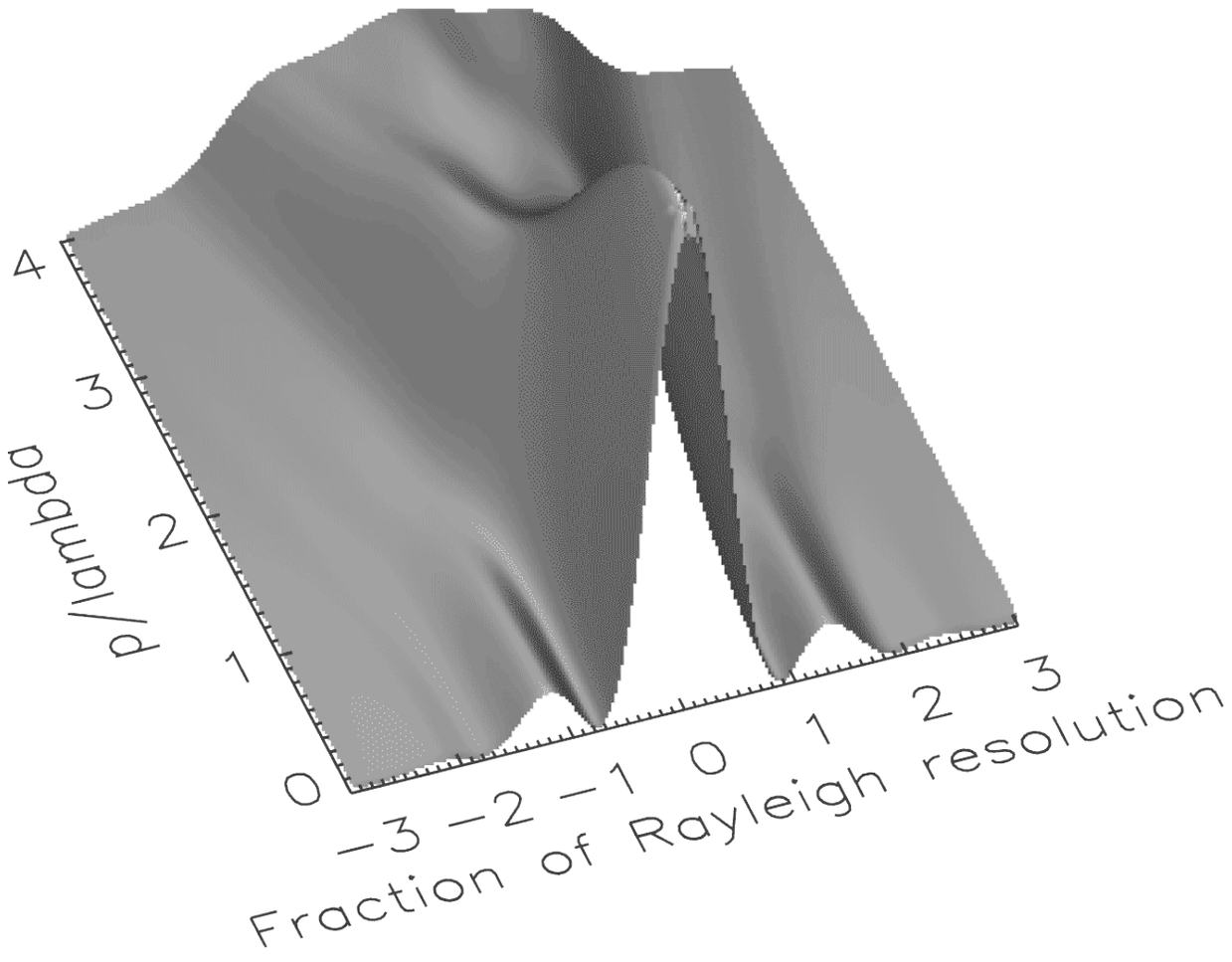

Effect on point spread function PSF
(50% central stop)

Jacobsen et al., Ultramicroscopy **47**, 55 (1992); Winn et al., J. Synch. Rad. **7**, 395 (2000).

2D imaging with Stony Brook STXMs

Scanning zone plate microscopes

U15 and X17t (1983-1987): Kirz (Stony Brook) and Rarback (NSLS).

X1A (since 1989): Kirz and Jacobsen (Stony Brook)

2D imaging is moderately useful but...

- Cannot track fluroescently-labeled proteins in living cells
- Resolution is inferior to cryoEM, though do not need to section
- Best utility may lie beyond simple 2D imaging

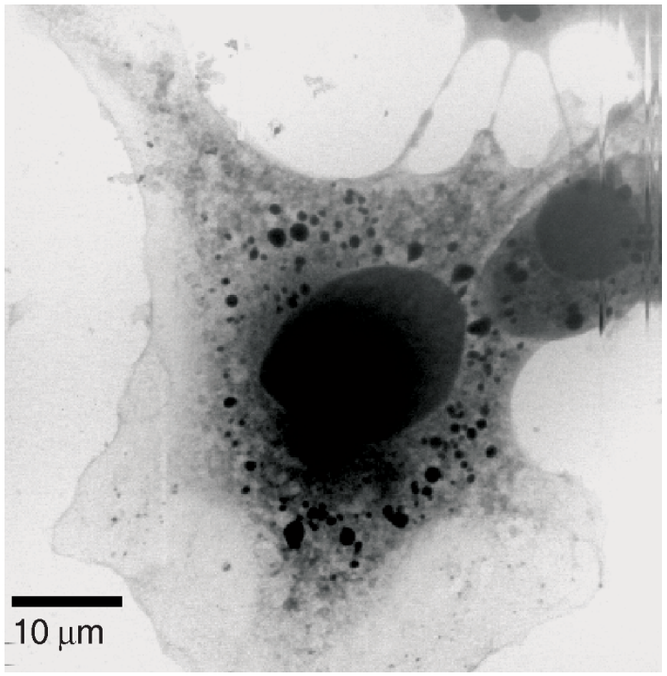

NIL 8 fibroblast (wet, fixed): Oehler *et al.*

Human sperm (unfixed): Wirick, Fleckenstein, Sheynkin *et al.*

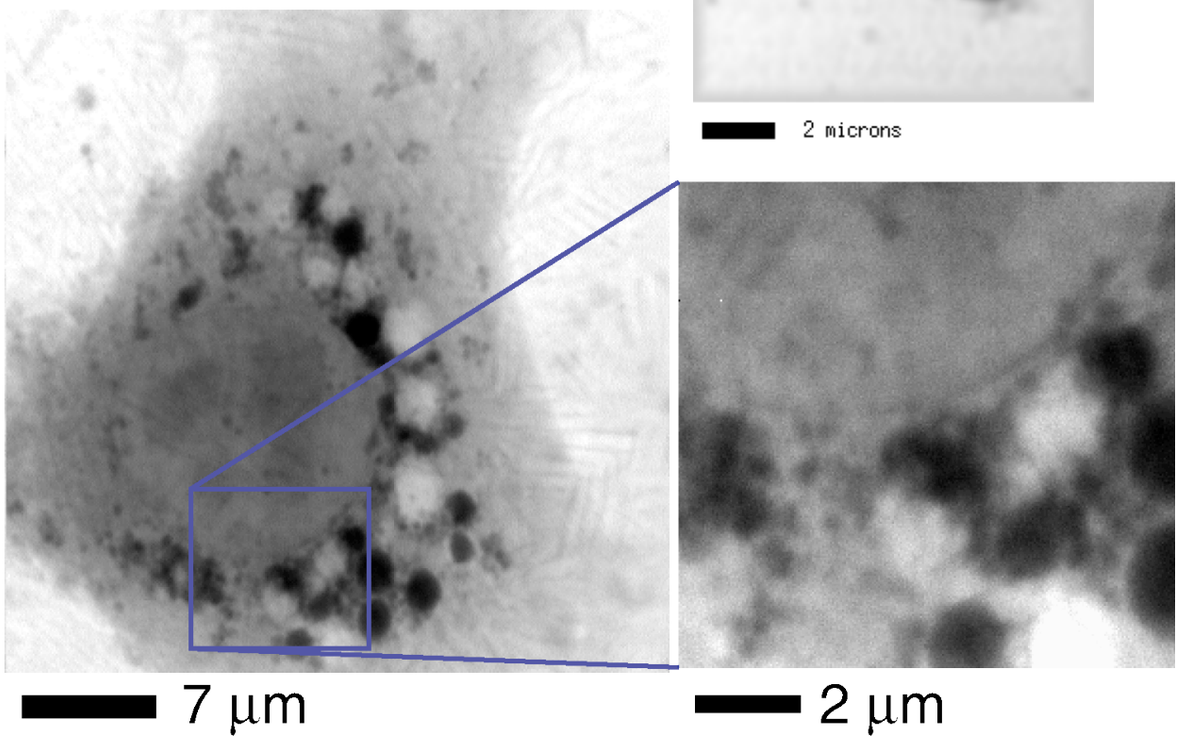

Fibroblast (frozen hydrated): Maser *et al.*, *J. Micros.* **197**, 68 (2000)

Absorption edges

Lambert-Beer law: linear absorption coefficient μ

$$I = I_0 \exp\left[-\mu(E) \bullet t\right] = I_0 \exp\left[-D(E)\right]$$

This coefficient makes a jump at specific elemental absorption edges!

This example: 0.1 μm protein, silica

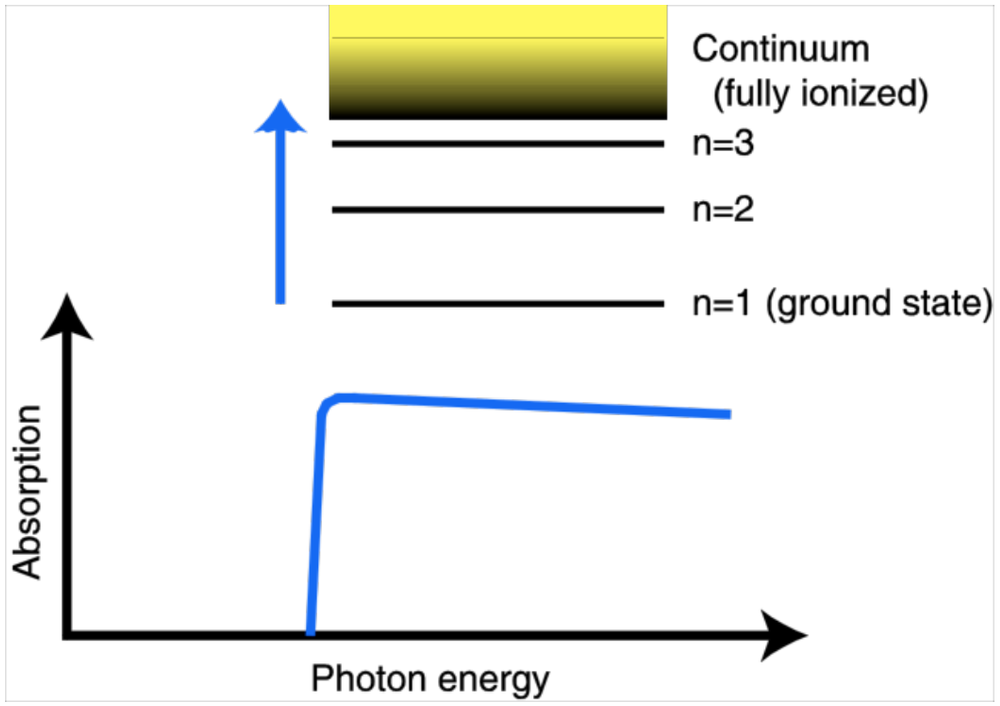

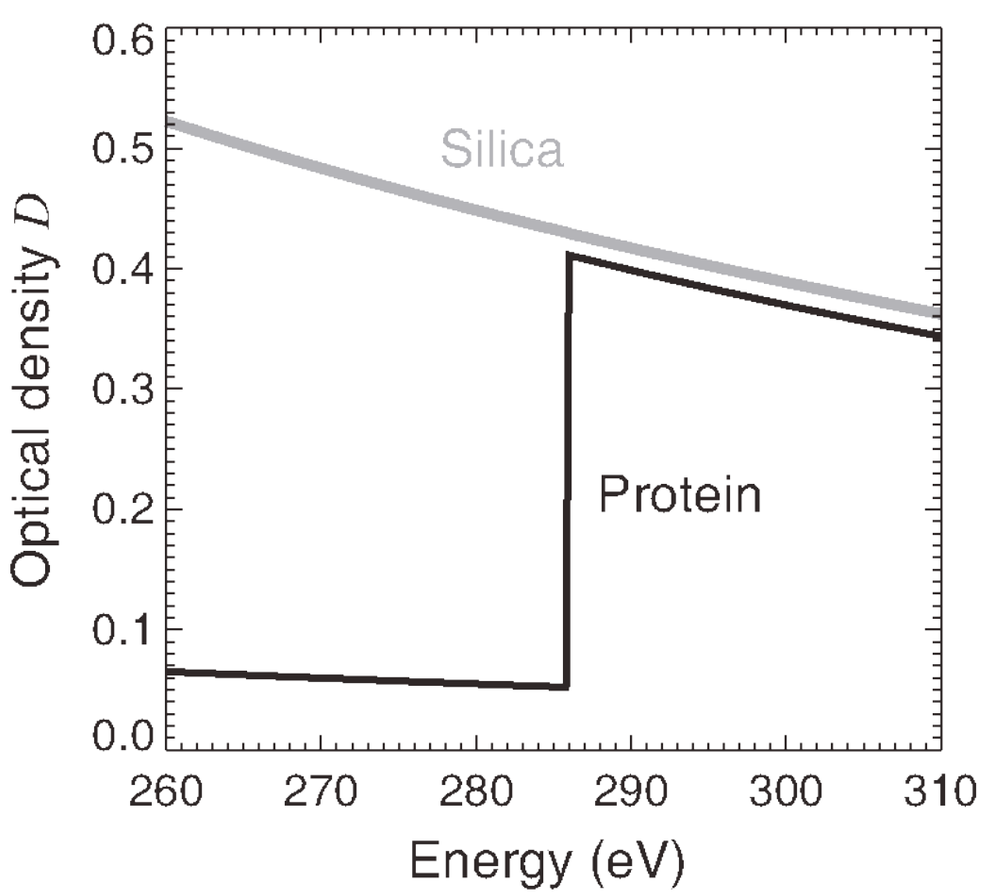

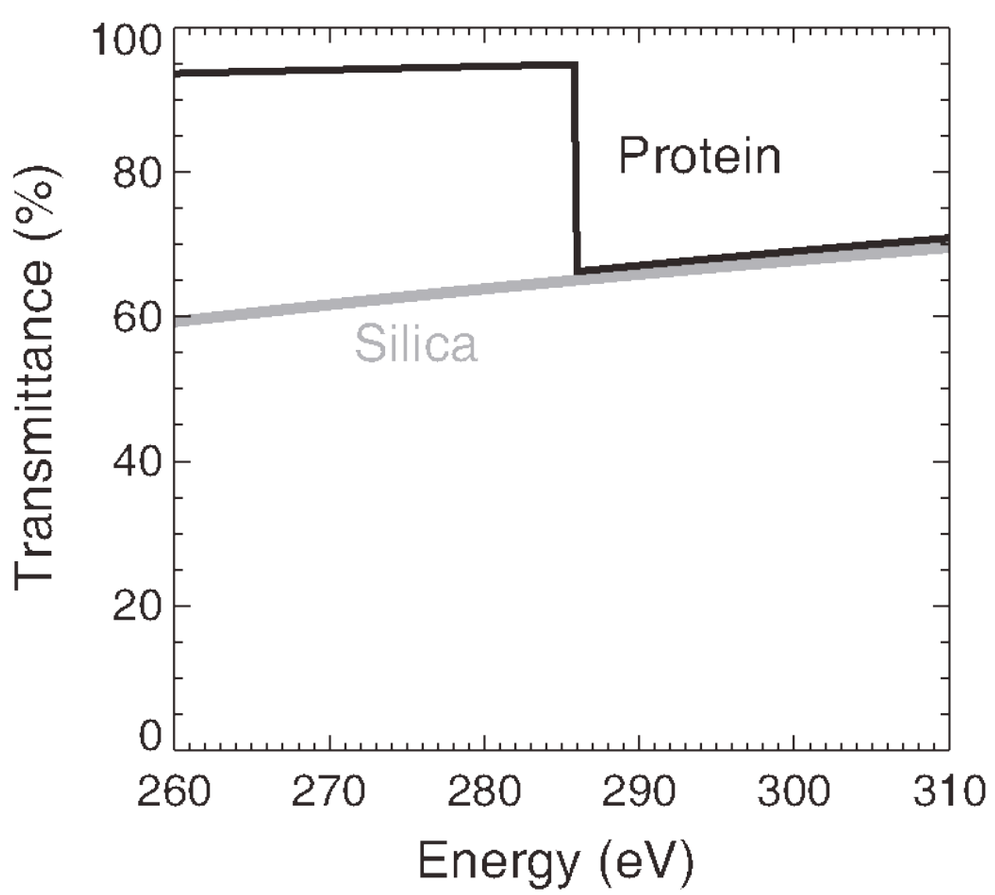

X-ray microscopy of colloids

- U. Neuhäusler (Stony Brook/Göttingen), S. Abend (Kiel), G. Lagaly (Kiel), C. Jacobsen (Stony Brook), Colloid and Polymer Science **277**, 719 (1999)
- Emulsion: water, oil droplets, clay, and layered double hydroxides (LDH)
- "Caged" part of oil droplet remains fixed; "uncaged" part can disperse

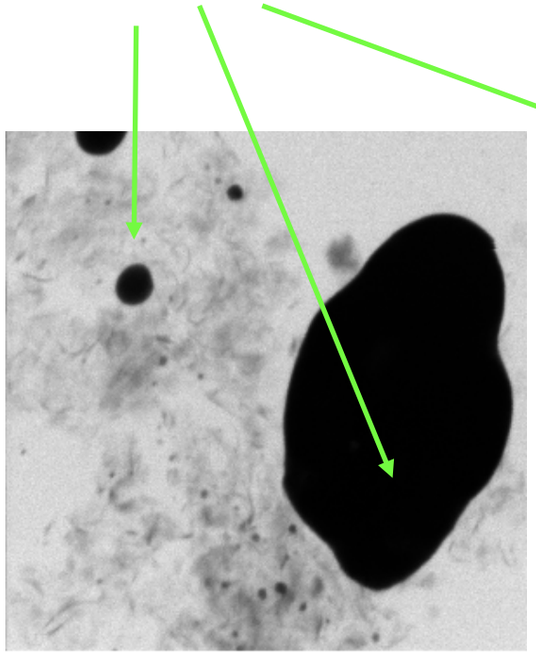

346 eV: calcium weakly absorbing. Clays and LDHs absorb equally

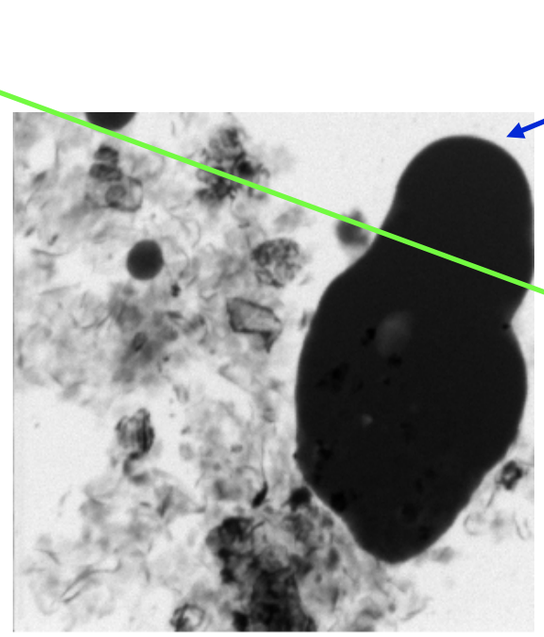

352.3 eV: calcium strongly absorbing. Calcium-rich LDHs are highlighted.

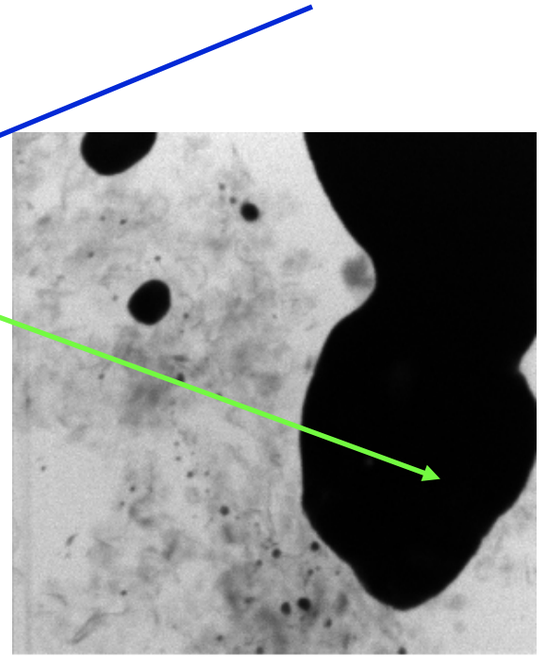

290 eV: carbon strongly absorbing

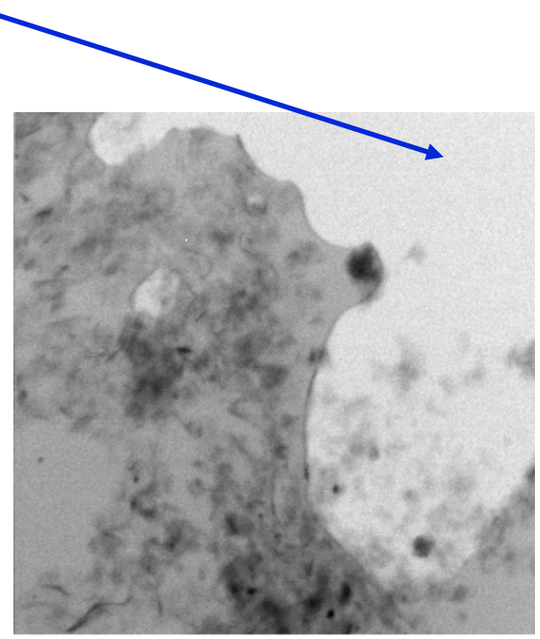

284 eV: carbon (oil drop) weakly absorbing

Near-edge absorption fine structure (NEXAFS) or X-ray absorption near-edge structure (XANES)

- Fine-tuning of the x-ray energy near an atom's edge gives sensitivity to the chemical bonding state of atoms of that type
- First exploitation for chemical state transmission imaging: Ade, Zhang *et al.*, *Science* **258**, 972 (1992) – Stony Brook/X1A

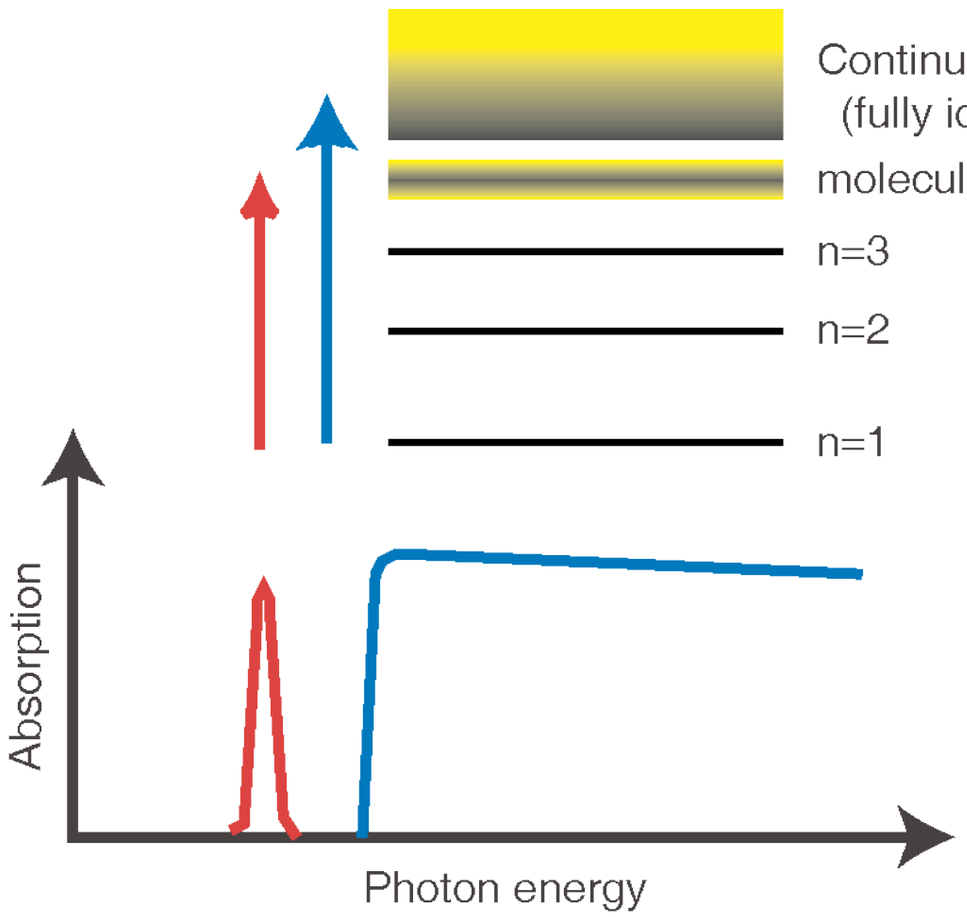

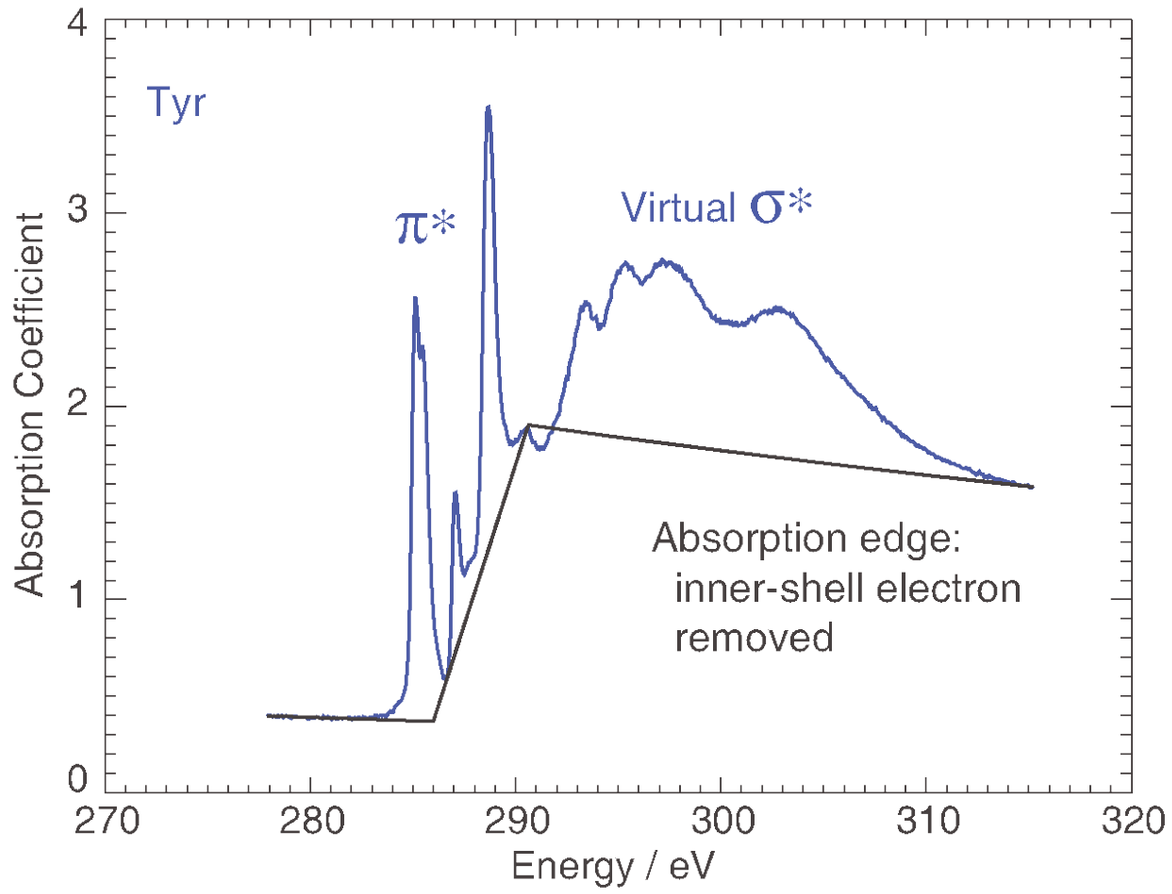

Compared with UV "tickling" of molecular orbitals, core-level electrons come from a single, well-defined state!

Near-edge spectroscopy: ELNES and XANES

ELNES (electron **E**nergy **L**oss)

- Plural inelastic scattering
- Many elements at once - but plasmon modes are always excited (damage)
- ΔE was ~0.6 eV, but now <0.1 eV in some cases

XANES (**X**-ray **A**bsorption)

- No plural scattering
- One element at a time - slow but less damage
- ΔE of 0.05-0.1 eV is common

Electrons ~1000x more damaging:

- Isaacson and Utlaut, *Optik* **50**, 213 (1978)
- Rightor *et al.*, *J. Phys. Chem. B* **101**, 1950 (1997).

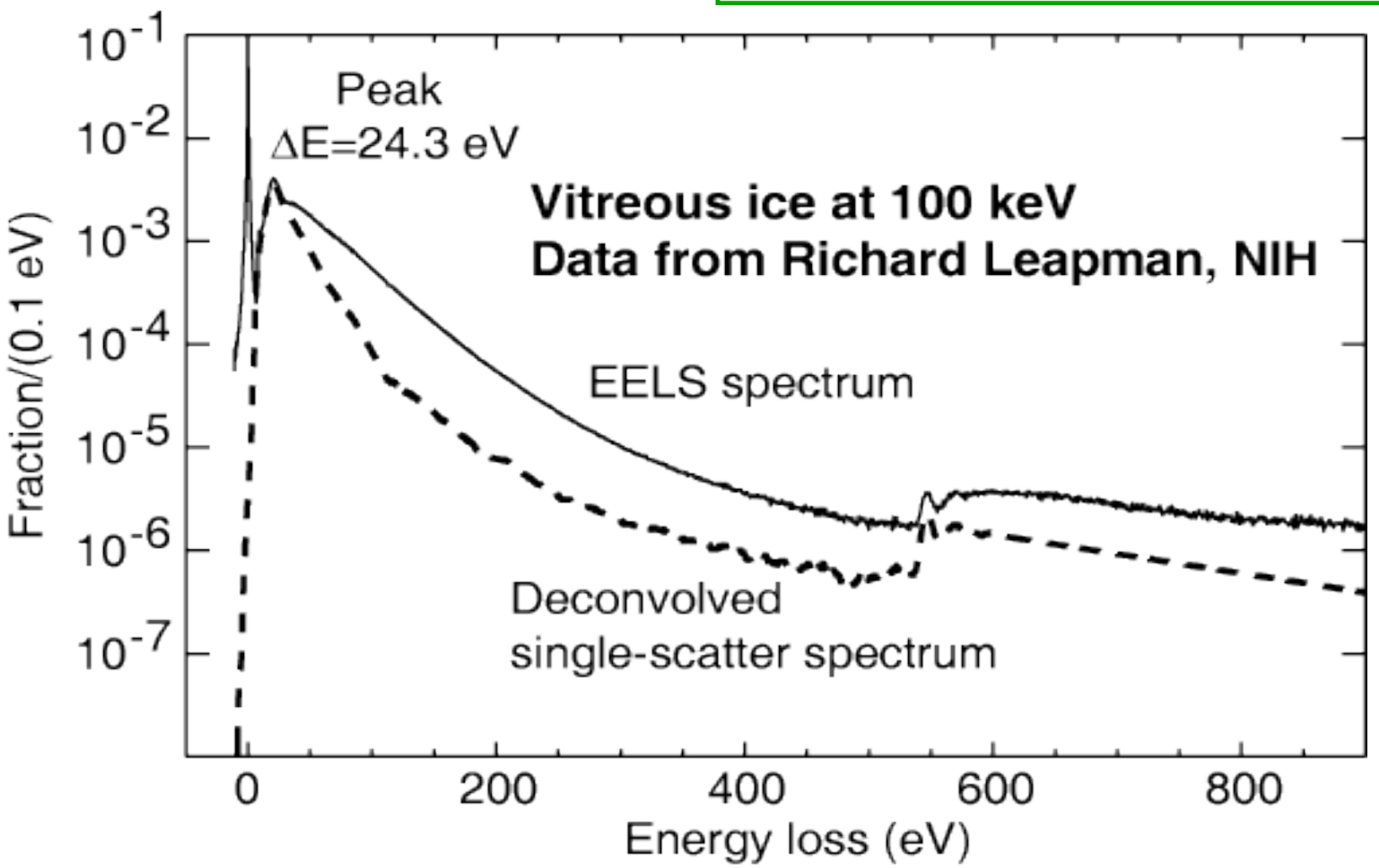

C-XANES spectral bands

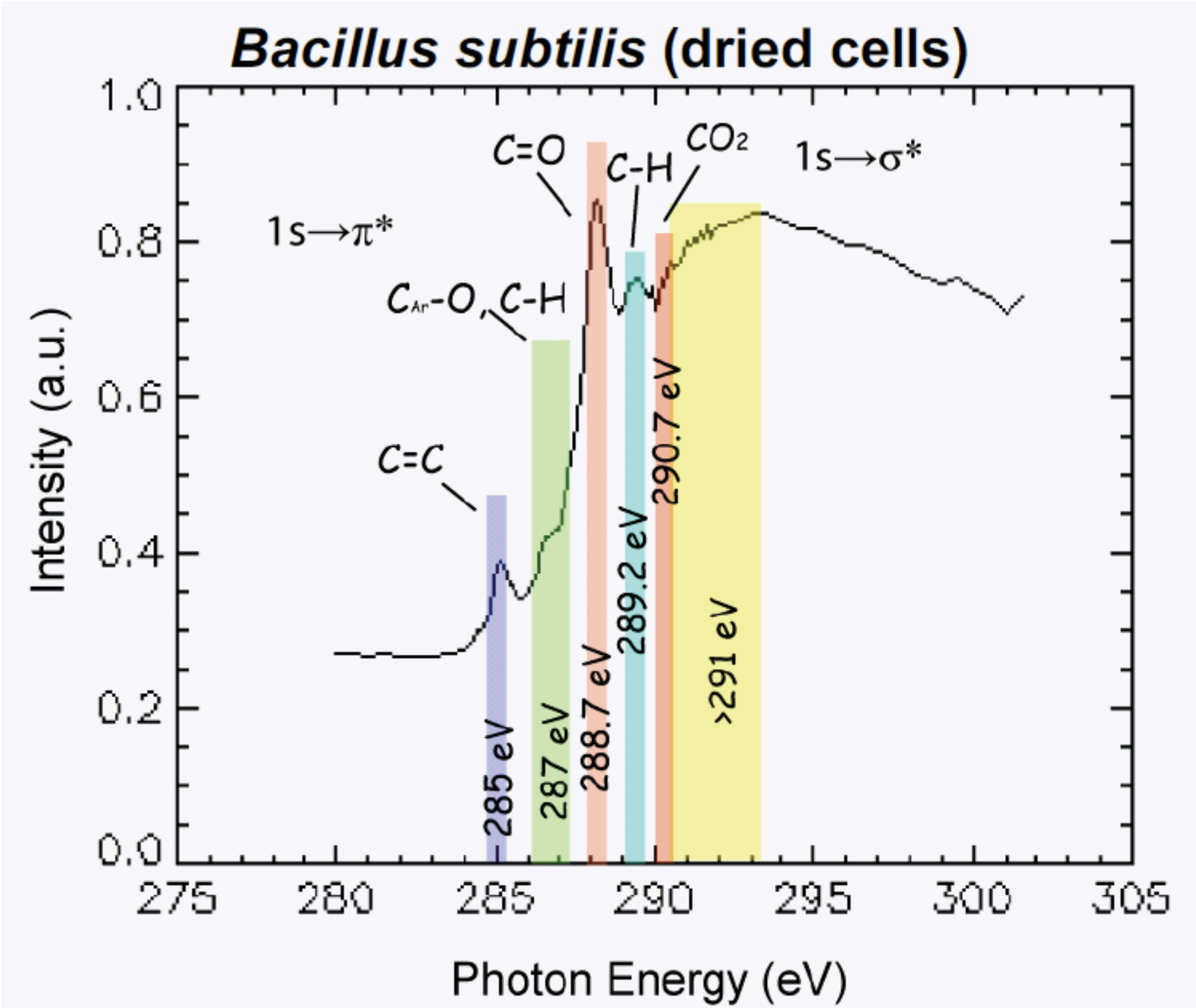

C-XANES of amino acids

- K. Kaznacheyev *et al.*, *J. Phys. Chem.* **A 106**, 3153 (2002)
- Experiment: K. Kaznacheyev *et al.*, Stony Brook (now CLS)
- Theory: O. Plashkevych, H. Ågren *et al.*, KTH Stockholm; A. Hitchcock, McMaster

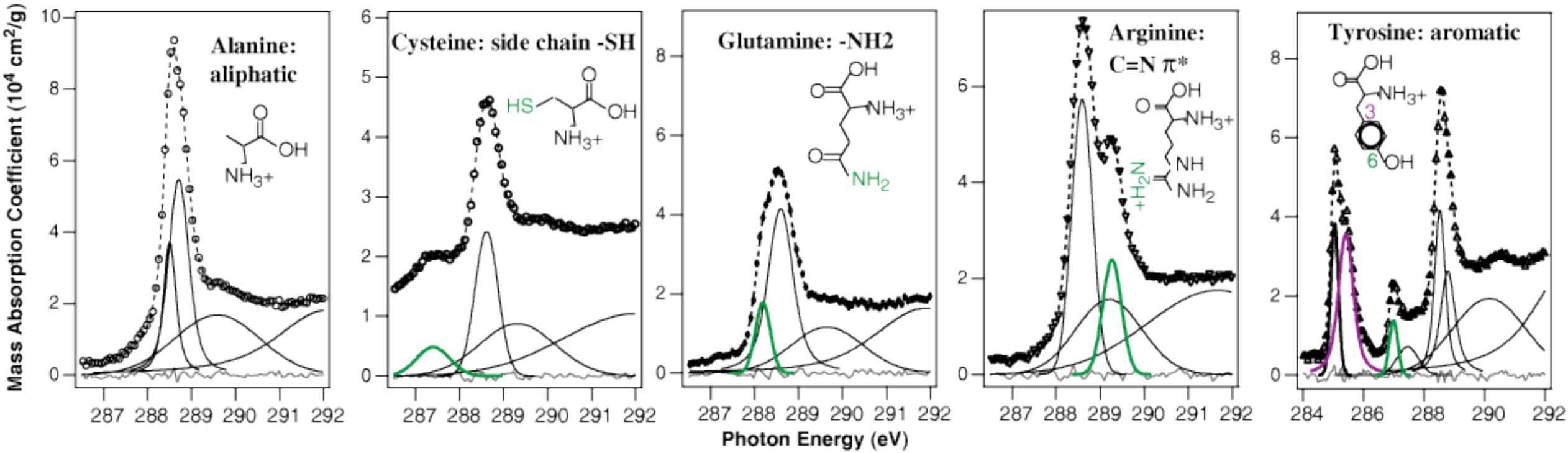

Polymers: see e.g., Dhez, Ade, and Urquhart, *JESRP* **128**, 85 (2003)

Spectromicroscopy from image sequences

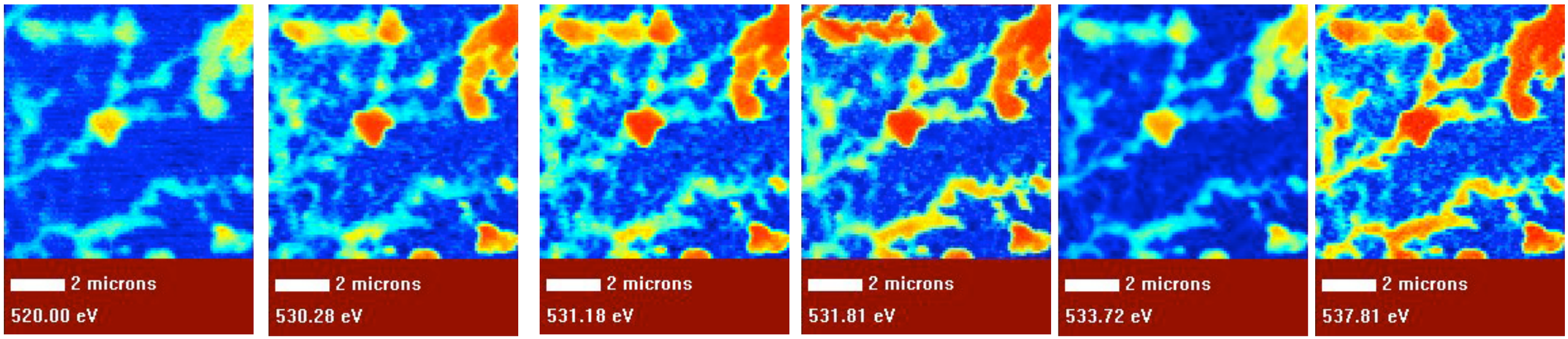

Lu in hematite (T. Schäfer)

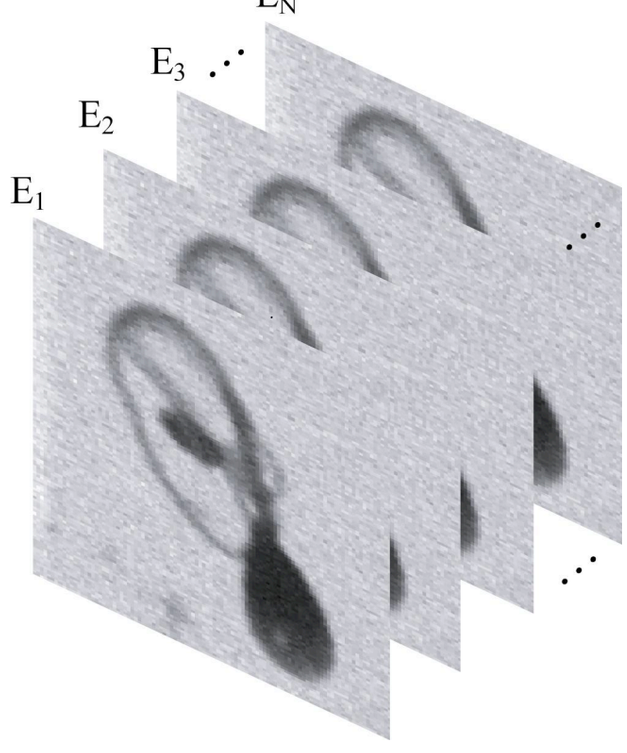

Aligned spectral image sequences: Jacobsen *et al.*, *J. Microscopy* **197**, 173 (2000)

10^4-10^5 spectra! Too many to analyze "by hand."

Complex mixtures *etc.*; life is not made up of uniform thin films.

How to deal with the complexity?

1. PCA for noise reduction, orthogonalization.
2. Cluster analysis to find patterns.
3. Non-negative matrix factorization for final analysis.

Spectromicroscopy analysis

We measure the optical density D=μt from I=I_0exp[-μt], which gives us a matrix over n=1..N energies and p=1..P pixels of the data:

$$D_{N\times P} = \begin{bmatrix} D_{11} & \text{pixels} & D_{1P} \\ \text{spectra} & & \vdots \\ D_{N1} & \dots & D_{NP} \end{bmatrix}$$

What we have

We wish we could interpret this in terms of a set of s=1..S components. We would then have a matrix of their spectra

$$\mu_{N\times S} = \begin{bmatrix} \mu_{11} & \text{components} & \mu_{1S} \\ \text{spectra} & & \vdots \\ \mu_{N1} & \dots & \mu_{NS} \end{bmatrix}$$

We would also have a matrix of their thicknesses

$$t_{S\times P} = \begin{bmatrix} t_{11} & \text{pixels} & t_{1P} \\ \text{components} & & \vdots \\ t_{S1} & \dots & t_{SP} \end{bmatrix}$$

What we wish we had

Doing the math

- We measure the data but want to interpret it as spectra times thicknesses:

$$\begin{bmatrix} D_{11} & \text{pixels} & D_{1P} \\ \text{spectra} & & \vdots \\ D_{N1} & \dots & D_{NP} \end{bmatrix} = \begin{bmatrix} \mu_{11} & \text{components} & \mu_{1S} \\ \text{spectra} & & \vdots \\ \mu_{N1} & \dots & \mu_{NS} \end{bmatrix} \cdot \begin{bmatrix} t_{11} & \text{pixels} & t_{1P} \\ \text{components} & & \vdots \\ t_{S1} & \dots & t_{SP} \end{bmatrix}$$

$$\text{or} \quad D_{N\times P} = \mu_{N\times S} \cdot t_{S\times P}$$

- If we know all S components and their spectra $\mu_{N\times S}$, we can obtain thickness maps:

$$t_{S\times P} = \mu^{-1}_{S\times N} \cdot D_{N\times P}$$

- Matrix $\mu_{N\times S}$ of all spectra can be inverted using singular matrix decomposition (SVD). See e.g., Zhang *et al.*, *J. Struct. Biol.* **116**, 335 (1996); Koprinarov *et al.*, *J. Phys. Chem. B* **106**, 5358 (2002).

What if we don't know the components or their spectra $\mu_{N\times S}$?

- "Natural" specimens, such as in biology or environmental science
- Reactive phases, rather than simple mixing
- Complexity! 300x300 pixel image contains 10^5 spectra!
- Let's reduce the complexity using principal component analysis or PCA

PCA in spectromicroscopy: King *et al.*, *J. Vac. Sci. Tech. A* **7**, 3301 (1989); A. Osanna & C. Jacobsen, XRM99 proceedings; Bonnet *et al.*, *Ultramicroscopy* **77**, 97 (1999).

Principal component analysis (PCA)

Can we find new orthogonal coordinates that better represent the data?

Scatterplot: pixels plotted based on signal at two different photon energies

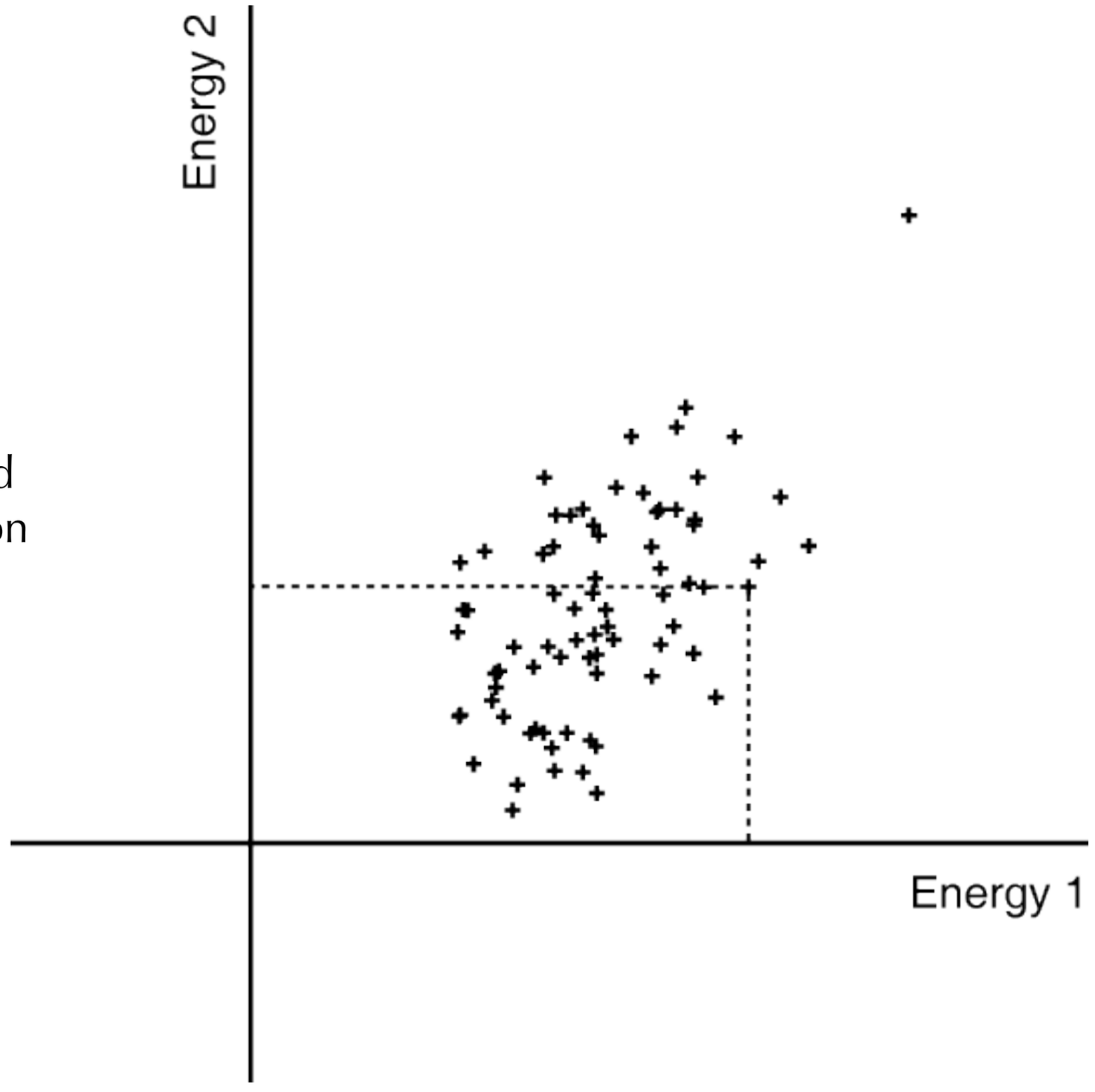

Principal component analysis (PCA)

Can we find new orthogonal coordinates that better represent the data?

1. Find the axis along which there is the greatest variance

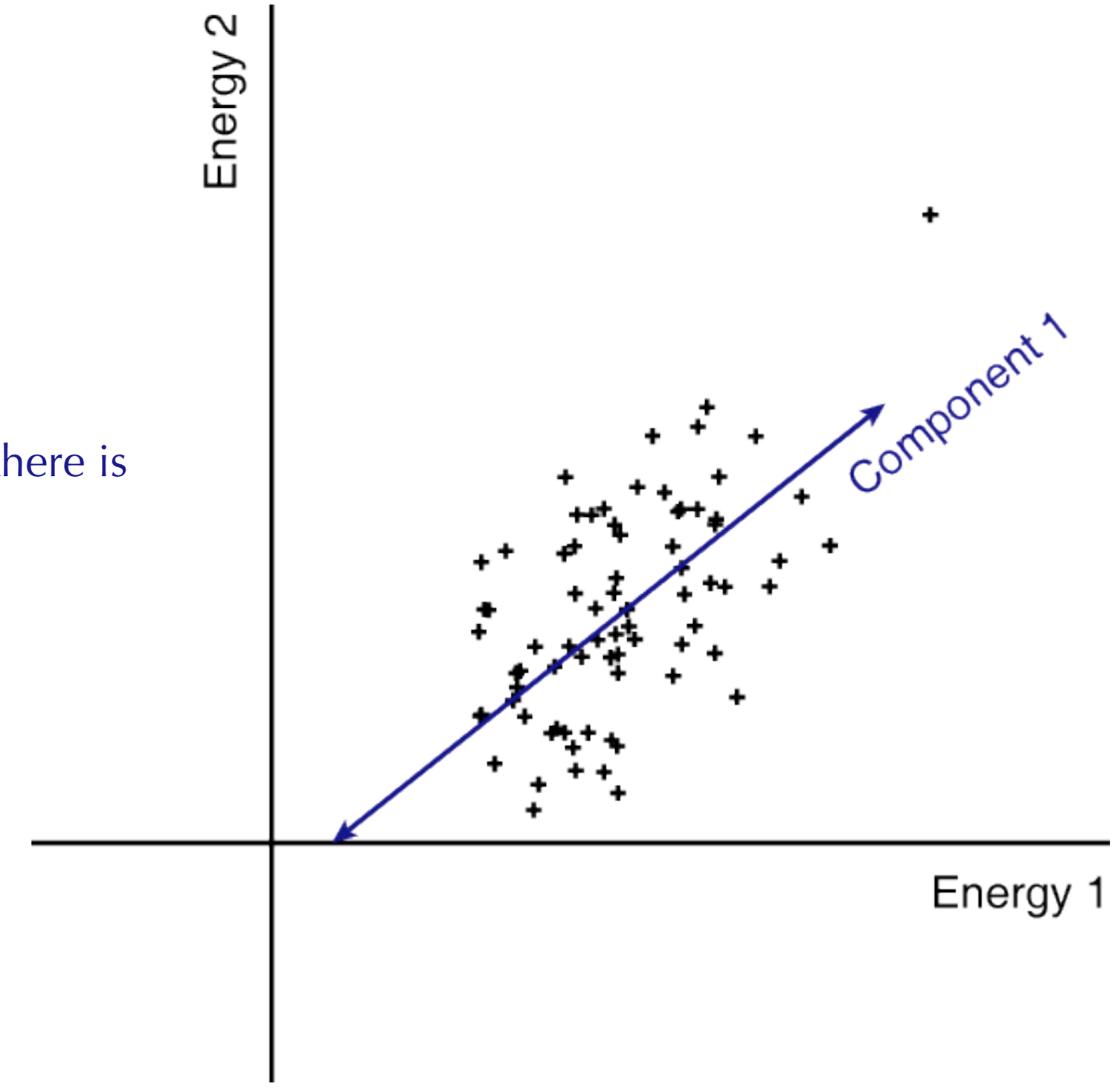

Principal component analysis (PCA)

Can we find new orthogonal coordinates that better represent the data?

1. Find the axis along which there is the greatest variance
2. Find an orthogonal axis of next greatest variance

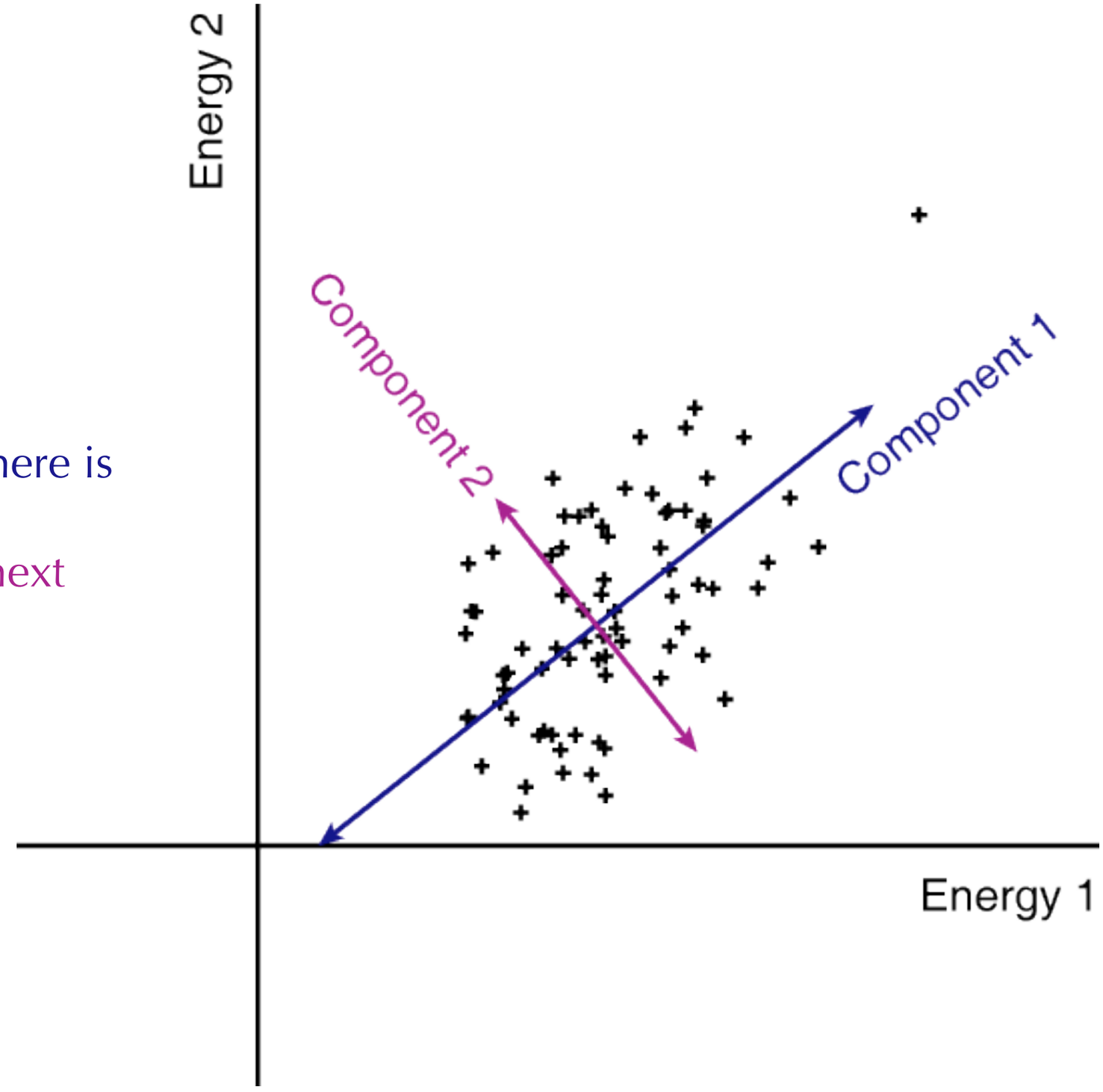

Principal component analysis (PCA)

Can we find new orthogonal coordinates that better represent the data?

1. Find the axis along which there is the greatest variance
2. Find an orthogonal axis of next greatest variance
3. Gives a new coordinate system

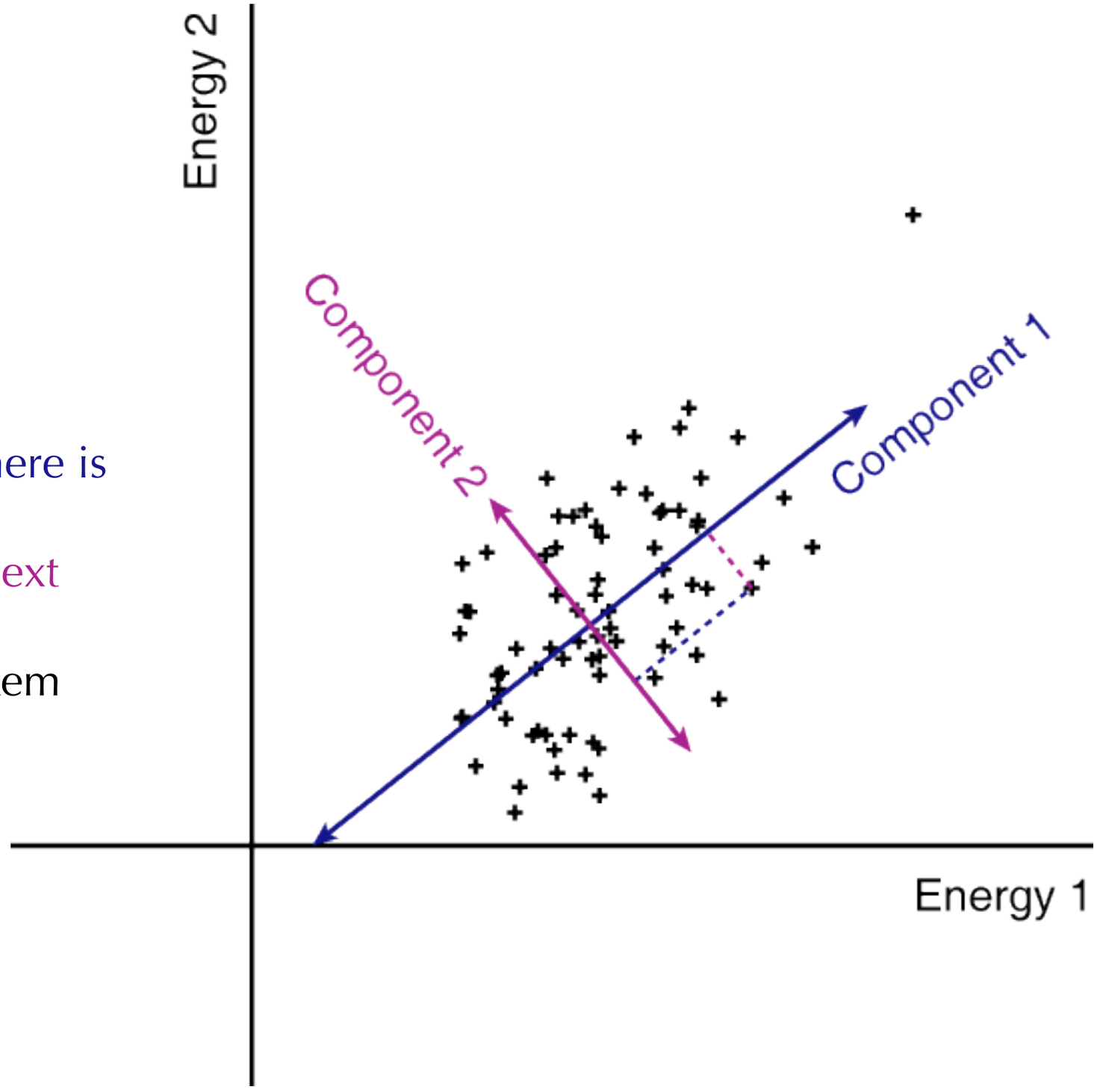

Principal component analysis (PCA)

Can we find new orthogonal coordinates that better represent the data?

1. Find the axis along which there is the greatest variance
2. Find an orthogonal axis of next greatest variance
3. Gives a new coordinate system
4. Rotate onto new, orthogonal coordinate system

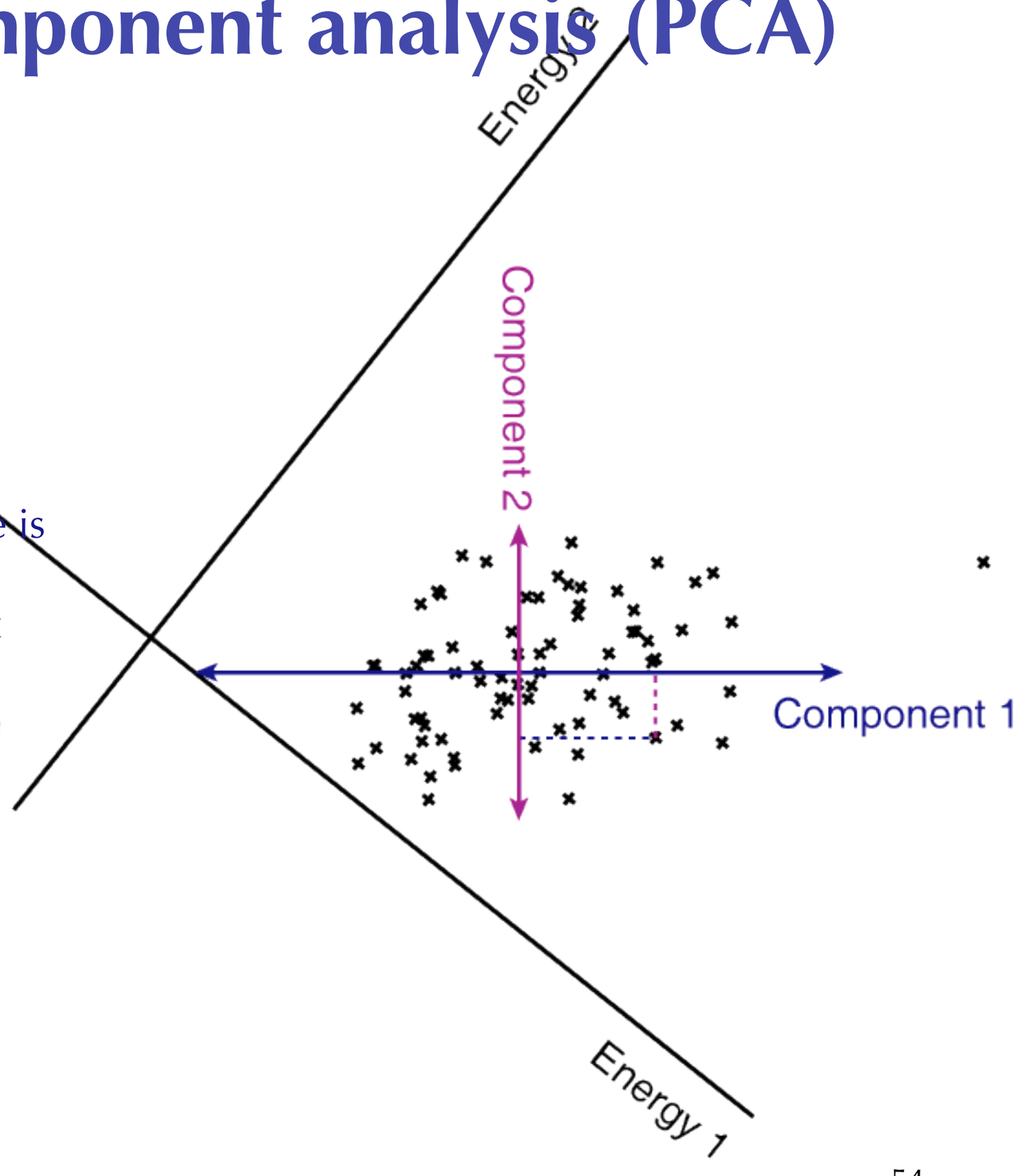

PCA and factor compression

For an abstract component: contribution is singular value times singular spectrum

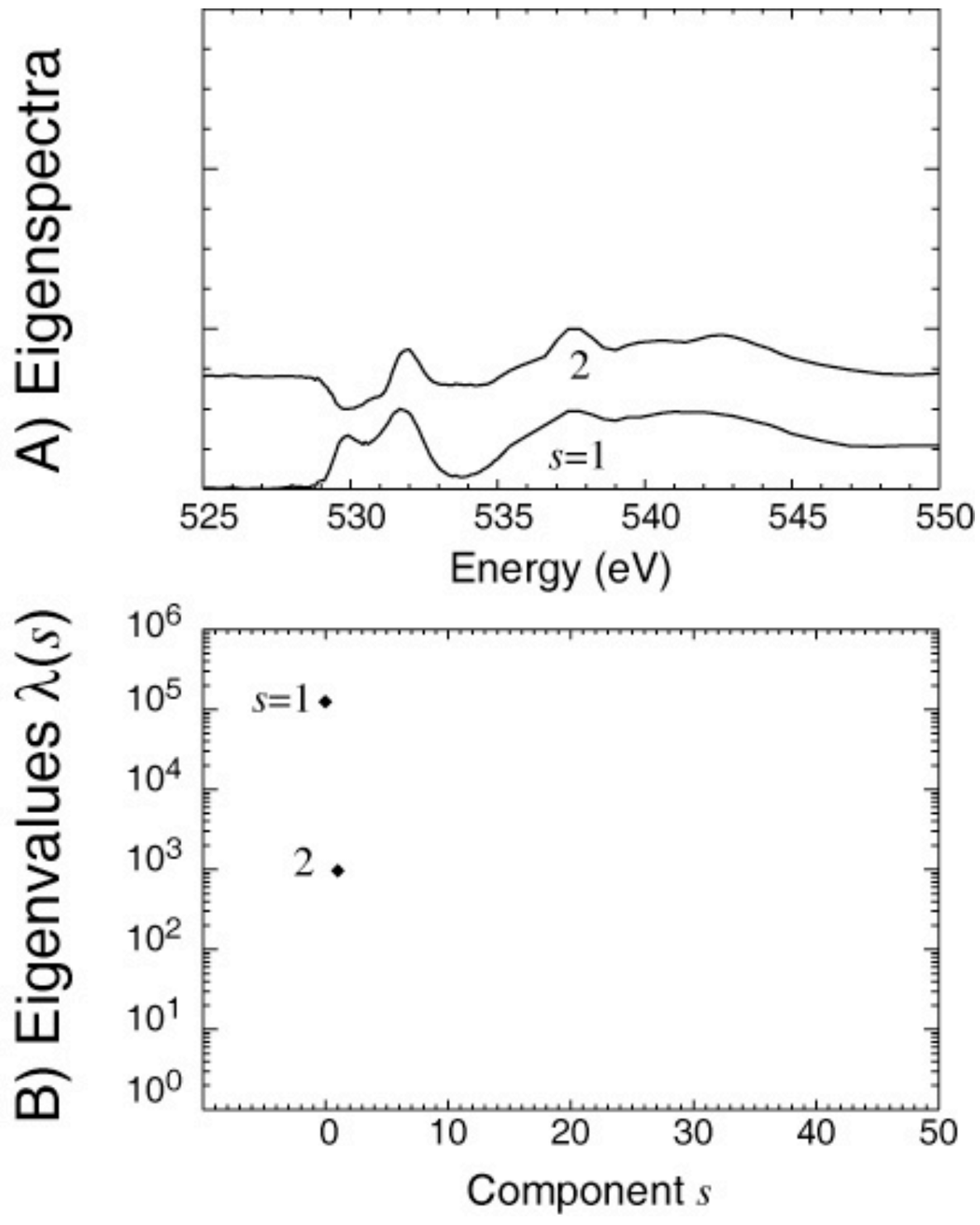

Find reduced number of **significant** components $\overline{S}_{abstract}$

PCA and factor compression

For an abstract component: contribution is singular value times singular spectrum

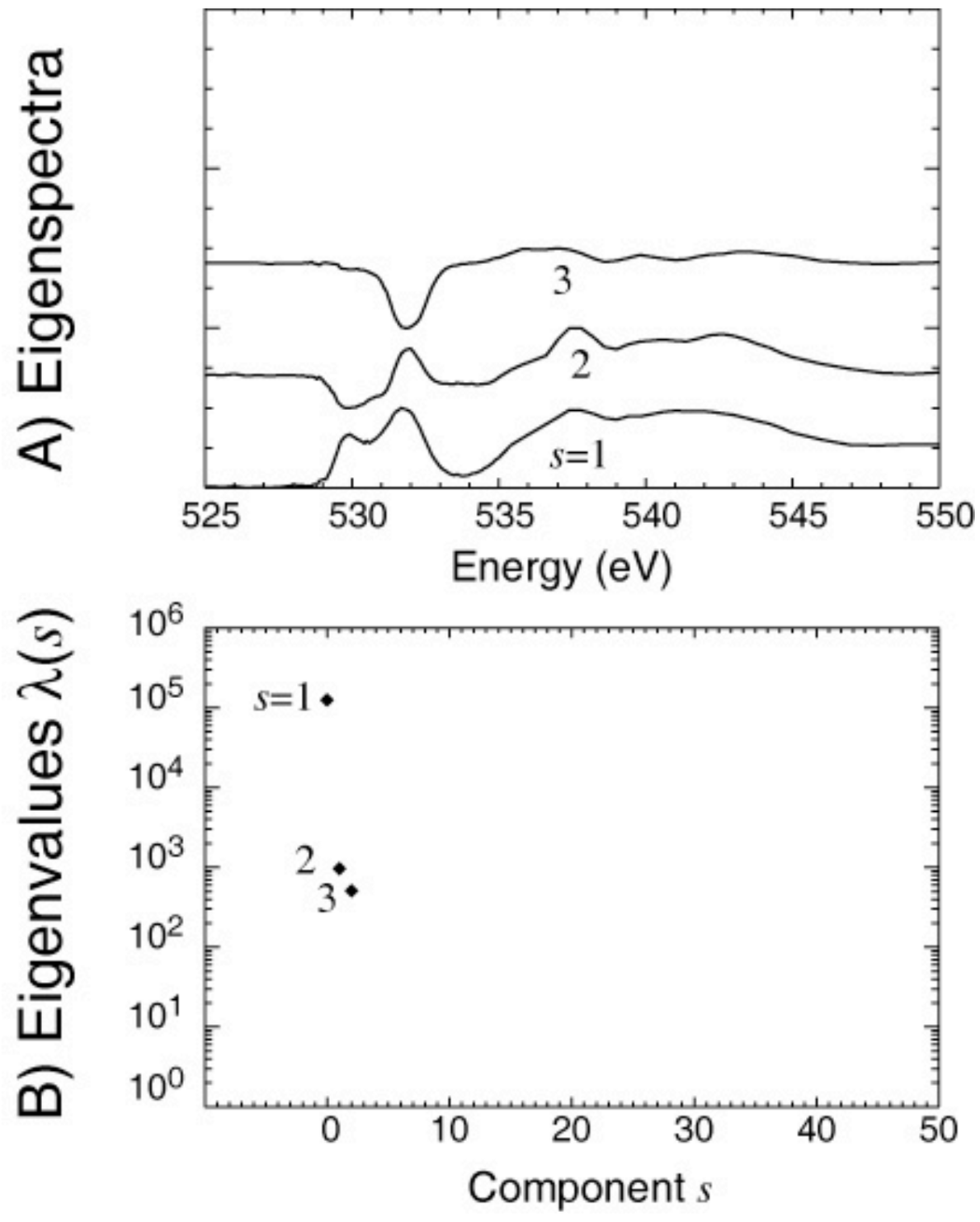

Find reduced number of **significant** components $\overline{S}_{abstract}$

PCA and factor compression

For an abstract component: contribution is singular value times singular spectrum

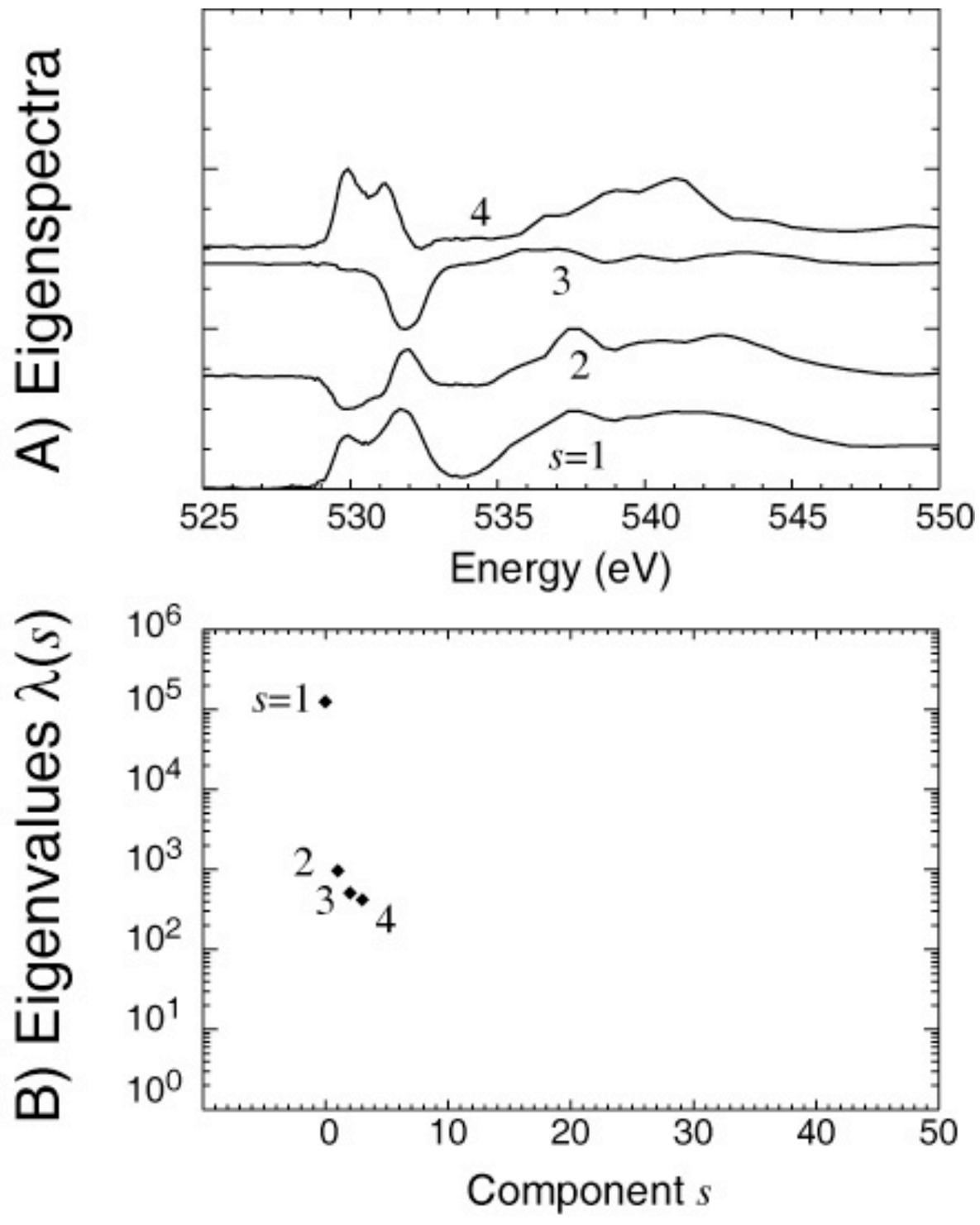

Find reduced number of **significant** components $\overline{S}_{abstract}$

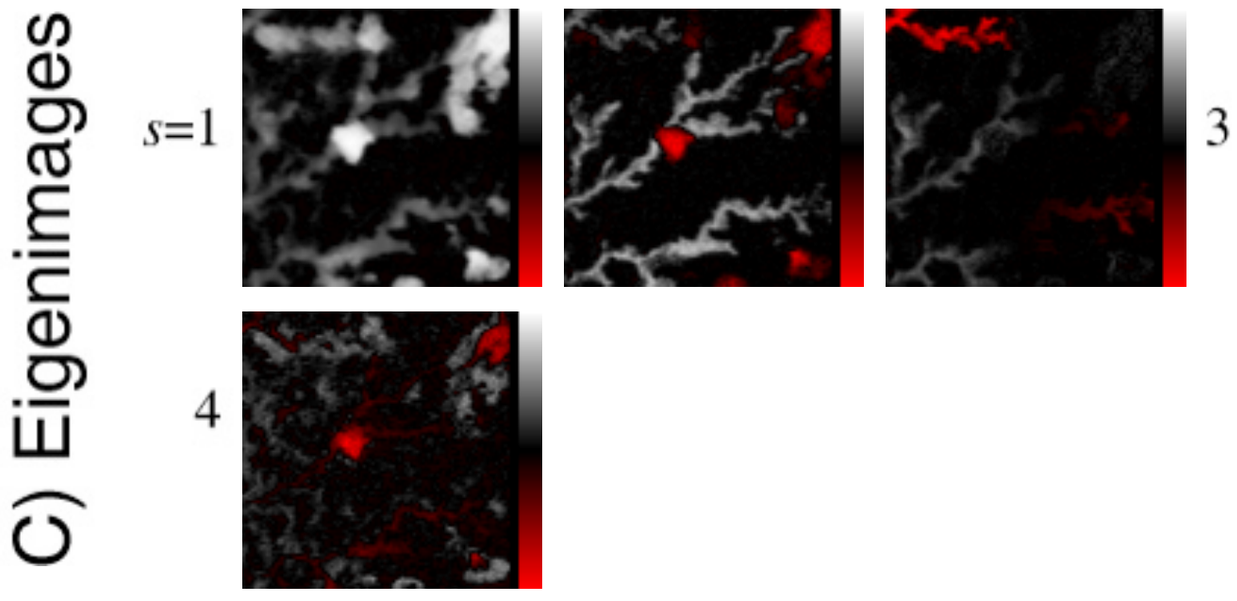

PCA and factor compression

For an abstract component: contribution is singular value times singular spectrum

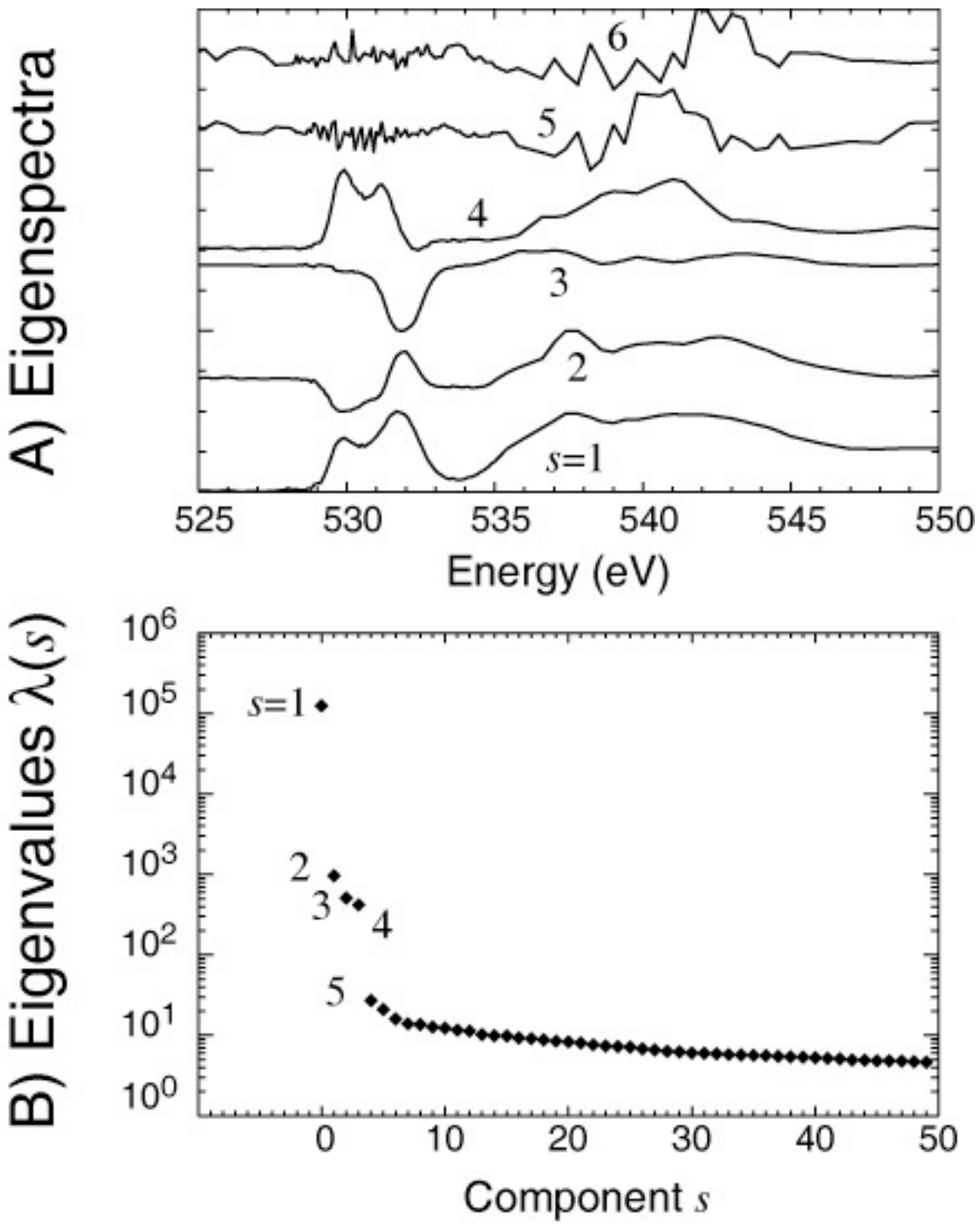

Find reduced number of **significant** components $\overline{S}_{abstract}$

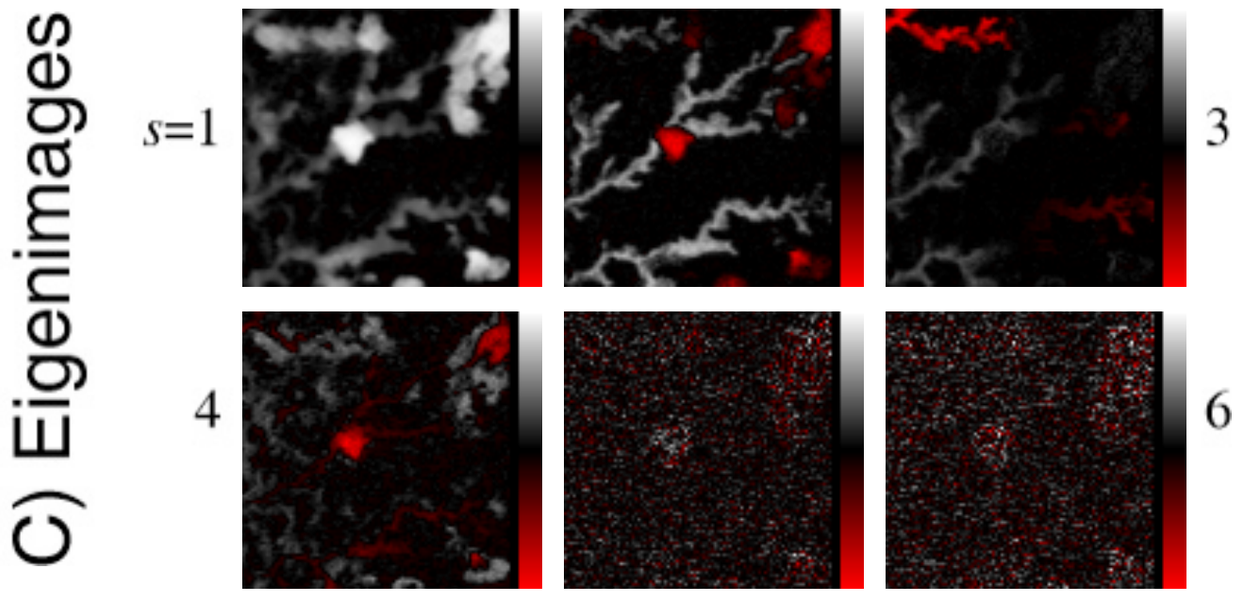

Eigenimages

1

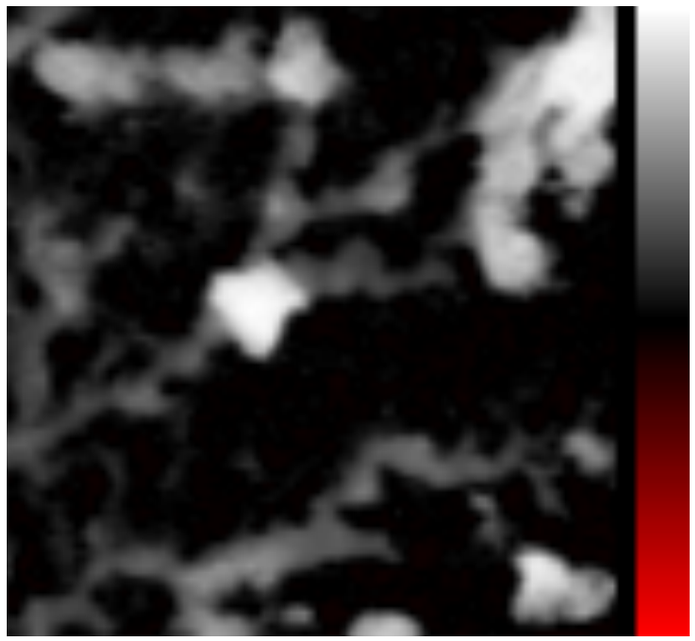

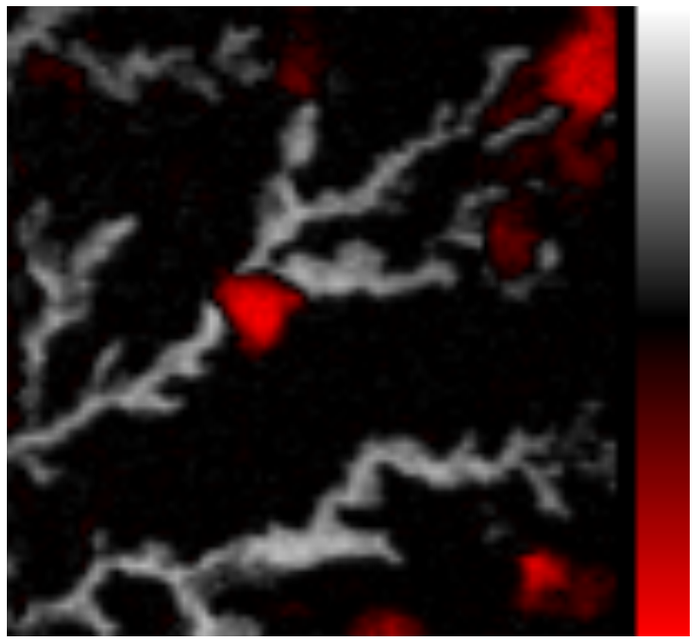

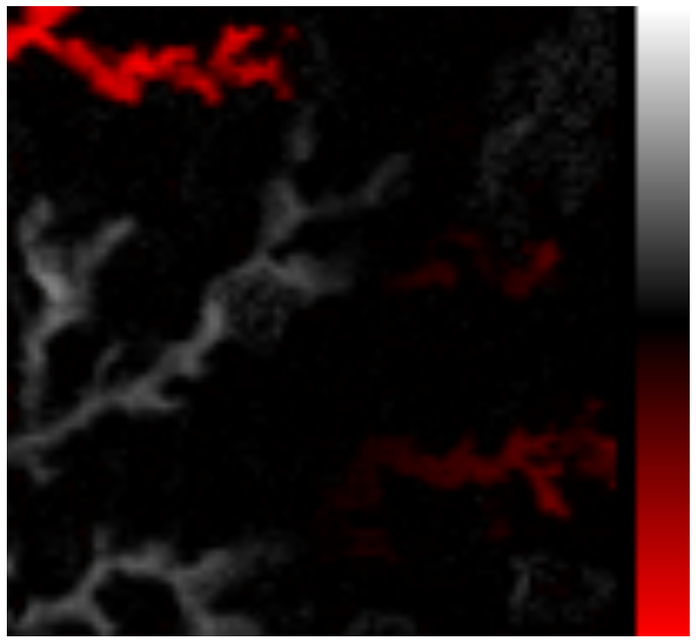

3

4

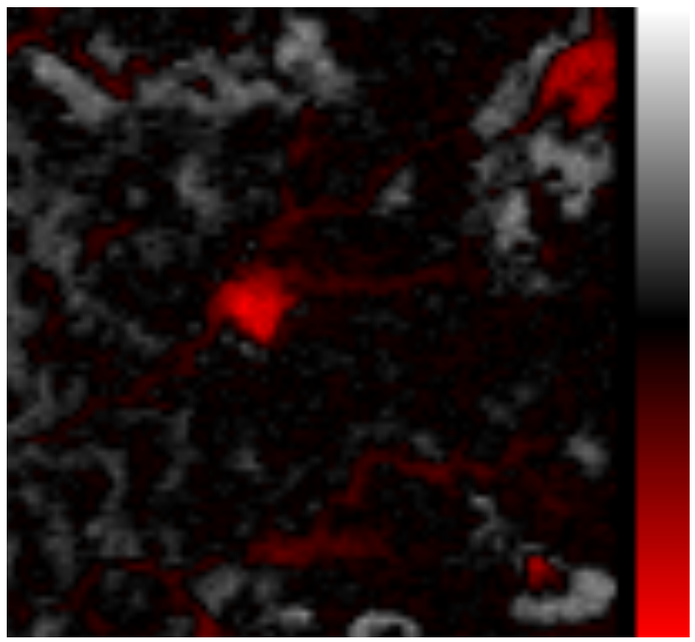

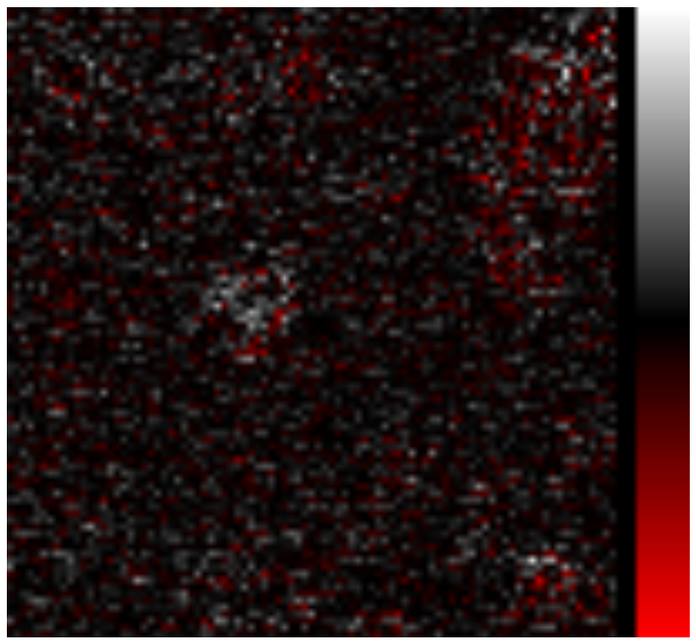

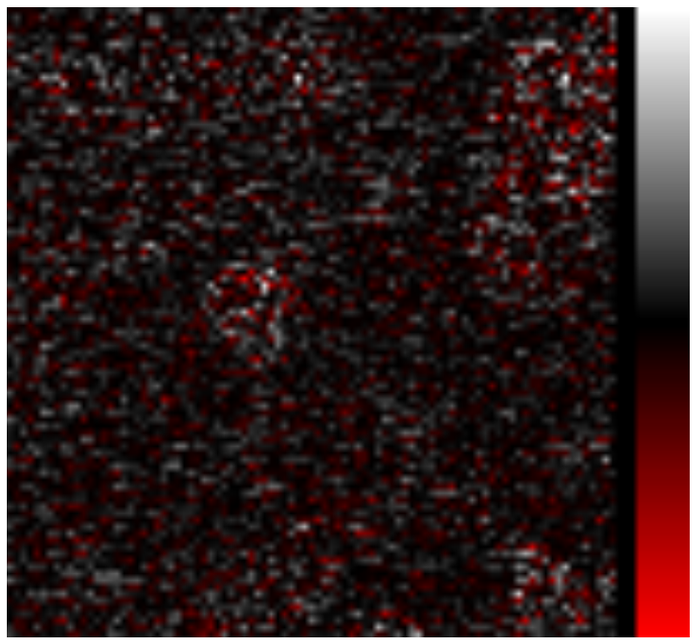

6

PCA gets us *something*…

- Principal component analysis lets you reduce and orthogonalize the data set!
- Reduction: filter out spectral variations that are poorly correlated throughout the dataset (smells like photon noise!). We went from N=140 energies to $\bar{S}_{\text{abstract}}$=4 components
- Orthogonality might have nice consequences

But we have a problem…

- Eigenspectra > 1 are abstract. They have negative optical densities, so they are not readily interpretable.
- "Rotating" eigenspectra to make them positive is not always sufficient; can have more distinct mixtures than eigenspectra.

A well-known problem

We chose to follow an approach which is well known in the literature:

"You can't always get what you want; but if you try sometimes, well you just might find you get what you need"

M. Jagger, K. Richards *et al.*, *Let it Bleed* **1**, 1 (1969)

Cluster analysis: Euclidian distance learning algorithm

- Kohonen, *Proc. IEEE* **78**, 1464 (1990)
- Pixels are scattered according to weighting of each component

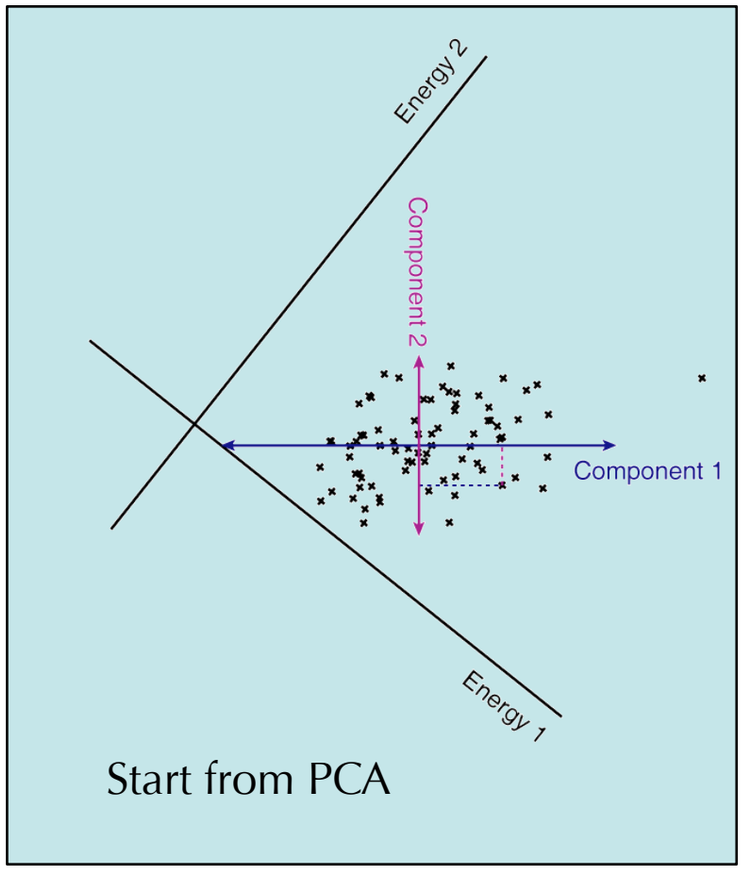

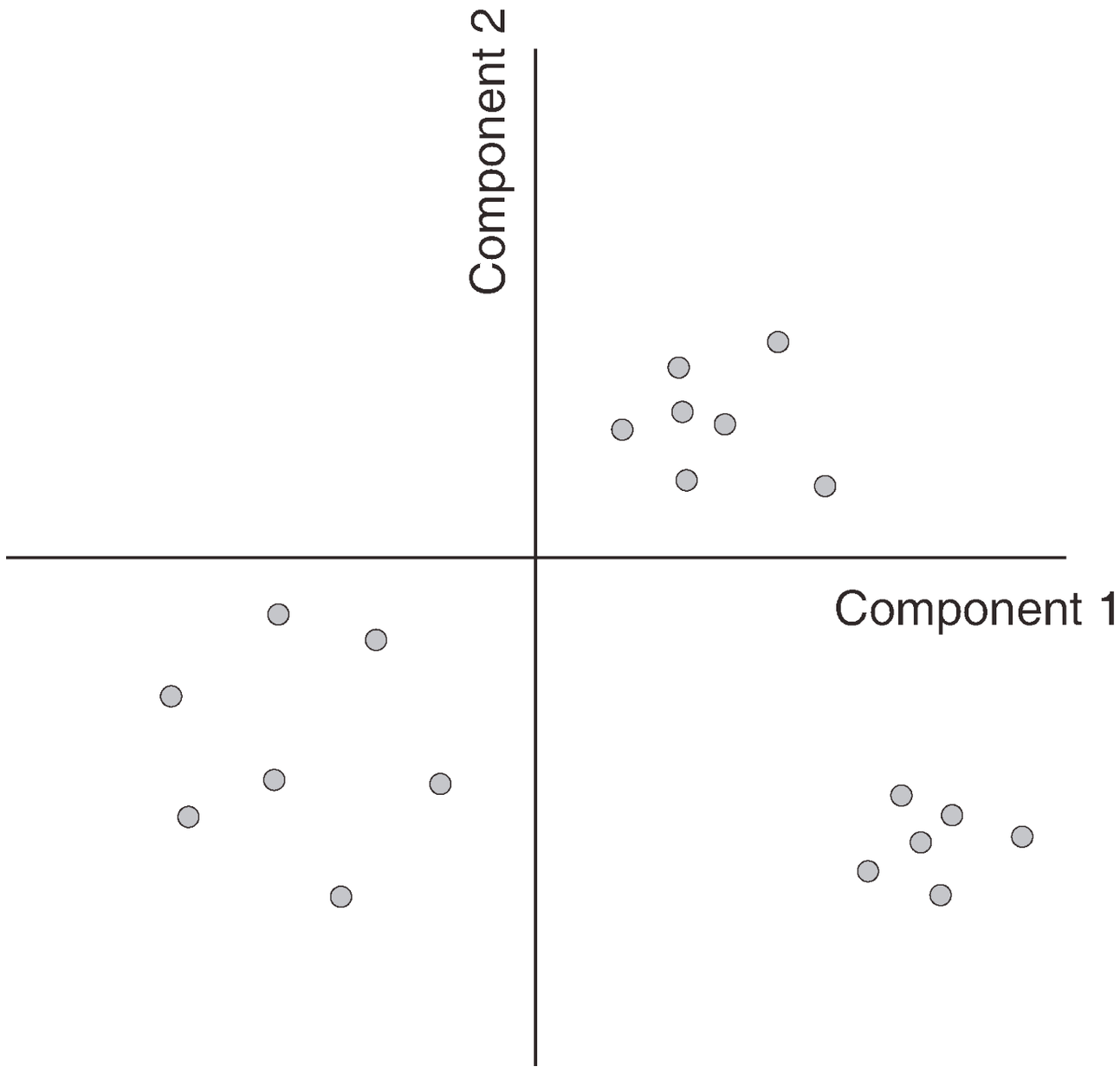

Cluster analysis: Euclidian distance learning algorithm

- Kohonen, *Proc. IEEE* **78**, 1464 (1990)
- Pixels are scattered according to weighting of each component
- Put down cluster centers at random positions.

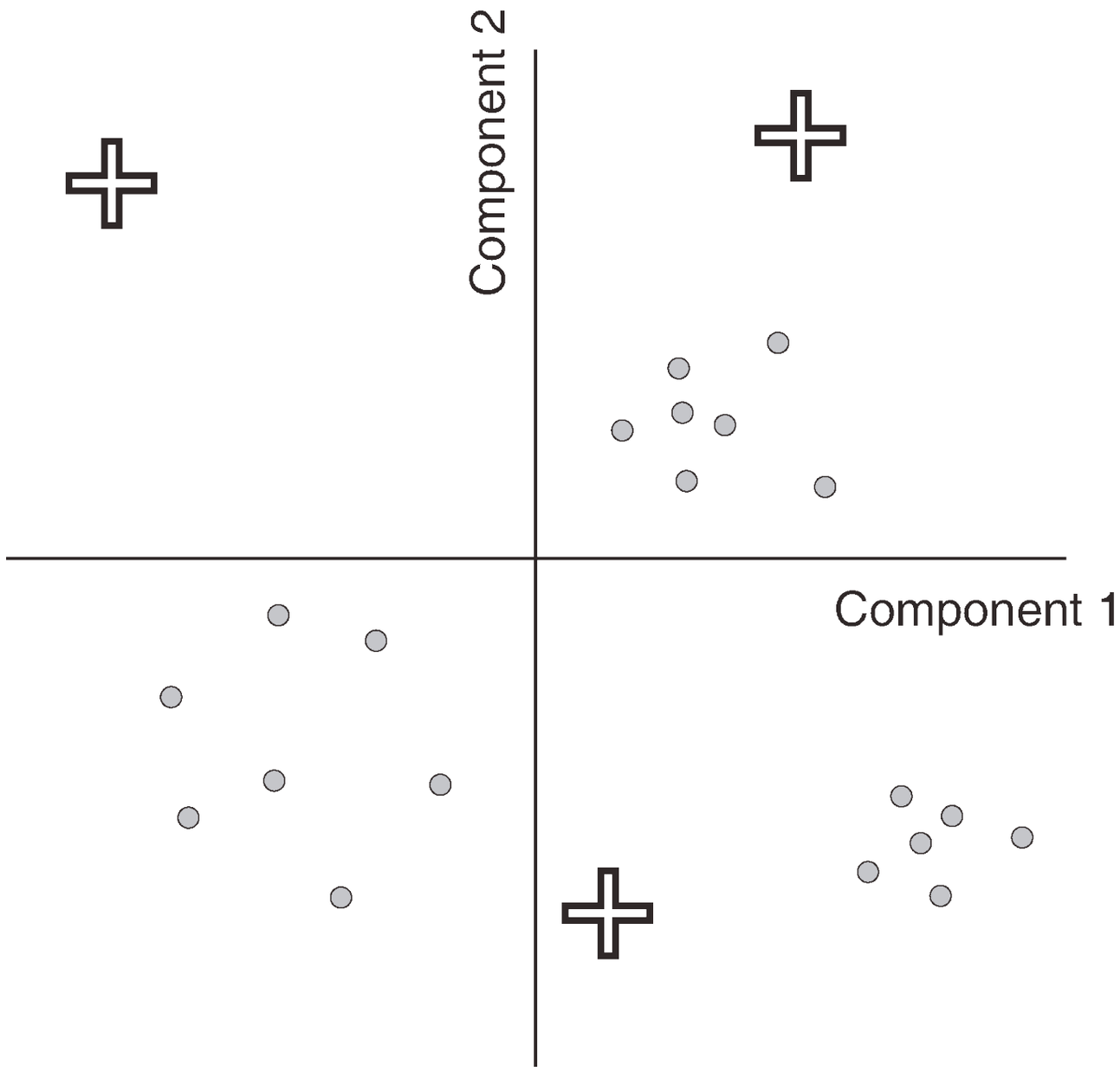

Cluster analysis: Euclidian distance learning algorithm

- Kohonen, *Proc. IEEE* **78**, 1464 (1990)
- Pixels are scattered according to weighting of each component
- Put down cluster centers at random positions.
- Iterate through all pixels, several times:
  - Calculate distances from one pixel to all cluster centers.

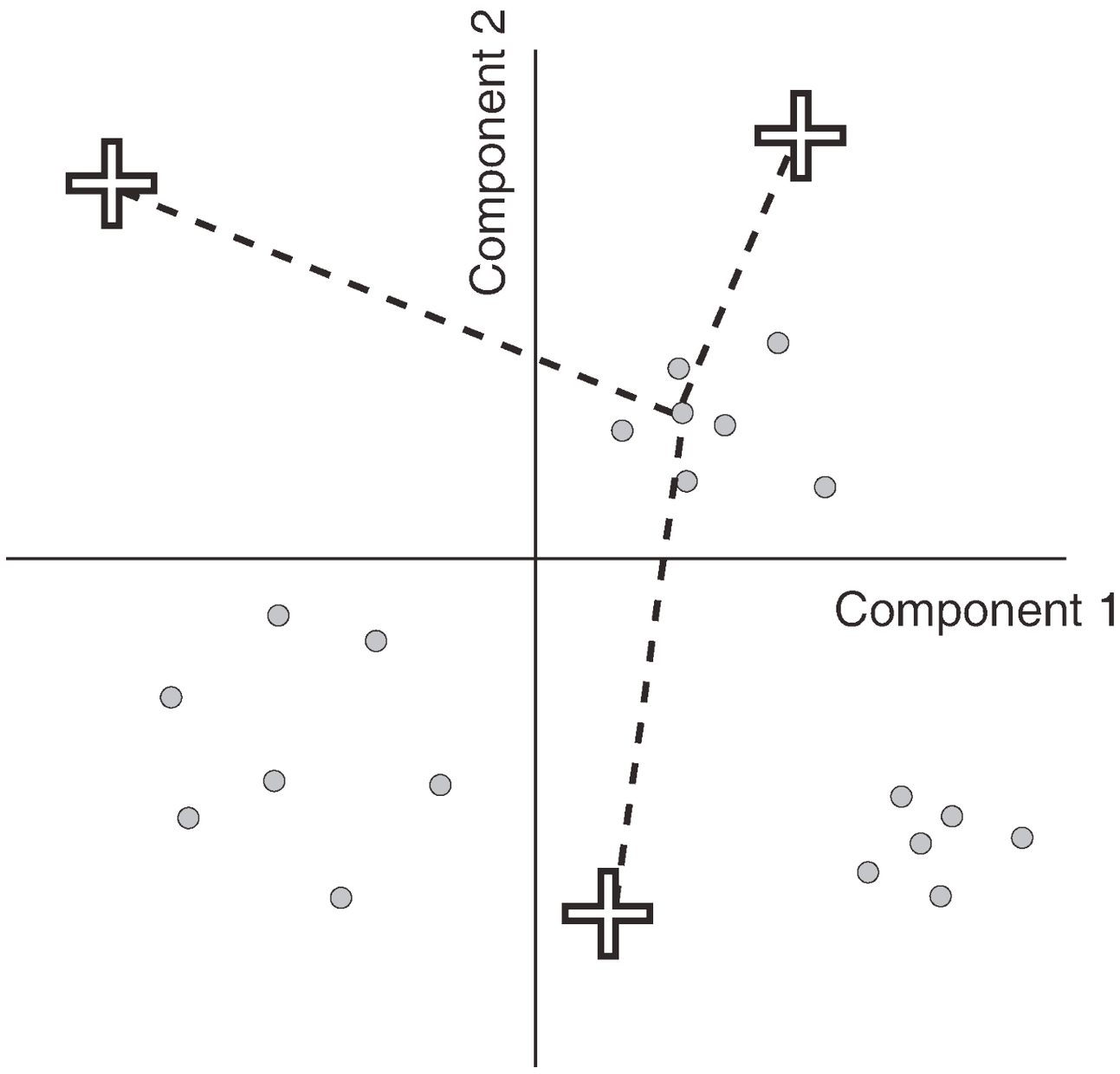

Cluster analysis: Euclidian distance learning algorithm

- Kohonen, *Proc. IEEE* **78**, 1464 (1990)
- Pixels are scattered according to weighting of each component
- Put down cluster centers at random positions.
- Iterate through all pixels, several times:
  - Calculate distances from one pixel to all cluster centers.
  - Pick shortest distance.
  - Move cluster center partway to pixel.

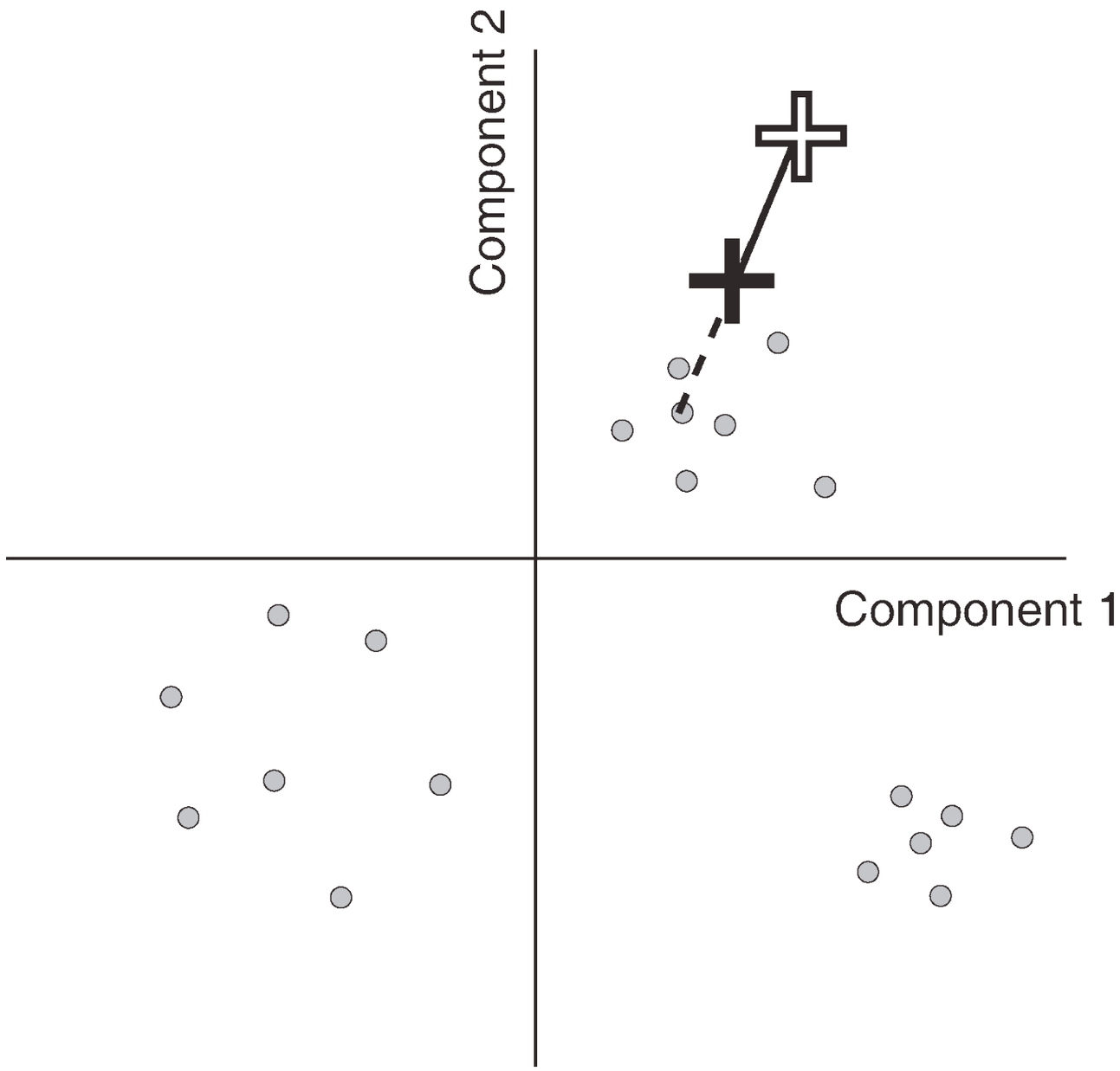

Cluster analysis: Euclidian distance learning algorithm

- Kohonen, *Proc. IEEE* **78**, 1464 (1990)
- Pixels are scattered according to weighting of each component
- Put down cluster centers at random positions.
- Iterate through all pixels, several times:
  - Calculate distances from one pixel to all cluster centers.
  - Pick shortest distance.
  - Move cluster center partway to pixel.
- Cluster pixels with their nearest cluster center

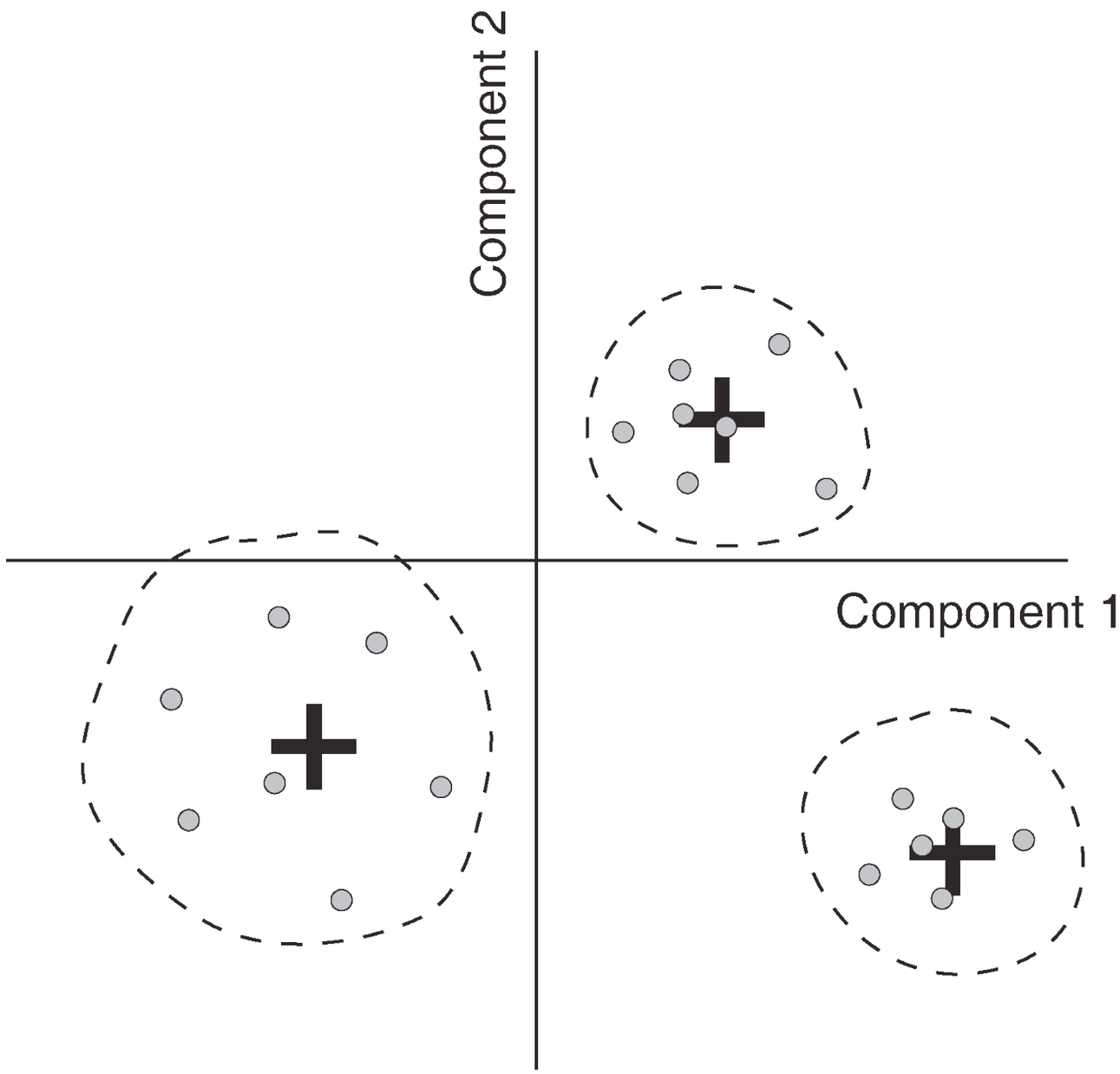

Cluster analysis: Lu in hæmatite

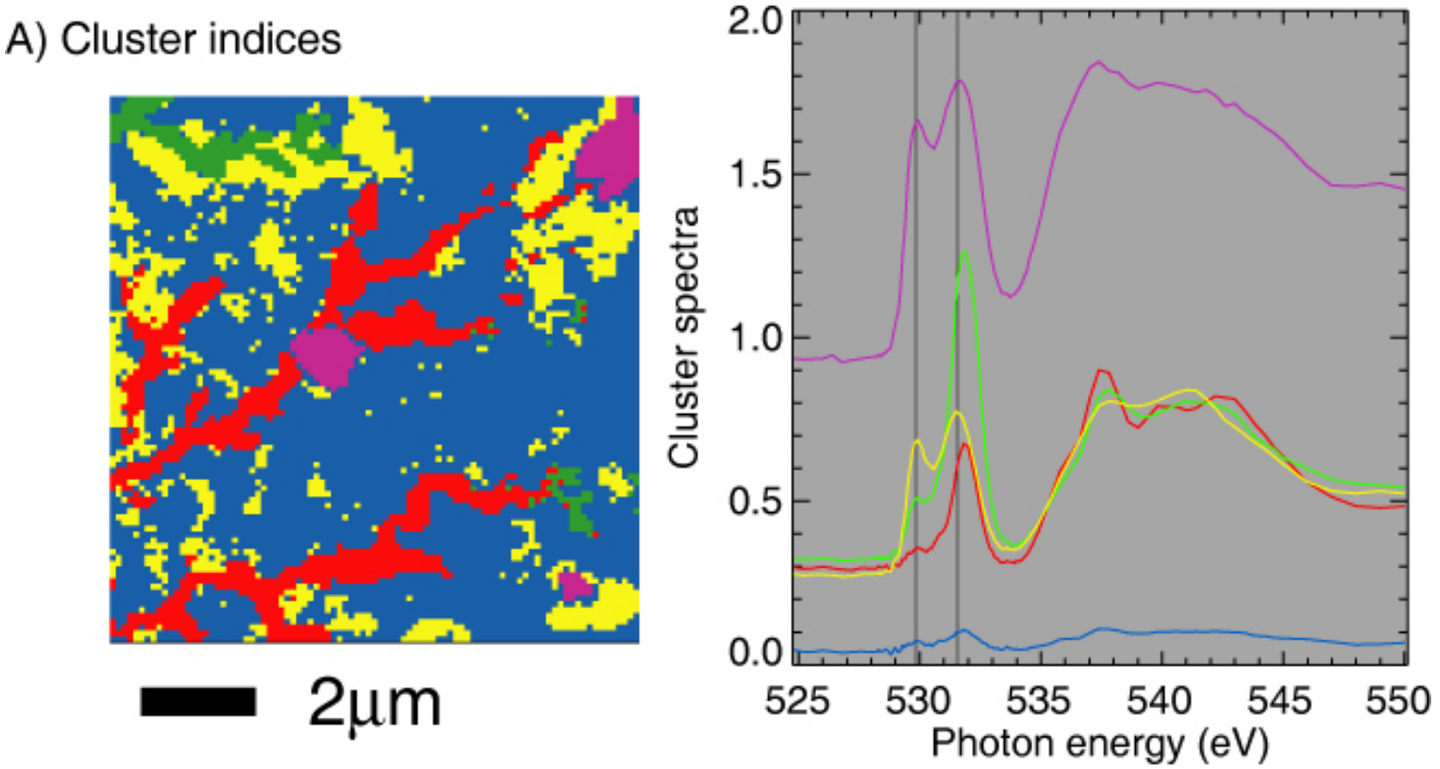

cluster 1

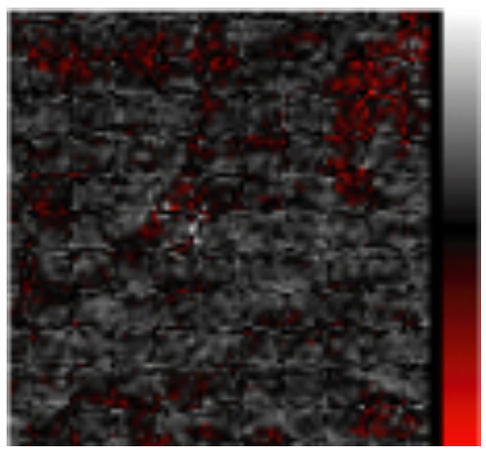

cluster 2

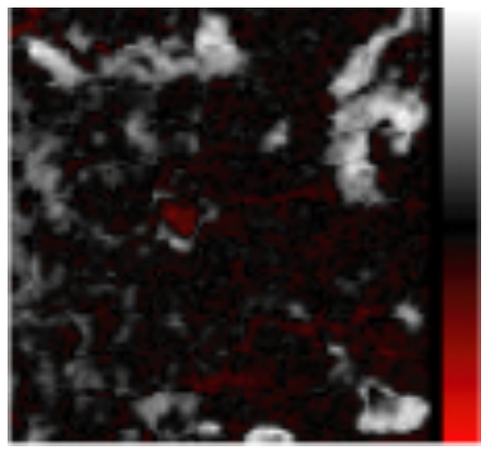

- Lu as a stand-in for Am in nuclear wastes; hæmatite can be a groundwater colloid that increases transport rate 1000x
- Oxygen XANES shows two different incorporation phases of Lu in hæmatite (clusters 2 and 5)
- Lerotic, Jacobsen, Schäfer, Vogt, *Ultramic*. **100**, 35 (2004)

cluster 3

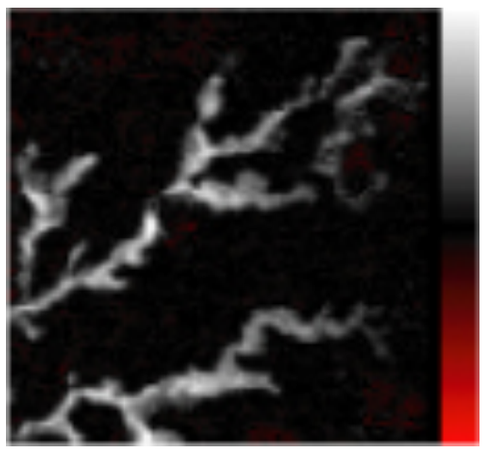

cluster 4

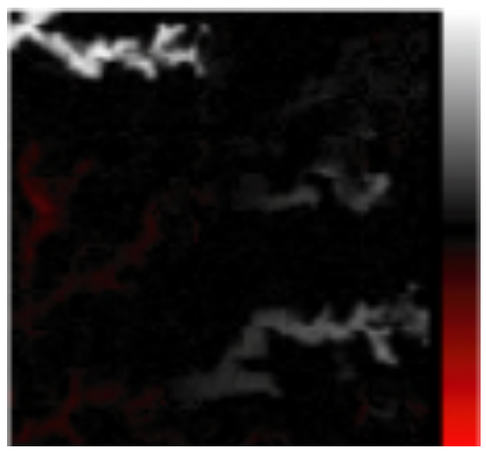

cluster 5

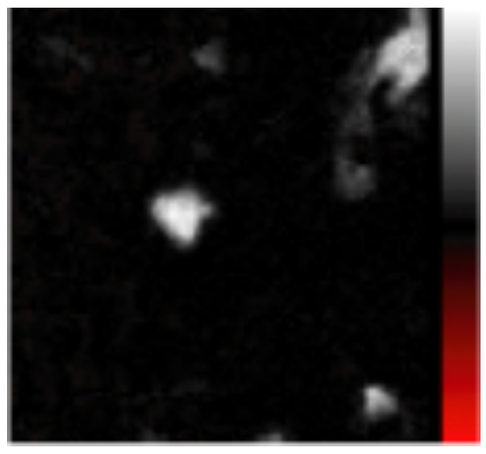

Red spots: negative values, because cluster spectra are not guaranteed to "span the set"

Cluster analysis: simplifying complexity

- Ethanol from lignocellulose materials is promising: large fraction of total biomass, easier cultivation.
- But there are great challenges in economically separating cellulose from lignin!
- Soft x-ray spectromicroscopy can map cellulose and lignin so that one can see the effects of various enzymes.

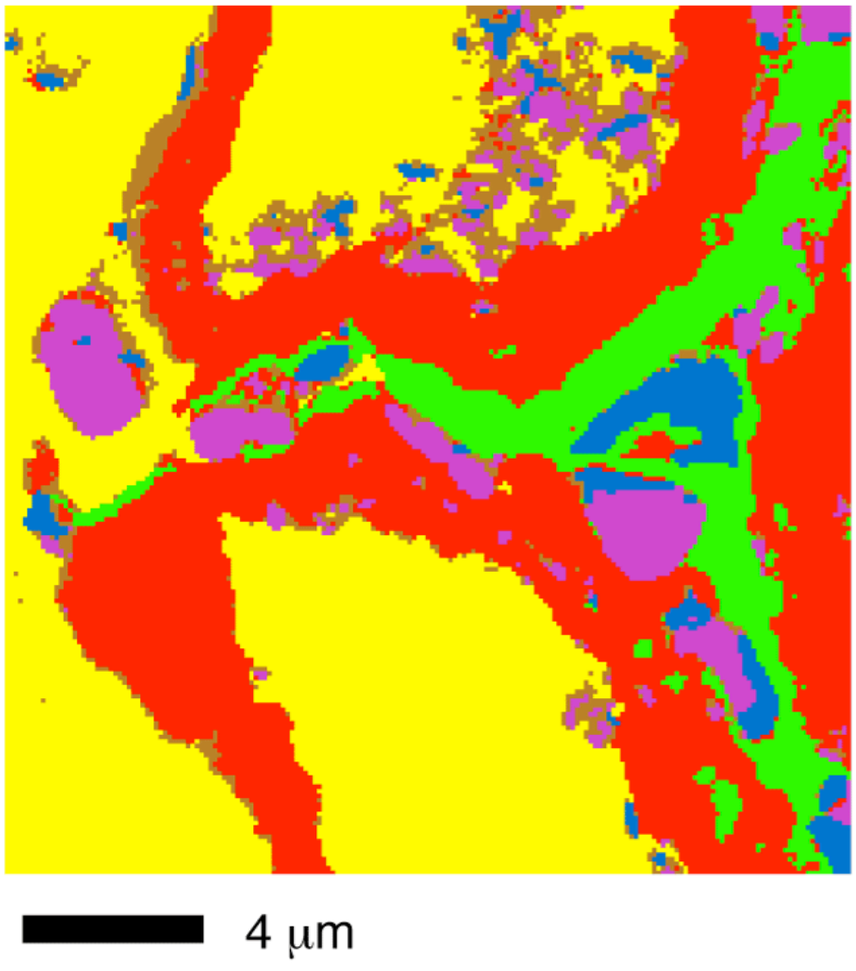

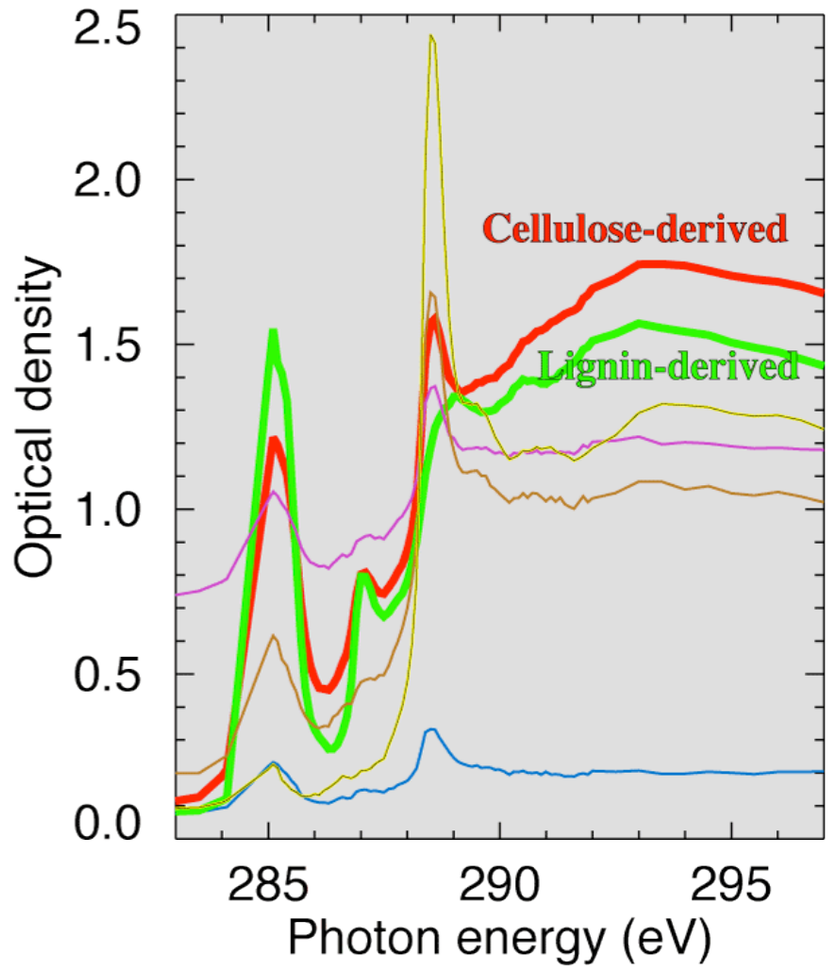

Lignin and cellulose in 400 million year old chert: Boyce *et al.*, *Proc. Nat. Acad. Sci.* **101**, 17555 (2004), with subsequent pattern recognition analysis by Lerotic *et al.*, *Ultramicroscopy* **100**, 35 (2004).

Cluster analysis: human sperm

Biochemical organization of sperm revealed directly from data: enzyme-rich region, DNA+histones, mitochondria and flagellar motor, lipid

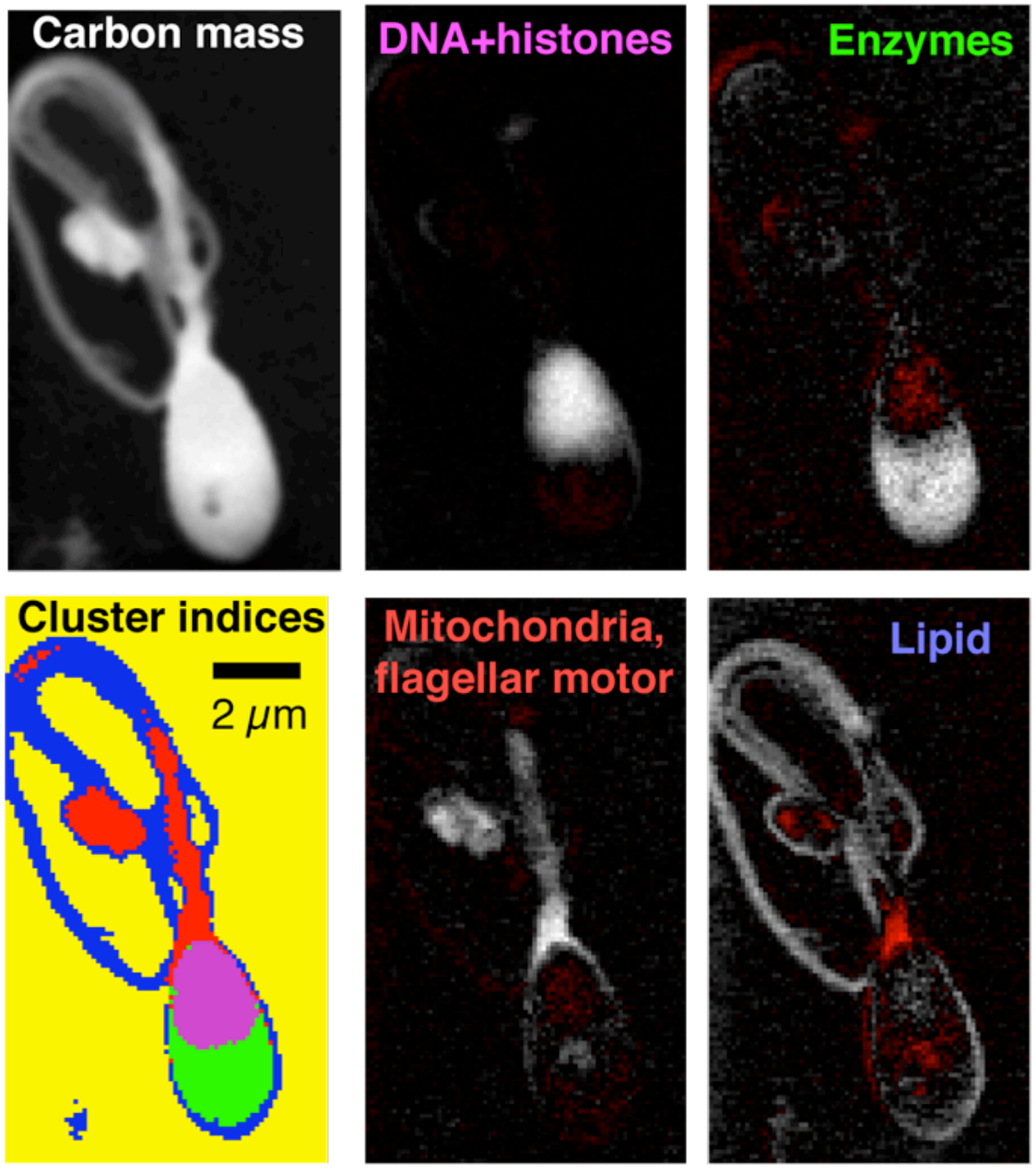

H. Fleckenstein, M. Lerotic, Y. Sheynkin *et al.*, Stony Brook. Human sperm, air-dried.

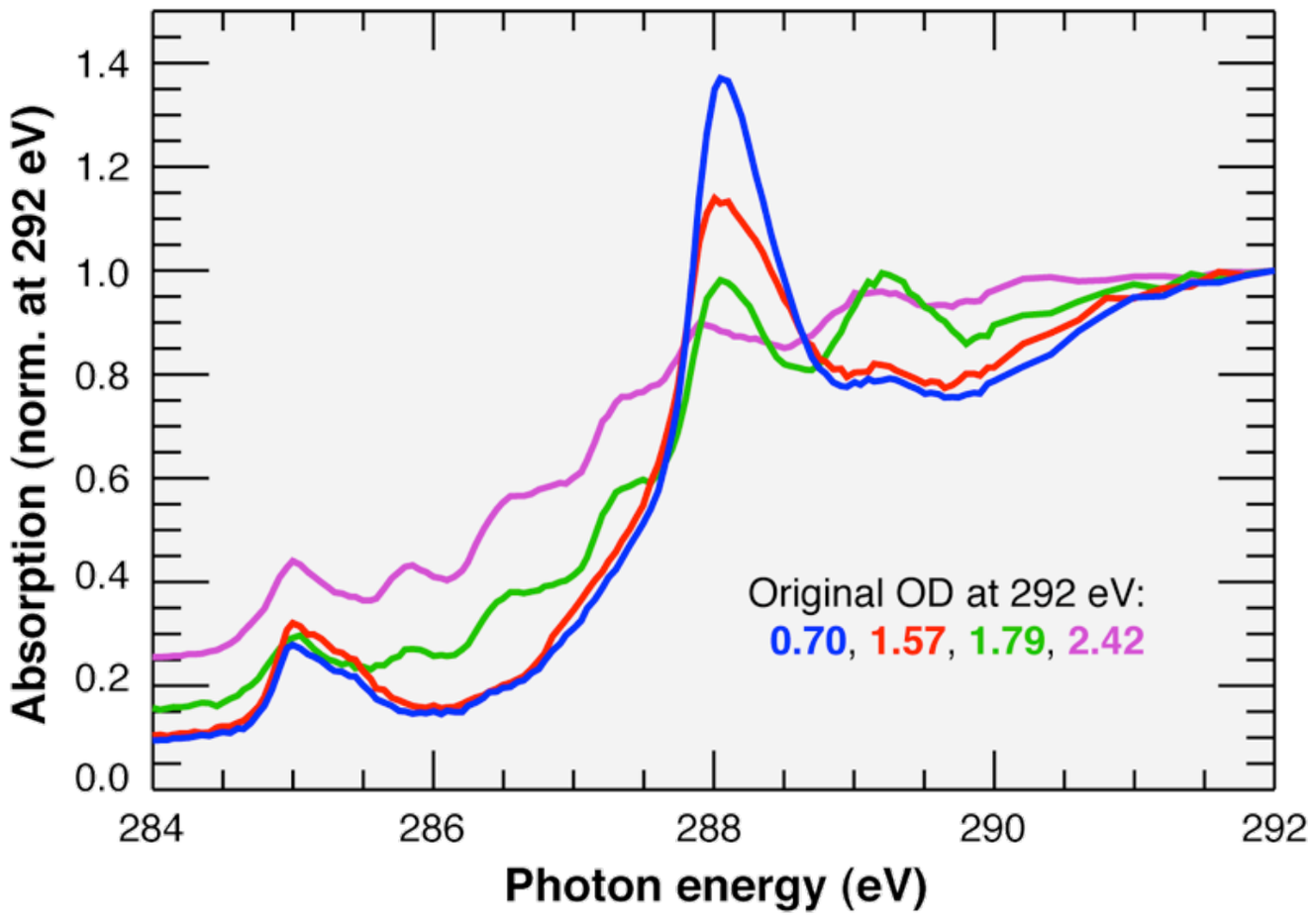

Red spots: negative values, because cluster spectra are not guaranteed to "span the set"

Spectromicroscopy can be damaging!

- Study: polyacrilimide-induced flocculation of clays (irrigation of loamy soils)
- Mass loss is visible after acquiring spectra with focused beam (wet sample at room temperature)
- U. Neuhaeusler, PhD Thesis (Stony Brook/Göttingen)

Calculating dose

- SI units for ionizing radiation: 1 Gray=1 J/kg=100 rad
- Lambert-Beer law with inverse absorption length μ(=1.3 mm for protein at 8.98 keV):

$$I = I_0 e^{-\mu x} \qquad \text{with} \qquad \mu = 2\frac{\rho N_A}{A} r_e \lambda f_2$$

- Energy per thickness:

$$\frac{dE}{dx} = h\nu \frac{dI}{dx} = h\nu\, \mu\, I_0 e^{-\mu \cdot 0} = I_0\, h\nu\, \mu$$

- Energy per mass:

$$\frac{dE}{dm} = \frac{dE}{dx}\frac{1}{\text{Area} \cdot \rho} = h\nu\, \mu\, I_0 \frac{1}{\text{Area} \cdot \rho} = h\nu\, \frac{I_0\, \mu}{\text{Area} \cdot \rho}$$

Dose numbers

- G factor: number of bonds broken per 100 eV. G~5 for many organic molecules (room temp.)
- Break 1 bond per atom:

$$\frac{(20\ \text{eV/atom}) \cdot (N_A\ \text{atoms/mol}) \cdot (1.6 \times 10^{-19}\ \text{J/eV})}{(12\ \text{g/mol}) \cdot (10^{-3}\ \text{kg/g})} = 1.6 \times 10^{8}\ \text{Gray}$$

- Representative dose in crystallography:

$$\frac{10^{14}\ \text{photons}}{(50\ \mu\text{m})^2} \frac{(8979\ \text{eV/photon}) \cdot (1.6 \times 10^{-19}\ \text{J/ev})}{(1300\ \mu\text{m}) \cdot (1.35\ \text{g/cm}^3) \cdot (10^{-4}\ \text{cm}/\mu\text{m})^3 \cdot (10^{-3}\ \text{kg/g})} = 3.3 \times 10^{7}\ \text{Gray}$$

- X-ray microscopy: doses of 10^6-10^8 Gray are common, depending on resolution

X-ray absorption: the aftermath

Primary electrons undergo multiple inelastic collisions

Continuous slowing down approximation (CSDA): range over which majority of energy is deposited

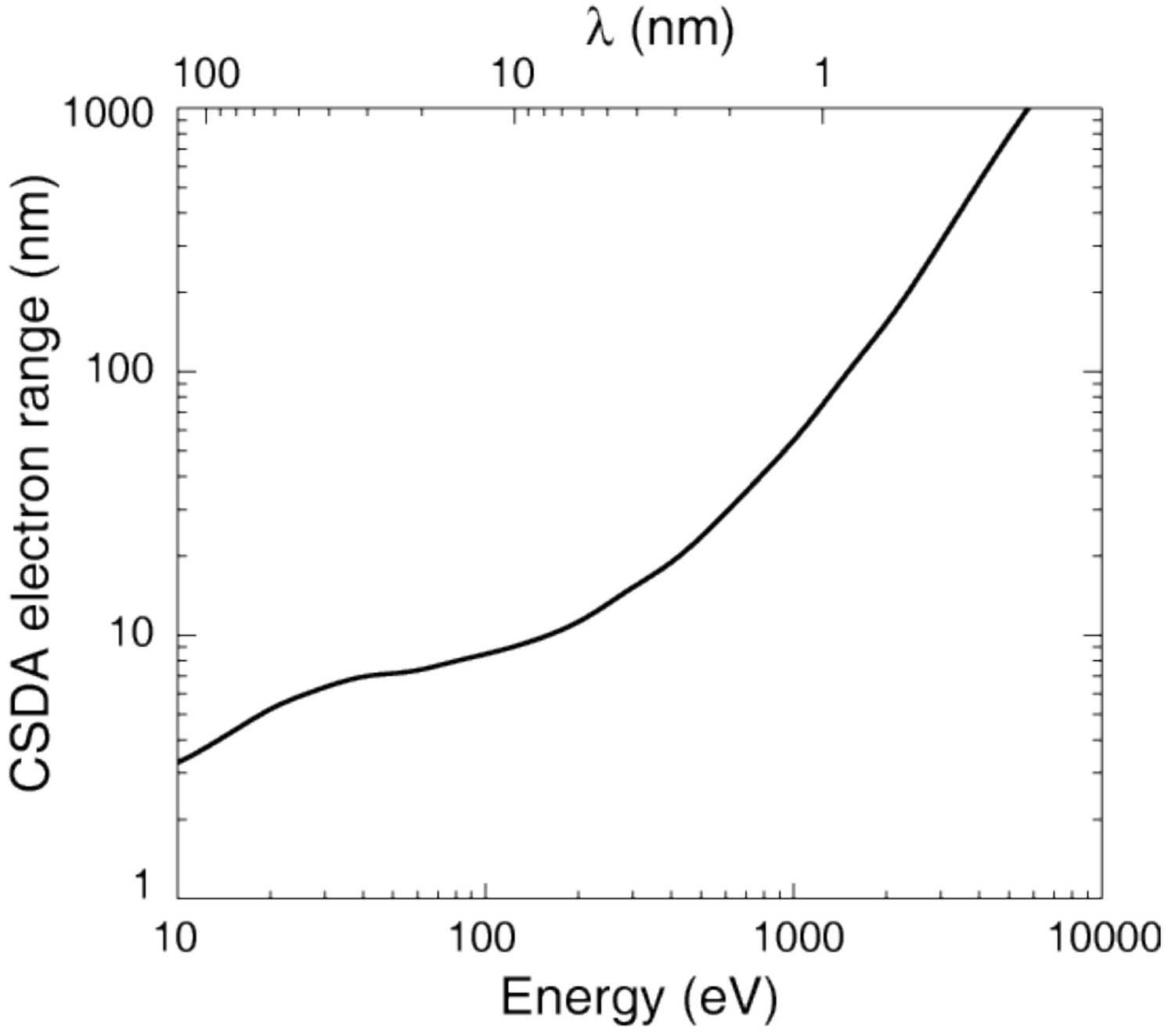

Radiation damage on (initially) living cells

- X-rays are ionizing radiation. The dose per high resolution image is about 100,000 times what is required to kill a person
- Makes it hard to view living cells!

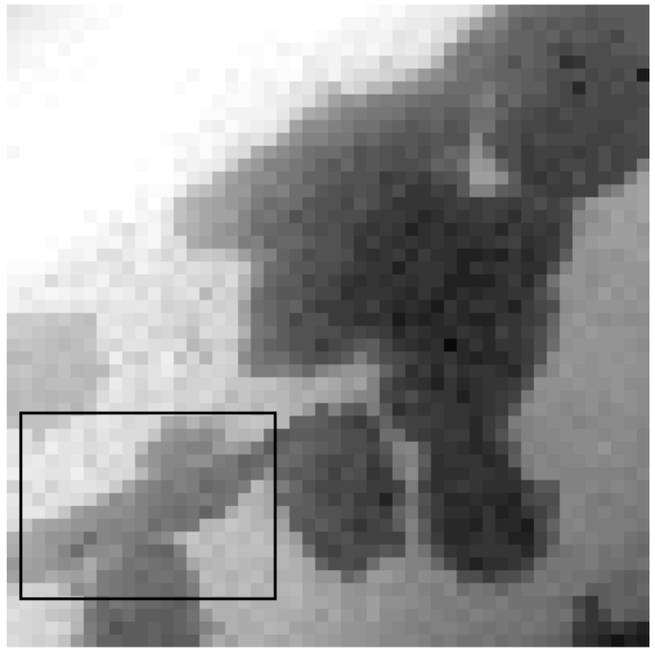

10 μm
$6.0 \cdot 10^2$ Gray, ET=2 min.

Experiment by V. Oehler, J. Fu, S. Williams, and C. Jacobsen, Stony Brook using specimen holder developed by Jerry Pine and John Gilbert, CalTech

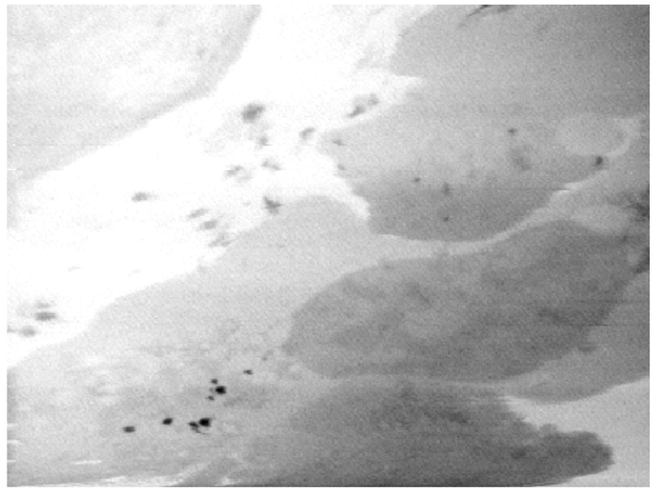

5 μm
$1.2 \cdot 10^5$ Gray, ET=9.5 min.

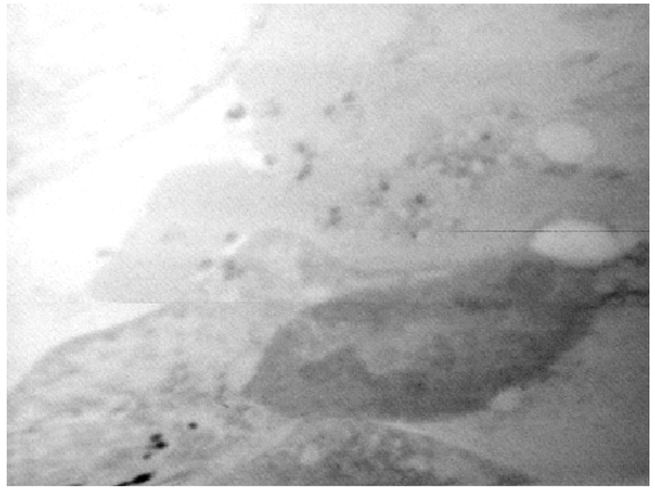

5 μm
$2.4 \cdot 10^5$ Gray, ET=17 min.

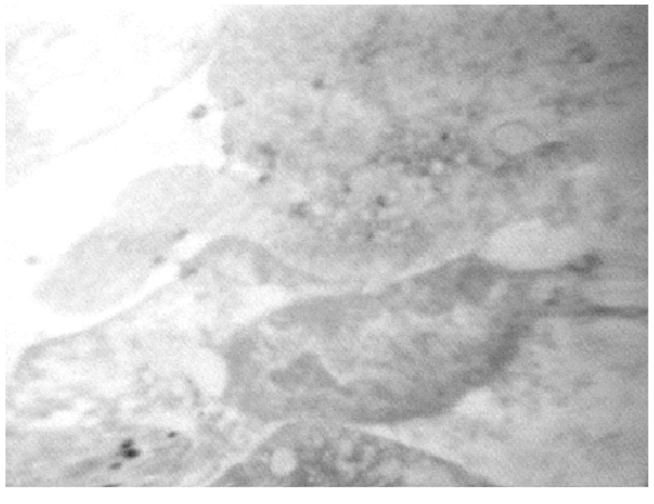

5 μm
$3.7 \cdot 10^5$ Gray, ET=24.5 min.

Wet, fixed samples: one image is OK

- Chromosomes are among the most sensitive specimens.
- V. faba chromosomes fixed in 2% glutaraldehyde. S. Williams et al., J. Microscopy **170**, 155 (1993)
- Repeated imaging of one chromosome shows mass loss, shrinkage

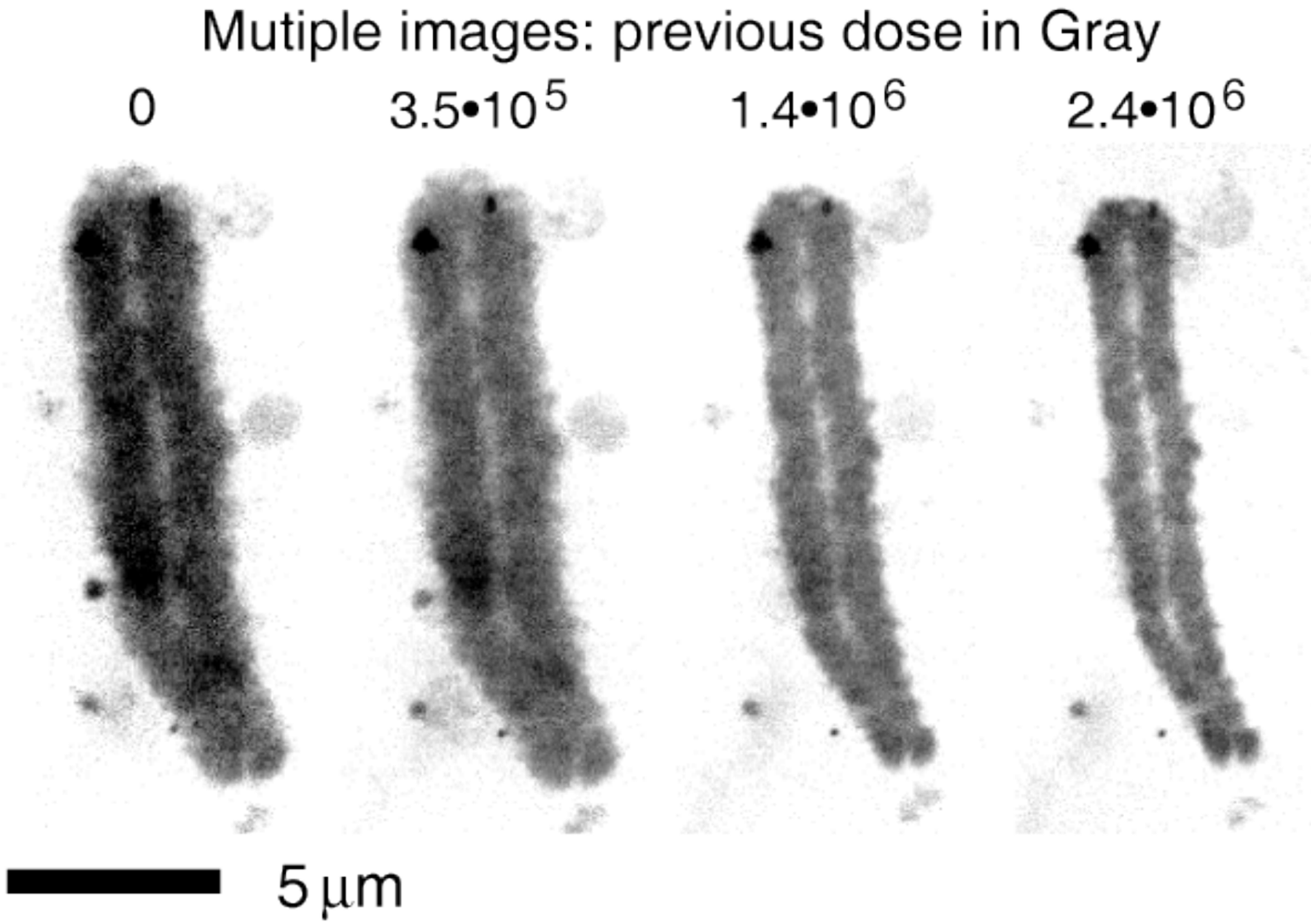

Frozen hydrated specimens

Grids with live cells are

- Taken from culture medium and blotted
- Plunged into liquid ethane (cooled by liquid nitrogen)

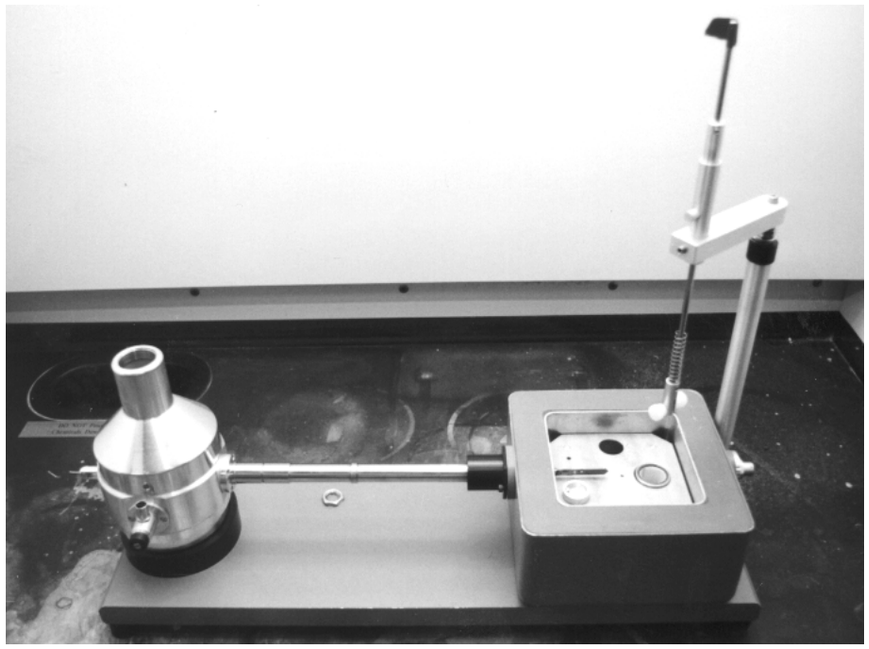

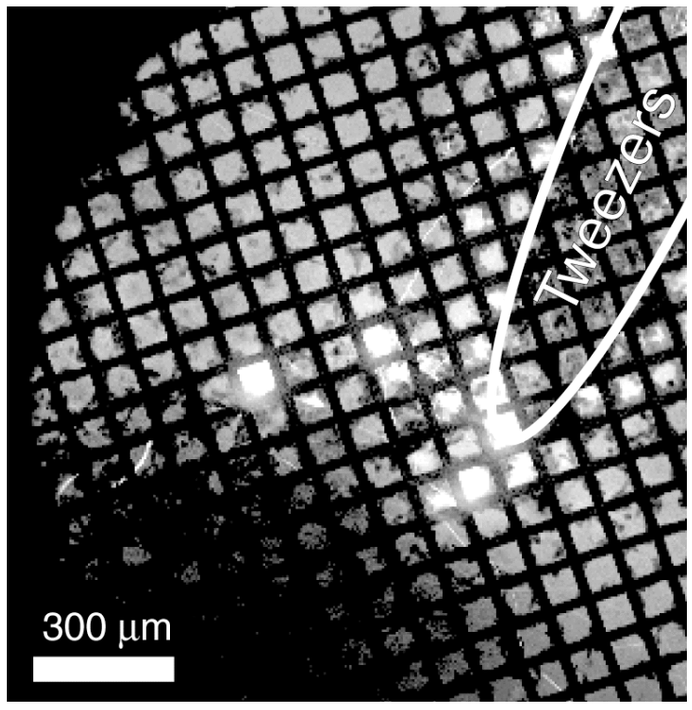

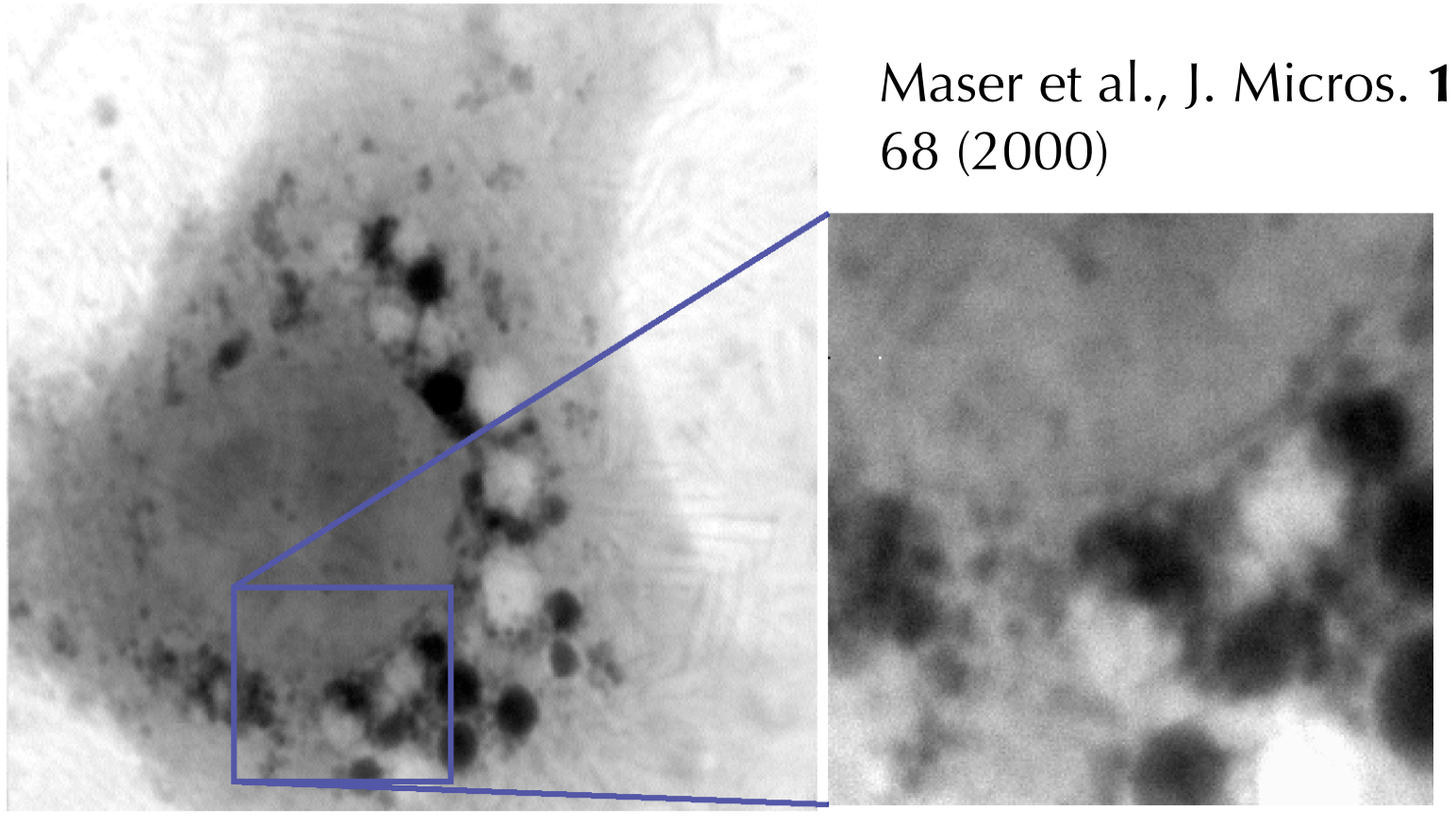

Maser et al., J. Micros. **197**, 68 (2000)

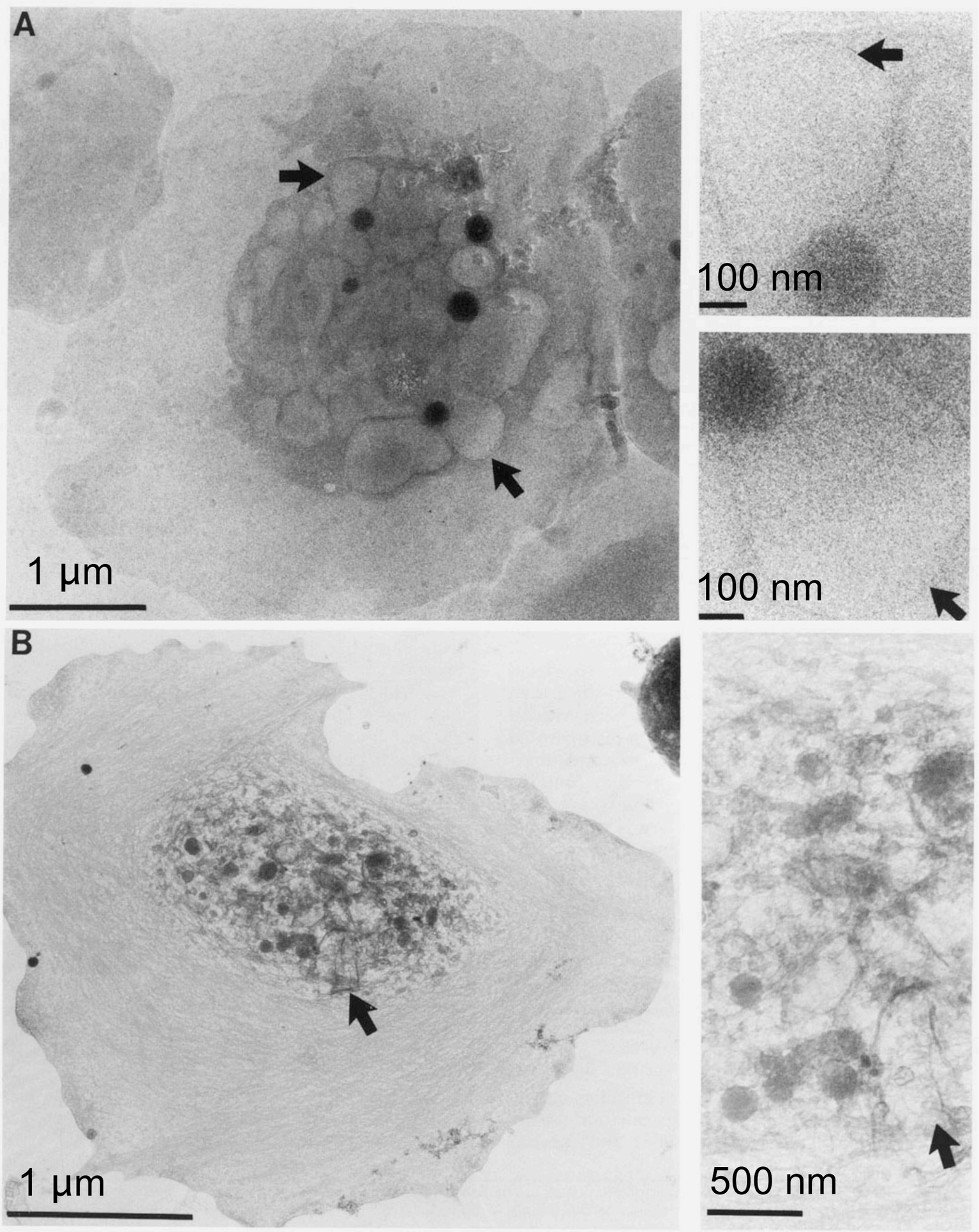

Frozen hydrated

- Human blood platelets
- 1 MeV transmission electron microscope (JEOL-1000)
- O'Toole, Wray, Kremer, and McIntosh, *J. Struct. Bio.* **110**, 55 (1993)

2% glutaraldehyde fix
1% OsO_4 postfix
critical-point dry

Electrons: frozen hydrated

Polymer spheres in amorphous ice viewed with low dose rate at 100 keV
Smaller spheres: PMMA
Larger spheres: PS
Doses are in Gray

From Y. Talmon, in Steinrecht and Zierold, **Cryotechniques in Biological Electron Microscopy** (Springer, 1987)

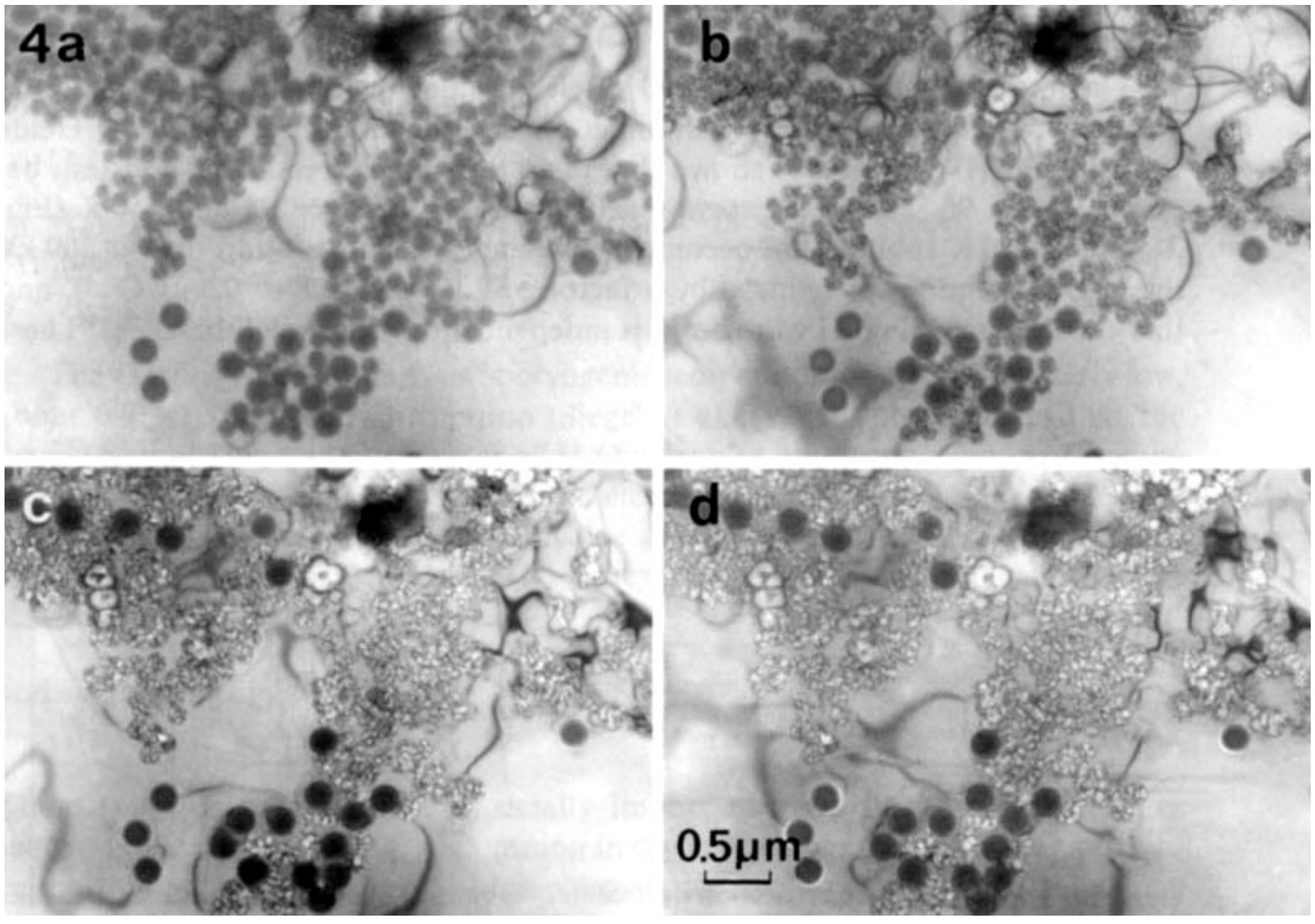

"Bubbling" dose in cryo electron microscopy: ~1000 e-/nm^2 or about 3x10^7 Gray. Bubbles: hydrogen gas [Leapman, Ultramic. **59**, 71 (1995); Sun et al., J. Mic. **177**, 18 (1995)]

Radiation damage resistance in cryo

Left: frozen hydrated image after exposing several regions to ~10^{10} Gray

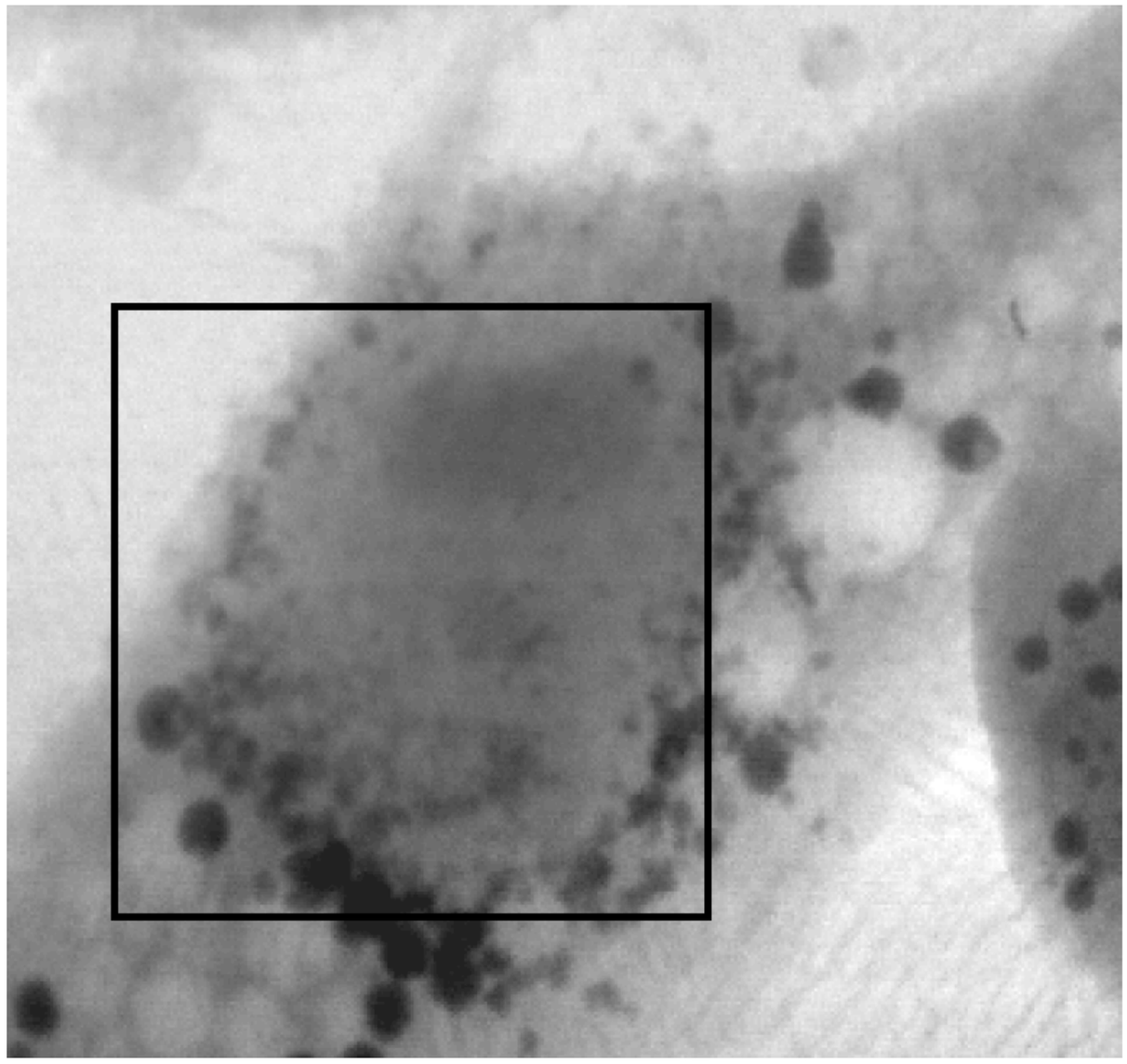

Maser et al., J. Micros. **197**, 68 (2000)

Right: after warmup in microscope (eventually freeze-dried): holes indicate irradiated regions!

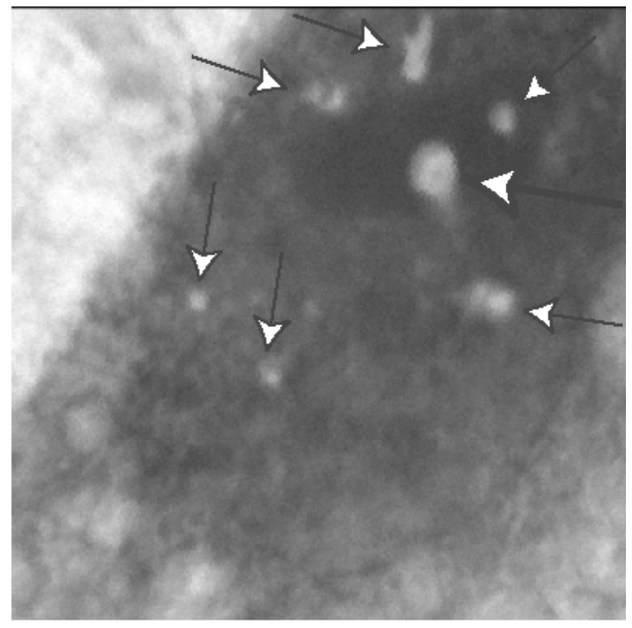

Hints of damage?

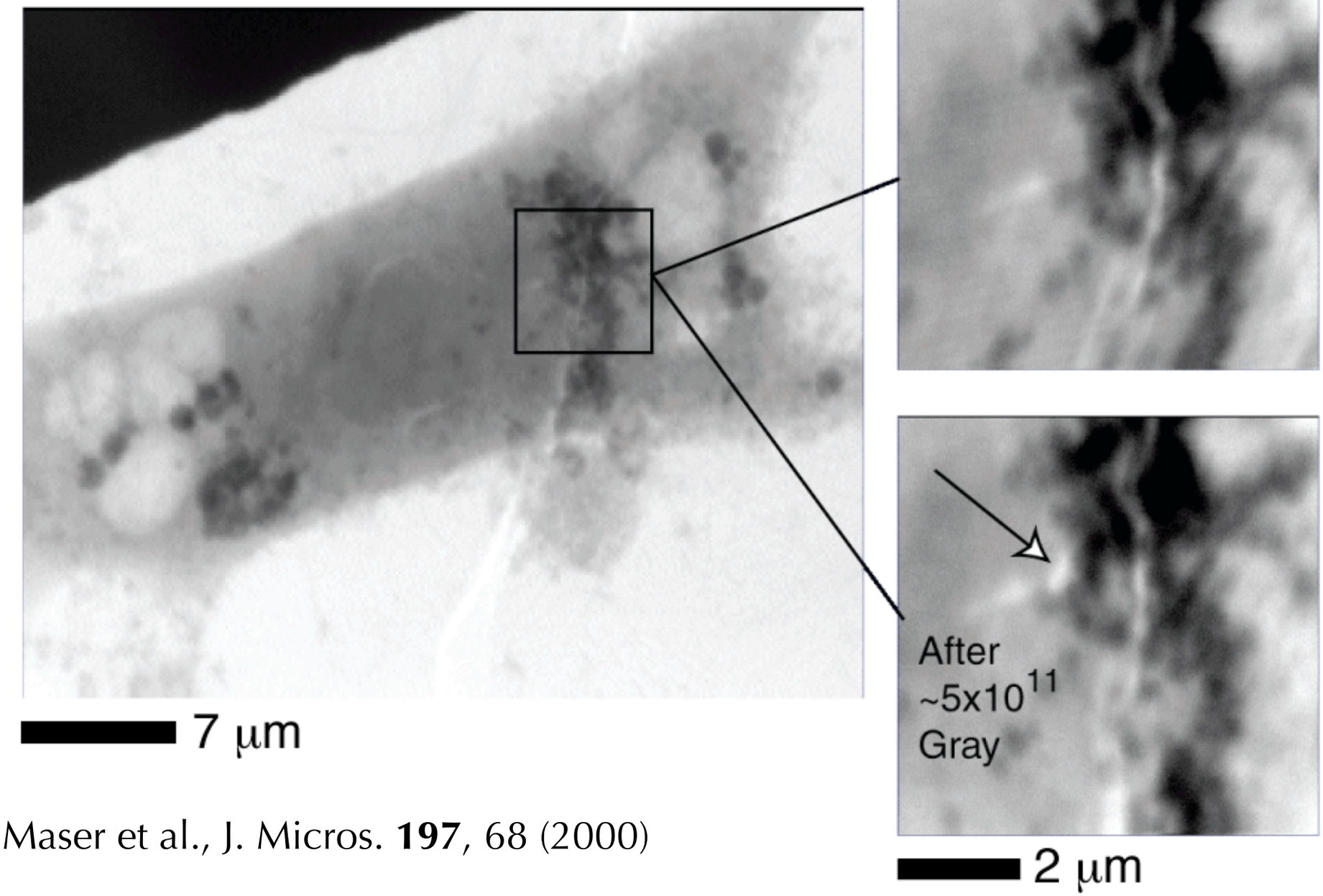

Maser et al., J. Micros. **197**, 68 (2000)

Note: we have never seen "bubbling" with soft x-rays. Lower relative dose in water, plus lower dose rate to allow for gas diffusion?

X-ray irradiation: poly(methyl methacrylate) (PMMA)

- PMMA: poly methyl methacrylate (plexiglass!) which is especially radiation sensitive – it's used as a resist for electron beam lithography
- X. Zhang et al., J. Vac. Sci. Tech. B **13**, 1477 (1995)

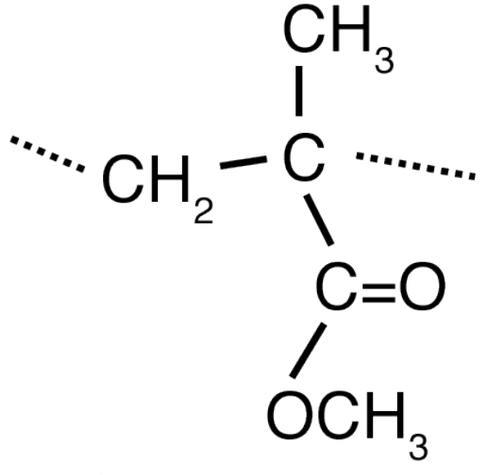

- Fine step size, high flux image for dose
- Slightly defocused beam for low dose image off XANES peaks
- At end, AFM for thickness

- Defocused beam for spectrum
- Gaussian fit to measure peak strengths at XANES resonances

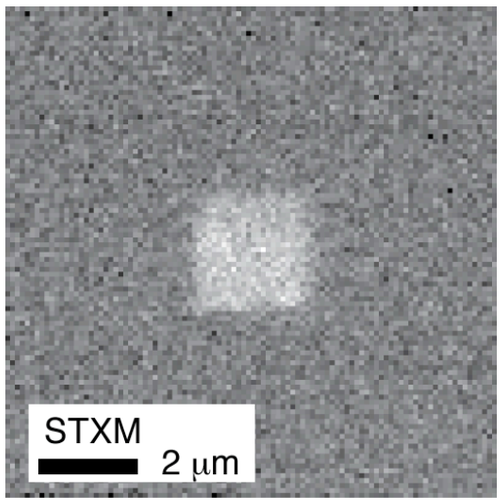

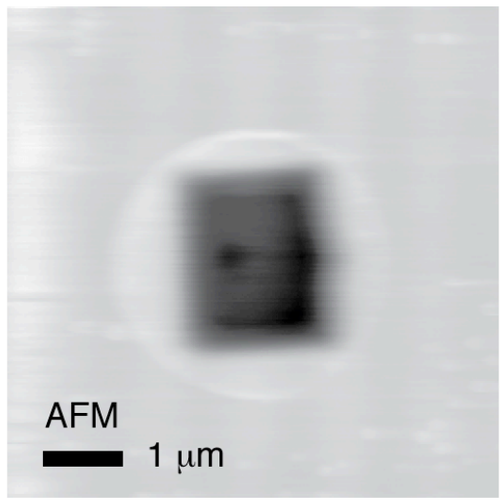

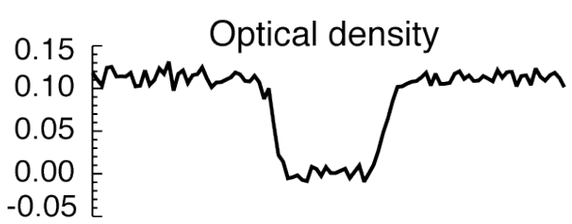

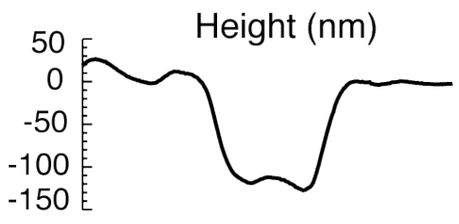

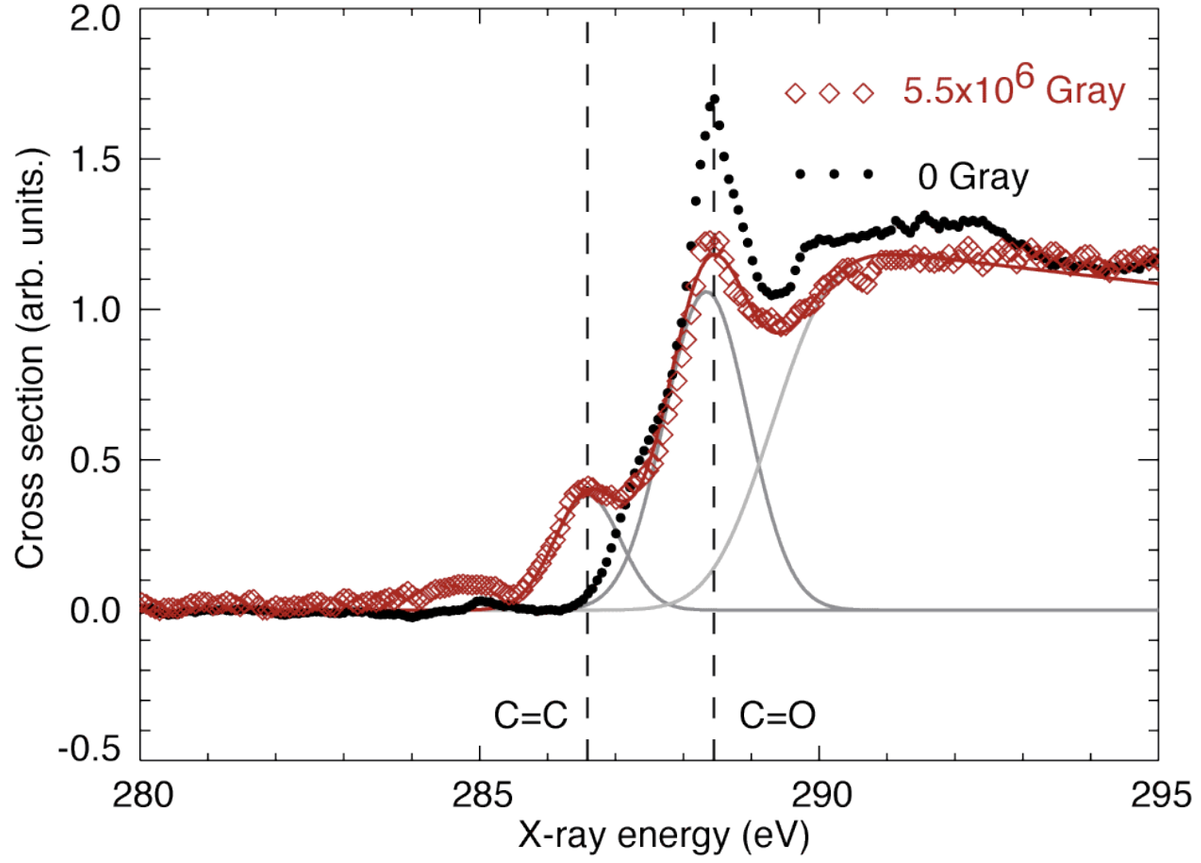

Mass loss: small pieces fly away

X. Zhang, C. Jacobsen, S. Lindaas, S. Williams, J. Vac. Sci. Tech. B **13**, 1477 (1995)

- Chain scission: C=0 peak decrease
- Crosslinking: C=C peak increase

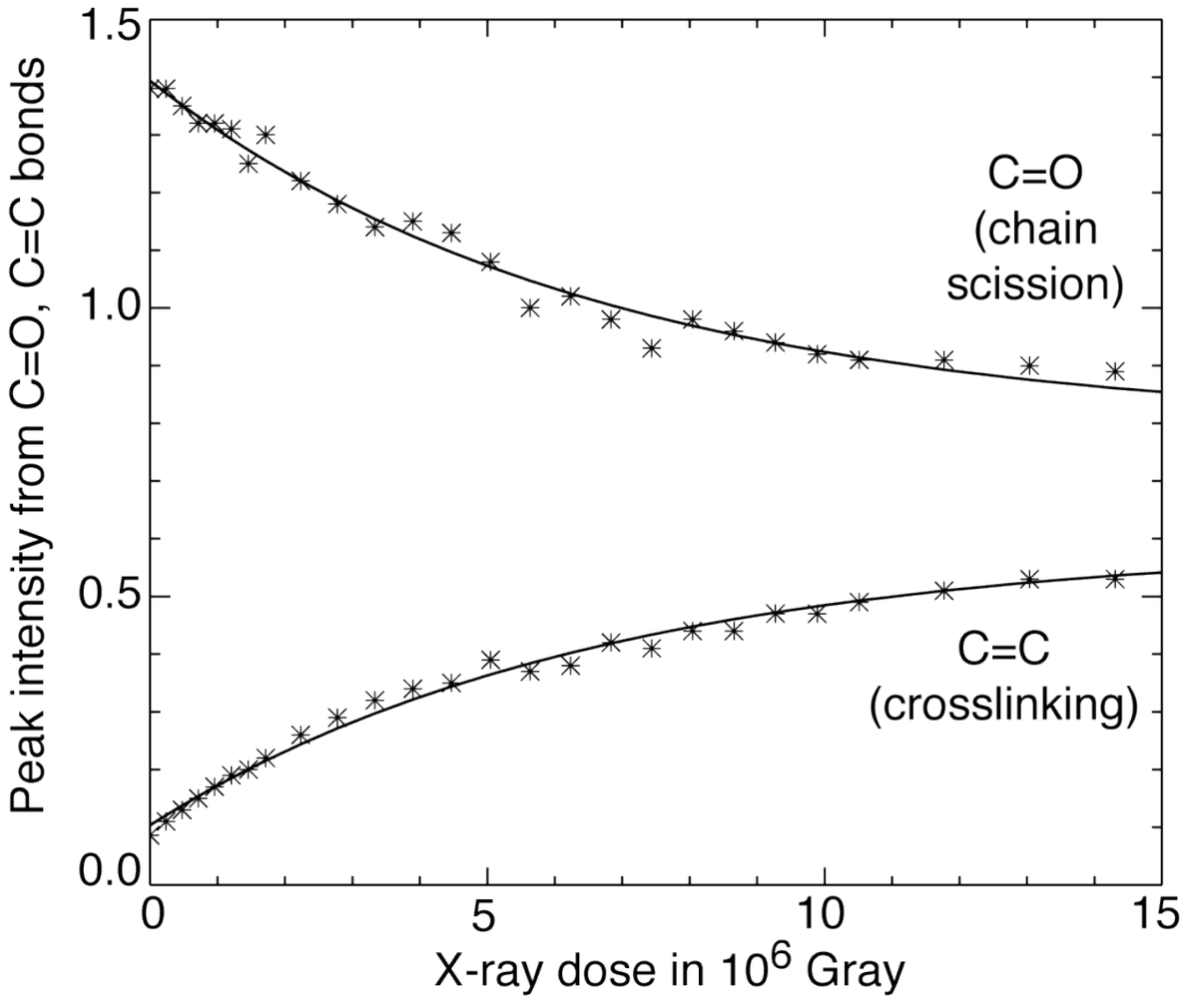

- Mass loss: optical density, AFM verification

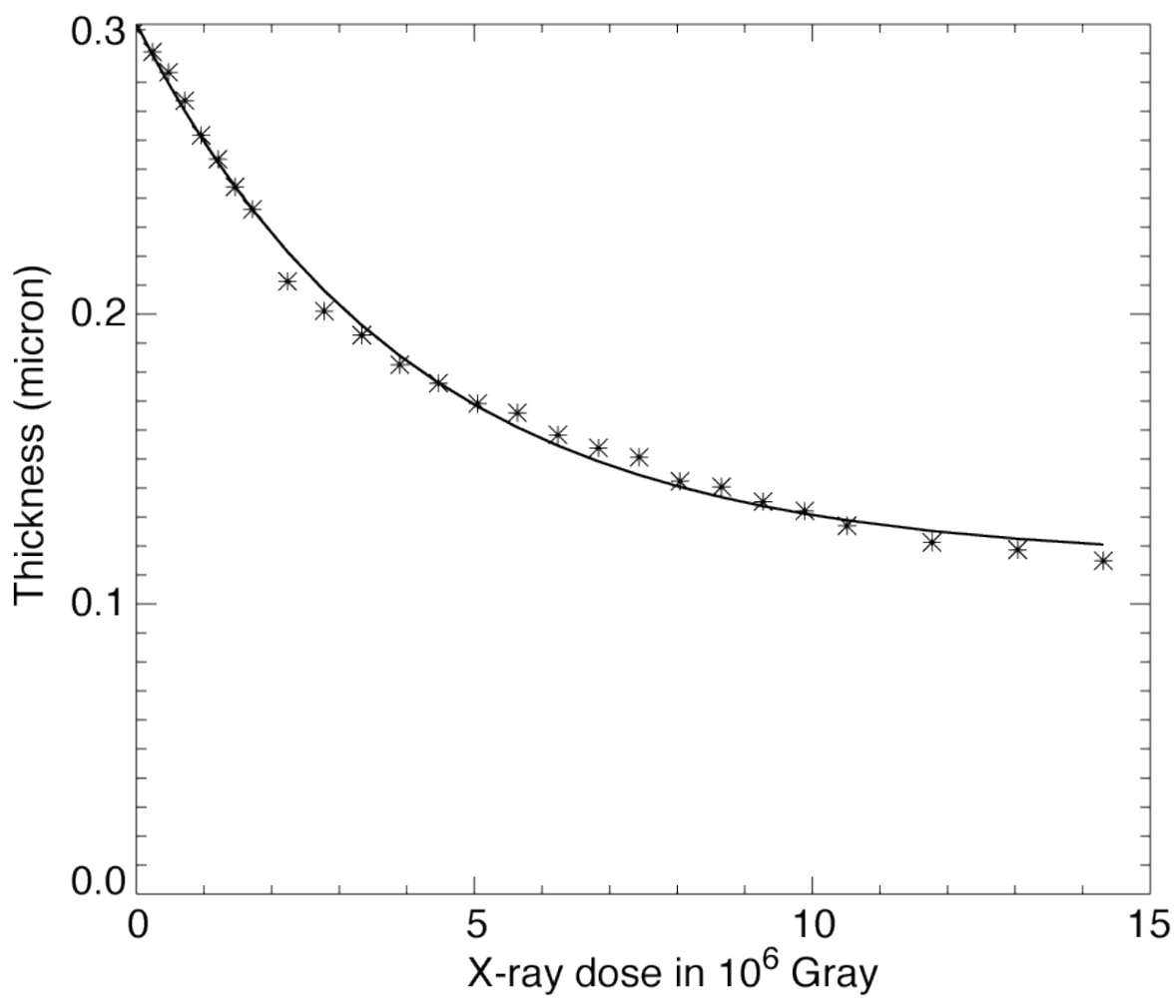

Mass spectroscopy of fragments: see Tinone et al., J. Vac. Sci. Tech. **A 13**, 1885 (1995)

PMMA at room, LN2 temperature

- Beetz and Jacobsen, J. Synchrotron Radiation **10**, 280 (2003)
- Repeated sequence: dose (small step size, long dwell time), spectrum (defocused beam)
- Images: dose region (small square) at end of sequence

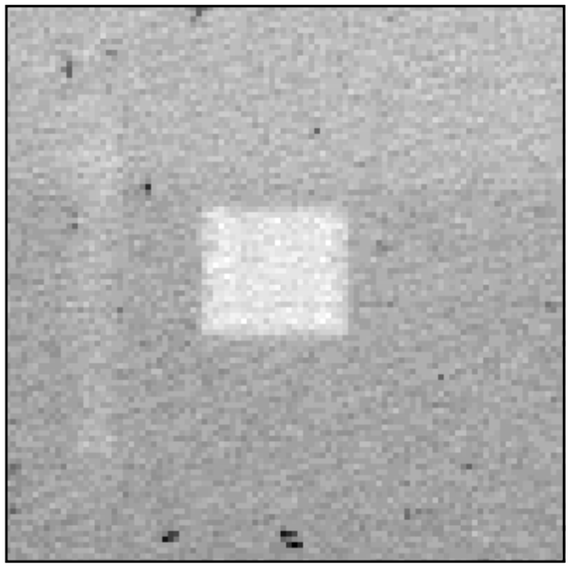

Room temperature: mass loss immediately visible

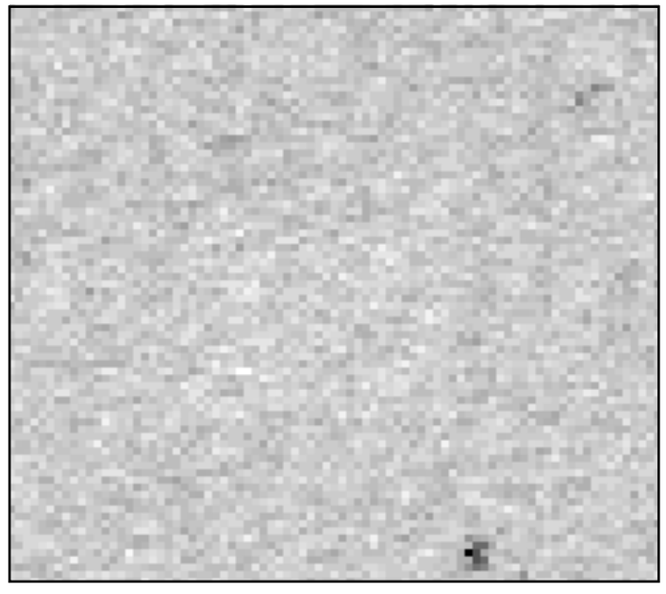

LN2 temperature: no mass loss immediately visible

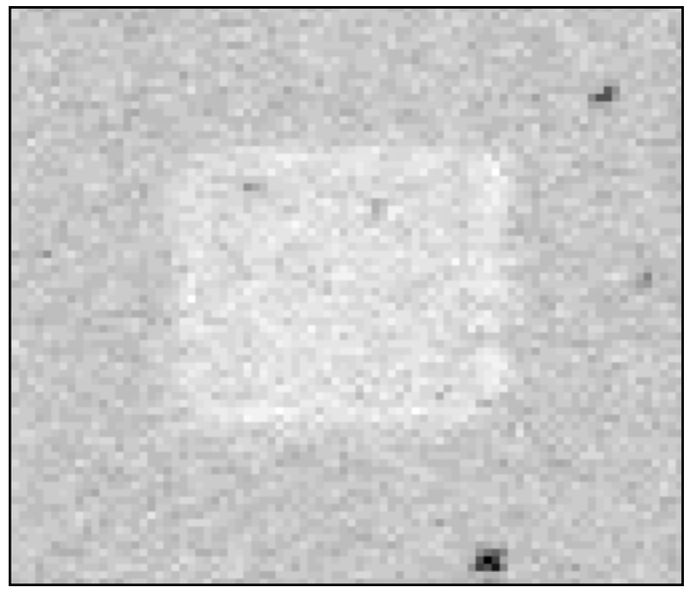

After warm-up: mass loss becomes visible

PMMA at LN2, room temperature: XANES spectra

- Peak at 531.4 eV: C=0 bond
- Plateau at 540 eV: total mass (plus some emphasis on oxygen σ* bonds)
- Beetz and Jacobsen, J. Synchrotron Radiation **10**, 280 (2003)

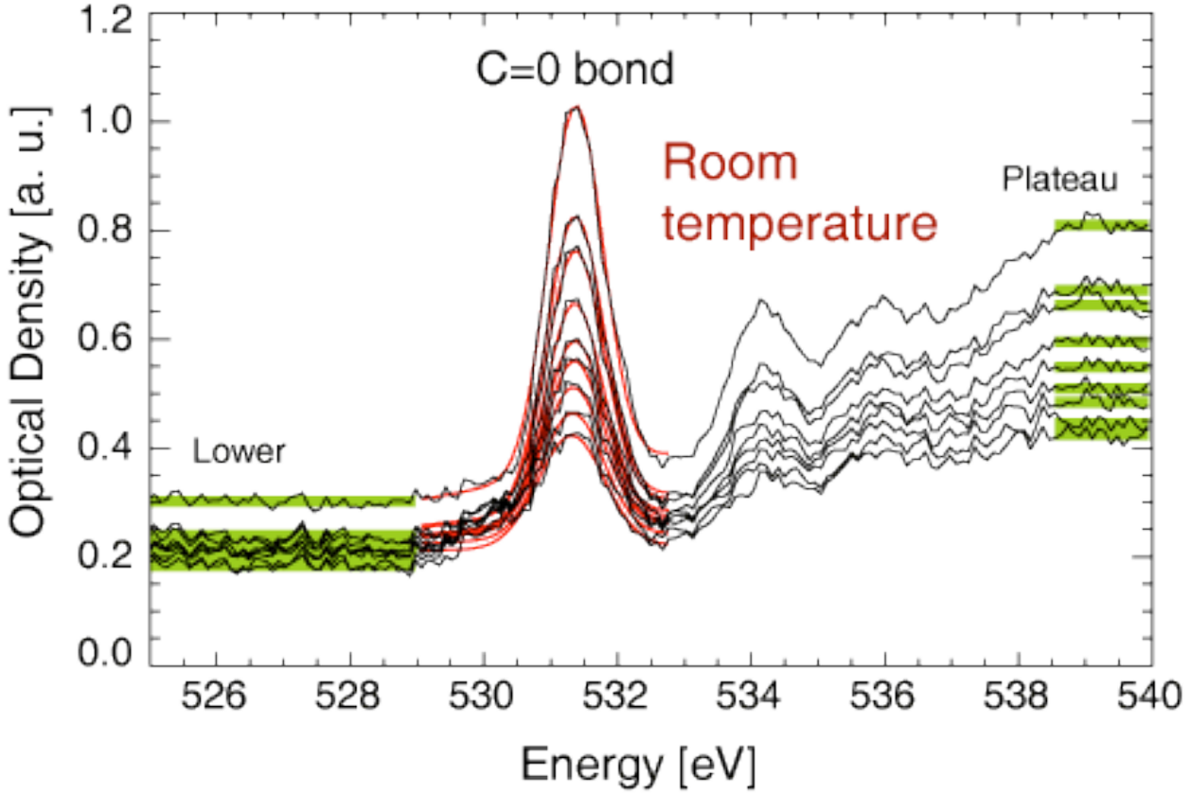

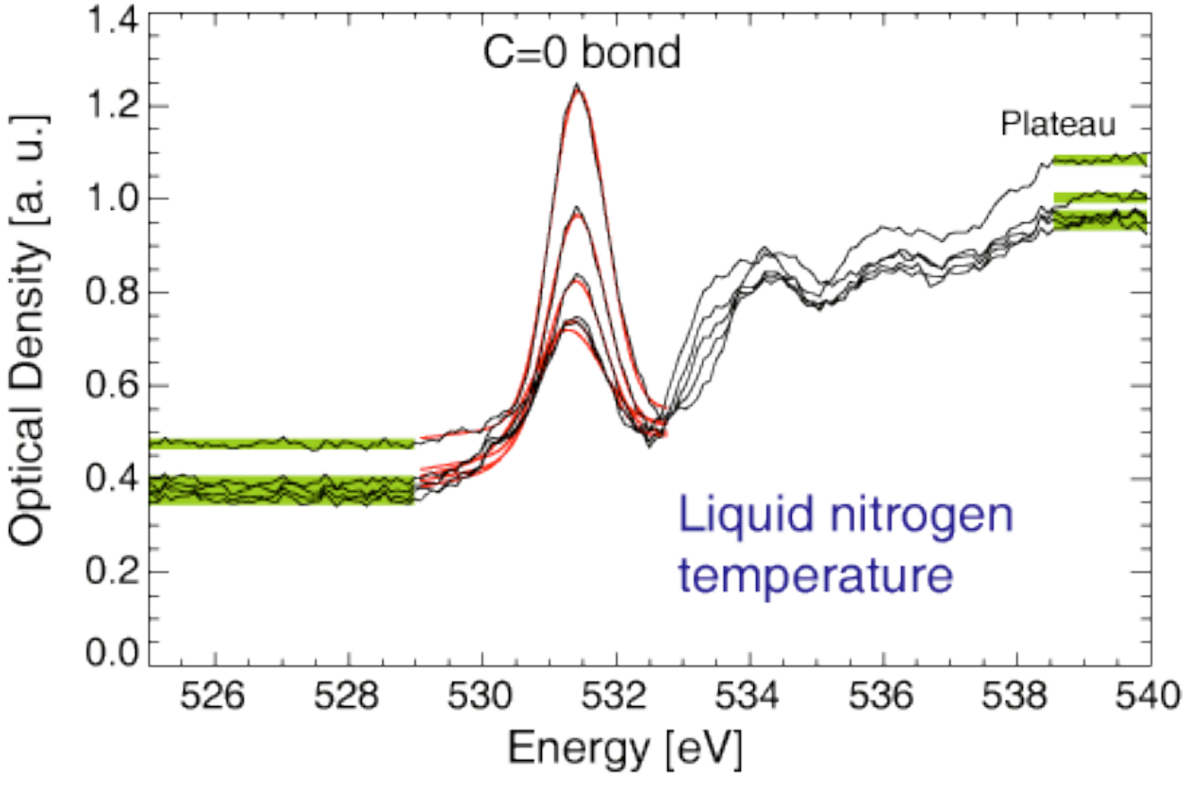

Results from fitting spectra

LN_2 temp: protection against mass loss, but not against breaking bonds (at least C=0 bond in dry PMMA)

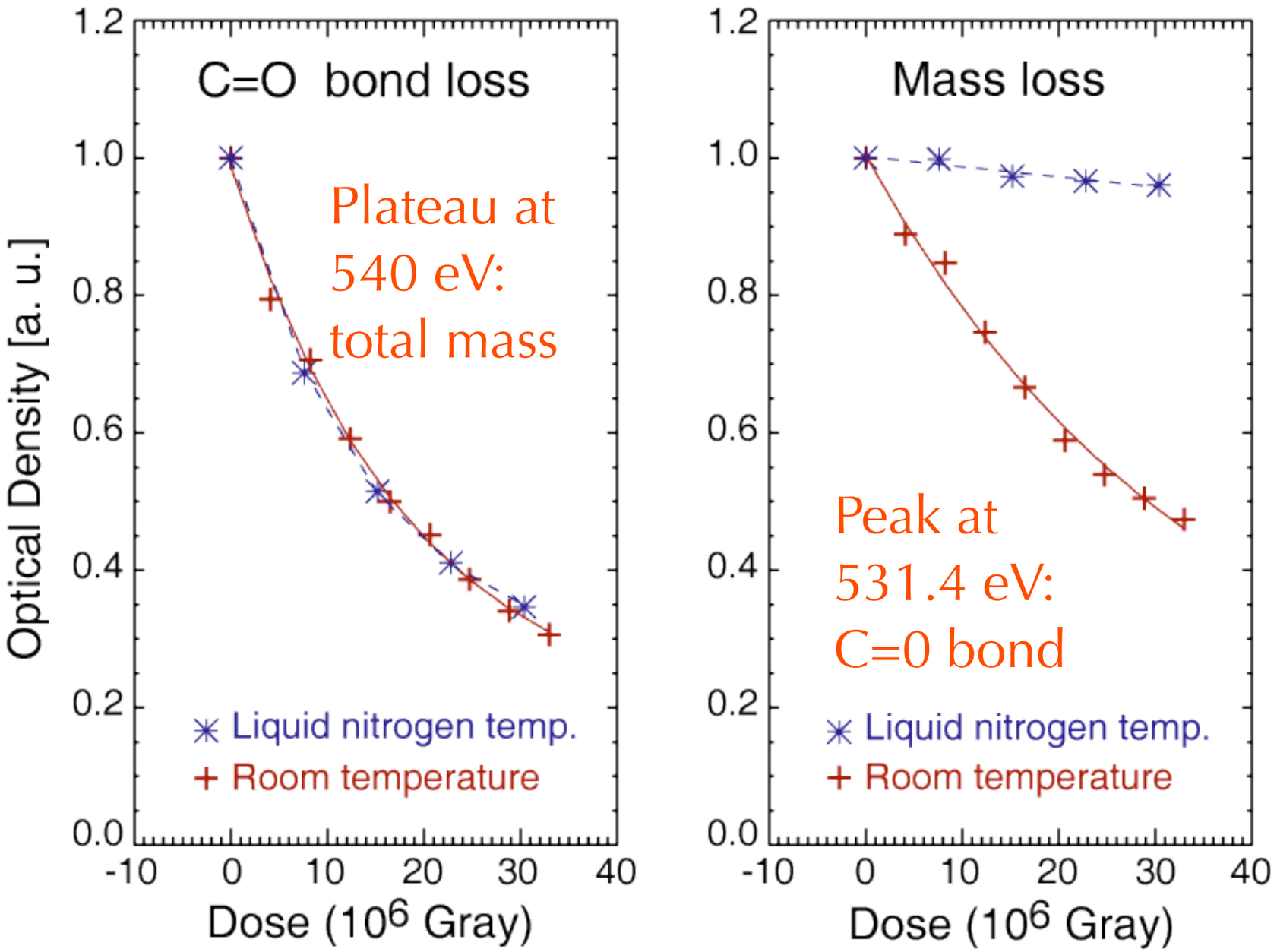

Beetz and Jacobsen, *J. Synchrotron Radiation* **10**, 280 (2003)

Tomography: projections in a microscope

Projections of a frozen hydrated 3T3 fibroblast. Y. Wang *et al.*, *J. Microscopy* **197**, 80 (2000)

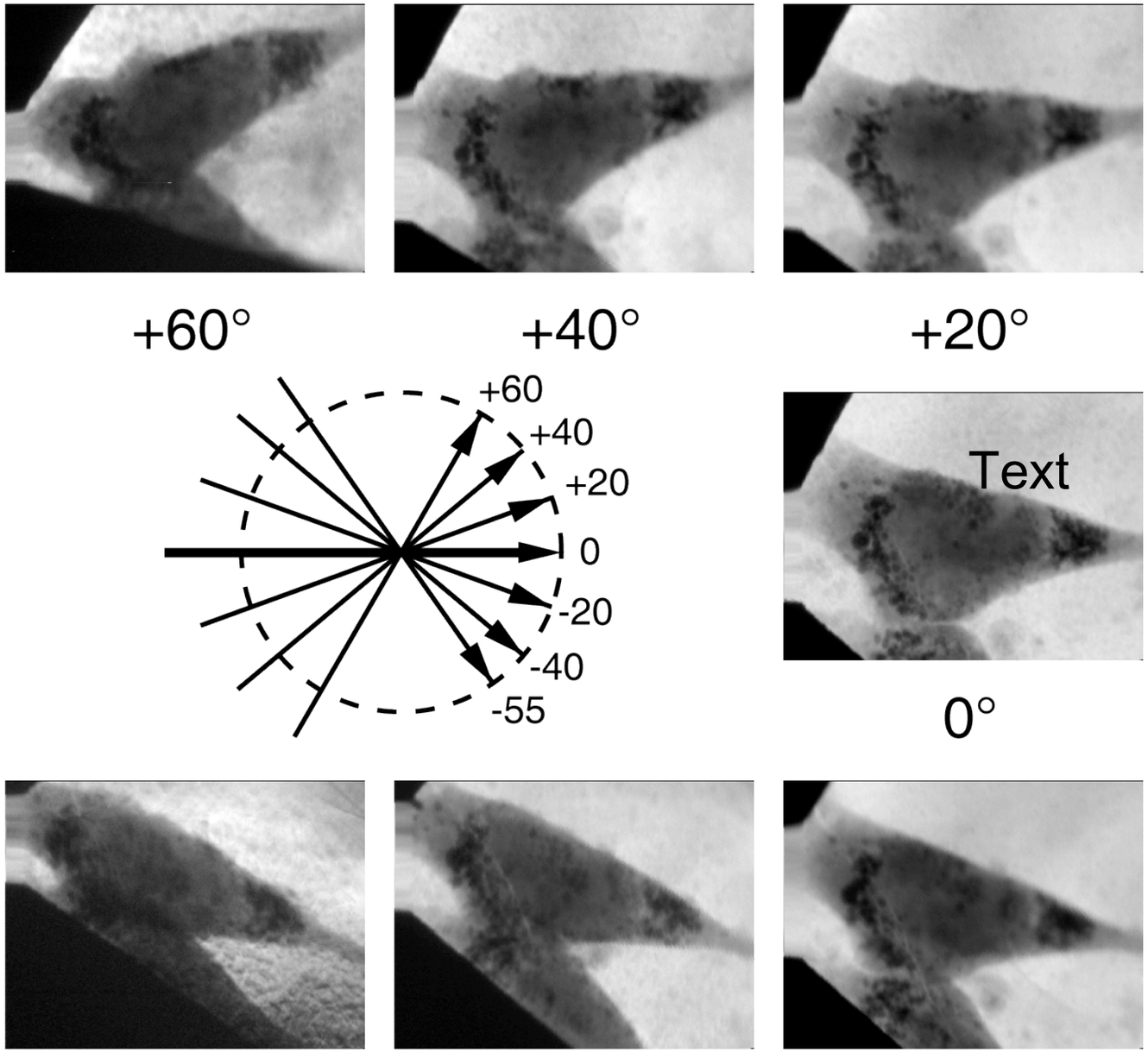

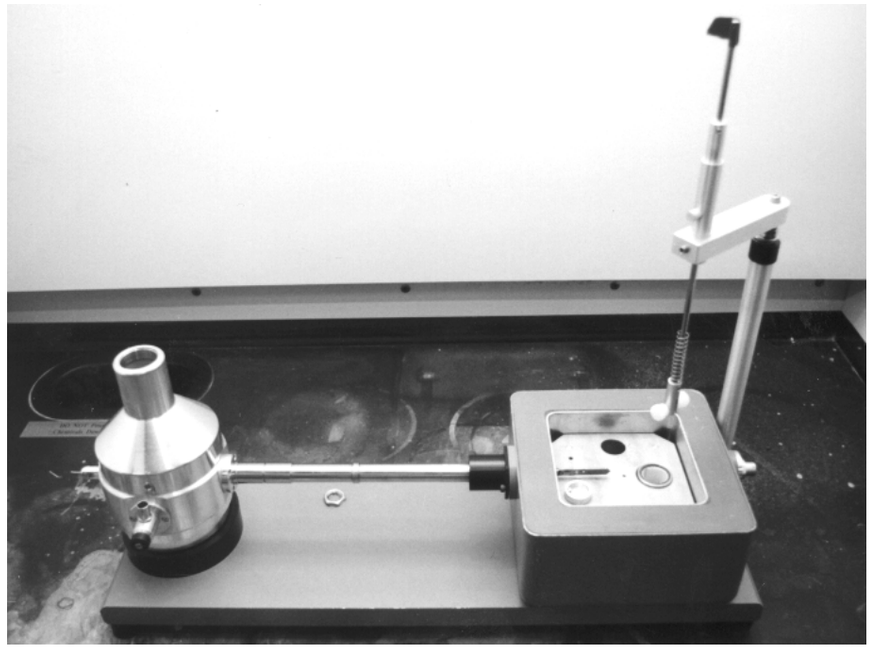

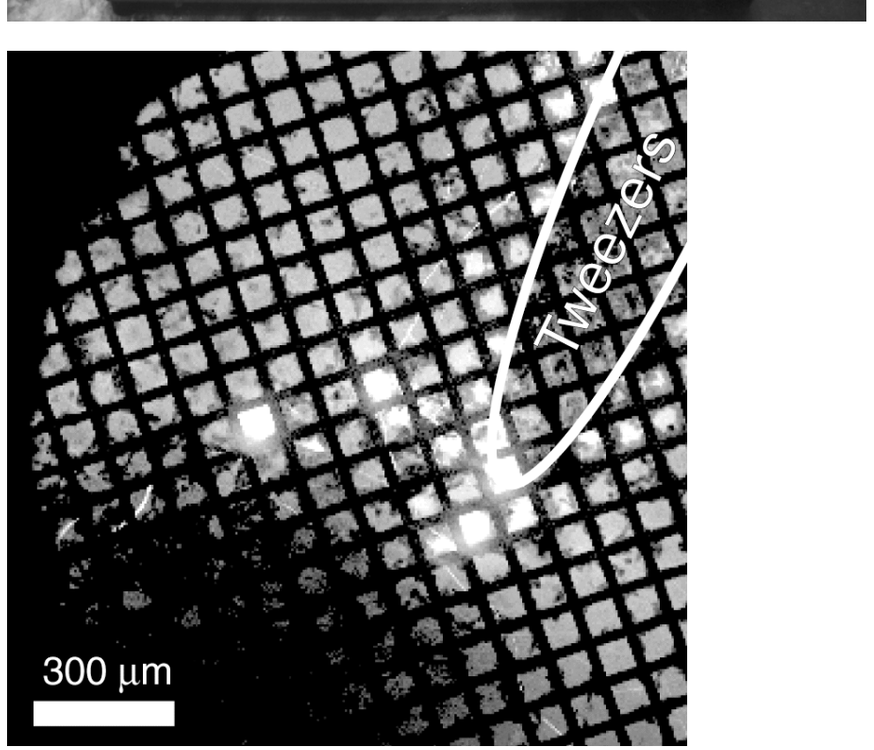

Maser *et al.*, *J. Micros.* **197**, 68 (2000)

Fibroblast reconstruction: Z slices

Y. Wang et al., J. Microscopy **197**, 80 (2000)

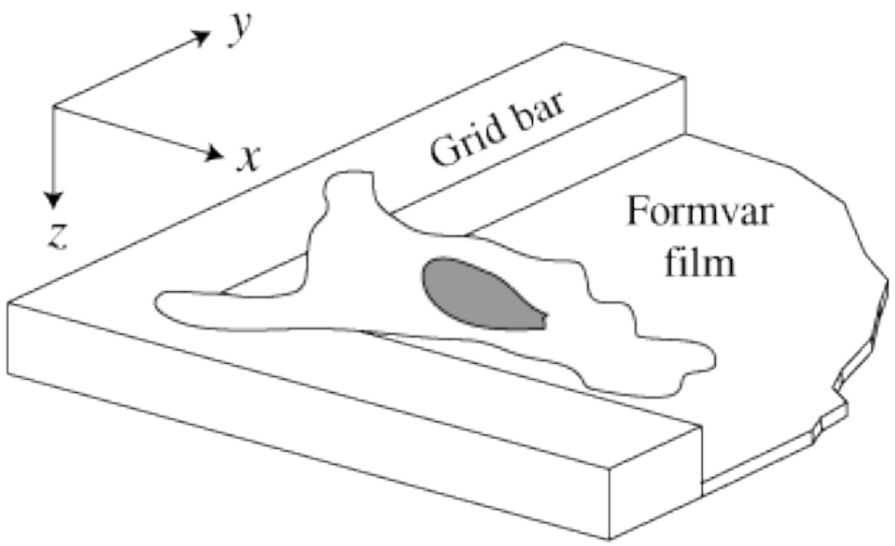

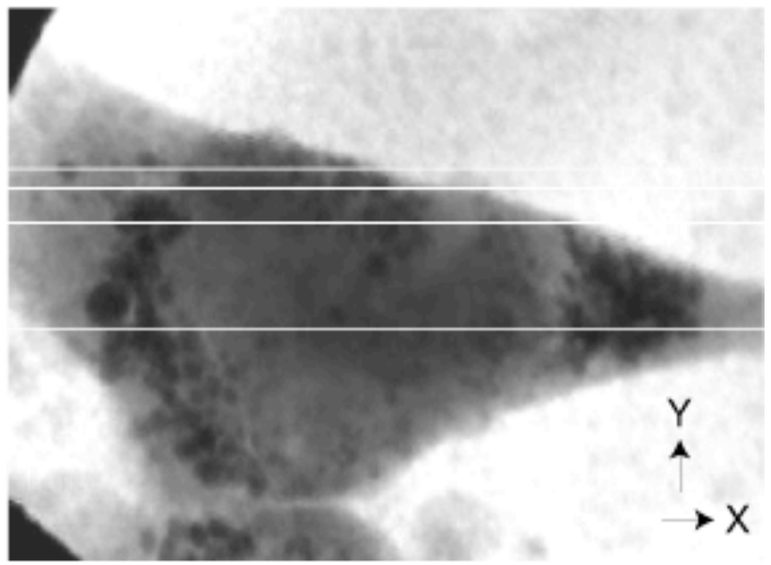

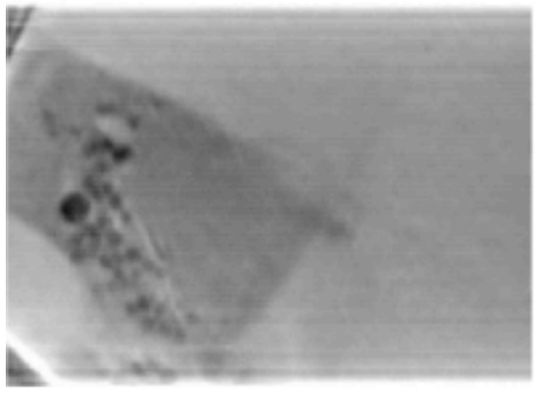

z = 12.7 μm

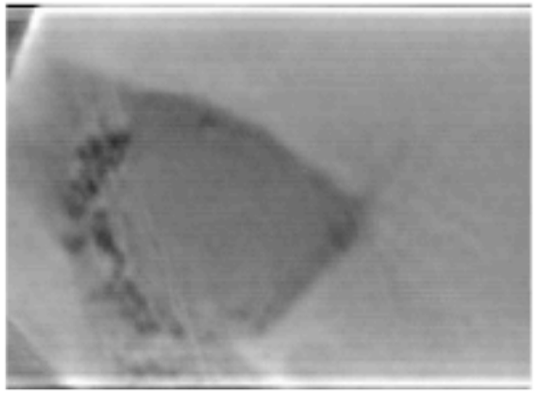

z = 15.1 μm

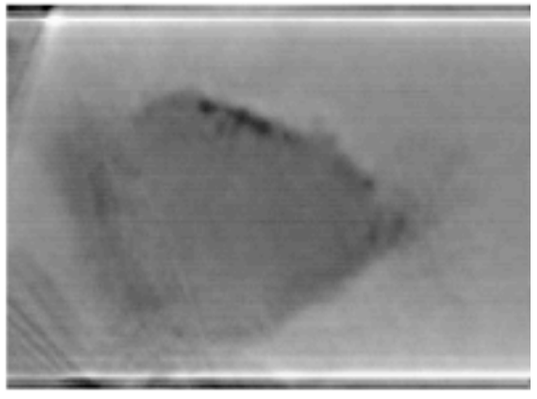

z = 17.6 μm

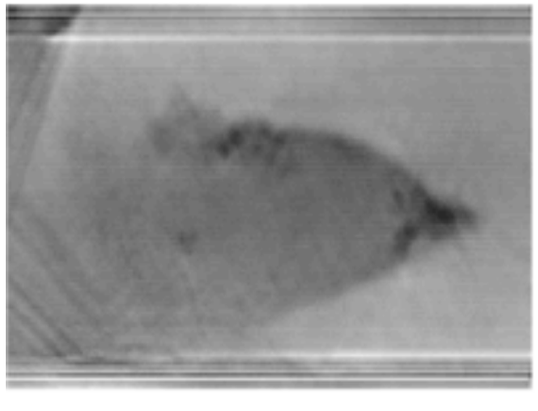

z = 20.0 μm

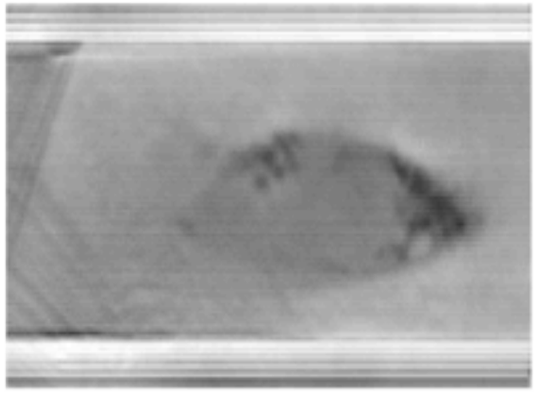

z = 21.6 μm

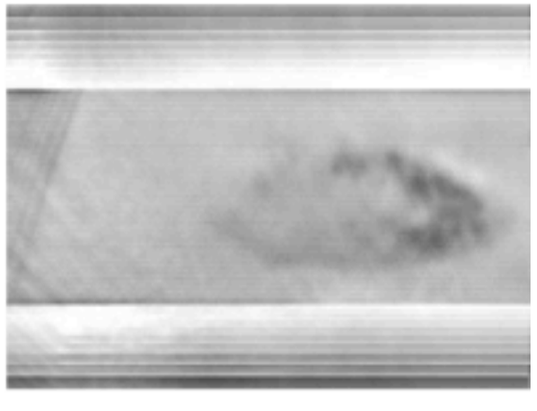

z = 23.1 μm

3D imaging with lenses

Transverse: $$\Delta_t \Rightarrow \frac{\lambda}{4\theta} = \frac{\Delta_{rN}}{2}$$

Longitudinal: $$\Delta_\ell \Rightarrow \frac{\lambda}{\theta^2} = 4\Delta_{rN}\,\frac{\Delta_{rN}}{\lambda}$$

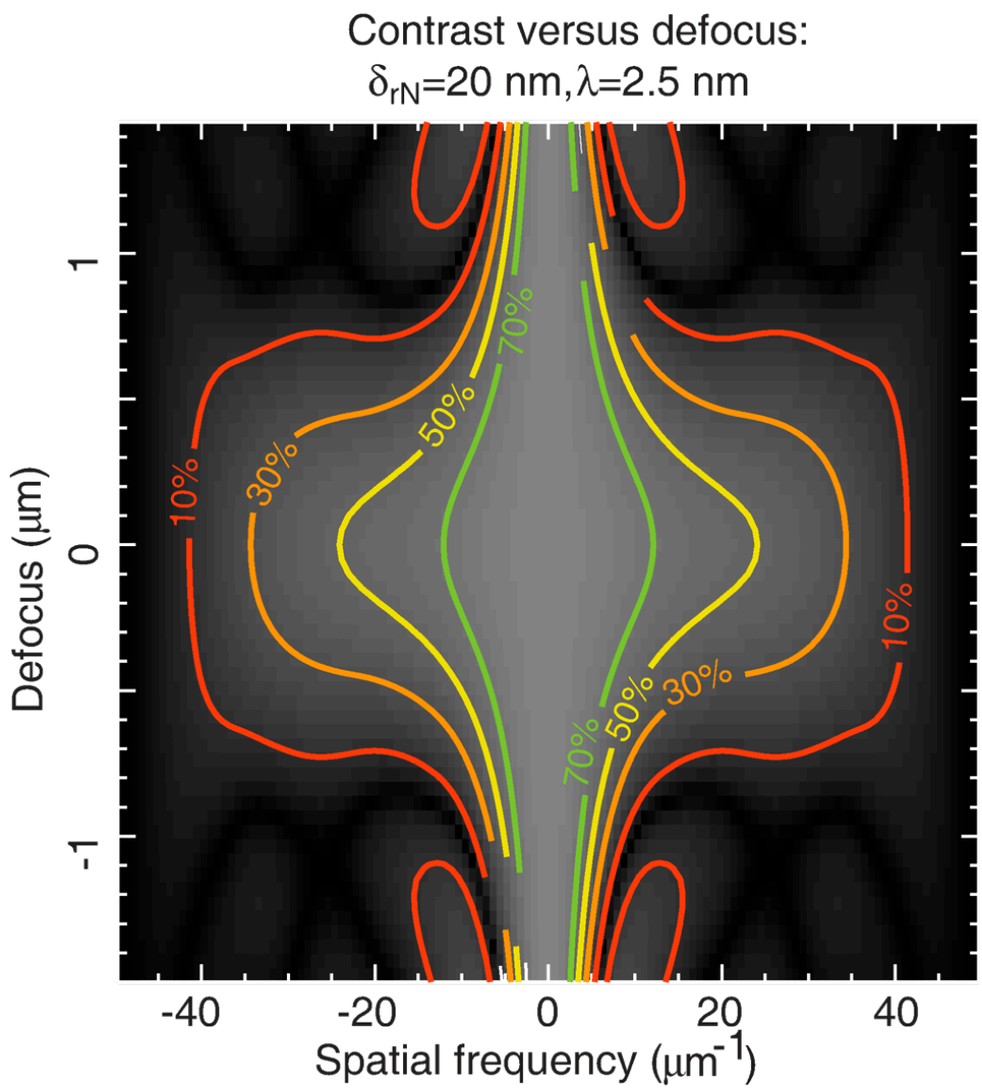

20 nm resolution at 520 eV: depth of field ~1 μm

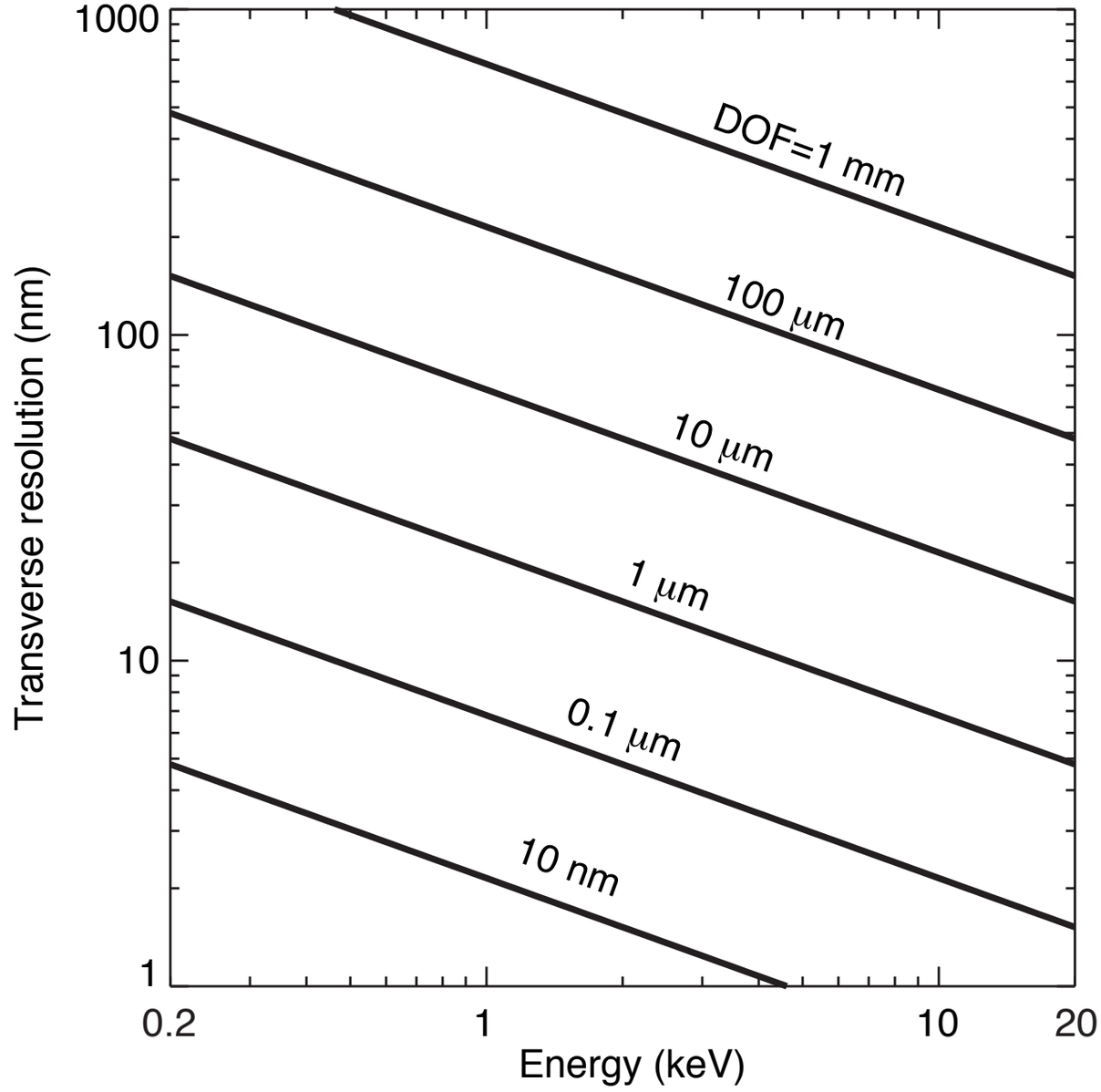

Through-focus deconvolution with lenses:

- Confocal: fully incoherent (fluorescence)
- EM: phase only, coherent
- TXM: partially coherent, equal absorption and phase contrast, need for experimental CTF

Soft x-ray tomography of algae shock-frozen in liquid ethane: Slices through a tomographic reconstruction

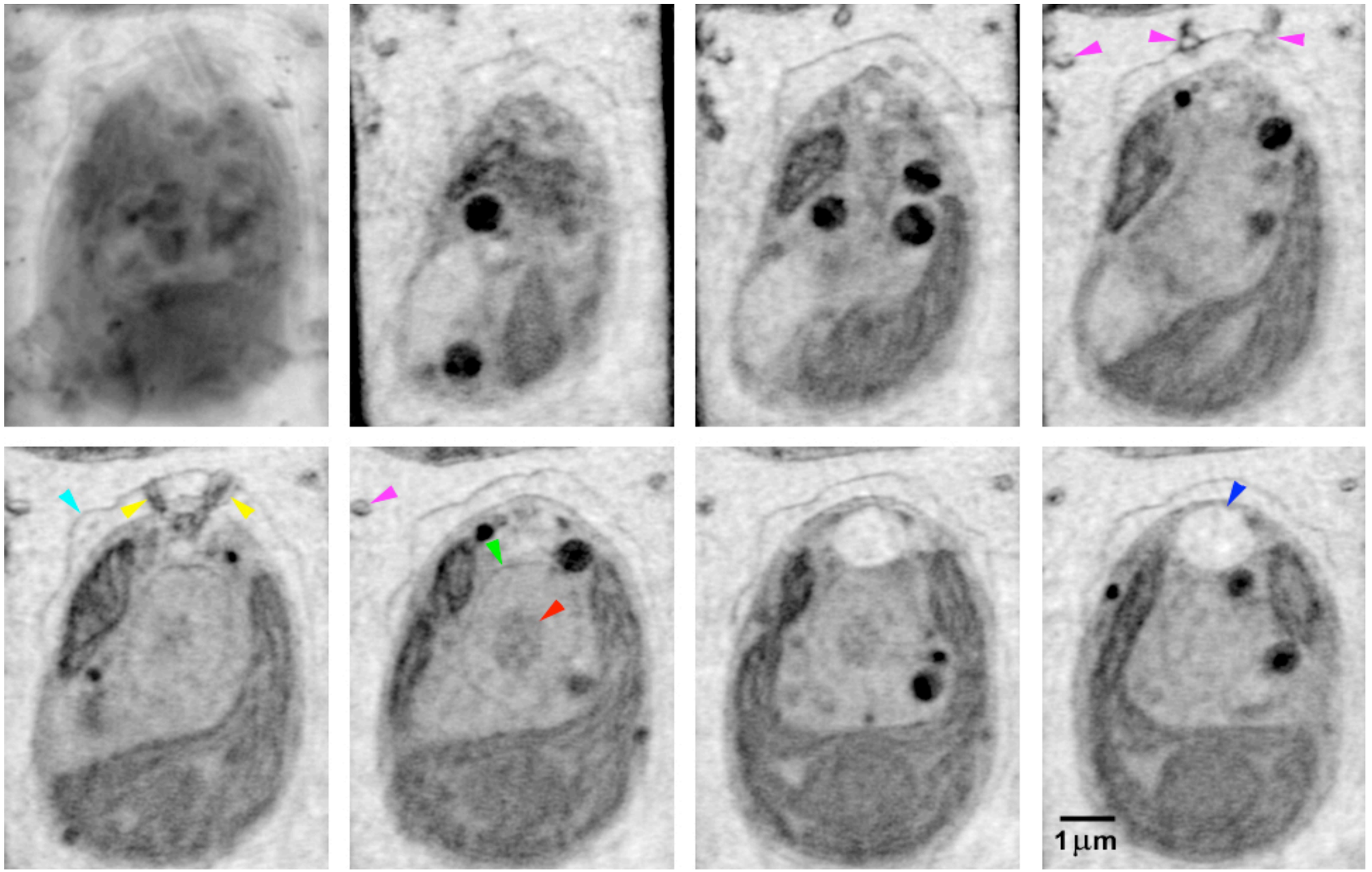

Vacuole

Nuclear membrane

Nucleolus

Flagellar roots and neuromotor

Cell wall

Flagella

Weiss, Schneider et al., Ultramicroscopy **84**, 185 (2000).
See also Larabell and Le Gros, Molecular Biology of the Cell **115**, 957 (2004)

National Center for X-ray Tomography

DoE/BER and NIH funded center at Advanced Light Source in Berkeley; sophisticated TXM for cryo tomography; Larabell, LeGros *et al.*

Parkinson *et al.*, *J. Struct. Bio.* **162**, 380 (2008): fission yeast *Schizosaccharomyces pombe*.
Nuclei, mitochondria, vacuoles…

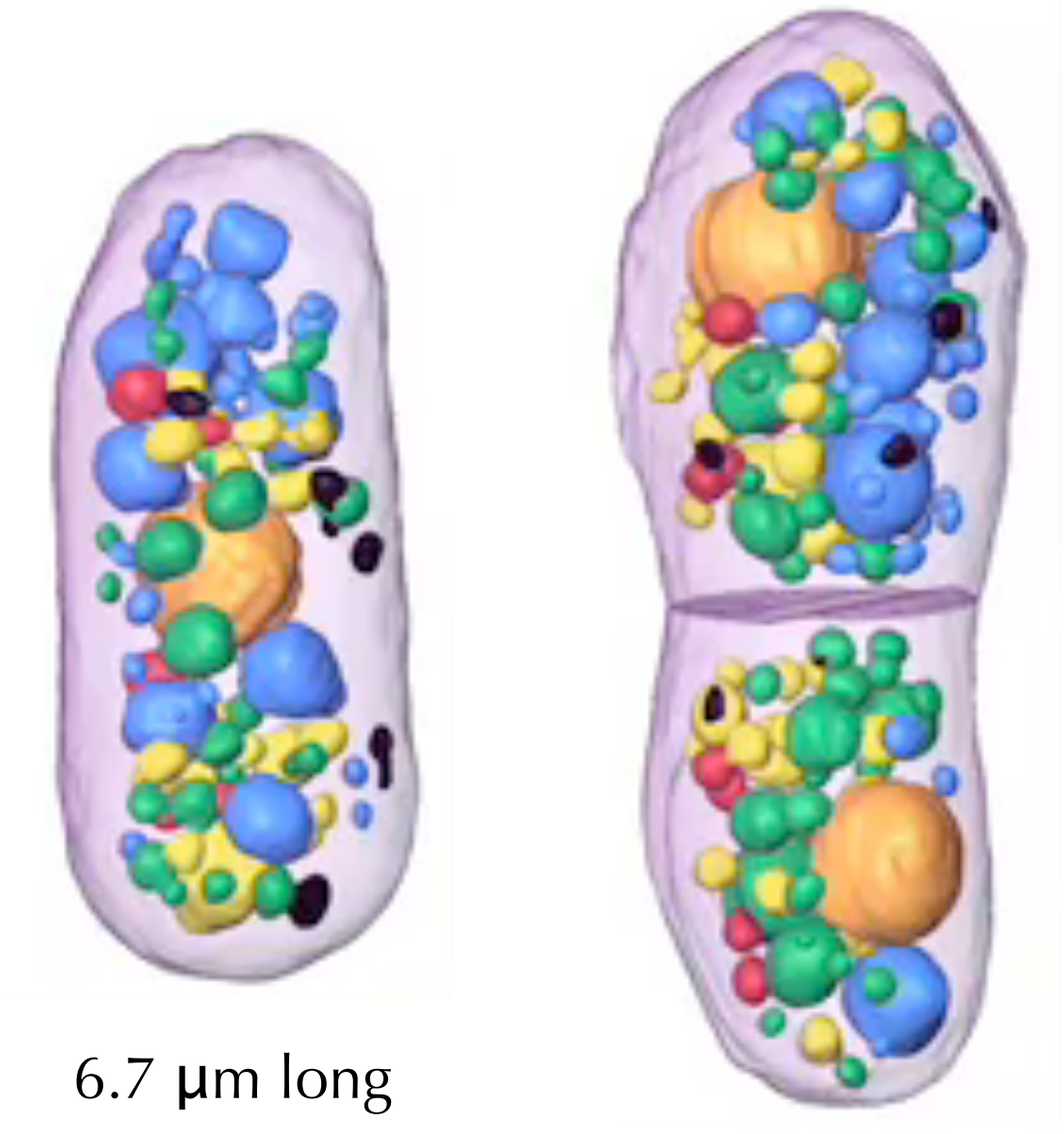

6.7 µm long

Radiation damage sets the ultimate resolution limit

- For many specimens, radiation damage sets the ultimate limit on achievable resolution.
- Lenses phase the signal, but lose the signal. Example: 20 nm zone plate with 10% efficiency, 50% window transmission, 20% modulation transfer function (MTF) for 15 nm half-period:

  net transfer of 1% for high spatial frequencies
- Can we avoid this ~100x signal loss, and also go beyond numerical aperture limit of available optics?

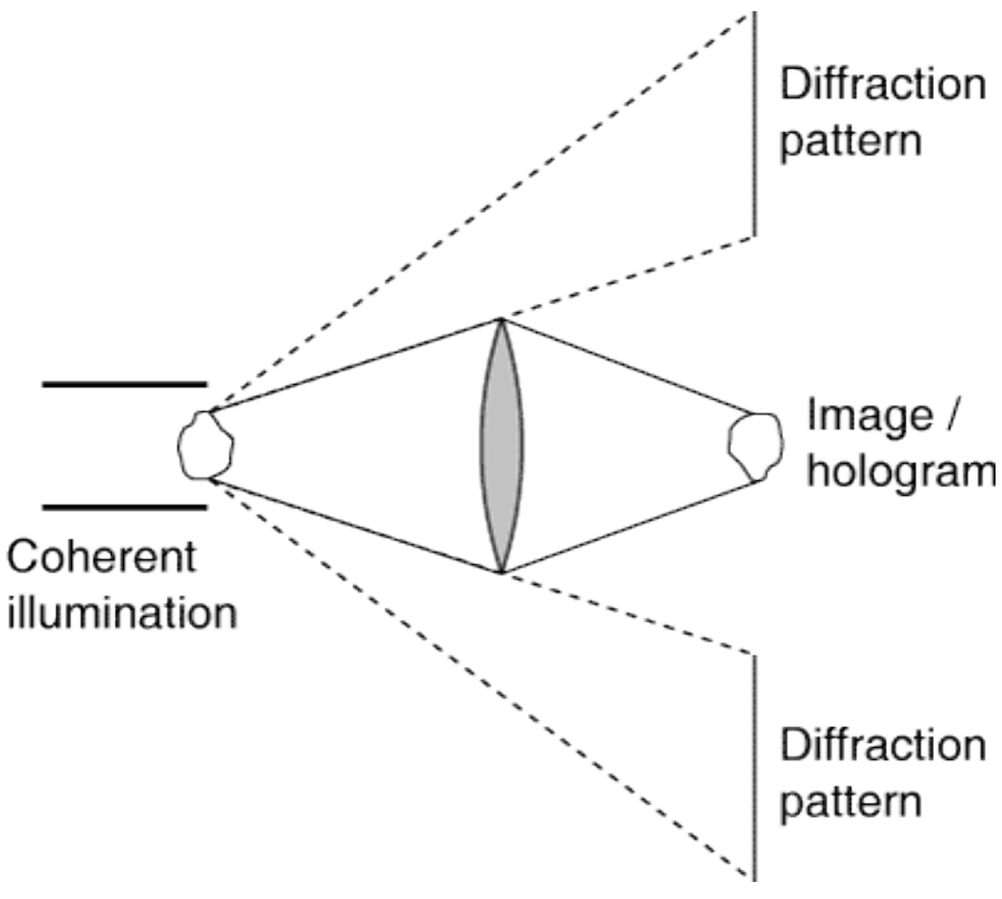

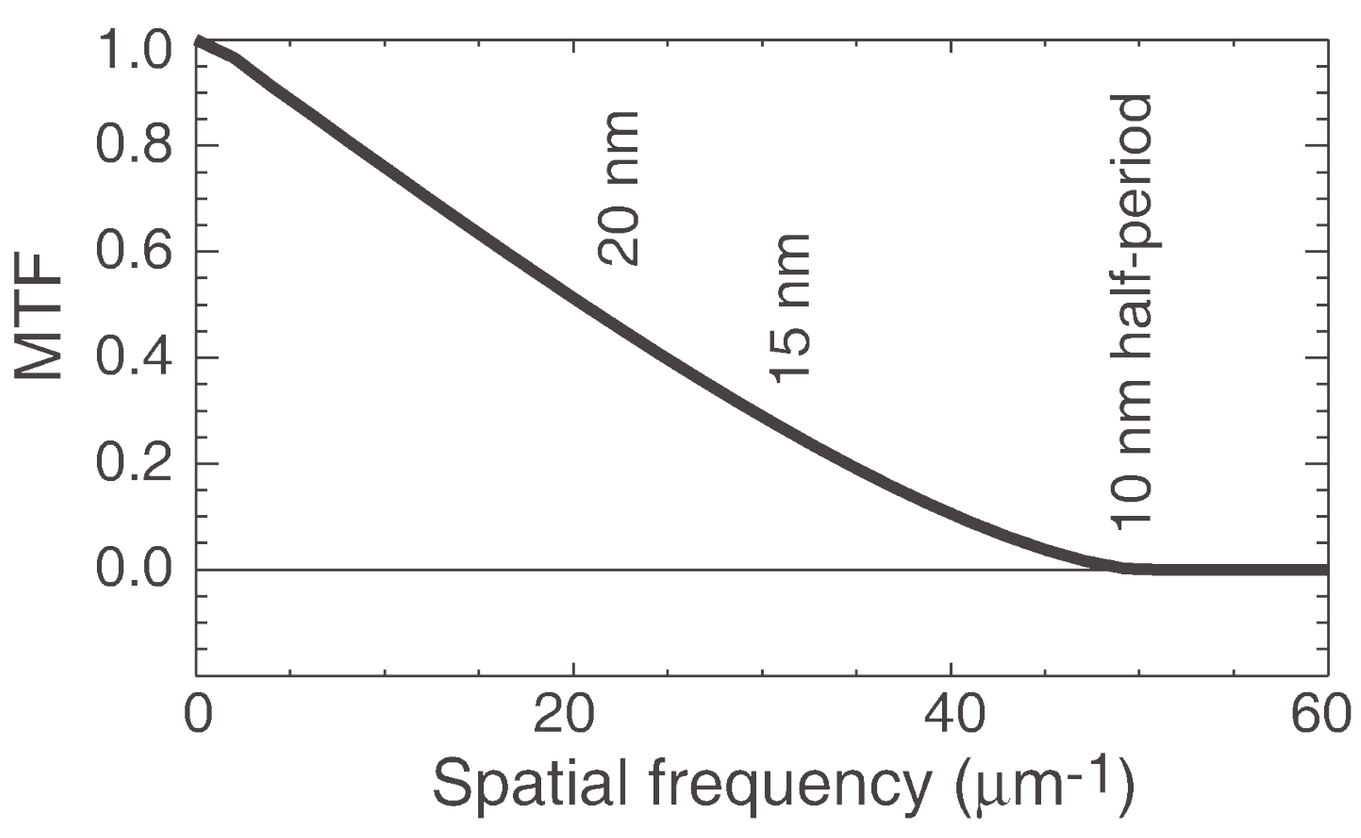

Phase matters

Image→ Fourier transform→ zero magnitude or phase→ inverse Fourier transform

Malcolm Howells
at La Clusaz

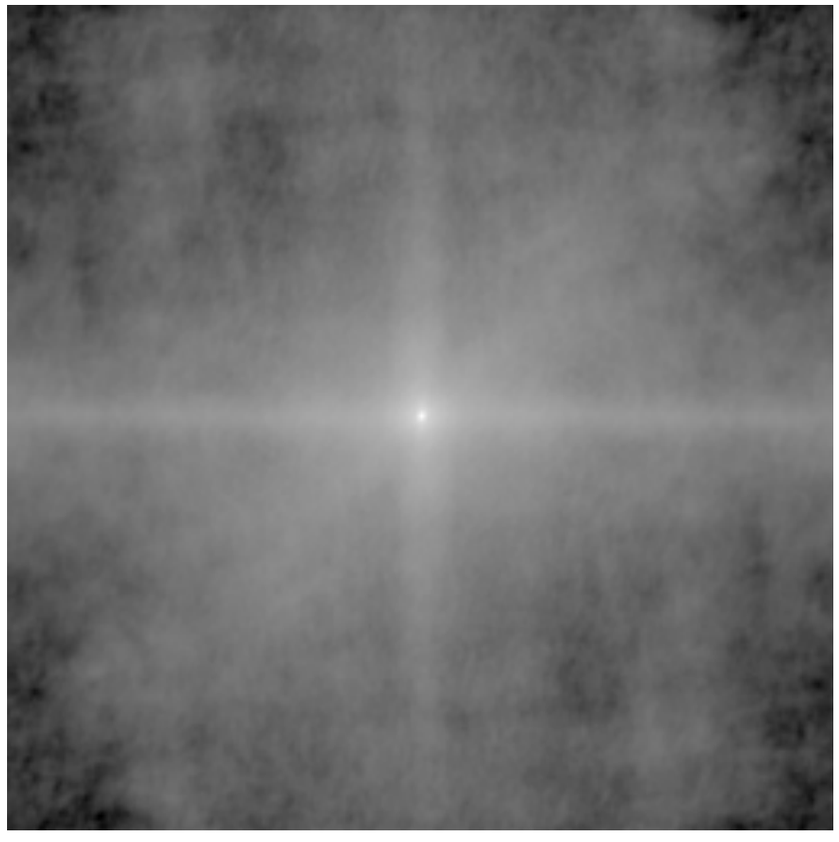

Image using only
Fourier magnitudes

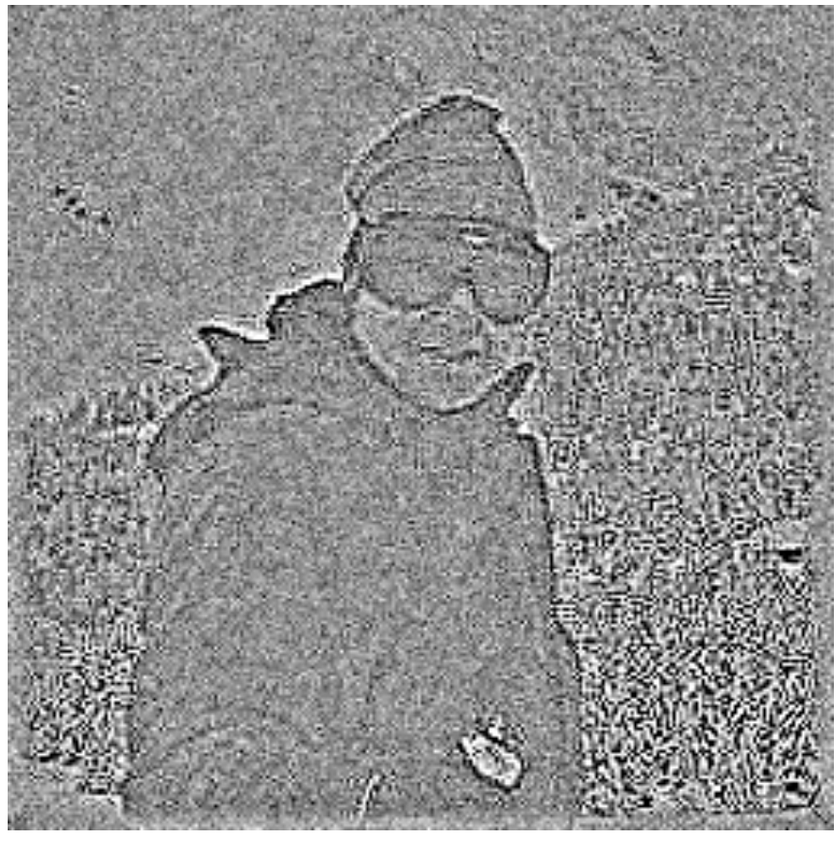

Image using only
Fourier phases

1 unit cell

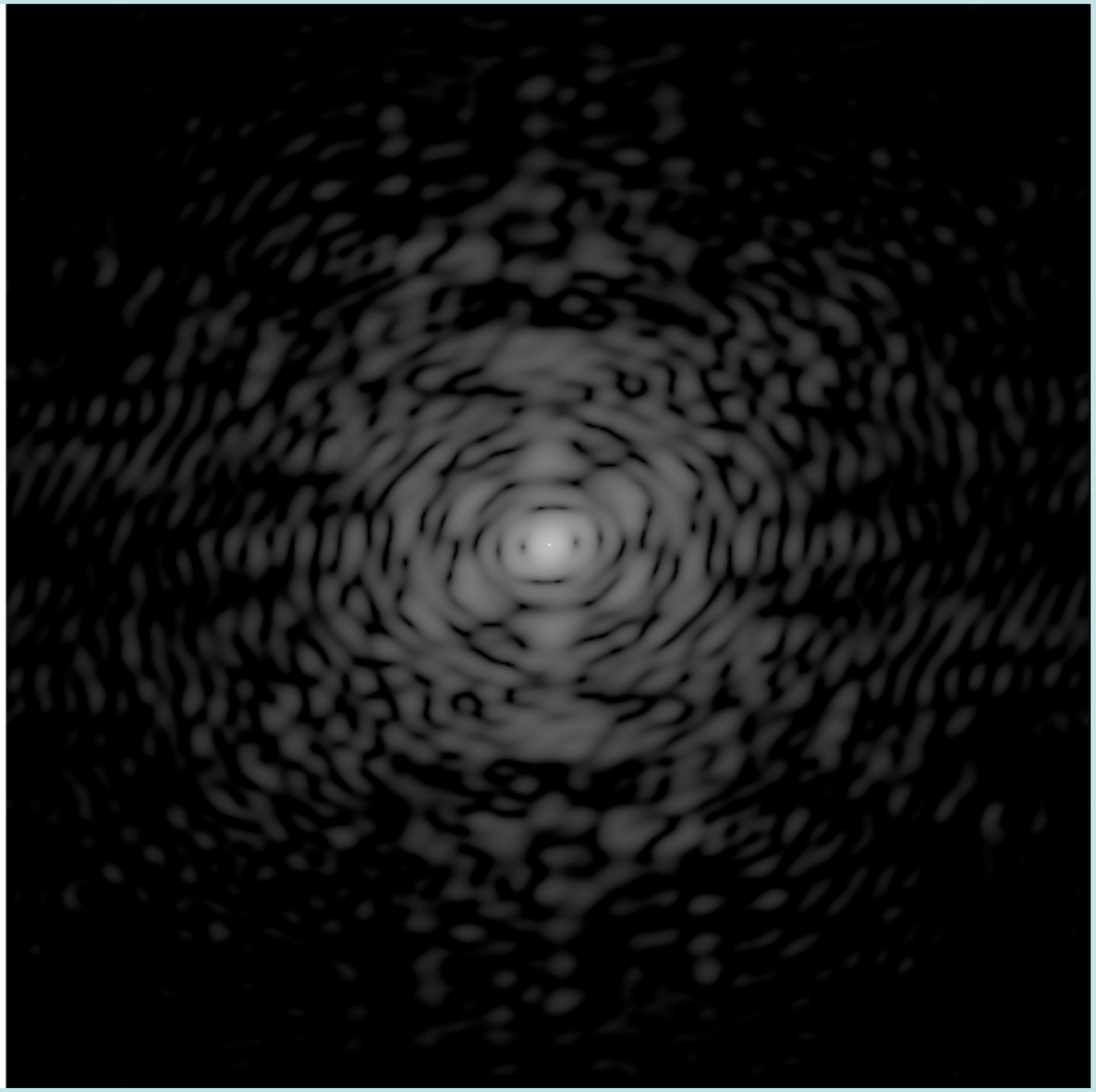

2x2 unit cells

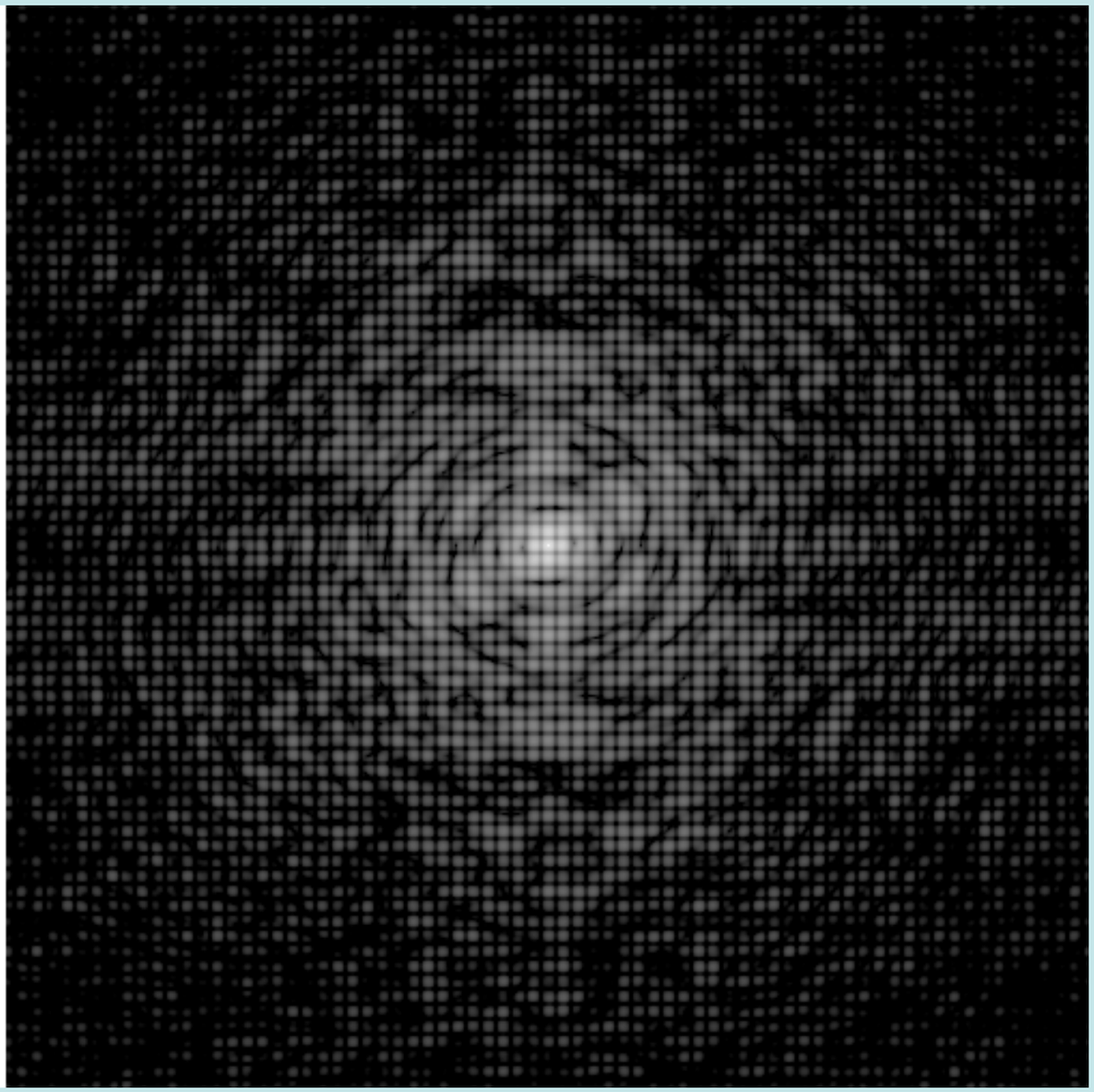

See e.g., D. Sayre, "Some implications of a theorem due to Shannon," *Acta Cryst*. **5**, 843 (1952)

3x3 unit cells

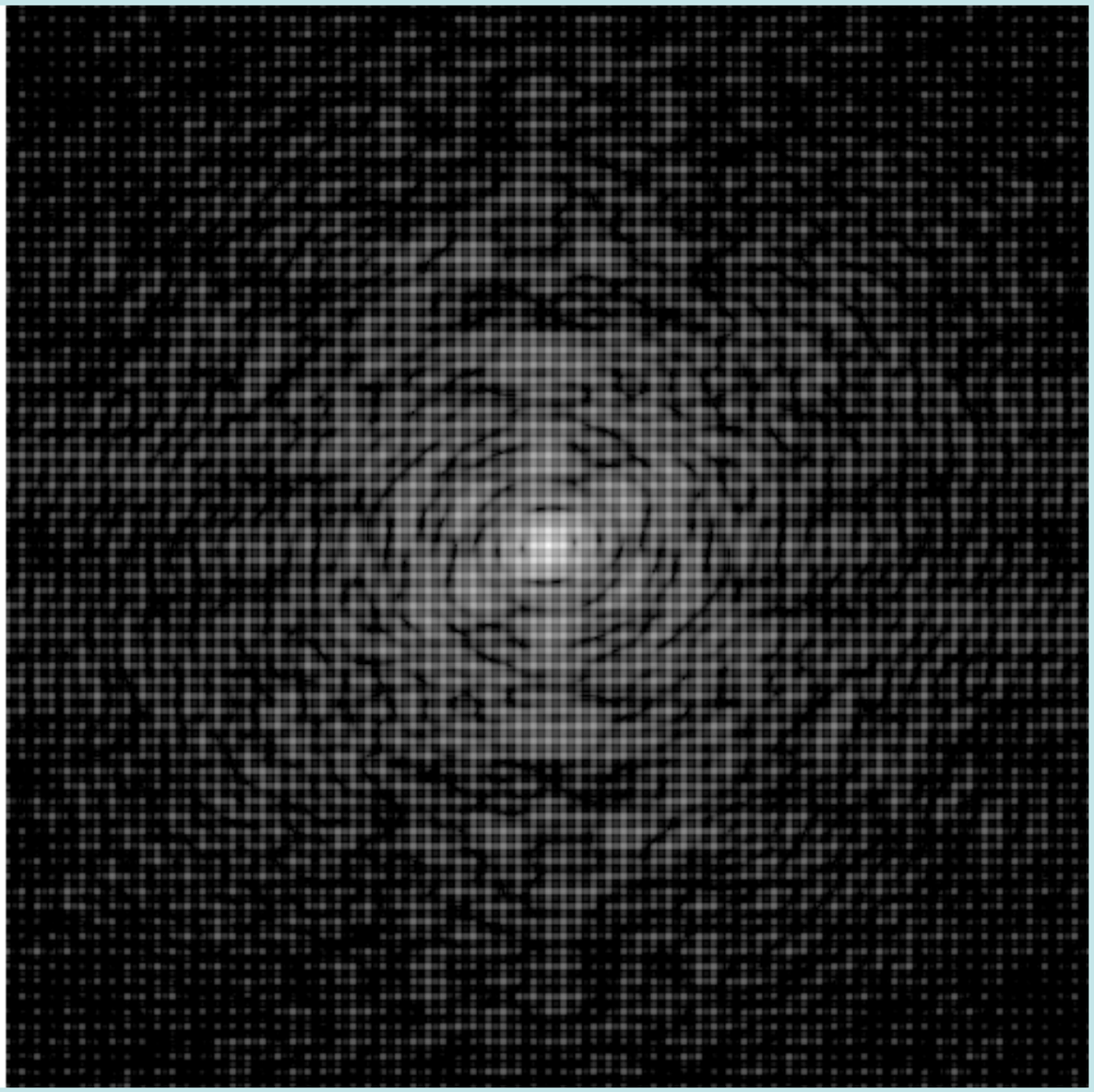

See e.g., D. Sayre, "Some implications of a theorem due to Shannon," *Acta Cryst.* **5**, 843 (1952)

4x4 unit cells

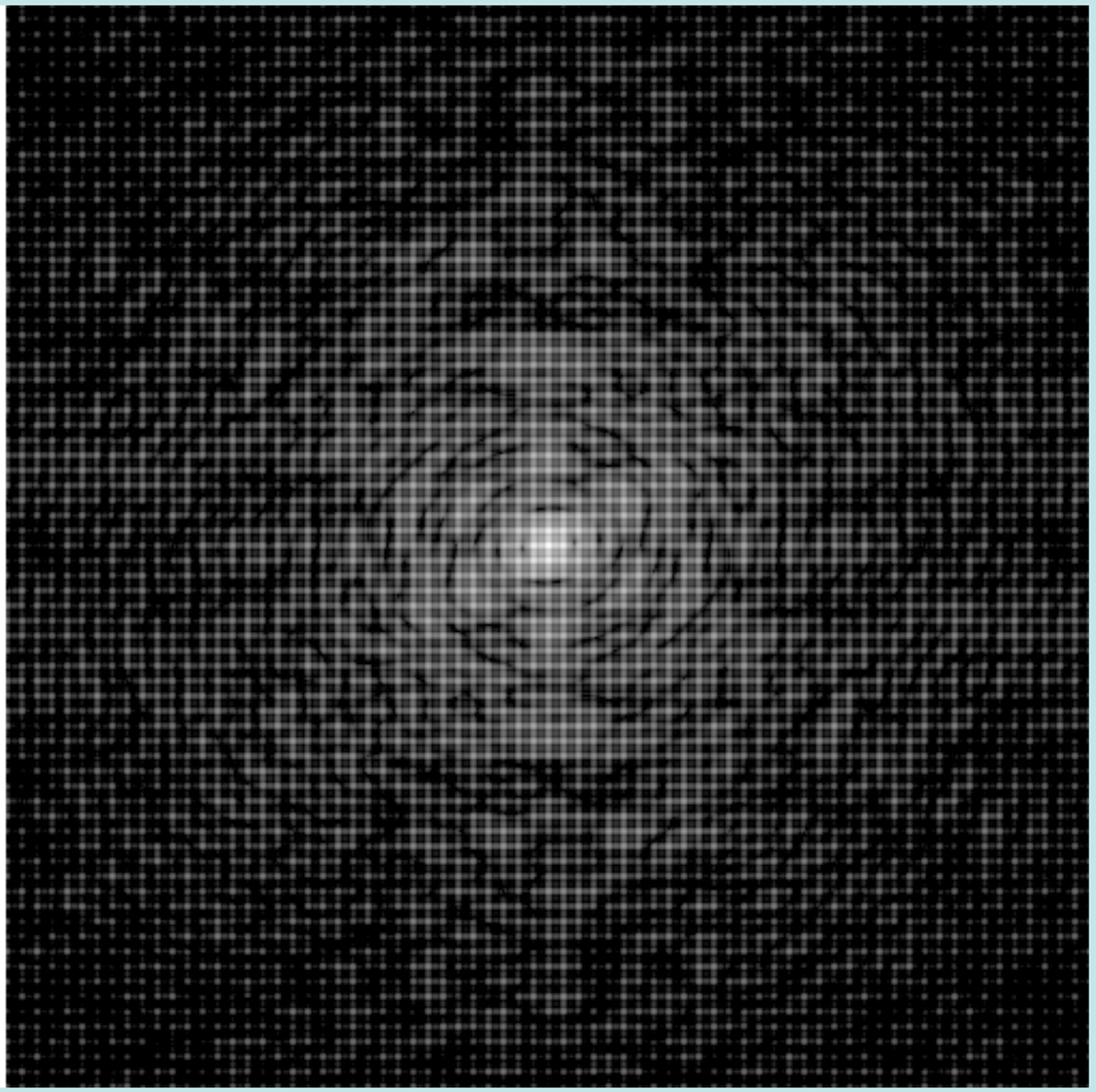

See e.g., D. Sayre, "Some implications of a theorem due to Shannon," *Acta Cryst*. **5**, 843 (1952)

5x5 unit cells

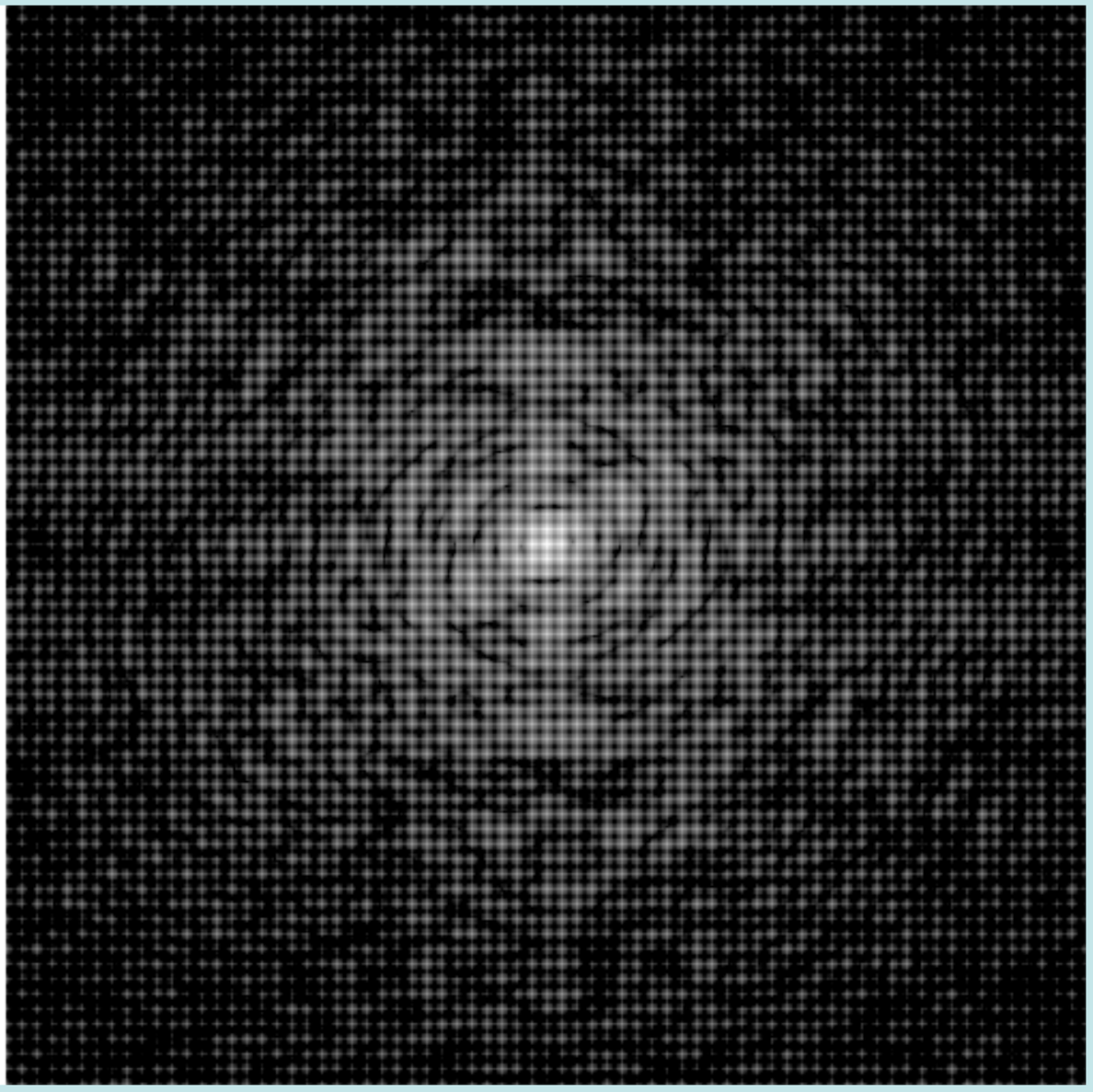

See e.g., D. Sayre, "Some implications of a theorem due to Shannon," *Acta Cryst*. **5**, 843 (1952)

1 unit cell

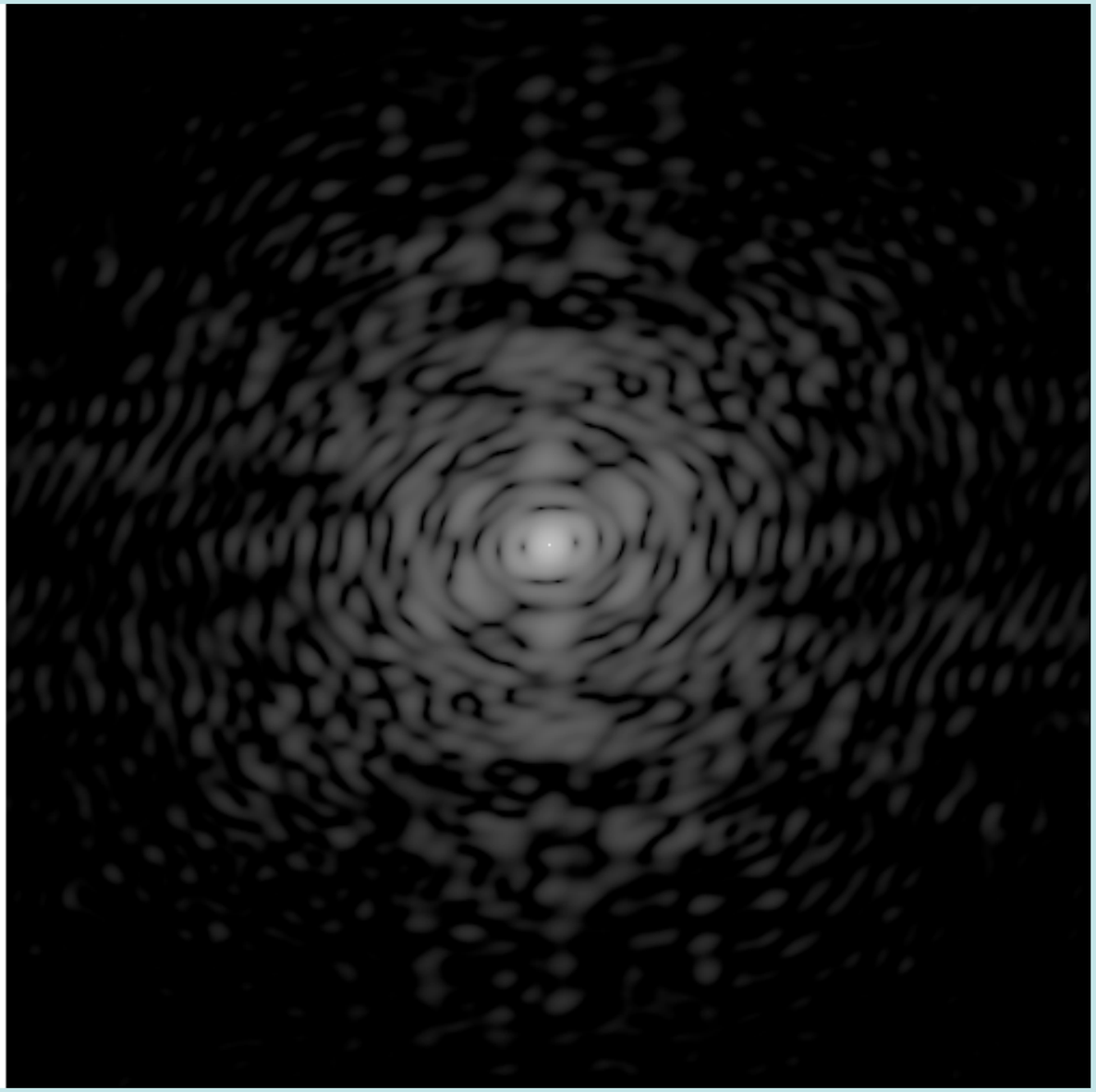

See e.g., D. Sayre, "Some implications of a theorem due to Shannon," *Acta Cryst*. **5**, 843 (1952)

Who else might be interested?

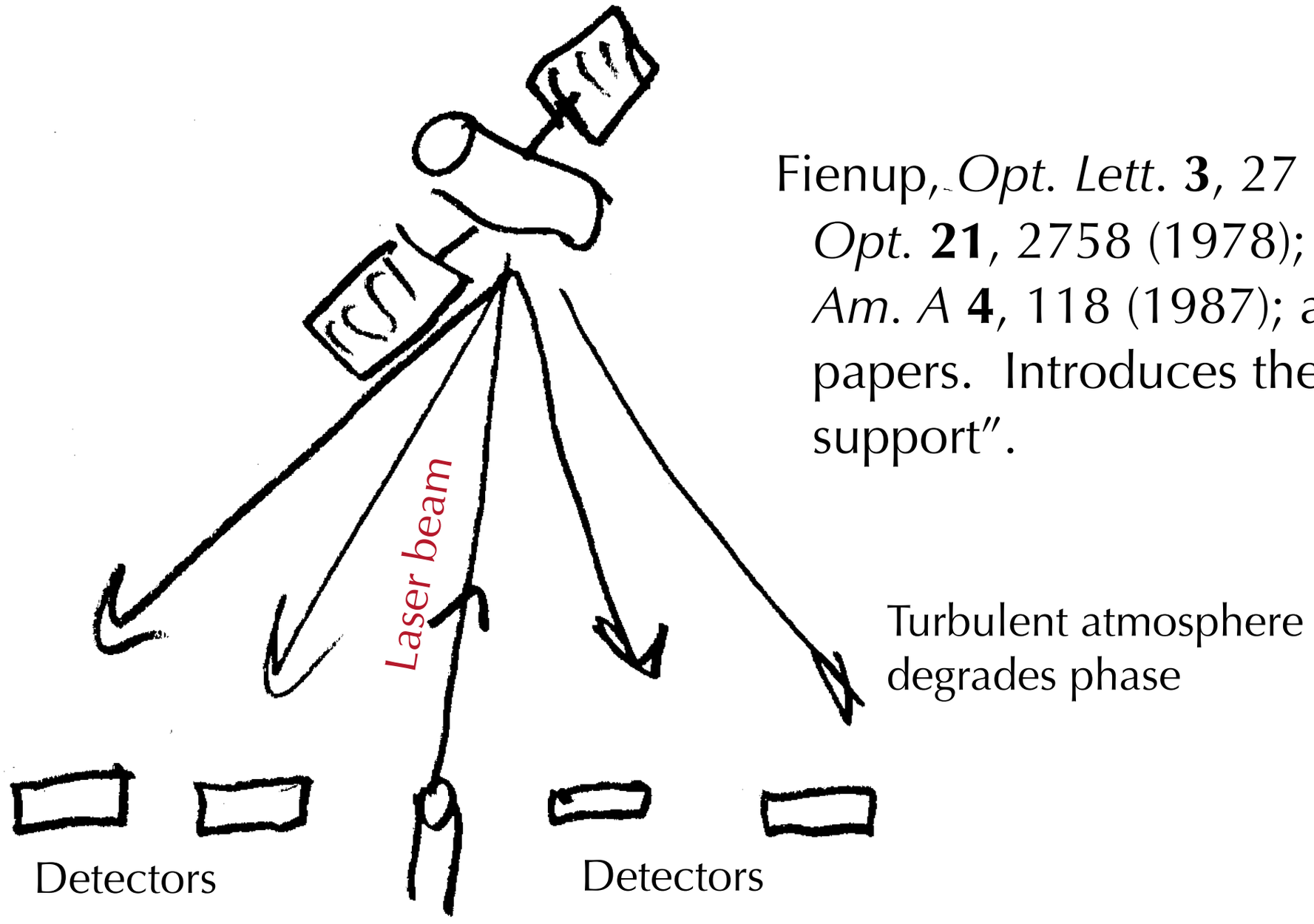

Fienup, *Opt. Lett.* **3**, 27 (1978); *Appl. Opt.* **21**, 2758 (1978); *J. Opt. Soc. Am. A* **4**, 118 (1987); and other papers. Introduces the use of a "finite support".

Cartoon based on presentations by Fienup from ERIM (Environmental Research Institute of Michigan). Fienup is now at U. Rochester

Imaging without lenses

- Avoid losses of lens efficiency and transfer function
- Must phase the diffraction intensities

Real space: finite support
(or other constraints)

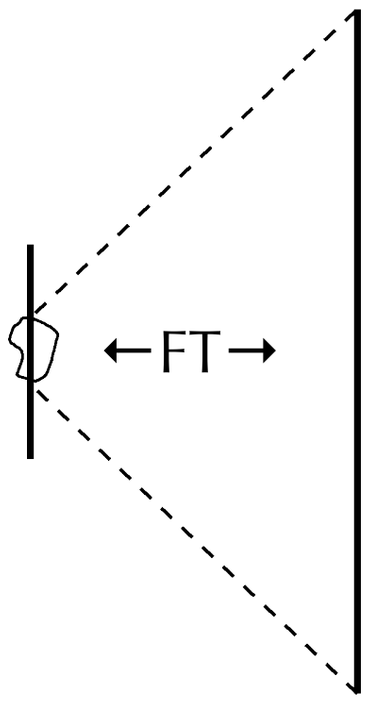

Fourier space: magnitudes known, but phases are not

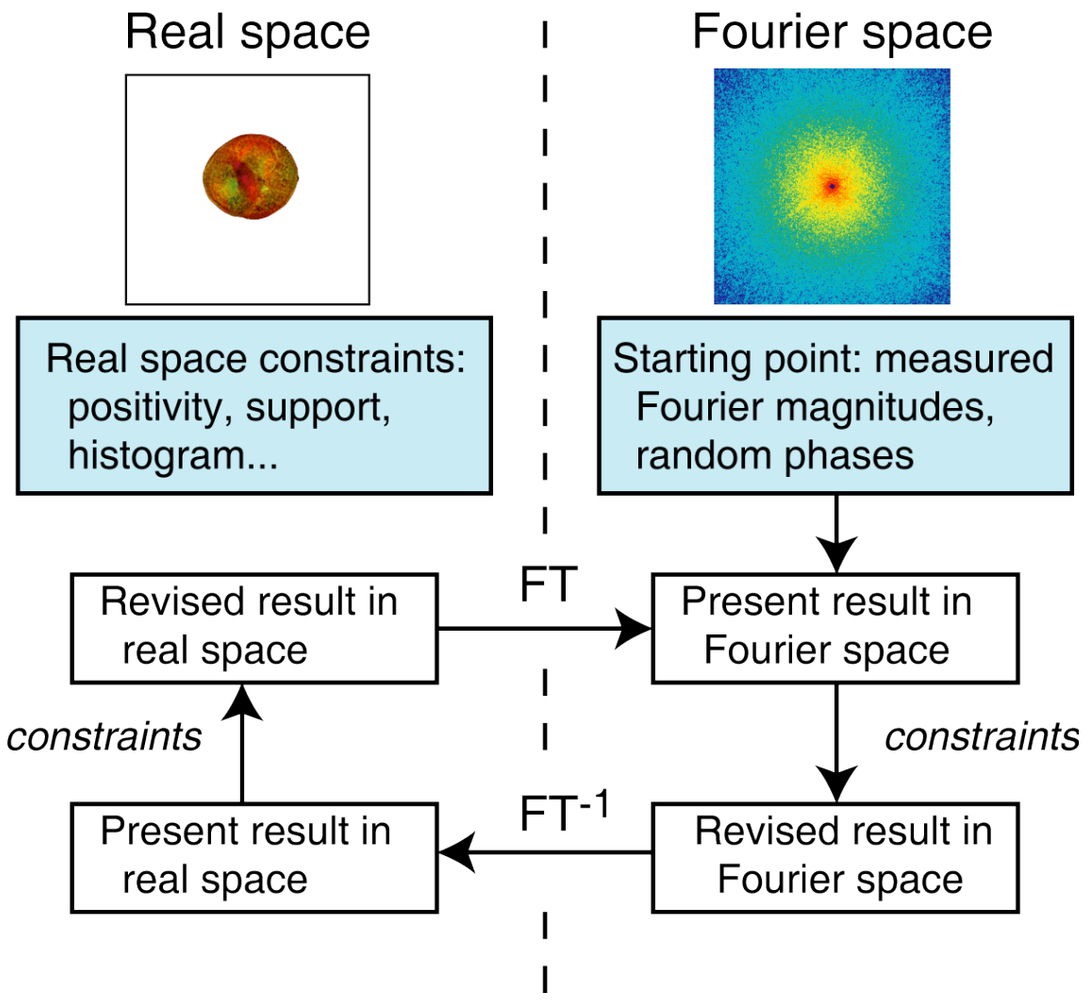

Phasing algorithms: Feinup, *Opt. Lett.* **3**, 27 (1978); Elser, *JOSA A* **20**, 40 (2003); and others. First x-ray demonstration: Miao *et al.*, *Nature* **400**, 342 (1999).

Iterative phasing: simple example

- High harmonic generation of XUV radiation from femtosecond lasers, illuminating two pinholes.
  - R. Bartels, A. Paul, H. Green, H.C. Kapteyn, M.M. Murnane, S. Backus, I.P. Christov, Y. Liu, D. Attwood, C. Jacobsen, *Science* **297**, 376 (2002)

Data

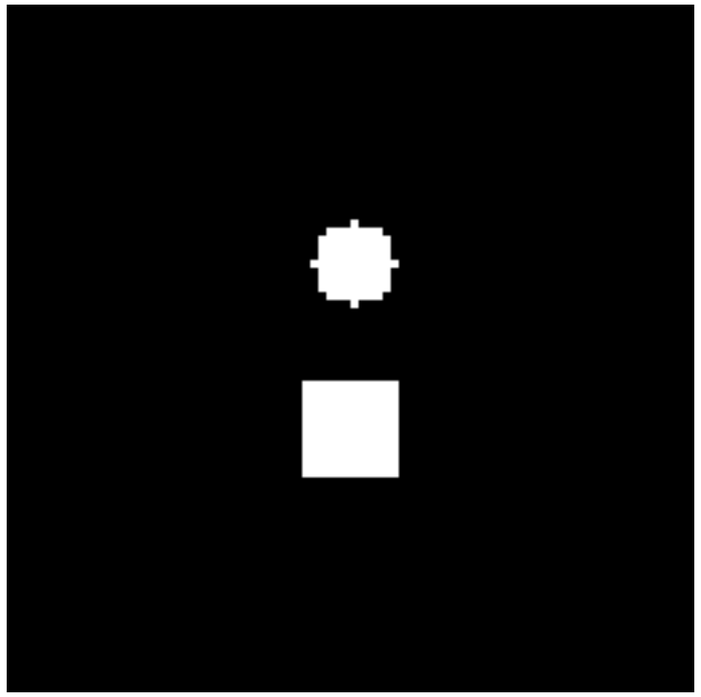

Support constraint
(very loose)

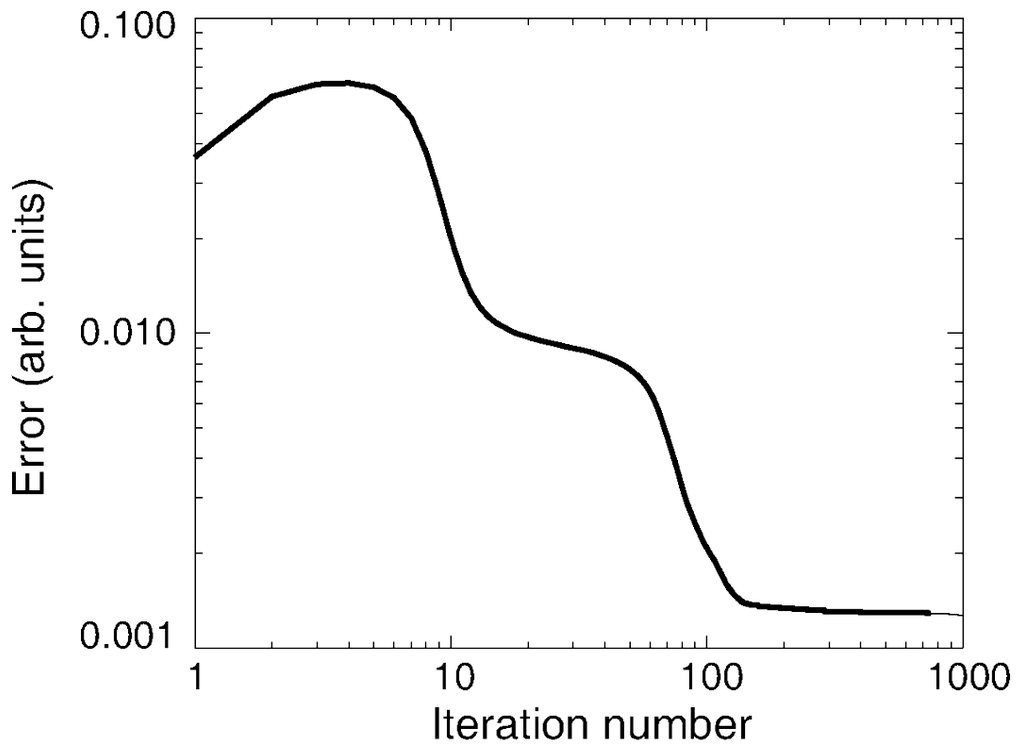

Reconstruction error

The reconstruction

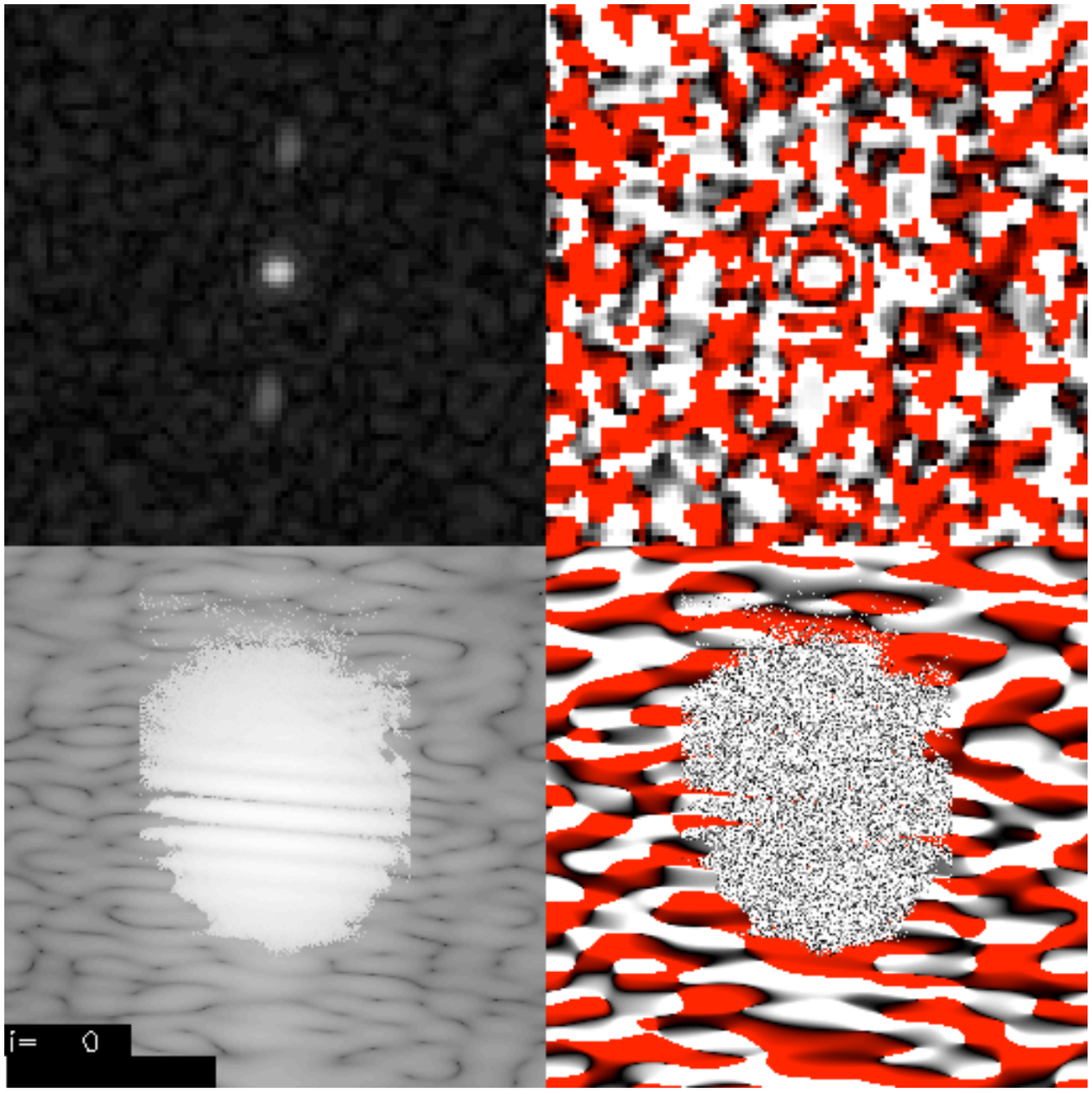

Real space Magnitude	Real space Phase
Far field Magnitude	Far field Phase

Fluctuating solutions

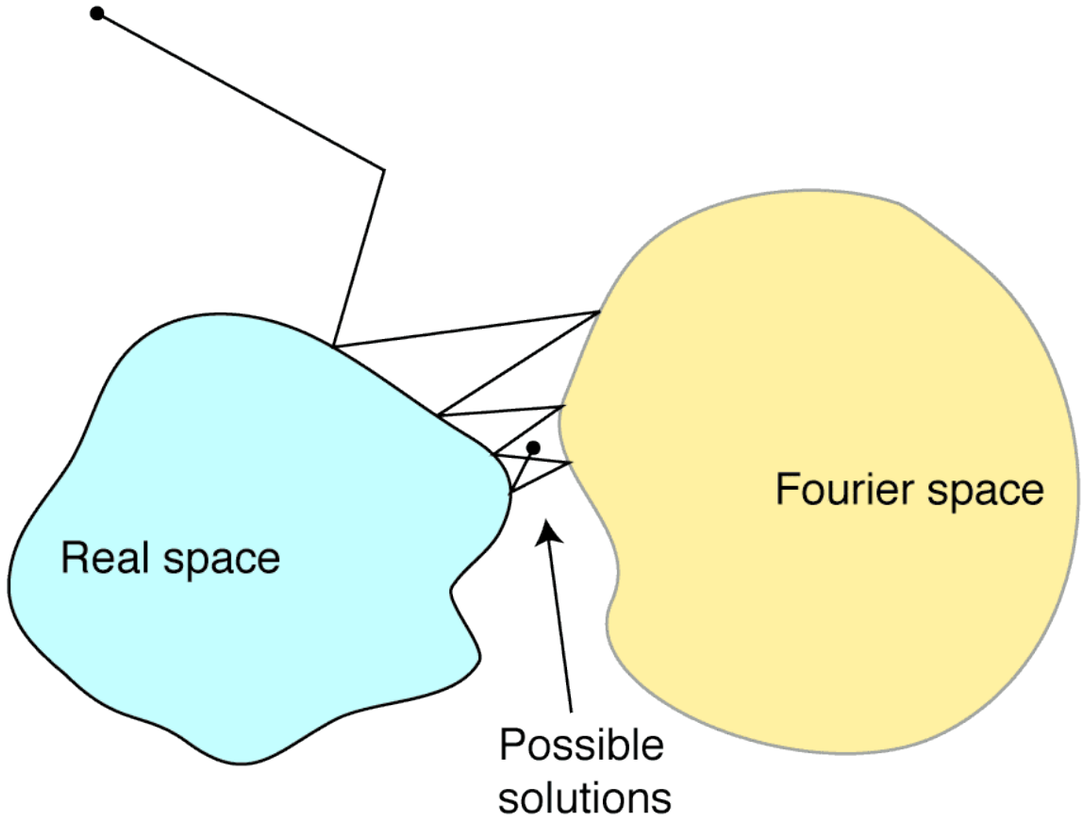

- Ideally, there would be a single point of best agreement between various constraints.
- Noise and incomplete constraints only provide a neighborhood of acceptable solutions.
- Choosing one iterate from one random starting phase as “the” solution is unwarranted!

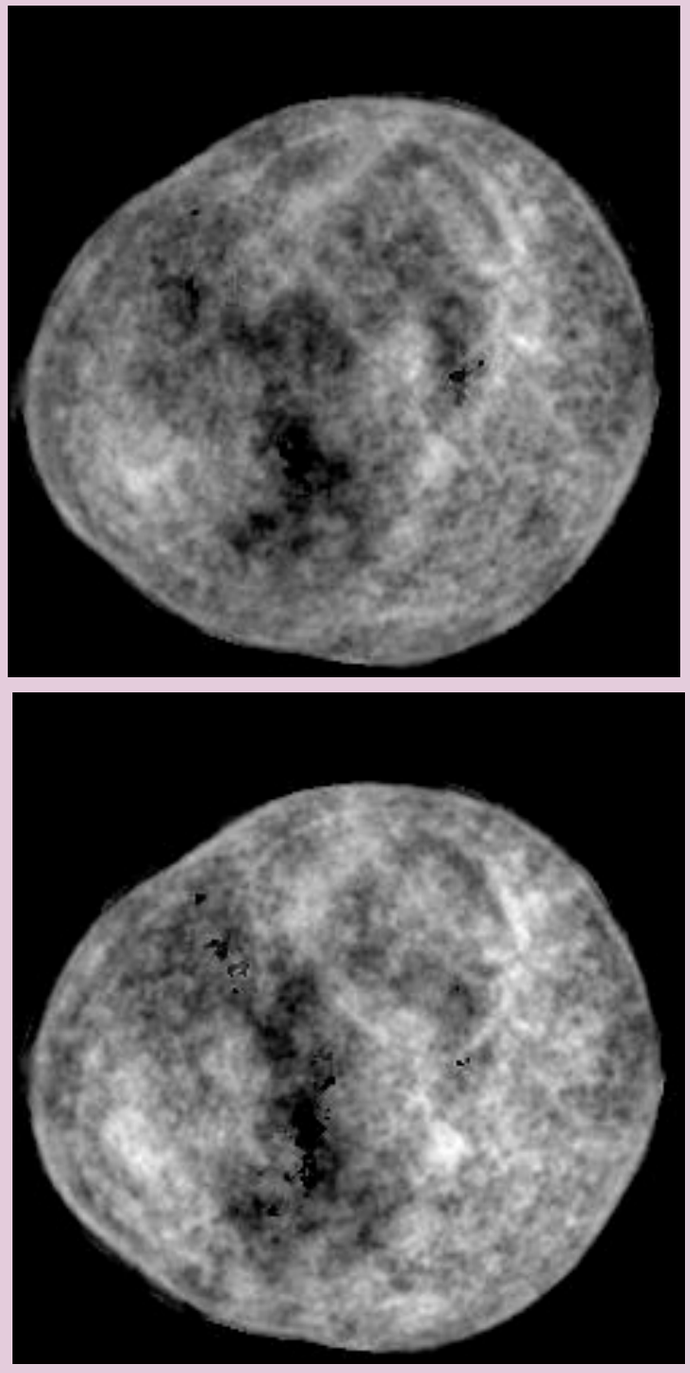

Two individual iterates

Iterate averaging

- If the solution fluctuates, let's take many samples and average them!
- Non-reproducible phases get washed out; reproducible phases get reinforced
- Thibault, Elser, Jacobsen, Shapiro, and Sayre, *Acta Crystallographica A* **62**, 248 (2006)
- Other approaches: compare results from several different starting random phases (*e.g.*, Miao, Robinson)

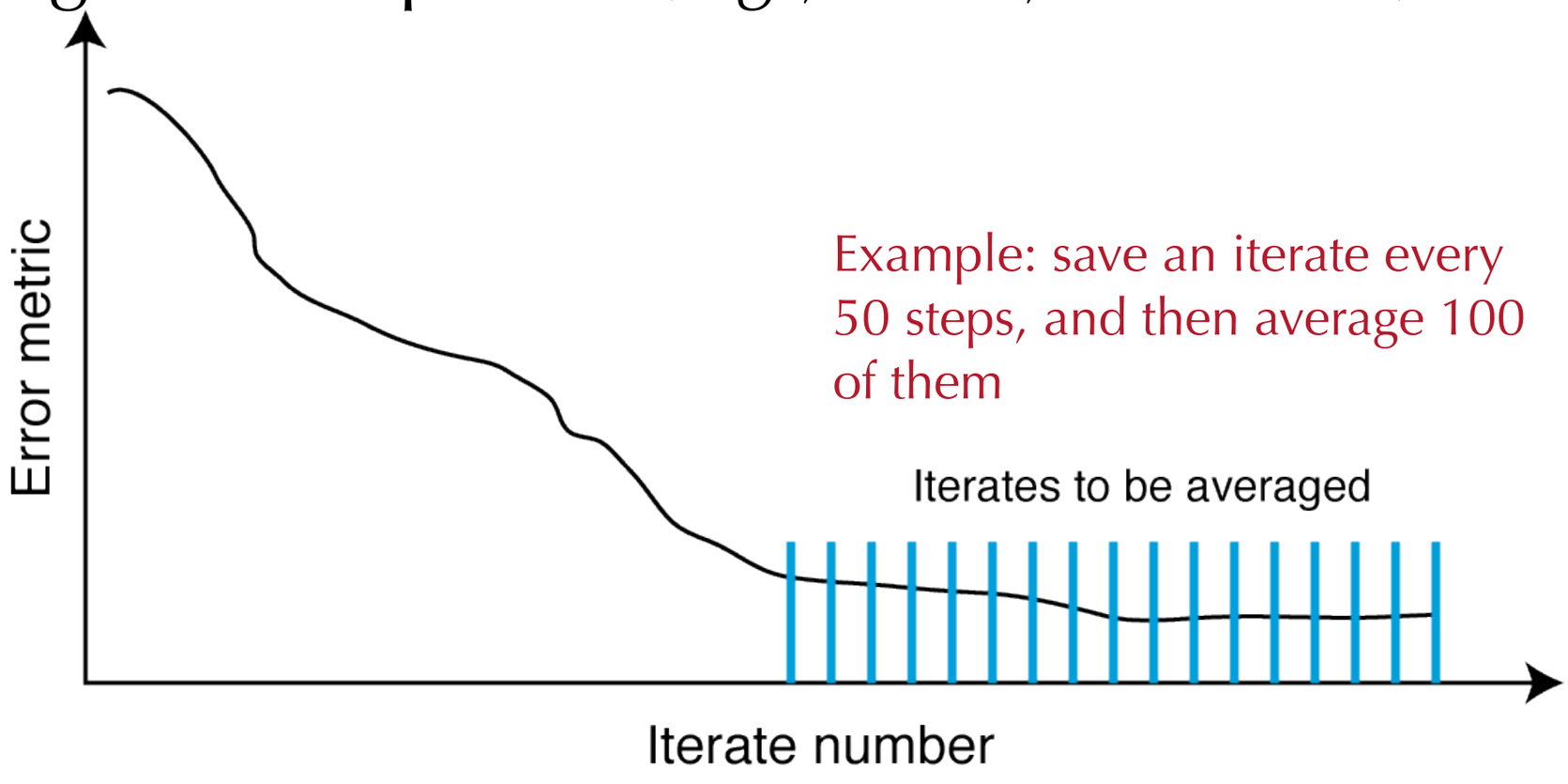

Different starting random phases

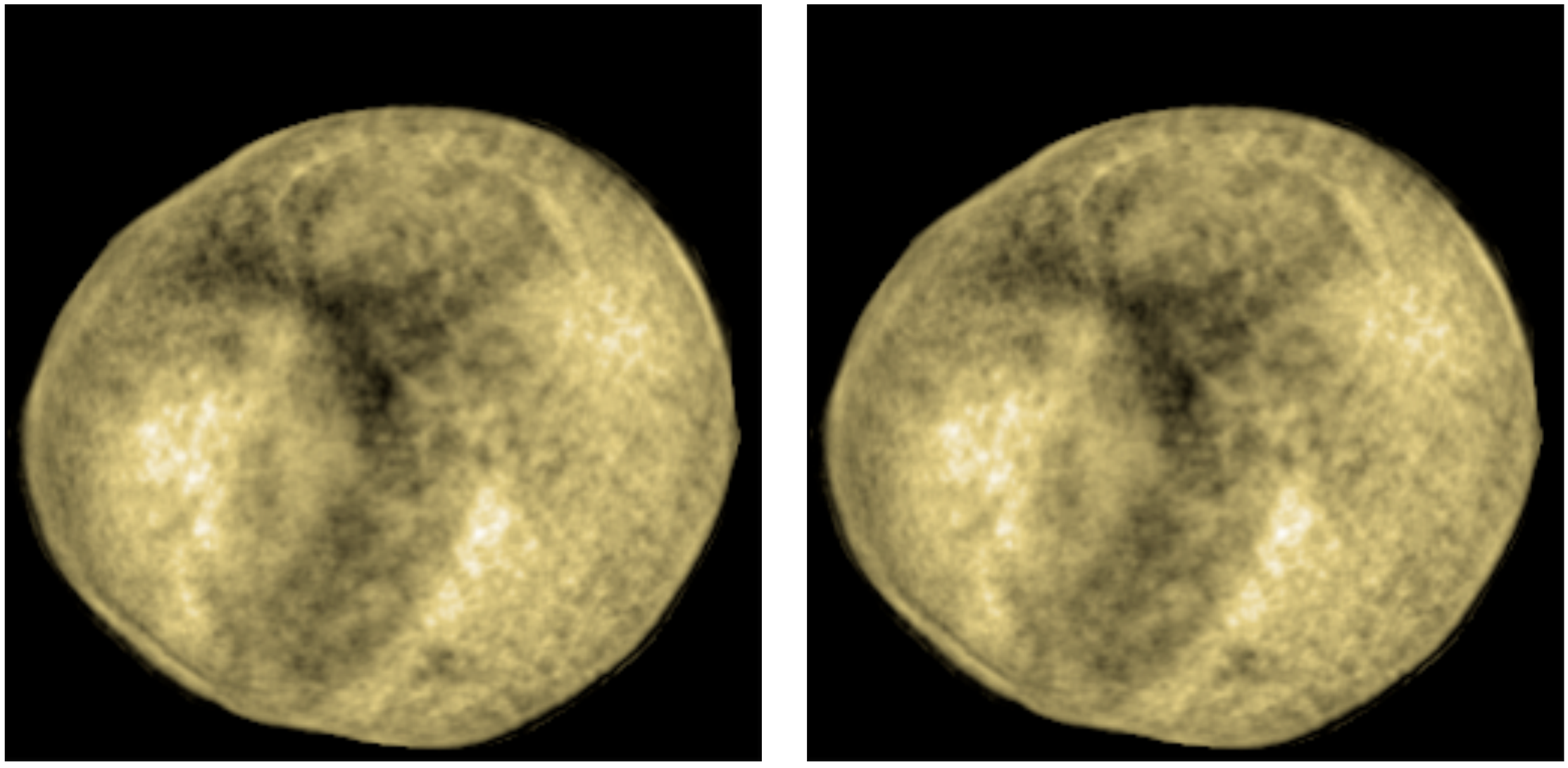

Two separate runs of algorithm with different random starting phases. In both cases, 125 iterates spaced 40 iterations apart were averaged (E. Lima).

Gold-labeled yeast

1.8 nm gold, silver-enhanced, dehydrated: J. Nelson *et al.*, Stony Brook/ALS

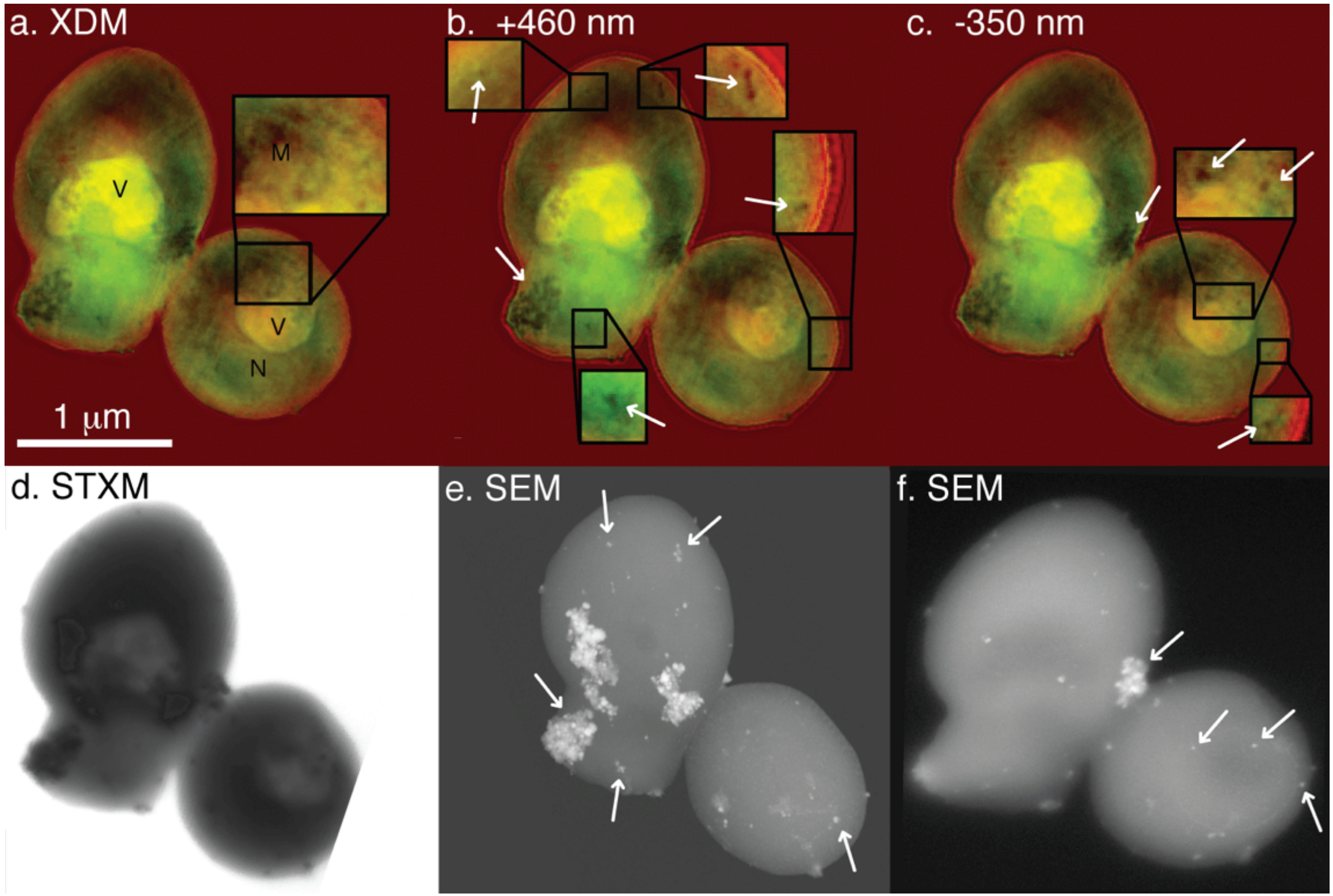

Crystallinity, and strain within nanocrystals

Domain boundaries in polycrystalline materials: Liu *et al.*, *Ultramicroscopy* **103**, 199 (2005).

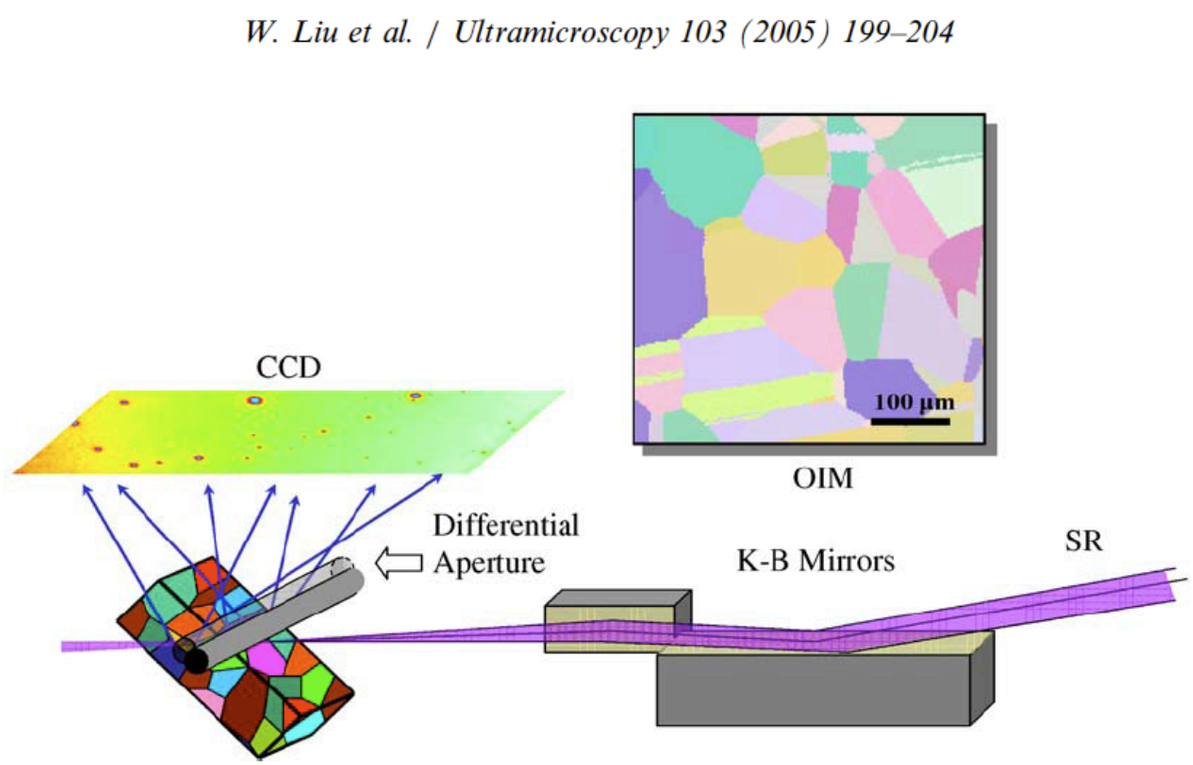

Coherent diffraction about a Bragg peak reveals the shape of and strain within a nanocrystalline domain at 40 nm resolution. Pfeiffer *et al.*, *Nature* **442**, 63 (2006).

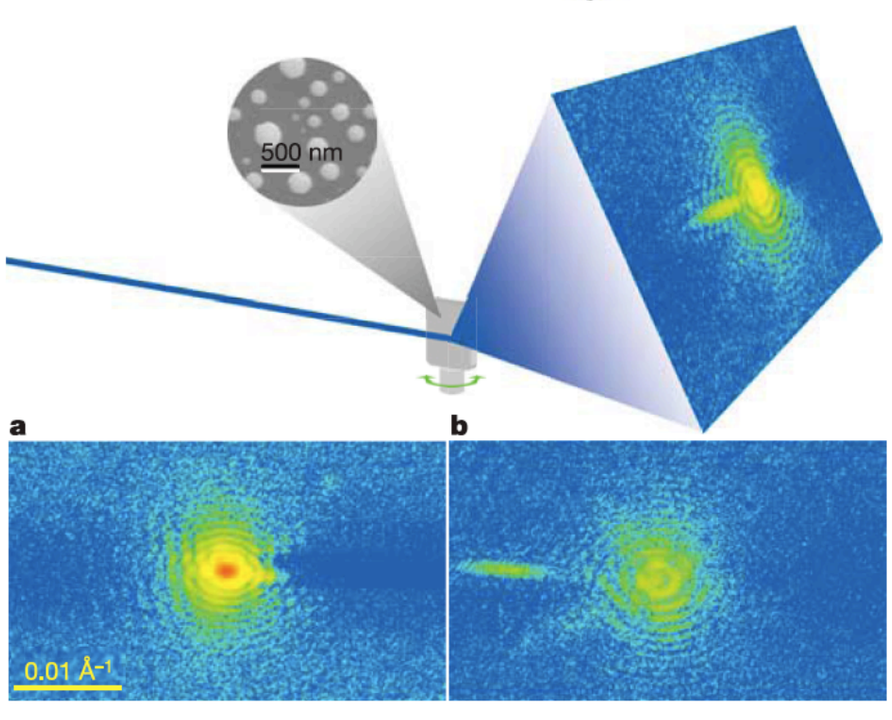

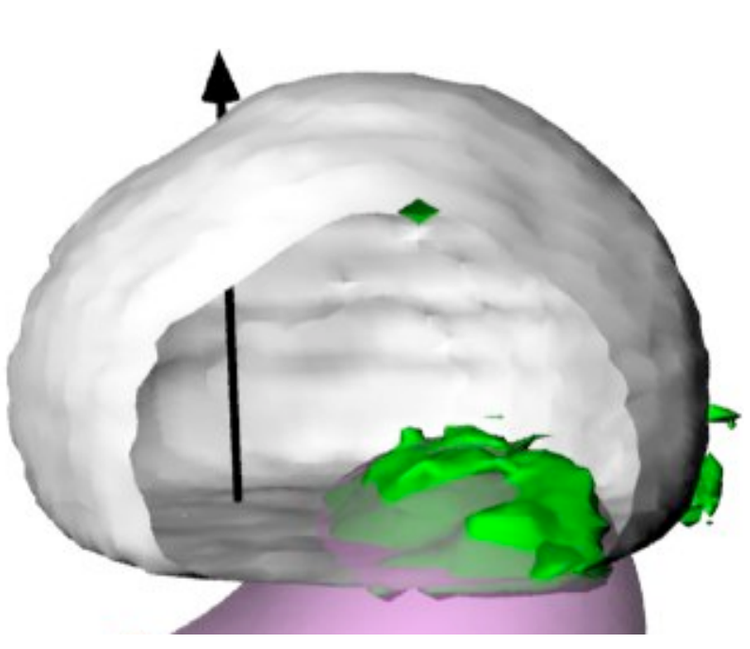

Ptychography

High-Resolution Scanning X-ray Diffraction Microscopy

Pierre Thibault,[1]* Martin Dierolf,[1] Andreas Menzel,[1] Oliver Bunk,[1] Christian David,[1] Franz Pfeiffer[1,2]

Coherent diffractive imaging (CDI) and scanning transmission x-ray microscopy (STXM) are two popular microscopy techniques that have evolved quite independently. CDI promises to reach resolutions below 10 nanometers, but the reconstruction procedures put stringent requirements on data quality and sample preparation. In contrast, STXM features straightforward data analysis, but its resolution is limited by the spot size on the specimen. We demonstrate a ptychographic imaging method that bridges the gap between CDI and STXM by measuring complete diffraction patterns at each point of a STXM scan. The high penetration power of x-rays in combination with the high spatial resolution will allow investigation of a wide range of complex mesoscopic life and material science specimens, such as embedded semiconductor devices or cellular networks.

SCIENCE VOL 321 18 JULY 2008 379

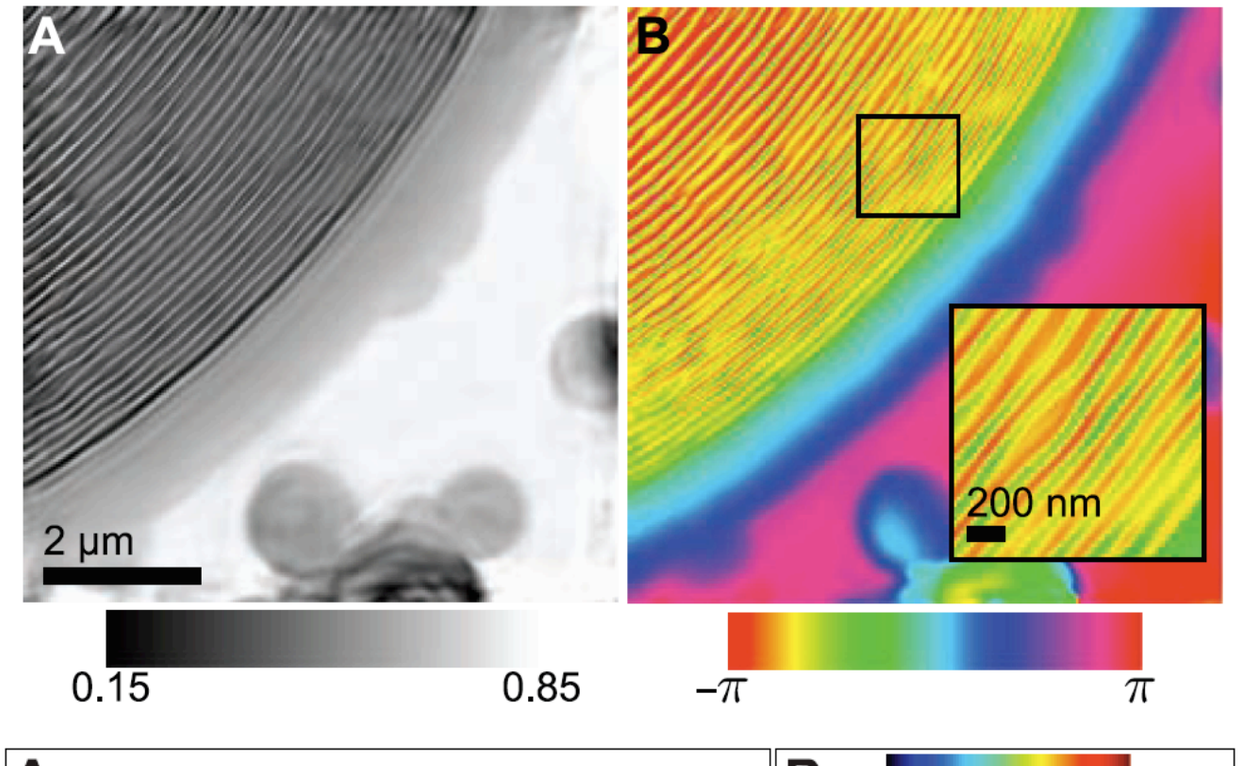

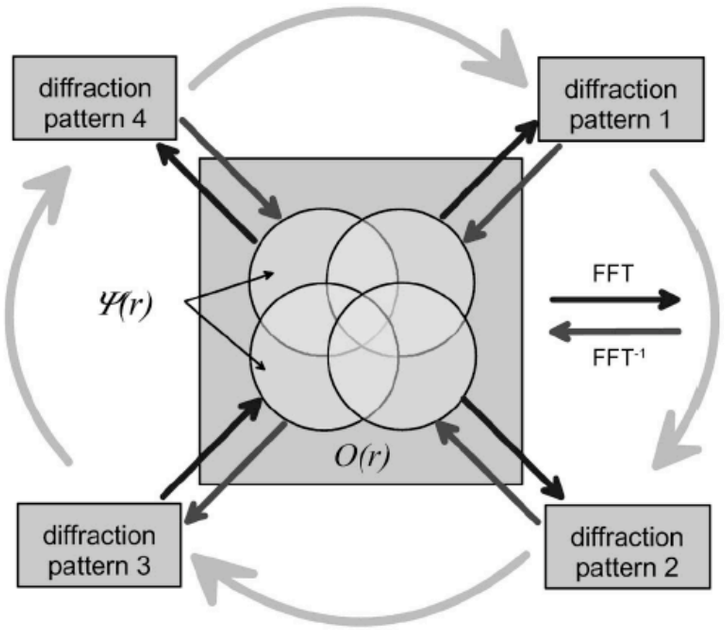

FIG. 2. Diagram of the phase-retrieval algorithm. The outer circular arrows indicate the position stepping within one iteration. The arrows within indicate (inverse) Fourier transforms and the desired input-output information.

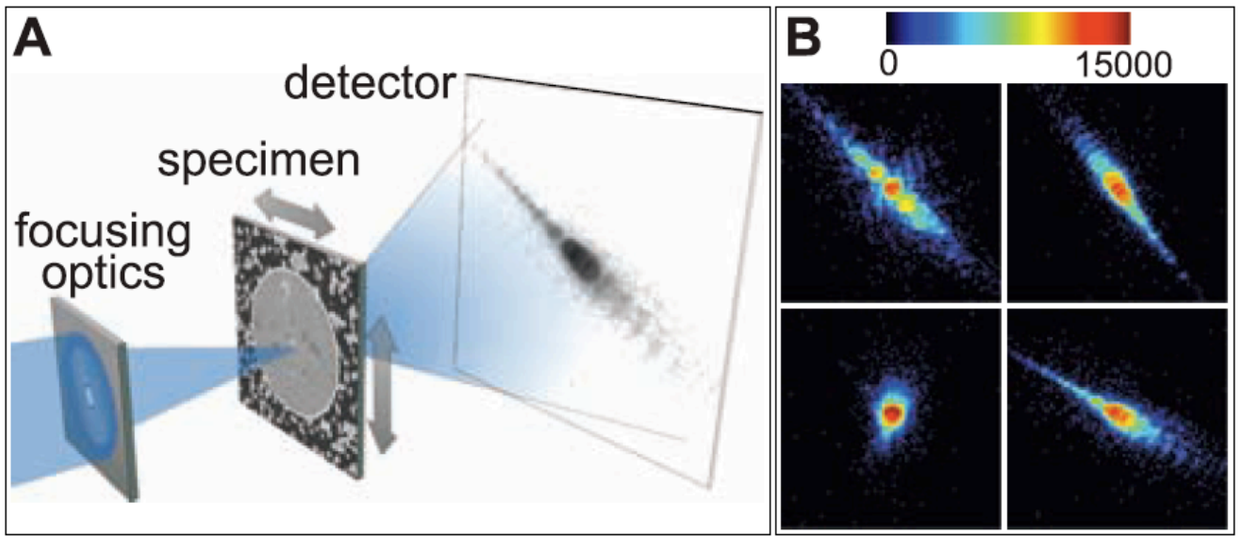

Rodenburg *et al.*, *Phys. Rev. Lett.* **98**, 034801 (2007)